Sustainable Urban Ecological Infrastructures: Multi-Functionality and Long-Term Dynamics for Water Management

PUBLICATIONS

Research Supervision Habilitation (HDR) Thesis
University of Strasbourg - Sciences

Presented and publicly defended by Paul BOIS
on Monday, November 9th 2020

Jury members:

M. Ellen BANZHAF	DR, UFZ, Leipzig	Main reviewer
M. Daniel L. CHILDERS	Pr, ASU, Phoenix	Reviewer
M. Nicolas FLIPO	Pr, Mines ParisTech, Paris	Reviewer
M. Thomas HEIN	Pr, BOKU, Wien	Main reviewer
M. Christelle LISON	Pr, Université de Sherbrooke	Main reviewer
M. Adrien WANKO	Pr, ENGEES, Strasbourg	Guarantor
M. Christiane WEBER	DR, CNRS, Montpellier	Reviewer

Université de Strasbourg

ENGEES

ICUBE

CNRS

Publications

Indicateurs de colmatage de filtres plantés de roseaux à écoulement vertical :

étude comparative de quatre stations de traitement après 10 ans de fonctionnement

■ P. BOIS[1], J. LAURENT[1], M. NUEL[1,2], A. WANKO[1]

Mots-clés : traitement de l'eau, filtre planté de roseau, vieillissement, comportement hydraulique, expériences de terrain

Keywords: wastewater treatment, constructed wetland, ageing, hydraulic properties, field experiments

Introduction

La directive ERU (eaux résiduaires urbaines) de 1991 a rendu obligatoires les installations de traitement pour les communes de plus de 2 000 équivalent-habitant (EH) et a ainsi entraîné la création d'installations de traitement supplémentaires. Parmi elles, les procédés extensifs et en particulier les filtres plantés de roseaux (FPR) ont prouvé leur efficacité pour le traitement des eaux usées domestiques depuis plus d'une quinzaine d'années [BOUTIN *et al.*, 1997] et dans de nombreux pays [VYMAZAL, 2002]. Sur le bassin Rhin-Meuse, les stations de type FPR ont fait leur apparition au milieu des années 1990. Le recours à ce procédé de traitement est aujourd'hui en pleine expansion pour les petites collectivités : une dizaine de stations de ce type sont construites chaque année dans le bassin Rhin-Meuse, pour un total de 146 FPR actuellement recensés [AERM, 2013]. Au total, ce type de stations représente 27 % des STEU de moins de 2000 EH recensées sur le bassin hydrographique. Toutes les stations de type FPR implantées dans ce bassin sont conçues et exploitées selon le modèle français. Une station comprend ainsi deux étages en cascade, l'alimentation en effluent est intermittente (en général un tiers du temps en alimentation et deux tiers du temps en repos) et par bâchées. Le granulat du premier étage est plutôt grossier pour éviter le colmatage et le granulat du second étage est plus fin ; l'écoulement de l'effluent est vertical sur les deux étages.

Parmi les stations de ce type recensées par l'agence de l'eau Rhin-Meuse (AERM), quatre sont en service depuis plus de 10 ans. Cette longévité et le nombre croissant d'installations de ce type posent les questions relatives à leur durée de vie et au nécessaire maintien des performances de traitement au cours de ce cycle de vie. En effet, le vieillissement des filtres plantés s'accompagne d'un certain nombre de phénomènes *a priori* indésirables, dont celui de colmatage, dû principalement aux phénomènes suivants [KADLEC et WALLACE, 2009] :

– dépôt de particules en suspension, surtout dans les horizons superficiels ;

– développement rapide d'un biofilm sur le support granulaire.

Le colmatage peut entraîner une diminution des performances de traitement par baisse de l'oxygénation des filtres colonisés jusqu'à un facteur 20 [PLATZER et MAUCH, 1997]. Il peut également arriver que l'accumulation de boues ne provoque pas de colmatage total, mais soit indésirable pour des raisons hydrauliques, notamment de répartition de l'effluent ou de conductivité hydraulique [MOLLE *et al.*, 2004]. On peut cependant remarquer que le vieillissement de ces

[1] Équipe MécaFlu, Laboratoire ICube – UMR 7357 CNRS/Engees/Unistra – 2, rue Boussingault – 67000 Strasbourg. Courriel : paul.bois@icube.unistra.fr

[2] Agence de l'eau Rhin-Meuse – Rue du Ruisseau – Rozérieulles – BP 30019 – 57161 Moulins-lès-Metz.

systèmes n'est pas forcément synonyme de dégradation des performances hydrauliques, comme l'ont remarqué CHAZARENC et MERLIN (2005). Il semble donc nécessaire de procéder à un suivi du vieillissement de ces systèmes, afin de s'assurer de la continuité de leur bon fonctionnement – hydraulique et épuratoire, ces deux aspects étant liés – au cours du temps.

Dans le cadre de cette étude, l'aspect hydraulique du vieillissement en lien avec le colmatage des filtres est étudié. Pour cela, une approche couplant expériences de terrain et de laboratoire a été adoptée : le comportement hydraulique, par l'intermédiaire de mesures de la vitesse d'infiltration [PEDESCOLL *et al.*, 2009], ainsi que la stratification verticale du granulat des quatre plus anciennes stations du bassin Rhin-Meuse ont été évalués sur le terrain. Un curage superficiel des parcelles échantillonnées a été réalisé pour simuler l'effet d'un curage des filtres ; cet effet a été repris en laboratoire lors de tests en éprouvette pour étudier l'évolution des vitesses d'infiltration au sein du massif filtrant. Cette évaluation est suivie par une évaluation en laboratoire de paramètres physico-chimiques et structuraux (teneur en matière organique, porosité, granulométrie) du granulat prélevé dans les filtres, là encore afin d'apporter des éléments d'explications aux résultats hydrauliques obtenus. Ainsi, les objectifs de cette étude sont :

– rendre compte de l'état de vieillissement hydraulique – colmatage – des filtres plantés de roseaux à écoulement vertical (FPRv) équipant des petites communes après 10 ans de fonctionnement ;

– étudier l'impact d'un curage de filtre sur les vitesses d'infiltration relevées sur le terrain ;

– mettre ces résultats en perspective, notamment des caractéristiques de l'effluent d'entrée.

1. Matériel et méthodes

1.1. Choix des sites d'étude

Les quatre stations choisies pour l'étude sont des stations de traitement des eaux usées de type filtres plantés de roseaux à écoulement vertical (FPRv), situées sur le bassin Rhin-Meuse. Elles ont été choisies

	A			B			C			D		
Mise en service	1999			1999			1998			2002		
Débit journalier (m^3/j)	105			150			40			12,5		
Débit de pointe (m^3/h)	14			12,6			5			1,5		
Capacité (EH)	350			500			200			150		
Bassins par étage	3			3			3			3 (1er étage) / 2 (2e étage)		
Surface totale (m^2)	E1	E2		E1	E2		E1	E2		E1	E2	
	668	496		474	518		375	255		190	128	
Lame d'eau (m/j)	0,68			0,67			0,32			0,95		
Porosité granulat (%)	E1F	E2F	E2Dr	E1F	E2F	E2Dr	E1F	E2F	E2Dr	E1F	E2F	E2Dr
	46	48	44	37	40	38	54	69	nd	66	43	56
CU	E2F	E2Dr		E2F	E2Dr		E2F	E2Dr		E2F	E2Dr	
	7,2	9,1		34	6,0		3,9	nd		34	2,6	
d_{10} (mm)	E2F	E2Dr		E2F	E2Dr		E2F	E2Dr		E2F	E2Dr	
	0,14	0,12		0,06	0,17		0,42	nd		0,06	0,36	
Teneur en fines (%)	E2F	E2Dr		E2F	E2Dr		E2F	E2Dr		E2F	E2Dr	
	0,59	0,46		0,39	0,14		0,25	nd		0,21	0,12	

E1 : premier étage ; E2 : second étage ; E1F : horizon filtrant du premier étage ; E2F : horizon filtrant du second étage ; E2Dr : horizon de drainage du second étage ; EH : équivalent-habitant ; CU : coefficient d'uniformité ; d10 : 10 % des grains de la matrice ont un diamètre (en mm) inférieur à la valeur du d10.

Tableau I. Caractérisation des stations étudiées

	A	B	C	D	MOLLE *et al.*, 2004
MES (g/m²/j)	52	49	37	79	50
DCO (g/m²/j)	117	89	83	105	100
DBO_5 (g/m²/j)	45	42	32	53	50
NTK (g/m²/j)	11	11	8	13	10
NH4 (g/m²/j)	8	7	6	9	-
Ptot (g/m²/j)	3	2	2	3	-

MES : matières en suspension ; DCO : demande chimique en oxygène ; DBO_5 : demande biochimique en oxygène ; NTK ; azote total Kjeldahl ; Ptot : phosphore total.
Tableau II. Charges de dimensionnement des stations. Les charges correspondent aux charges d'entrée dans la station

car elles sont les plus âgées en service sur le bassin (> 10 ans) recensées par l'agence de l'eau Rhin-Meuse [AERM, 2013]. Elles sont situées sur les communes d'Erckartswiller (14 ans de fonctionnement, notée A par la suite), Deuxville (14 ans de fonctionnement, notée B par la suite), Nixéville-Blercourt (15 ans de fonctionnement, notée C par la suite) et Saint-Julien-sous-les-Côtes (11 ans de fonctionnement, notée D par la suite). Les caractéristiques de ces stations sont données *tableaux I* et *II*. Toutes ces stations comprennent deux étages de filtration, fonctionnent de manière alternée et intermittente [MOLLE *et al.*, 2004] et ont été plantées de roseaux communs *Phragmites australis* lors de leur mise en œuvre. Les prélèvements ont été réalisés le 28 mai 2013 (A), le 29 mai 2013 (B), le 30 mai 2013 (C) et le 3 juin 2013 (D). Lors de l'étude, les filtres du premier étage de la station D présentaient un phénomène de colmatage total.

1.2. Stratégie de prélèvement

Sur chaque station, les prélèvements et les mesures *in situ* ont été réalisés sur le filtre qui était en phase de repos. Les conventions suivantes ont été adoptées pour la dénomination des échantillons *(figure 1)* :
– selon l'étage : les échantillons réalisés sur le premier étage sont notés E1, ceux réalisés sur le second étage sont notés E2 ;
– selon le point de prélèvement : pour le premier étage, deux types de prélèvement ont été réalisés afin de prendre en compte l'hétérogénéité spatiale du système. Les échantillons situés à 1 m et 2 m de l'alimentation en effluent sont notés respectivement P1 et P2. Pour le second étage, la répartition des rampes d'alimentation homogénéisant l'effluent en surface du filtre a permis de définir un seul point de prélèvement équidistant des rampes pour toutes les stations étudiées ;
– selon l'horizon de prélèvement : les horizons de prélèvement sont référencés comme de « dépôt » D (horizon superficiel composé uniquement de matière accumulée), de « filtration » F (horizon situé immédiatement sous l'horizon précédent et composé d'un mélange de granulats et de matière accumulée) et enfin de « drainage » Dr (uniquement pour le second étage, correspond à l'horizon situé en dessous de l'horizon de filtration).

Ces notations sont récapitulées dans le *tableau III*.

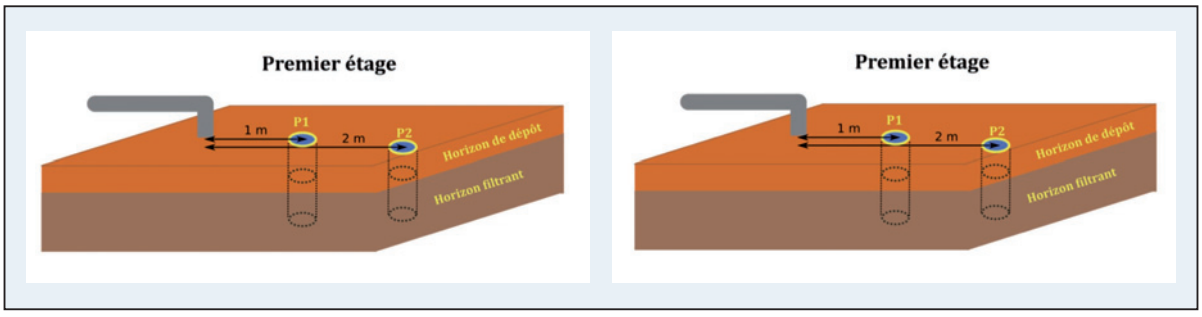

Figure 1. Localisation des points de prélèvement. Quatre échantillons ont été définis sur le premier étage et trois sur le second

	Horizon de dépôt	Horizon filtrant	Horizon de drainage
1er étage	E1P1D, E1P2D	E1P1F, E1P2F	–
2e étage	E2D	E2F	E2Dr

Tableau III. Nomenclature des échantillons

1.3. Vitesse d'infiltration

1.3.1. Mesure *in situ*

L'infiltration cumulée est mesurée à l'aide d'un infiltromètre à double-anneau *(figure 2)*, l'incertitude associée à cette mesure sur le terrain étant de l'ordre de 20 % [BOIVIN, 1990]. La mesure est réalisée en plusieurs étapes selon la norme NF X 30-418 de la façon suivante :

• préparation de l'aire d'essai qui consiste principalement à la coupe au sécateur des végétaux au ras de la surface du filtre de manière à faciliter l'implantation des anneaux sans déstructurer le milieu poreux et le système racinaire en place ;

• mise en place des anneaux concentriques dont l'enfoncement de quelques centimètres dépendra de la résistance du milieu ;

• mise en eau des deux compartiments de l'infiltromètre à la même hauteur d'eau afin que celle-ci s'infiltre à la même vitesse autour et dans l'anneau de mesure. L'écoulement dans l'anneau extérieur va favoriser l'infiltration verticale de l'eau contenue dans l'anneau intérieur en la canalisant. Le flux d'infiltration est alors quantifié par la mesure de la diminution de la hauteur d'eau dans l'anneau interne – lecture de l'échelle apposée sur la face interne *(figure 2)* et chronométrage simultané. On obtient ainsi une courbe donnant l'infiltration d'eau cumulée en fonction du temps ; la vitesse d'infiltration du filtre est ensuite déduite de la partie linéaire de cette courbe. Pour chaque point, deux mesures sont effectuées :

Figure 2. Perméamètre à double-anneau en fonction

– la première réalisée sur le granulat colonisé sans déstructuration du massif (la partie aérienne des plantes ayant été au préalable taillée délicatement à l'aide d'un sécateur). La vitesse d'infiltration mesurée correspond alors à l'hydrodynamique du filtre après 10 ans de fonctionnement ;

– la seconde réalisée au même endroit que la première, mais après curage de la couche de dépôt, correspond à la vitesse d'infiltration du filtre après simple curage du dépôt.

1.3.2. Mesure en laboratoire

500 mL d'échantillons sont placés dans une éprouvette perforée à la base et dont les perforations sont protégées par une géogrille. Le dispositif et la méthode pour le calcul des vitesses d'infiltration sont ceux d'un test de Grant [COOPER *et al.*, 1996]. Trois mesures successives sont effectuées pour chaque échantillon.

1.4. Caractérisation physico-chimique des granulats

1.4.1. Stratification verticale

La densité racinaire sur les différents étages a été évaluée par des critères qualitatifs sur la base des observations de terrain : elle est évaluée comme faible ou forte.

La stratification verticale du filtre a été déterminée consécutivement aux mesures de vitesse d'infiltration en mesurant l'épaisseur des horizons rencontrés. Dans le cas de la station D, le phénomène de colmatage total constaté a entraîné au cours du fonctionnement la formation d'une couche d'effluent densifié non minéralisé, non représentatif d'une accumulation/minéralisation progressive des boues.

Les données de charge d'entrée utilisées pour le dimensionnement *(tableau II)* sont ramenées à l'unité de surface de filtre pour s'affranchir des différences de surface entre stations ; elles sont donc exprimées en g/m^2/j. Les données de charge d'entrée en fonctionnement ont été obtenues sur le système d'information en ligne mis en place par l'agence de l'eau Rhin-Meuse [AERM, 2013] et ont également été exprimées en g/m^2/j ; elles regroupent les données

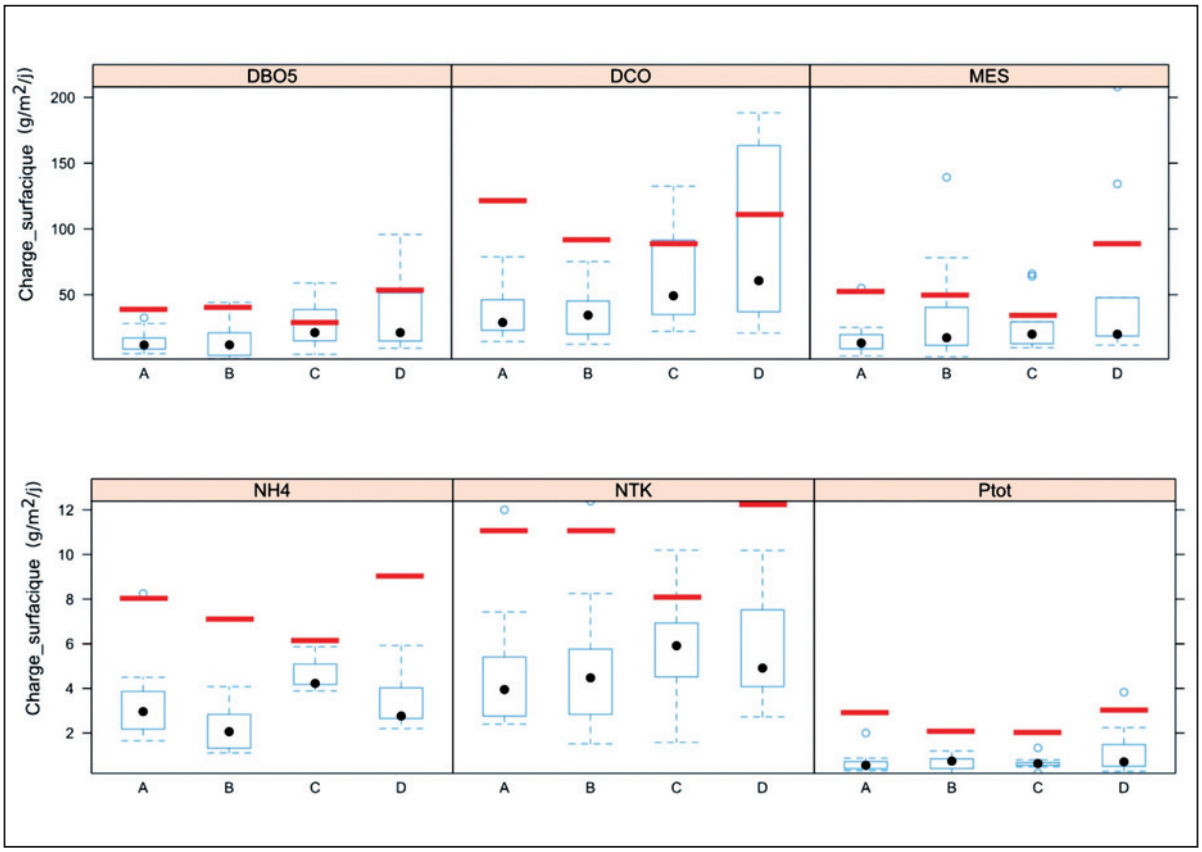

Figure 3. Comparaison entre les charges surfaciques relevées sur le terrain (boîtes à moustaches) et les charges surfaciques utilisées pour le dimensionnement (trait rouge horizontal)

mesurées à l'entrée de chaque station entre 2004 et 2011, à raison d'environ une mesure par an. Elles sont représentées sous forme de boîtes à moustache, ce qui permet de rendre compte de leur variabilité *(figure 3)*. Ces représentations ont été réalisées à l'aide du logiciel R [R CORE TEAM, 2013].

1.4.2. Teneur en matière organique

L'échantillon est séché à 105 °C dans une coupelle jusqu'à obtention d'une masse constante. Trois réplicats sont ensuite pesés (M_0) puis placés à 450 °C pendant 3 heures pour réaliser la combustion des matières volatiles (MV) assimilées à la matière organique. La pesée des réplicats après combustion (M_1) permet de déterminer la quantité de MV par différence. On en déduit finalement la teneur en matières organiques selon la formule suivante :

$$\text{Teneur en matières organiques} = \frac{MV}{M_0} = \frac{M_1 - M_0}{M_0}$$

1.4.3. Porosité et granulométrie

Afin de caractériser le granulat mis en œuvre à la construction d'un point de vue structural, porosité et granulométrie des granulats prélevés sur le terrain ont été mesurées. Pour la porosité, une éprouvette de 1 L de masse connue est pesée après ajout de 200 mL ($V_{apparent}$) d'échantillon séché à 105 °C dans une étuve. Un volume de 200 mL d'eau est alors ajouté, ce qui donne le volume $V_{initial\ éch+eau}$; le volume de l'ensemble est mesuré une fois celui-ci stabilisé, ce qui donne le volume $V_{final\ éch+eau}$. La porosité du granulat prélevé sur le terrain est alors déterminée par différence :

$$\text{Porosité} = \frac{V_{initial\ éch+eau} - V_{final\ éch+eau}}{V_{apparent\ échantillon}}$$

La détermination de la distribution de la taille des granulats constituant les échantillons lavés est réalisée par un granulomètre mécanique selon la norme NF EN 933-1. Les valeurs de ces paramètres figurent dans le *tableau I*.

1.5. Récapitulatif

Les analyses réalisées et les échantillons analysés sont récapitulés dans le *tableau IV*.

2. Résultats et discussion

2.1. Hydrodynamique des filtres

2.1.1. Impact d'un curage simulé sur la vitesse d'infiltration (terrain)

Sur le premier étage, on observe tout d'abord des différences de vitesses d'infiltration variables en fonction des sites *(figure 4)* : sur la station A, V_{inf} = 0,0060 ± 0,0010 mm/s ; sur la station B, V_{inf} = 0,75 ± 0,15 mm/s ; sur la station C, V_{inf} = 0,034 ± 0,015 mm/s ; sur la station D, V_{inf} = 0,0085 ± 0,0065 mm/s. Pour les stations A, C et D, ces vitesses sont d'un ordre de grandeur comparable à la conductivité hydraulique à saturation mesurée sur un filtre vertical âgé de 9 ans (0,0042 mm/s) par MORVANNOU et coll. [2013]. La vitesse d'infiltration bien plus élevée obtenue pour la station B peut s'expliquer par l'accumulation de boues plus faible constatée sur cette station.

	Mesure		Horizon		
	Sur le terrain	En laboratoire	Dépôt	Filtration	Drainage
Vitesse d'infiltration (I)	✓		✓	✓	
Vitesse d'infiltration (II)		✓		✓ (lavé)	✓ (lavé)
Stratification verticale	✓		✓	✓	✓
Teneur en matières organiques		✓	✓	✓	✓
Porosité		✓		✓	✓
Granulométrie		✓		✓	✓

Tableau IV. Récapitulatif des analyses. Le protocole de chaque analyse est détaillé dans la partie « matériel et méthodes »

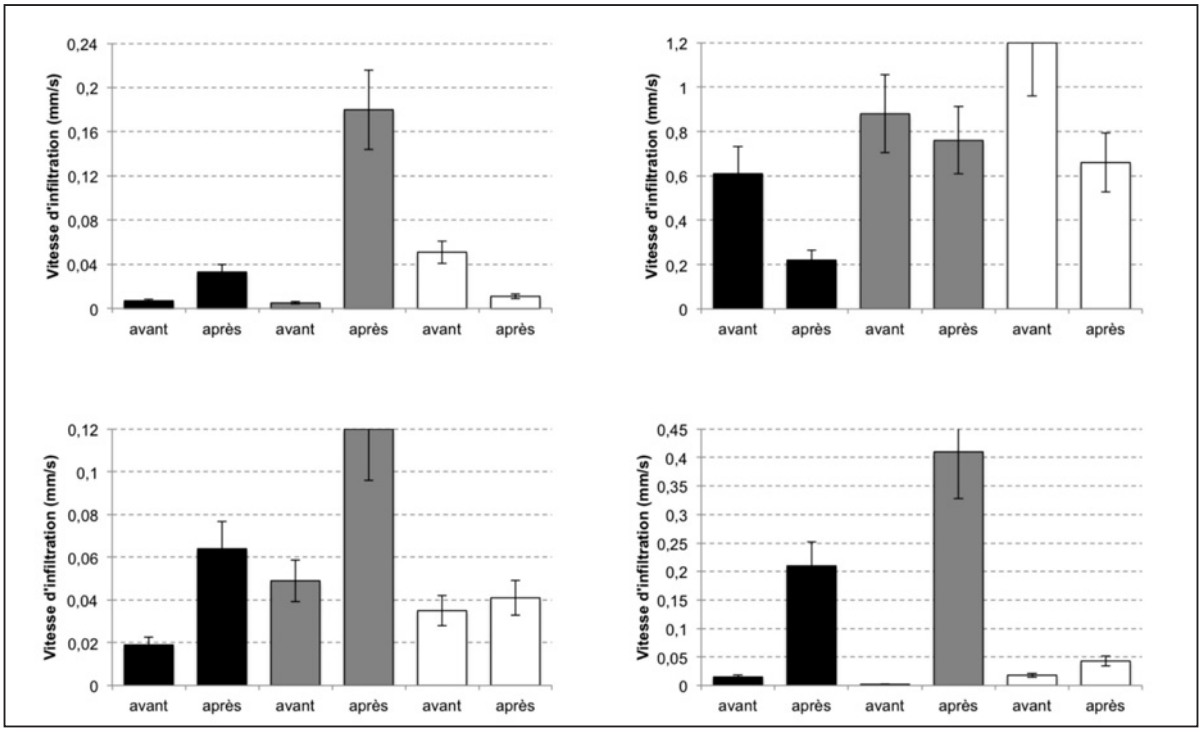

Figure 4. Évolution des vitesses d'infiltration sur le terrain. De gauche à droite et de haut en bas : A, B, C, D. Noir : E1P1 ; gris : E1P2 ; blanc : E2. Les barres d'erreur représentent la variabilité associée aux mesures d'infiltration par infiltromètre double-anneau sur le terrain. La notation « avant » correspond à la vitesse d'infiltration du filtre après 10 ans de fonctionnement. La notation « après » correspond à la vitesse d'infiltration du filtre après curage des boues

Sur le second étage, on observe des vitesses d'infiltration plus élevées que sur le premier étage, probablement en raison de l'accumulation moins forte de boues. Ainsi on relève : sur la station A, V_{inf} = 0,05 mm/s ; sur la station B, V_{inf} = 1,2 mm/s ; sur la station C, V_{inf} = 0,035 mm/s ; sur la station D, V_{inf} = 0,018 mm/s. Cette tendance est inverse à celle recherchée initialement, c'est-à-dire un temps d'infiltration plus élevé (et donc une vitesse d'infiltration plus faible) sur le second étage que sur le premier. Ces valeurs sont inférieures à celle de conductivité hydraulique à saturation (1,5 mm/s) trouvée par MORVANNOU et coll. [2013] sur cet étage, sauf pour la station B dont l'accumulation est moins élevée (cf. paragraphe précédent). Cela peut s'expliquer par le fait que les filtres étudiés sont plus âgés, entre 11 et 15 ans, contre 9 ans pour le filtre étudié dans ces travaux.

Le colmatage est donc plus important sur le premier étage, ce qui entraîne une vitesse d'infiltration plus faible que sur le second étage en dépit de la granulométrie plus grossière et de la vitesse d'infiltration initiale plus élevée sur le premier étage.

Lorsque l'on procède au curage de la boue, on observe sur le premier étage un effet similaire sur les deux points de mesure (*figure 4*) : amélioration significative pour les stations A ($V_{curé}/V_{init}$ = 4,7 pour P1 et $V_{curé}/V_{init}$ = 36 pour P2), C ($V_{curé}/V_{init}$ = 3,4 pour P1 et $V_{curé}/V_{init}$ = 2,4 pour P2) et D ($V_{curé}/V_{init}$ = 14 pour P1 et $V_{curé}/V_{init}$ = 205 pour P2) et évolution non significative (due à la variabilité associée aux mesures par infiltromètre double-anneau, rapportée par BOIVIN [1990]) pour la station B. On remarque que l'amélioration la plus forte est logiquement constatée sur la station D, qui présentait un colmatage total lors de l'étude. Sur le second étage, l'effet est moins marqué : amélioration pour les stations C ($V_{curé}/V_{init}$ = 1,2) et D ($V_{curé}/V_{init}$ = 8,3), diminution pour les stations A ($V_{curé}/V_{init}$ v = 0,55) et B ($V_{curé}/V_{init}$ = 0,21). Cette atténuation de l'effet du curage est à relier à l'accumulation de matière plus faible sur le second étage que sur le premier, et à une modification consécutivement plus faible de la perméabilité de l'ensemble. On remarque également que le curage a pour effet de rétablir une vitesse d'infiltration plus élevée sur le premier étage que sur le second.

Ces modifications de vitesse d'infiltration à la suite de la présence de solides accumulés ont déjà été reportées dans la littérature pour des filtres contenant des granulats de taille similaire à celle des filtres étudiés, dans le sens d'une amélioration ou d'une dégradation ; ainsi l'étude de KNOWLES et DAVIES [2009] a relevé une diminution de la conductivité hydraulique concomitante à une accumulation de solides alors que CHAZARENC et MERLIN [2005] ont observé une amélioration de la percolation d'un facteur 5. Les résultats de la présente étude tendent, eux, à montrer que l'opération de curage semble diminuer de manière significative le colmatage superficiel lié au dépôt de surface et en conséquence améliore les capacités d'infiltration des filtres du premier étage des FPR. Du point de vue opérationnel, cela permettrait ainsi d'envisager une dissociation du curage de l'horizon de dépôt et du remplacement du granulat, pour permettre de restaurer la capacité hydraulique du filtre.

2.1.2. Vitesse d'infiltration du granulat lavé (laboratoire)

Les vitesses d'infiltration des granulats lavés sont bien plus élevées en moyenne que celles des granulats curés sur le terrain (*figure 5*). Cela provient probablement du protocole expérimental différent qui a été employé, mais également du fait que le curage sans remplacement de l'horizon profond simulé sur le terrain ne joue pas sur le colmatage lié à la croissance de la biomasse sur le support granulaire. On constate également que la vitesse d'infiltration du granulat du

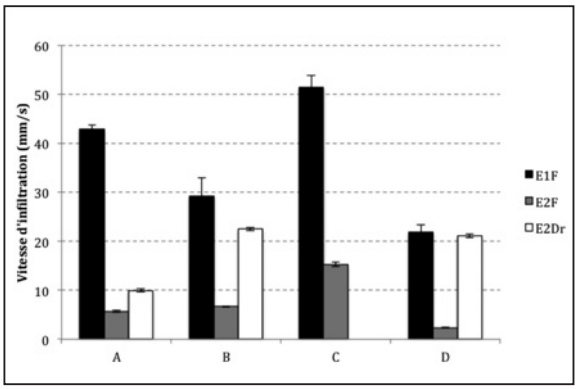

Figure 5. Vitesses d'infiltration du substrat lavé (tests en laboratoire)

premier étage est significativement plus importante que celle du granulat du second étage, ce qui est cohérent avec les tailles des granulats mis en œuvre (gravier pour le premier étage, sable pour le second) et à relier aux fonctions prévues pour ces deux étages (filtration des matières en suspension MES pour le premier, lente filtration pour permettre la nitrification pour le second).

2.1.3. Comparaison curage superficiel/remplacement du granulat

Au-delà de la nécessaire évacuation de la boue accumulée, le curage superficiel permet donc une amélioration significative de la vitesse d'infiltration dans les filtres, qui n'est toutefois pas équivalente à l'amélioration obtenue par le remplacement total du granulat de la couche filtrante. Ainsi, le *tableau V* quantifie les évolutions obtenues : dans 13 cas sur 16, le curage ou le remplacement du granulat améliorent la vitesse d'infiltration. Le curage permet un gain de l'ordre d'un facteur 10, le remplacement permettant lui un gain de l'ordre d'un facteur 100.

2.2. Caractérisation du dépôt

2.2.1. Stratification verticale

De façon globale, la densité racinaire est plus importante sur le premier étage du filtre que sur le second (*figures 6* et *7*), probablement en raison de la plus grande quantité de substrat disponible sur le premier étage. On constate une densité racinaire nettement plus importante sur le premier étage des stations A, C et D que sur celui de la station B. Ces différences de densité racinaire constatées au niveau du premier étage entre stations peuvent provenir de la prédominance des espèces végétales : les roseaux prédominaient sur les stations A (*figure 8*), C et D tandis que les orties prédominaient sur la station B (*figure 9*). Après discussion avec les exploitants des sites étudiés, il apparaît que cette répartition dépend fortement des pratiques d'exploitation, notamment de l'entretien des plantations au sein des filtres, surtout pendant les premiers mois d'exploitation.

Figure 6. Coupe de l'horizon de dépôt sur le 1er étage du filtre (site A)

Figure 7. Coupe de l'horizon de dépôt sur le 2e étage du filtre (site A)

V_{inf}/V_{inf_10}	E1		E2	
	Curé	Lavé	Curé	Lavé
A	18,0	397,4	0,2	518,4
B	0,7	59,2	0,5	10,1
C	2,6	673,3	1,2	372,4
D	36,6	70,3	2,4	55,1

Tableau V. Rapport des vitesses d'infiltration après maintenance sur la vitesse d'infiltration (Vinf) après 10 ans de fonctionnement. E1 : premier étage du filtre ; E2 : second étage du filtre

Figure 8. Premier étage de filtres plantés de roseaux (site A)

Figure 9. Premier étage de filtres plantés de roseaux (site B)

Avant d'analyser l'accumulation de matière observée sur les stations, il convient de vérifier les paramètres de dimensionnement des filtres. Tout d'abord, la surface de premier étage par équivalent-habitant (EH) est égale à 1,34 m^2/EH (A), 1,35 m^2/EH (B), 1,88 m^2/EH (C) et 1,27 m^2/EH (D). La règle de dimensionnement en France préconise une surface comprise entre 1,2 et 1,3 m^2/EH [BOUTIN *et al.*, 1997]. Seule la station C présente un surdimensionnement de l'ordre de 45 %. Les trois autres stations étudiées sont donc correctement dimensionnées. En ce qui concerne l'adéquation des charges de fonctionnement réelles avec les charges de fonctionnement utilisées pour le dimensionnement, les charges réelles sont quasiment toutes inférieures aux charges nominales, voire similaires dans le cas de la demande chimique en oxygène (DCO) pour la station D *(figure 3)*. Les stations étudiées fonctionnent donc à une capacité inférieure à la charge nominale.

Les épaisseurs des différents horizons sont présentées dans la *figure 10*. On observe une accumulation de boues variable entre les stations étudiées, aussi bien au niveau du premier que du second étage. L'accumulation la plus élevée est observée sur la station A (22,5 cm) et la moins élevée sur la station B (10 cm). On observe également une hétérogénéité d'accumulation au sein du premier étage pour les stations A et C, malgré la présence de plaques de béton au droit des points d'alimentation destinées à limiter l'affouillement et à favoriser la distribution de l'effluent [KNOWLES *et al.*, 2011] en surface des filtres. Sur le premier étage, l'horizon de dépôt atteint en moyenne 22,5 cm pour la station A, 10 cm pour la station B et 17,5 cm pour la station C. Pour le second étage, on observe une forte accumulation de boues (20 cm) sur la station A, alors que l'on observe une accumulation beaucoup plus faible, comprise entre 1 et 5 cm et inférieure à celle des premiers étages respectifs, pour les autres stations. Cela semble cohérent, la charge des effluents diminuant après le premier étage de traitement (86 % d'abattement en MES, 79 % en DCO d'après MOLLE et coll. [2004]. Pour toutes les stations, l'épaisseur de la couche de filtration (F) était supérieure à 50 cm sur les deux étages de filtre.

Les valeurs obtenues peuvent être comparées aux valeurs données dans l'étude de MOLLE et coll. [2004]. Les auteurs y indiquent un taux d'accumulation de 1,5 cm de boues par an sur un filtre de premier étage, pour une charge de fonctionnement analogue à celles des stations étudiées *(tableau II)*. Les valeurs relevées sont similaires pour la station A avec 22,5 cm relevés (soit 1,6 cm/an) contre 21 cm potentiels et, pour la station C, avec 17,5 cm relevés (soit 1,2 cm/an) contre 22,5 cm potentiels, mais

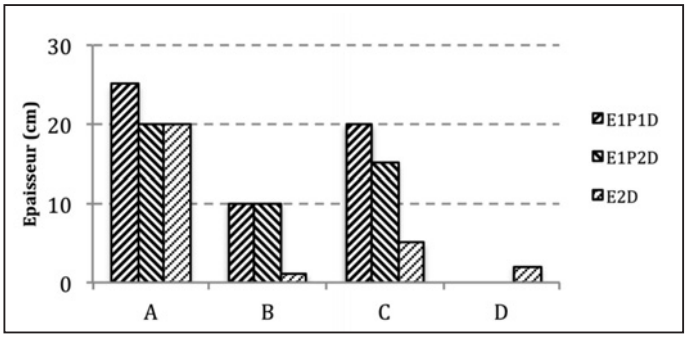

E1P1D : horizon de dépôt du premier étage, premier point de prélèvement ; E1P2D : horizon de dépôt du premier étage, second point de prélèvement ; E2D : horizon de dépôt du second étage.

Figure 10. Épaisseur des horizons. L'absence de barre indique une absence de valeur

peuvent également différer fortement dans le cas de B avec 10 cm relevés (soit 0,7 cm/an) pour 21 cm potentiels. La différence relevée dans le cas de la station B pourrait s'expliquer par la présence importante d'eaux claires parasites sur le site. Celles-ci, estimées à 222 % des eaux usées, entraînent une surcharge hydraulique et le déversement fréquent d'effluent par le by-pass. Enfin, ce calcul ne peut pas s'appliquer à la station D en raison du récent remplacement du support granulaire dont elle a fait l'objet.

2.2.2. Teneur en matière organique

La teneur en matière organique est peu variable entre les points E1P1D et E1P2D d'une part, et entre les points E1P1M et E1P2M d'autre part ; les valeurs moyennes de chaque horizon sur le premier étage sont donc présentées. On observe de manière globale *(figure 11)* que les horizons échantillonnés présentent une faible teneur en matière organique, comprise entre 0,45 % et 20 %, excepté pour l'horizon de dépôt de la station C (40 %). Ces valeurs sont cohérentes avec celles données par des études précédentes faisant état d'une teneur en matière organique comprise entre 3 et 20 % [CASELLES-OSORIO *et al.*, 2007 ; KNOWLES *et al.*, 2011] pour ce type d'échantillon. Cette faible teneur en matière organique sur les FPR provient de la minéralisation de la matière organique au sein de ces filières de traitement. La forte teneur en matière organique, observée pour la station C, pourrait provenir de la présence sur cette station d'un ouvrage de dessablage en tête (contrairement aux autres stations de l'étude), ce qui réduit la part de matière minérale entrant dans la station et augmente ainsi relativement la part organique de l'effluent entrant. En résumé, en calculant la moyenne des valeurs obtenues sur les quatre stations, on obtient les résultats suivants : sur le premier étage de ce type de filière, la teneur en matière organique de l'horizon de dépôt est d'environ 18 % (17,6 ± 9,8 %), celle de l'horizon de filtration est d'environ 2 % (1,9 ± 0,5 %). Le dépôt d'eau usée se faisant sur l'horizon superficiel, il est normal que ce dernier soit le plus riche en matière organique. Sur le second étage, la teneur en matière organique de l'horizon de dépôt est d'environ 11 % (10,9 ± 3,8 %), celle de l'horizon de filtration est d'environ 2 % (1,8 ± 0,5 %) et celle de

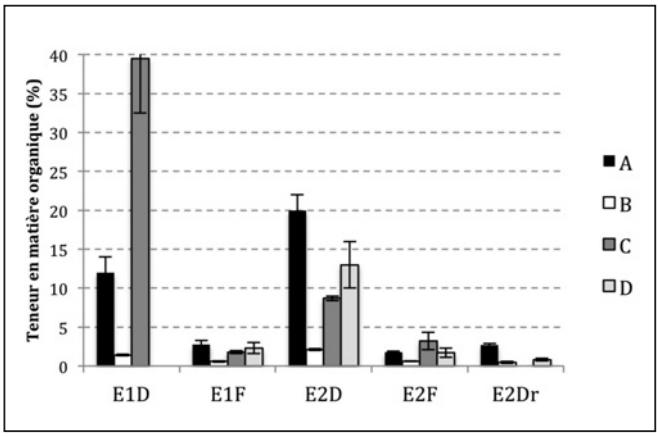

E1D : horizon de dépôt du premier étage ; E1F : horizon de filtration du premier étage ; E2D : horizon de dépôt du second étage ; E2F : horizon de filtration du second étage ; E2Dr : horizon de drainage du second étage.

Figure 11. Teneur en matière organique des échantillons de terrain

l'horizon de drainage est d'environ 1,3 % (1,3 ± 0,6 %). Là encore l'horizon sur lequel se fait le dépôt est le plus riche en matière organique. La décroissance de teneur en matière organique entre les horizons superficiels et les horizons filtrants/de drainage ainsi calculée est confirmée par les observations visuelles de terrain.

2.3. Effet des différents paramètres externes

On a vu que les charges de dimensionnement utilisées sont proches des valeurs de fonctionnement pour toutes les stations et que la surface allouée par EH n'explique pas les variations obtenues. Il est donc plus probable que les différences observées au niveau de l'accumulation de boues, du colmatage des filtres ou des plantes présentes proviennent de différences d'exploitation ou d'incidents de fonctionnement/exploitation au cours de la vie de la station. Cela est notamment le cas pour la station D pour laquelle la granulométrie est faible comparée aux recommandations, ce qui a entraîné le phénomène de colmatage. Ou encore pour la station B, où une surcharge hydraulique avérée entraîne un déversement anormalement fréquent de l'effluent par le by-pass.

Enfin, l'état des différents FPR au moment de l'étude dépend notamment fortement de la maintenance réalisée sur ces stations et des conditions météorologiques récentes. L'évaluation précise de la situation nécessiterait donc un suivi plus régulier sur le long terme.

Conclusion

Quatre stations de traitement des eaux usées de type FPRv fonctionnant selon un mode opératoire français ont été étudiées afin d'évaluer le vieillissement de ce type d'ouvrages après plus de 10 années de fonctionnement. Les charges surfaciques entrantes relevées en fonctionnement [AERM, 2013] montrent que ces stations fonctionnent à un niveau de charge cohérent avec celui utilisé pour le dimensionnement, ce qui laisserait supposer *a priori* d'une évolution classique pour ces stations.

L'accumulation constatée sur les stations étudiées confirme dans certains cas (sites A et C) le taux d'accumulation de 1,5 cm/an relevé par MOLLE et coll. [2004]. De même, la teneur en matière organique du granulat accumulé en surface des filtres varie entre 0,45 % et 20 %, en raison de la minéralisation de la matière organique et de la rémanence de la matière minérale au cours du fonctionnement de la station. La présence d'un ouvrage de traitement primaire de type dessableur fait cependant varier cette teneur de manière significative pour atteindre 40 % (station C). Les tests de curage effectués sur le terrain ont mis en évidence une amélioration significative de la vitesse d'infiltration, sans toutefois parvenir à retrouver la vitesse d'infiltration initiale évaluée lors de tests en laboratoire. Dans le cadre d'un entretien courant, il peut donc être suffisant de retirer la couche superficielle sans toucher au granulat pour retrouver une vitesse d'infiltration compatible avec un bon fonctionnement hydraulique du filtre. Les différences de colmatage observées entre les différents sites d'étude semblent être principalement liées à des différences de maintenance ou d'exploitation.

Remerciements

Les auteurs remercient Marie-Pierre Ottermatte pour son aide, les exploitants des stations étudiées pour leur collaboration et l'agence de l'eau Rhin-Meuse pour le financement de cette étude.

Bibliographie

AERM (2013) : « Service d'Information sur l'Eau Rhin-Meuse ». http://rhin-meuse.eaufrance.fr, 2013, consultation le 20 février 2014.

BOIVIN P. (1990) : « Caractérisation de l'infiltrabilité d'un sol par la méthode Muntz : variabilité de la mesure ». *Bulletin - Réseau Erosion ;* 10 : 14-24.

BOUTIN C., LIENARD A. et ESSER D. (1997) : « Development of a new generation of reed-bed filters in France: First results ». *Water Science and Technology ;* 35(5) : 315-322.

CASELLES-OSORIO A., PUIGAGUT J., SEGU E., VAELLO N., GRANES F., GARCIA D., GARCIA J. (2007) : « Solids accumulation in six full-scale subsurface flow constructed wetlands ». *Water Research ;* 41 : 1388-1398.

CHAZARENC F., MERLIN G. (2005) : « Influence of surface layer on hydrology and biology of gravel bed vertical flow constructed wetlands ». *Water Science and Technology ;* 51(9) : 91-97.

COOPER P.F., JOB G.D., GREEN M.B., SHUTES R.B.E. (1996) : *Reed beds and constructed wetlands for wastewater treatment.* WRc plc, Swindon, 1996, 184 p.

KADLEC R. H., WALLACE S. (2009) : *Treatment wetlands,* 2nd edition. Londres, New York : CRC Press, 1016 p.

KNOWLES P., DAVIES P.A. (2009) : « A method for the in-situ determination of the hydraulic conductivity of gravels as used in constructed wetlands for wastewater treatment ». *Desalination and Water Treatment ;* 5 : 257-266.

KNOWLES P., DOTRO G., NIVALA J., GARCIA J. (2011) : « Clogging in subsurface-flow treatment wetlands : Occurrence and contributing factors ». *Ecological Engineering ;* 37 : 99-112.

MOLLE P., LIENARD A., BOUTIN C., MERLIN G., IWEMA A. (2004) : « Traitement des eaux usées domestiques par marais artificiels : état de l'art et performances des filtres plantés de roseaux en France ». *Ingénieries ;* n° spécial : 23-32.

MORVANNOU A., FORQUET N., VANCLOOSTER M., MOLLE P. (2013) : « Characterizing hydraulic properties of filter material of a vertical flow constructed wetland ». *Ecological Engineering ;* 60 : 325-335.

PEDESCOLL A., UGGETTI E., LLORENS E., GRANES F., GARCIA D., GARCIA J. (2009) : « Practical method based on saturated hydraulic conductivity used to assess clogging in subsurface flow constructed wetlands ». *Ecological Engineering ;* 35 : 1216-1224.

PLATZER C., MAUCH K. : (1997) « Soil clogging in vertical flow reed beds - mechanisms, parameters, consequences and ... solutions? » *Water Science and Technology ;* 35(5) : 175-181.

R CORE TEAM (2013) : *R: A Language and Environment for Statistical Computing*.

VYMAZAL J. (2002) : « The use of sub-surface constructed wetlands for wastewater treatment in the Czech Republic: 10 years experience ». *Ecological Engineering ;* 18 : 633-646.

Résumé

P. BOIS, J. LAURENT, M. NUEL, A. WANKO

Indicateurs de colmatage de filtres plantés de roseaux à écoulement vertical : étude comparative de quatre stations de traitement après 10 ans de fonctionnement

L'effet du vieillissement sur le colmatage de quatre stations de traitement de type filtre planté de roseaux a été étudié sur le terrain et en laboratoire. Il ressort de l'étude qu'un curage de la boue déposée permet d'améliorer la vitesse d'infiltration sur le premier étage (trois cas sur quatre) et parfois sur le second étage (deux cas sur quatre). Le renouvellement du granulat permet lui une augmentation de la vitesse d'infiltration d'un facteur 100 environ. Les taux d'accumulation de boue relevés varient entre 0,7 et 1,6 cm/an sur le premier étage des filtres. La teneur en matière organique du dépôt varie entre 0,45 % et 20 % en fonction de la présence d'ouvrages de traitement primaire en amont de la station. Les différences de colmatage observées entre les différents sites d'étude semblent être principalement liées à des différences de maintenance ou d'exploitation. L'utilisation d'un infiltromètre double-anneau pourrait permettre de s'assurer du bon fonctionnement hydraulique du système et de planifier les opérations de curage des filtres.

Abstract

P. BOIS, J. LAURENT, M. NUEL, A. WANKO

Vertical flow reed bed filter aging indicators: comparative study of four constructed wetlands after ten years of operation

A study on the effect of ageing on 4 constructed wetlands designed for wastewater treatment is carried out on the field and in the laboratory. Sludge removal allows improving infiltration speed on the first (3 out of 4 sites) and sometimes on the second stage (2 out of 4 sites) of the station. Granular medium renewal enables a 100-fold infiltration speed increase. Sludge accumulation rate ranges between 0.7 and 1.6 cm/yr on the first stage. Deposit organic matter content ranges between 0.45% and 20%, depending on the presence of primary treatment systems before the plant. Clogging differences that are observed seem to be mainly due to maintenance and operation. Double-ring infiltrometer could be used as a tool to monitor hydraulic functioning of the system and to help planning removal sequences on the filters.

esa ECOSPHERE

Confirming a plant-mediated "Biological Tide" in an aridland constructed treatment wetland

Paul Bois,[1,2] Daniel L. Childers,[3,]† Thomas Corlouer,[2] Julien Laurent,[1,2] Antoine Massicot,[2] Christopher A. Sanchez,[3] and Adrien Wanko[1,2]

[1]*ICube (UMR 7357 ENGEES/CNRS/Unistra), 2 rue Boussingault, 67000 Strasbourg, France*
[2]*LTSER France, Zone Atelier Environnementale Urbaine, 3 Rue de l'Argonne, 67000 Strasbourg, France*
[3]*School of Sustainability, Arizona State University, Tempe, Arizona 85287 USA*

Citation: Bois, P., D. L. Childers, T. Corlouer, J. Laurent, A. Massicot, C. A. Sanchez, and A. Wanko. 2017. Confirming a plant-mediated "Biological Tide" in an aridland constructed treatment wetland. Ecosphere 8(3):e01756. 10.1002/ecs2.1756

Abstract. As urban populations grow and the need for sustainable water treatment increases, urban constructed treatment wetlands (CTWs) are increasingly being used and studied. However, less is known about the effectiveness of this "turquoise infrastructure" in arid climates. In a recent publication, we presented evidence of plant-mediated control of surface hydrology, using a water budget approach, in a CTW in Phoenix, Arizona, USA. We also demonstrated how this transpiration-driven wetland surface flow made this treatment marsh more effective at pollutant removal than its counterparts in cooler or more mesic environments. Water budget-based calculations estimated that nearly 20% of the water overlying the marsh was transpired daily by the plants (40–60 $L \cdot m^{-2} \cdot d^{-1}$) during the hottest summer months. We estimated the associated water velocity to be about 40 cm/h. In this paper, we report on hydrodynamic experiments that confirmed the existence of this phenomenon that we refer to as the "Biological Tide," and verified the rate at which transpiration by the marsh vegetation moves surface water into the biogeochemically active marsh. We combined a water budget-based approach and dye tracer experiments to quantify and confirm this phenomenon. Because of the low velocities estimated from our water budget approach (a few cm/h), we used a fixed-wall flowthrough marsh flume to limit the lateral dye movement during the tracer experiments. We measured actual flow rates of 7–50 cm/h (with 5–8% precision) during these experiments, which closely conformed to the values estimated from our water budget-based approaches. The flow was largely dispersive due to the extensive impedance imparted by dense plant stems in the marsh. From these summer flow rates, we calculated that residence time of the water overlying the marsh in this CTW averaged about 13 d, but could be as low as four days. Again, these values were reasonably close to the 15–20% replacement rate for marsh water we estimated using the water budget approach. This is the first time, to our knowledge, that plant-mediated biological control of surface hydrology in a wetland, without connection to groundwater, has been reported.

Key words: constructed treatment wetland; dye tracer experiment; ecological engineering; transpiration; urban sustainability; wastewater treatment.

Received 14 December 2016; revised 13 February 2017; accepted 13 February 2017. Corresponding Editor: Ryan A. Sponseller.

† **E-mail:** Dan.childers@asu.edu

Introduction

Humans are becoming an increasingly urban species: Since 1900 the proportion of people living in cities has increased from 10% to over 50% globally, and will likely be 80% by 2050 (Grimm et al. 2008). In the last 100 yr, many cities have transformed into "sanitary cities," with highly centralized, capitalized, and expensive infrastructure designed to keep inhabitants healthy (Melosi 2000, Grove 2009). Often this infrastructure has imparted large systemic inertias on cities that hinder novel or transformative new solutions to growing problems (Childers et al. 2014). Still, there are many ways to design urban infrastructure so as to optimize key ecosystem services by using "design with nature" approaches that make cities more resilient and sustainable (Pickett et al. 2013). When these urban designs incorporate terrestrial ecological features, they are typically called "green infrastructure," while "blue infrastructure" refers to aquatic systems. One example of "designing with nature" is the increasing use of constructed treatment wetlands (CTWs) as part of urban wastewater treatment in place of expensive and energy-intensive treatment technologies. Wetlands have both terrestrial and aquatic ecological characteristics, and because of the color that results when green and blue are mixed, we refer to such urban wetlands as "turquoise infrastructure" (Childers et al. 2015).

Constructed treatment wetlands are a relatively low cost and low maintenance solution to urban wastewater and water reclamation challenges (Wallace and Knight 2006, Nivala et al. 2013). Most CTWs are designed to "polish" partially treated municipal effluent with a mix of open water areas, macrophytic vegetation, and waterlogged soils (Fonder and Headley 2013). Designs are often highly dependent on local or regional variables, including water quality regulations and site-specific conditions (Fonder and Headley 2010, Tanner et al. 2012), and rely on different flow types (subsurface [SSF] vs. free water surface [FWS] flow). While CTWs may be relatively similar in design and expectations, particular attention must be paid to the way these systems function in different climatic settings.

Arid environments make up more than 30% of the earth's land surface, and cities in these regions increasingly face water scarcity issues. To address these issues, many are turning to the reuse of treated municipal effluent for various urban uses (Greenway 2005), but the challenge is that reclaimed water used in densely populated areas must be clean. Notably, in the aridland city of Phoenix, Arizona, USA—where we conducted the research reported here—virtually all municipal effluent is reused (Metson et al. 2012), and the only real export of water from the city is to the atmosphere. Constructed treatment wetlands are a viable "design with nature" solution, but building these wetlands in hot, arid cities such as Phoenix may expose them to unique challenges associated with large losses of water via evaporation and plant transpiration. With this in mind, since summer 2011 we have been quantifying these water fluxes in a CTW operated by the City of Phoenix Water Services Department while also measuring wetland plant biomass and estimating the whole-system water and nutrient budgets (Sanchez et al. 2016, Weller et al. 2016). Our objective has been to understand the effect of atmospheric water losses on the whole-system water budget and on the ability of this CTW to remove nitrogen from wastewater effluent. We found large losses of water from the emergent marshes via plant transpiration during the hot, dry summer months—as much as 20–25% of the water overlying the vegetated marsh daily—and we identified a horizontal advection of surface water from nearby open water areas as the only way to replace this transpired water. We call this phenomenon a "biological tide" (hereafter Biological Tide; Sanchez et al. 2016), which is a different phenomenon from evapotranspiration-driven movements of shallow groundwater (White 1932, Bauer et al. 2004, McLaughlin and Cohen 2014). Transpiration-driven movement of shallow SSF water has been documented in a number of wetlands, including with tree islands in the Okavango Delta in Botswana (Bauer-Gottwein et al. 2007, Ramberg and Wolski 2008) and in the Florida Everglades (Bazante et al. 2006, Troxler-Gann and Childers 2006, Sullivan et al. 2014). However, to our knowledge, this is the first time that biotic control of surface hydrology has been demonstrated in any wetland. In this paper, we present data from two different approaches that independently corroborated this plant-driven movement of water into a CTW marsh, verifying that this unique, never-before-described phenomenon exists.

Furthermore, this plant-mediated Biological Tide is actually increasing the nutrient removal efficacy of the CTW we studied: The vegetated marsh consistently removed virtually all of the inorganic nitrogen (N) made available to it, despite high rates of transpirational water loss (Sanchez et al. 2016). By bringing additional water and solutes into the vegetated marsh and its soils, from adjacent open water areas, the Biological Tide actually enhanced the ability of the marsh to remove N relative to CTWs found in cooler or more mesic settings (Sanchez et al. 2016).

The objective of this work was to measure actual surface water flow within the marsh and to compare these flow rates to those estimated using our transpiration-based water budget calculations. Often water flow measurement experiments conducted in wetlands include the entire system or flow rates on the order of cm/s (Leonard and Luther 1995, Leonard and Croft 2006). In this case, though, the spatial scale of our experiment was small and the magnitude of expected velocities was very low—a few cm/h. These challenges required a different methodological approach. One of the easiest ways to measure water velocities is with a flowmeter, but this technique will not work at low flow velocities (~0.4 cm/s) because of inappropriate detection limits. Doppler velocimetry is an alternative, but Doppler flowmeters typically require a minimum water depth on the order of 0.25–0.5 m (Meselhe et al. 2004), and the water overlying vegetated wetlands is often shallower than this. Plant stems also interfere with the propagation of the acoustic signal, making Doppler results from vegetated wetlands difficult to obtain or analyze. In our CTW study site, water depths in the vegetated marsh averaged roughly 0.25 m, plant densities and productivity were high (Weller et al. 2016), and by our estimates, the Biological Tide flowed at only a few cm/h. Therefore, the only viable technique for documenting this flow was a tracer experiment.

The application of tracer studies to wetlands is not new (Bowmer 1987). Such tracer experiments have been used to calibrate hydrodynamic models of secondary and tertiary treatment wetlands (Giraldi et al. 2009, Laurent et al. 2015), to study on the effects of vegetation on flow dynamics (Bodin et al. 2012), to study internal wetland flows (Williams and Nelson 2011), and to examine the influence of water flow on CTW capacity (Worman and Kronnas 2005). Measuring water flow with tracers generally involves either direct water sampling or image recording. Either approach is relatively straightforward, and both are adapted to the low velocities that characterize vegetated environments (Meselhe et al. 2004). These very low flow rates create another complication, though: Lateral dispersion of the tracer may exceed directional advective–dispersive flow, decreasing our ability to longitudinally detect the tracer signal. To overcome this challenge, we added to our experimental design a fixed-wall flowthrough marsh flume to contain the dye tracking the Biological Tide flow within the vegetated marsh (for flume details, see Childers and Day 1988, 1990*a*, *b*, Childers 1994, Bouma et al. 2007, Harvey et al. 2011, Chang et al. 2015).

Methods

Site description

This work was conducted at a CTW associated with the largest wastewater treatment plant in Phoenix, Arizona, United States. We have focused our work on a 42-ha wetland that is part of this CTW, half of which is fringing vegetated marsh and half of which is mostly open water with several small upland islands (Fig. 1). The CTW is bounded by levee roads; it received from 95,000 to over 270,000 m^3/d of effluent, depending on the time of year. Water depths in the fringing marshes were consistently about 25 cm, while open water depths were 1.5–2 m; these depths did not vary because of the way water was managed in the system. The marshes were vegetated by seven emergent wetland species that are native to Arizona: *Typha latifolia, Typha domingensis, Schoenoplectus acutus, Schoenoplectus americanus*, *Schoenoplectus californicus, Schoenoplectus maritimus,* and *Schoenoplectus tabernaemontani* (Weller et al. 2016).

Plant transpiration measurements

We measured plant transpiration on a bimonthly schedule (January, March, May, July, September, and November), beginning in July 2011, using a LI-6400XT handheld infrared gas analyzer (LI-COR, Lincoln, Nebraska, USA). Leaf-level, plant-specific transpiration measurements were taken on individual *T. latifolia, T. domingensis, S. acutus, S. americanus, S. californicus,* and *S. tabernaemontani* plants along 10 transects evenly spaced

Fig. 1. Aerial image of the 42-ha Tres Rios constructed treatment wetland. White lines are the locations of the 10 marsh transects (each 50–60 m long), and blue arrows show the water inflow and outflow points. The star indicates where the July 2015 controlled-flow dye study was conducted.

around the fringing vegetated marsh, as well as along vertical (water surface to plant tip) and temporal (morning to afternoon) gradients (see Weller et al. 2016 for details on the experimental design). We used custom-made foam pads to create an airtight seal on the IRGA sampling chamber and to minimize plant damage when plant stems were thick or round, such as with *Schoenoplectus* plants. The IRGA also made measurements of ambient atmospheric conditions, including photosynthetically active radiation (PAR), air temperature, and relative humidity (see Sanchez et al. 2016 for sampling details).

We scaled these instantaneous leaf-level transpiration rates to whole-system transpiration volumes by relating the IRGA data to key whole-system datasets. Leaf-level transpiration rates were scaled across space with our bi-monthly estimates of whole-system species-specific macrophyte biomass (Weller et al. 2016, see *Plant biomass measurements* for more details). We used hourly meteorological data provided by the City of Phoenix, from an on-site meteorological station, to scale leaf-level transpiration rates in time, accounting for water losses when we were not sampling (Sanchez et al. 2016).

Transpirational water losses estimated since summer 2011 followed a strong seasonal pattern, with the greatest rates in July, when plant biomass, air temperature, and PAR were at annual maxima (Sanchez et al. 2016, Weller et al. 2016). It would follow that the plant-mediated Biological Tide would thus be strongest during the summer. As such, we conducted this study in July of 2014 and 2015. We used a water budget approach to estimate the magnitude of the Biological Tide that involved estimating the total volume of water overlying the vegetated marsh, accounting for volume displaced by standing live plants, and comparing this to bi-monthly transpirational water losses from July 2011 through September 2015.

Plant biomass measurements

We used bi-monthly estimates of live plant biomass to scale our leaf-specific plant transpiration measurements to the entire 21 ha of marsh. To quantify whole-system biomass, we developed phenometric models that allowed us to non-destructively estimate live biomass for all plant species using simple allometric measurements made in the field (Daoust and Childers 1998, Childers et al. 2006). Every two months, we measured all of the plants in five 0.25-m^2 quadrats that were randomly located along each of the 10 marsh transects, for a total of 50 0.25-m^2 quadrats sampled (Weller et al. 2016). We used simple linear interpolation to extrapolate plant biomass between bi-monthly samplings, producing daily

estimates of live macrophyte biomass from July 2011 through September 2015. Because the phenometric biomass models were not statistically different for *T. latifolia* and *T. domingensis* or for *S. acutus* and *S. tabernaemontani*, we combined these pairs of species into two species groups for calculations and analysis (Weller et al. 2016).

Summer 2015 dye tracer experiment

The summer 2015 Rhodamine dye tracer experiment was centrally located in our 42-ha study area (see white star on Fig. 1). We temporarily installed a fixed-wall flowthrough flume (2 m wide, 16 m long, 0.5 m high; Fig. 2) in the marsh, oriented perpendicular to the marsh–water interface and located approximately 10 m into the vegetated marsh. The walls were made from clear high-gauge plastic sheeting with metal chain hemmed into the bottom edge to hold the walls against the soil surface. The walls were held up with PVC poles located every 2 m.

We deployed five autosamplers (ISCO 6700) close to the flume on an existing boardwalk (Fig. 3). Sampler tube intakes were installed in the center of the flume 1, 3, 5, and 7 m inland from the Rhodamine dye injection point. One-liter samples were collected by the autosamplers at approximate half-water depth (i.e., ~12 cm from the bottom) either every 30 min or every hour over two-day experimental runs. The amount of water collected in these samples was negligible relative to the volume of water in the flume. We used a 30-min sampling time interval for the 1-m location to enhance measurement resolution. Two dye experiments were run a week apart, which allowed all residual Rhodamine to dissipate between the experiments. In the first experiment, we used 5 g Rhodamine B dye tracer powder (Fisher Scientific, Bridgewater, New Jersey, USA), while in the second we used 1 g. We made 1 L dye solutions on site using Tres Rios water, and the dye was gently injected into the marsh water at the injection point (Fig. 3).

Sample preparation and fluorescence analysis

Concentrations of Rhodamine B dye are easily determined using excitation fluorometry. We analyzed all samples on a Fluoromax 4 fluorometer (Horiba, Kyoto, Japan) after first diluting all samples (field samples and calibration solutions) tenfold with distilled water to avoid sensor saturation. The pH of Tres Rios water was effectively neutral and was stable (7.3 $\pm$ 0.1 SE), minimizing this possible source of fluorescence variation (Smart and Laidlaw 1977). Excitation and emission wavelengths were determined by recording the optimal response curve on an excitation–emission wavelength scan; we used an excitation wavelength of 546 nm and an emission wavelength of 590 nm. We also controlled for any possible background fluorescence in ambient Tres Rios water (e.g., by dissolved organics) by running field water blanks.

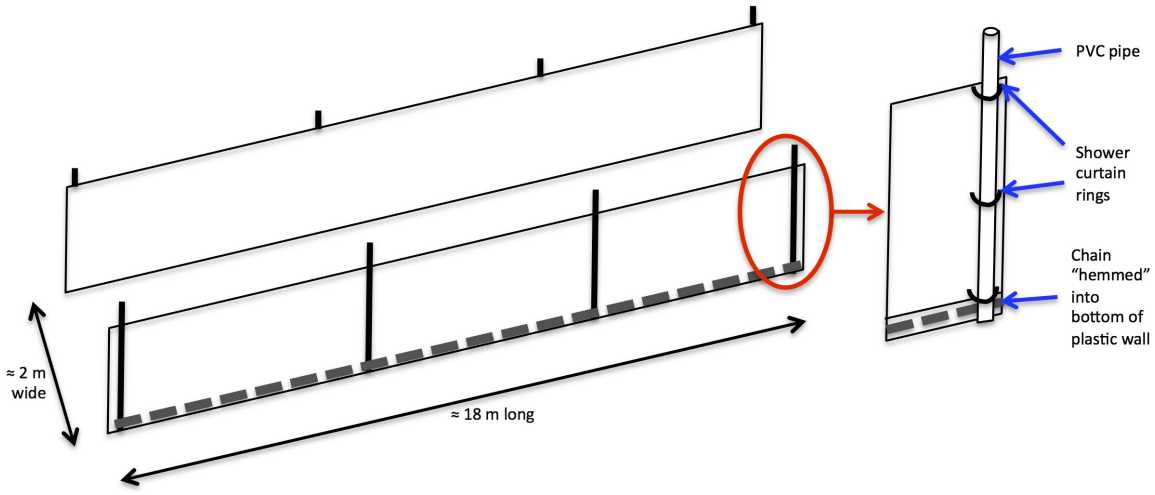

Fig. 2. Schematic of the temporary fixed-wall flowthrough marsh flume design, as modified from the approach used by Davis et al. (2001*a*, *b*).

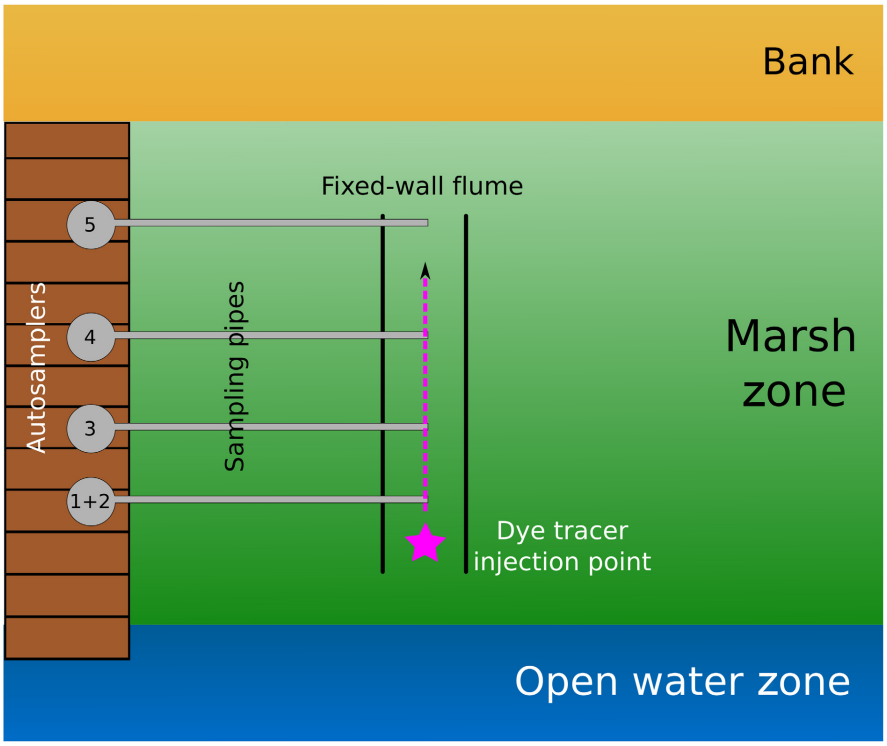

Fig. 3. Experimental design, including the approximate location of the 2 × 16 m flume (shown as "fixed-wall flume") adjacent to a boardwalk (left) and within the 50 m wide marsh. Sampling pipes allowed the autosamplers to collect water from within the flume without any disturbance of the marsh or soils during the experiment. The purple star indicates the dye tracer injection point.

Data analysis

We observed a low level of background fluorescence (due to the presence of dissolved organic matter), and we systematically accounted for it by subtracting the fluorescence values from the field water blanks from the sample signals. The resulting dye tracer breakthrough curves (BTCs) were used to compute residence time distribution (RTD) curves (Eq. 1, Table 1). The nth moments of the RTD curve ($\int_{t_0}^{t_f} E(t) \times t^n \times \mathrm{d}t$) allowed us to subsequently determine the characteristics of the flow: The first moment ($n = 1$) corresponded to the mean residence time $\bar{t}$ (or MRT; Eq. 2, Table 1) and the second central moment ($n = 2$) corresponded to σ^2, where σ is the standard deviation (Eq. 3, Table 1).

We computed three different velocities:

1. The maximum velocity was based on the time when the first significant fluorescence signal appeared. It was computed as the ratio between the sampler position to the injection point and this first signal time of appearance. We calculated the associated precision with the time span between two samples (i.e., 0.5 or 1 h depending on the location);
2. The local mean velocity was computed as the ratio between the sampler position to the injection point and the mean residence time $\bar{t}$ (Eq. 4, Table 1);
3. The flume mean velocity was obtained by averaging the local mean velocities (when they could be computed) of the different sampling points for a given experiment.

Water displacement has three important characteristics: advection, dispersion, and diffusion. Advection is the global movement of the fluid particles due to the mean velocity. In cases where multiple flowpaths are possible, different velocities may result when different flowpaths are followed: This is dispersion. The third mechanism, diffusion, results from thermal movement

Table 1. Summary of the formulas and equations used.

Eq. no.	Parameter	Symbol	Unit	Formula
(1)	Residence time distribution	$E(t)$	h^{-1}	$E(t) = \frac{C(t)}{\int_{t_0}^{t_t} C(t) \times dt} \left(\int_{t_0}^{t_t} E(t) \times dt = 1 \right)$
(2)	Mean residence time	$\bar{t}$	h	$\bar{t} = \int_{t_0}^{t_t} E(t) \times t \times dt$
(3)	Standard deviation	σ	h	$\sigma = \sqrt{\int_{t_0}^{t_t} E(t) \times (t - \bar{t})^2 \times dt}$
(4)	Local mean velocity	$\bar{V}$	cm/h	$\bar{V} = \frac{\Delta X}{\bar{t}}$
(5)	Peclet number	Pe	–	$\frac{\sigma^2}{\bar{t}^2} = \frac{2}{Pe} + \frac{8}{Pe^2}$
(6)	Transpiration flow	Q_{ET}	m^3/h	$Q_{ET} = V_{ET}/t_{transpiration}$
(7)	"Biological Tide" velocity	$\nu_{Biological\ Tide}$	cm/h	$\nu_{Biological\ Tide} = Q_{ET}/S_{flow-through}$

Notes: t_0, starting time of the experiment. t_t, ending time of the experiment.

of molecules and is isotropic. For Rhodamine B, diffusion-induced displacement would be around 1 mm/h (Gendron et al. 2008) and was thus considered to be negligible in our case (see *Results*). To further characterize the flow within the marsh, we estimated the dispersive flow (Levenspiel 1998) by computing the Peclet number, a dimensionless number equal to the ratio of advective to dispersive flow ($Pe = (U \times L)/D$), where U and L are the typical velocity and magnitude of the flow, and D is the dispersion coefficient of the flow (Kadlec and Wallace 2009). The higher the Peclet number, the more advection dominates the flow (see *Results* section for the threshold values). The Peclet number can be computed from the value of the standard deviation σ (as defined above). The exact formulation of the equation linking the Peclet number and this variance depends on the boundary conditions of the experimental system —in this study, we used the formulation adapted to an open inflow–open outflow channel (Eq. 5, Table 1), which fits the flowthrough marsh flume that we used.

As we noted above, we ran two independent dye study experiments in July 2015, using the marsh flume. These were started at two different times: In the first, we injected the dye at 9 a.m. and the experiment ran for 24 h (Experiment 1), while the second was started at 4 p.m. and the experiment ran for 40 h (Experiment 2). These starting times were chosen to, respectively, cover day–night and night–day succession, in an attempt to differentiate any potential diurnal dynamics.

Velocities comparison

As an extension of our earlier work, we used our transpiration-based water budget to estimate Biological Tide water velocities in the marsh based on daily volumes of marsh water that must be replaced due to transpirational losses (Sanchez et al. 2016, Eq. 6, Table 1). We applied this same water budget approach to the 32 m^2 of marsh contained within our fixed-wall flume after measuring plant biomass and transpiration rates in the flume immediately after the dye experiments were completed. Using the flume cross section ($S_{flow\text{-}through}$), we estimated a Biological Tide water velocity $\nu_{Biological\ Tide}$ within the flume (Eq. 7, Table 1) using the same transpiration-based water budget approach. The Rhodamine dye measurements, however, were a direct measure of surface advective velocity ($\nu_{measured\ Biological\ Tide}$), which we compared with the two transpiration-based water budget estimates. Notably, the degree of coherence among these three independent flow rate values also served to validate our whole-system water budget calculations and estimates (sensu Sanchez et al. 2016).

Results

We adopted a three-pronged approach in this work, based on a whole-system water budget, a flume water budget, and a dye tracer experiment. In this part of the study, we will start by presenting the results of the global evapotranspiration measurements and the related Biological Tide calculations, subsequently converting them into hydraulic residence time and velocity. We will then present the calculations and results similarly obtained with the second approach. Finally, we will present the results of the dye tracer experiments, calculating velocities, and characteristic parameters of the flow.

Plant transpiration and Biological Tide calculations

Whole-system biomass and transpiration values for the study period (summer 2015) were consistent with annual and inter-annual trends that we have observed since July 2011, as reported in Sanchez et al. (2016) and Weller et al. (2016). Average aboveground biomass in July 2015 was 1462 ± 152 (SE) g dw/m^2. Across the 21-ha marsh, this equated to a total biomass of 332 MT dw (Fig. 4). *Typha* spp. was the dominant macrophyte across the wetland and at the site of our controlled-flow dye experiment; it represented 89% of the July 2015 biomass. The total whole-system plant transpiration in July 2015 was 194,580 m^3/month, or 2.7 cm/d (Fig. 4). While this was lower than the 343,760 m^3/month that we estimated for July 2011, these transpiration rates were still markedly higher than rates reported for wetlands in more mesic or temperate climates (Sanchez et al. 2016).

We calculated transpiration-based estimates of the magnitude of the Biological Tide phenomenon (Sanchez et al. 2016) as the fraction of water overlying the marsh that was lost every day via plant transpiration—and that thus needed to be replaced by surface water movement into the marsh from adjacent open water areas (Fig. 5). This renewal rate varied from 1% to 5% during colder winter months, when whole-system transpiration losses were approximately 500–1500 m^3/d, equivalent to 0.2–0.6 cm/d, to as high as 15–20% during the hot, dry summer months, when transpirational losses were 9000 to over 12,000 m^3/d, equivalent to 3.8–5.1 cm/d (Fig. 4). It follows that, in the summer, hydraulic residence times of water overlying the vegetated marsh were likely 5–6 d or less. Our marshes are roughly 50 m wide, so replacing 20% of the overlying water every day can be equated to a daily horizontal flow rate of about 10 m/d, or about 42 cm/h. We further note that these values are conservative, as they do not account for the volume of water displaced by extensive dead and thatched vegetation on the marsh. We did account for the volume of standing live plant stems that displace marsh water; without subtracting that stem volume, the volume of water overlying the marsh (to a mean depth of 0.25 m) would be 52,500 m^3.

We used this same transpiration-driven water budget approach to estimate flow rates within the 16 × 2 m fixed-wall flume, which held roughly 5.94 m^3 of water—maximal because we did not account for the displacement volume of

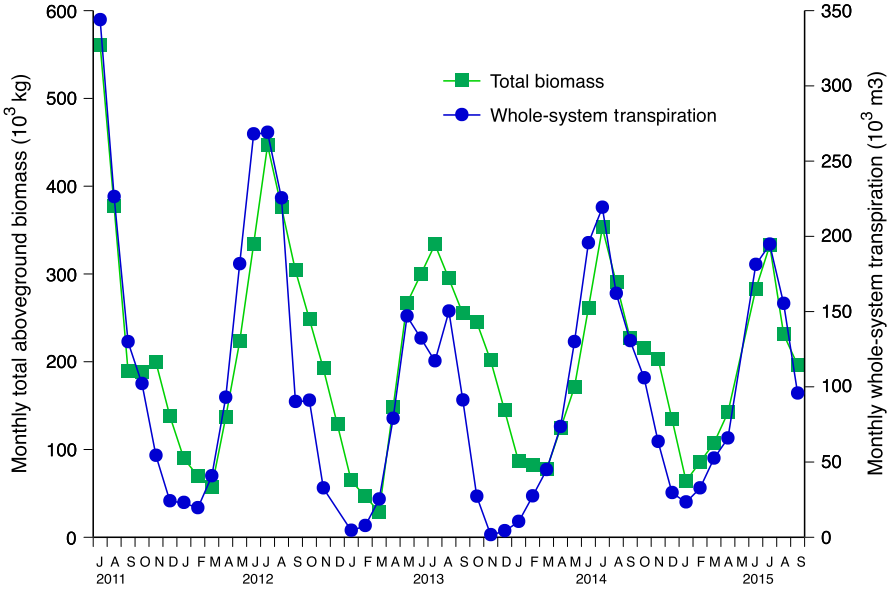

Fig. 4. Aboveground plant biomass and monthly total whole-system transpiration data from July 2011 through September 2015, including July 2015 when the controlled-flow dye experiment took place.

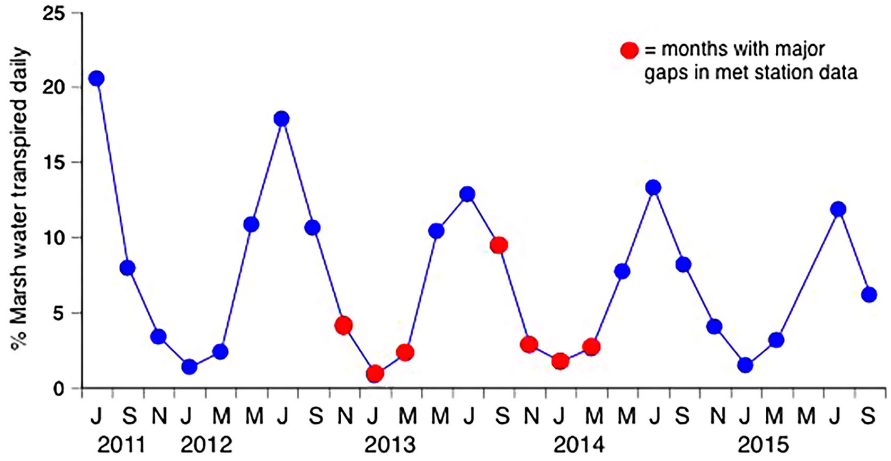

Fig. 5. Monthly average (±SE) fraction of the water overlying the marsh that was transpired daily from July 2011 through September 2015. Red circles represent months where transpiration was measured but could not be temporally scaled because of missing meteorological station data (see Sanchez et al. 2016 for details). Blue circles represent the percentage of marsh water transpired daily.

dead plant litter (wrack) or non-emergent aquatic vegetation (*Hydrocotyl* sp.). In July 2015, the 32 m^2 of marsh within the flume contained 30.3 kg dw of *Typha* sp. biomass that transpired 68 L/h (0.95 m^3/d or 3.0 cm/d) of water (taking into account 14 h of sunlight/d)—16% of the maximal volume of water within the flume. To replace this daily transpirational loss, new water would have had to flow into the flume at a rate of 2.57 m/d or 11 cm/h.

Dye experiments

Considering that (1) the water flow cross section within the flume was quite large compared with the tubing section of the autosampler and (2) the fixed walls of the flume were not impervious at the bottom, it was clearly very difficult to achieve a high tracer mass recovery. Neither a high recovery rate, nor the knowledge of the full RTD was the primary goal of this present work, though. We performed our calculations on the basis of the obtained BTCs (available in Appendix S1), which represent the fraction of the tracer mass we recovered. We got around 1% mass recovery for Experiment 1 and between 4% and 12% mass recovery (around 12% for the 1-m, 5% for the 3-m, and 4% for the 5-m sampling point) for Experiment 2. This low recovery rate had no impact on the data analysis in this study and the conclusions that are drawn, since the BTCs at the different sampling points gave valuable information.

For Experiment 1, we only calculated maximum velocity (see *Discussion*). For Experiment 2, the dye peak progressed down the flume in a predictable way, demonstrating that water was clearly, if slowly, advecting/dispersing into the marsh (Fig. 6). Additionally, the down-flume progression of the peak, from the marsh–open water interface toward the shore, confirmed the expected direction of water movement. In the first experiment, we calculated a high flow rate, 200 cm/h or 48 m/d, at the 1-m sampling location (Table 2). Otherwise, maximum velocities for both experiments ranged from 29 to 50 cm/h, or 7 to 12 m/d. The precision for these values was 5–8%. We found that the corresponding local mean velocities at the specific sampling points ranged from 7 to 25 cm/h (Table 2). The resulting flume mean velocity for this experiment was 16 cm/h, corresponding to 3.8 m/d.

In addition to advection, water flow is also characterized by dispersion and diffusion, and in low-flow situations where there are obstacles to flow—such as our marsh—dispersion may be a large component of flow. A simple measure of dispersion is the degree to which the fluorescence peaks widen and their tail increases with distance—and thus time—from the injection point. We found that the dispersion of the curves

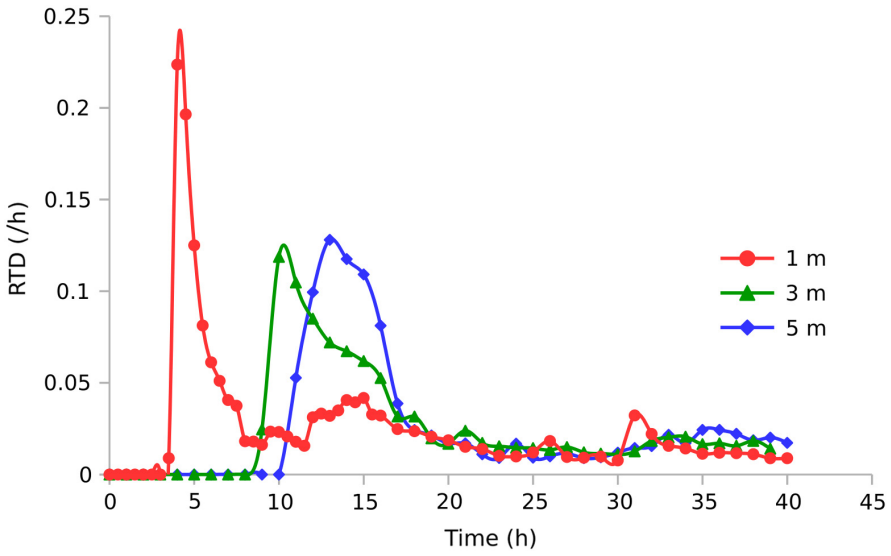

Fig. 6. Fluorescence curves for Experiment 2. Red circles (curve "1 m"), green triangles (curve "3 m"), and blue diamonds (curve "5 m"), respectively, represent the fluorescence at 1, 3, and 5 m from the injection point.

increased over distance (Fig. 6), demonstrating that the Biological Tide flow was (to a certain extent) dispersive. We were able to calculate Peclet numbers for only Experiment 2, because the calculation method required the use of the mean residence time, which we lacked for Experiment 1. One meter away from the injection point, the Peclet number was 6.2. Three and 5 m away from the injection point, its value was 12 and 13, respectively. As the characteristic length (L) and velocity (U) of the flow are 10 m and 16 cm/h (i.e., 4.4×10^{-5} m/s), the dispersion coefficient ($U \times L/\mathrm{Pe}$) for the flow ranges from 3.4×10^{-5} to 7.2×10^{-5} m^2/s. Finally, the recorded maximum velocities based on the fluorescence peaks observed at the 5-m sampling point were close to each other for both experiments (50 ± 2.8 and 45 ± 2.3 cm/h; Table 2), but not at the 1-m sampling point (200 and 29 ± 2.4 cm/h; Table 2). Based on these values, the difference between day to night (Experiment 1) and night to day (Experiment 2) flow rates were minimal, but additional experiments are needed to conclude this.

Discussion

We propose to compare the velocity of the Biological Tide with the velocities encountered in other wetlands, showing the relative magnitude of this phenomenon. We will then focus on the flow characteristics, especially its velocity range and dispersion features, providing comparison with the literature to situate the Biological Tide among the other types of flows already documented in

Table 2. Parameters calculated from the dye tracer experiments.

Experiment	Distance from injection point (m)	MRT (h)	Standard deviation σ (h)	Maximum velocity (cm/h)	Local mean velocity (cm/h)	Flume mean velocity (cm/h)	Peclet number (–)
1	1	na	na	200	na	na	na
	5	na	na	50 ± 2.8	na		na
2	1	15	11	29 ± 2.4	7	16 ± 5	6.2
	3	19	9	33 ± 2.1	16		12
	5	20	9	45 ± 2.3	25		13

Notes: MRT, mean residence time. Local mean velocity is defined as the ratio of the sampler position (i.e., distance from injection point) to the mean residence time for a given sampler (Eq. 3, Table 1). The flume mean velocity is defined as the average of all local mean velocities for a given experiment.

wetlands. A discussion about the relevance of the triple approach chosen in this study will follow, and we will conclude this part of the study by advancing management considerations involving comparison with wetlands displaying similar hydrodynamic features (namely velocity) or purposes (namely FWS CTW).

Marsh water velocity

The surface flow rates that we calculated from our July 2015 tracer experiments ranged from 29 to 45 cm/h. Using plant biomass and transpiration data from July, we estimated flow rates up to about 40 cm/h using our water budget approach. When we applied this same budget approach to the marsh within our 2 × 16 m fixed-wall flume, we calculated a conservative flow rate estimate of 11 cm/h. While these three independent approaches did not generate the same velocity, the estimates are reasonably close to each other and are thus believable. We found only one study where such low velocities have been reported: Kaplan et al. (2015) measured comparable surface flow velocities of 15–147 cm/h in a small (1.5 ha, 9000 m^3) vegetated tropical wetland that had an average water residence time of 90 d (Kaplan et al. 2011). By comparison, our Tres Rios CTW system was 42 ha in size—21 ha of which was vegetated marsh—held approximately 357,500 m^3 of water, and had a four-day design residence time. Our marsh surface flow velocities were much lower than those reported by Leonard and Luther (1995) for a tidal marsh in Florida—from 2 to 10 cm/s—although it is worth noting that tidal or gravity-based energy produced the currents in their tidal marsh, whereas plant transpirational water loss was the energy driving the Biological Tide in our CTW system. Regardless, there is considerable evidence that emergent vegetation in wetlands reduces both flow rates and turbulence (Leonard and Croft 2006).

The fluorescence value reached at the end of the Experiment 1 was too far from the baseline to compute the mean velocity value, unlike in Experiment 2. Indeed, the definition of a mean velocity implied that we were able to define the end point of the experiment (corresponding to the time when the fluorescence values return to background); this is a requirement to compute the MRT (Eq. 2, Table 1) and subsequently the local mean velocity (Eq. 3, Table 1).

The magnitude of the Biological Tide means that the renewing water will cover the marsh width (50 m) in approximately 13 d, based on the flume mean velocity (16 cm/h), but only 4.2 d for the fastest moving water parcels (50 cm/h). These maximum velocities (from 29 to 50 cm/h, Table 2) are the result of differential advective flow paths, characteristic of this dispersive flow. The Biological Tide is thus an advective–dispersive flow. The Peclet number was, in all cases, below the threshold value of 100 (Table 2), indicating that the flow we measured was largely dispersive (Levenspiel 1998). This can be explained by the high density and irregularity of plant stems within our marsh flume—almost 60% of flume surface and 2.4% of total water volume in the flume were occupied by live emergent plant stems—and more generally across the marsh. This leads to a multitude of possible flow paths for the water, which creates dispersion. This phenomenon has been documented in other wetland settings, including in other free surface water vegetated wetlands similar to our CTW (Keefe et al. 2004, Lightbody and Nepf 2006, Laurent et al. 2015). In our experiments, the dispersion coefficient ranged from 3.4×10^{-5} to 7.2×10^{-5} m^2/s, which is lower than previously encountered values: Coefficients between 1.3×10^{-4} and 6.3×10^{-4} m^2/s, 0.016 and 0.18 m^2/s, 2.5×10^{-3} and 2.1×10^{-2} m^2/s were, respectively, computed by Keefe et al. (2004), Variano et al. (2009), and Kaplan et al. (2015). This is most likely due to the lower velocities we observed in the Tres Rios marsh, as the Peclet numbers were quite similar among the aforementioned wetlands (respectively, around 30, 6–41 and 4–8).

The precision of our flow measurements ranged from 5% to 8%, which is reasonable for a field experiment under low velocity conditions. By comparison, the precision of most flowmeters and velocimeters is 2–20%. This precision and technical limitations (e.g., detection limit, measurement difficulty in a densely vegetated marsh) confirmed that a dye tracer experiment was the best way to measure the actual flow rates of the Biological Tide.

Comparison of transpiration-based water budget estimates and dye study results

We compared our water budget-based estimates of water replacement rates (Fig. 4) with water flow and replacement rates based on the

controlled-flow dye study conducted in July 2015 (Table 2). From transpiration calculations, we estimated a water velocity of 35–42 cm/h for a 50 m wide marsh in mid-summer, and a water residence time of 5–6 d for the water overlying the marsh (Fig. 5). The Rhodamine dye experiments confirmed velocities ranging from 25 cm/h (local mean velocity) to 45 cm/h (maximum velocity). The coherence between these two independent flow rate calculations is strong. As yet another methodological check, immediately after the dye experiment ended we also measured plant biomass and transpiration rates for the marsh within the 2 × 16 m fixed-wall flume itself, and used our water budget approach to estimate a replacement rate for the water in the flume. We estimated transpirational water loss within the flume area as roughly 950 L/d, or (a conservatively calculated) 16% of the total water volume within the flume. By extrapolation, we estimated that the rate of water flow that would be needed to replace this 16% loss, if the flume was closed at the downstream end, was 11 cm/h. This flume-specific water budget-based flow estimate is lower than, but still aligns reasonably well with, both our long-term whole-system transpiration-based estimates and the actual flow rates that we measured from the controlled-flow dye study.

Management considerations

Our five years of research at the Tres Rios CTW has documented that the most biogeochemically active zone of the system is the vegetated marsh (Sanchez et al. 2016, Weller et al. 2016). This is not surprising. But the management implications are important—if inorganic nitrogen, and presumably many other contaminants, gets into the marsh proper, they are effectively removed from the water (Weller et al. 2016). But the design water residence time for the entire 42-ha system, only 21 ha of which is vegetated marsh, is only four days, and it is likely that a considerable amount of the water entering the system leaves four days later without ever coming into contact with the biogeochemically active marsh. The high rates of summer water loss via plant transpiration, and the Biological Tide that is being driven by this, move more water and nitrogen into the marsh from the open water areas than would happen in a similar CTW in a cooler or more mesic climate. Thus, the biotically mediated surface hydrologic phenomenon that we have documented here, for the first time, is actually increasing the effectiveness of this CTW, simply because it is located in a hot, dry climate. Because of this, we would recommend a design for CTW in hot arid climates that either increases the relative area of vegetated marsh or increases the hydraulic likelihood that any given parcel of water in the system will come into contact with vegetated marsh.

Another design recommendation also focuses on water residence time. To demonstrate the potential importance of this hydraulic characteristic, we compared data from our CTW with similar values from a natural wetland located in the tropics (Costa Rica). The mean water residence time in natural La Reserva wetland was 100 d compared with 4 d in the Tres Rios CTW (Kaplan et al. 2011). This difference is largely because the water outflow rate at the latter was much higher (Table 3). One could expect that the higher water residence time in the La Reserva wetland would result in a higher nutrient uptake efficiency. However, the nitrogen removal efficiency of the La Reserva system (51–98.5%) was only double that of the Tres Rios CTW (22–48%, see Sanchez et al. 2016). If the Tres Rios CTW was designed for a longer whole-system water

Table 3. Comparison of hydraulic characteristics between a constructed treatment wetland (Tres Rios) and a natural wetland (La Reserva; Kaplan et al. 2011, 2015).

Parameters	TR	LR	TR/LR Ratio
Average outflow (m^3/h)	5000	6.25 ± 3.31†	523–1700
Volume (m^3)	351,500	7400–10,000†	35–48
Whole-system residence time (d)	4	30–110†	0.036–0.13
Marsh velocity (cm/h)	16	25–110‡	0.15–0.64
Marsh width (m)	50	–	–
Marsh residence time (d)	13	100†	0.13

Note: TR, Tres Rios wetland; LR, La Reserva wetland.

† Values from Kaplan et al. (2011). Intervals shown are 95% confidence intervals.

‡ Values from Kaplan et al. (2015). The lowest value corresponds to the wetland western average velocity; the highest one corresponds to the wetland eastern average velocity.

residence time, in conjunction with a physical design that allowed for more water contact with the vegetated marsh—and perhaps a higher marsh/open water ratio—we predict that its whole-system nutrient uptake efficiency, which is different from the marsh-specific uptake efficiency of nearly 100%, would be considerably higher.

Finally, in order to enlarge the comparison with systems sharing the same purpose and hydrological type, we put in perspective the removal efficiency of our wetland with a literature review of the removal performances of FWS CTWs (Kadlec and Wallace 2009). The reported mean removal rates reach 60% for ammonia, with a mean hydraulic loading rate of 7.3 cm/h (N = 118), and 46% for nitrate, with a mean hydraulic loading rate of 11.4 cm/h (N = 72). It thus appears that the Tres Rios CTW is fairly efficient, since the removal rates we measured reach 48% for ammonia and 22% for nitrate (Sanchez et al. 2016), while the hydraulic loading rate is roughly four times higher—42.9 cm/h. We can hypothesize that the Biological Tide we confirmed in the Tres Rios CTW, although not optimally utilized, already allows for significant nitrogen removal efficiency.

We are currently using a spatially articulate cell-based hydrodynamic model of the Tres Rios CTW, in conjunction with a biogeochemical processing model, to experiment with different hypothetical design options for this and other CTW systems.

Conclusions and next steps

We have used more than six years of data on plant community composition and biomass production, transpiration and evaporation rates, and water quality to verify the efficacy of nitrogen removal by the Tres Rios CTW. We have also used our whole-system water budget to demonstrate a plant-mediated, transpiration-driven Biological Tide that brings new water and nitrogen into the vegetated marsh of this CTW, where it is effectively removed and processed (Sanchez et al. 2016, Weller et al. 2016). In the research we present here, we used an empirical controlled-flow tracer study to confirm not only the existence and flow rates of the Biological Tide, but to verify the accuracy of our water budget-based estimates of flow rates. As we noted above, this is (to our knowledge) the first time that biotic control of surface hydrology has ever been demonstrated in a wetland ecosystem.

Our next steps involve using numerical modeling to further articulate how the Biological Tide phenomenon is enhancing nutrient removal in the wetlands of this CTW, and to explore design options for hypothetical CTW systems that optimize for this phenomenon. We are developing and parameterizing a spatially articulate hydrodynamic model, based on the current design of the Tres Rios CTW, that accounts for actual water flow rates between the marsh and open water bodies and that accurately simulates whole-system water residence times. We will then use this model to test various hypothetical design scenarios, including (1) different ratios and configurations of marsh and open water, (2) different open water flow paths, including a scenario where all water entering the system must come in contact with vegetated marsh, (3) various macrophyte community compositions, and (4) different plant densities (Kjellin et al. 2007). Ultimately, these modeling exercises will inform both improved management practices for the Tres Rios CTW and future designs that maximize the ecosystem services provided by CTW "turquoise" infrastructure in aridland cities around the world.

Acknowledgments

The first year of this work was supported by the U.S. Geological Survey through a grant from the Arizona Water Resources Research Institute. Additional support was provided by the National Science Foundation through the Central Arizona-Phoenix Long-Term Ecological Research Program (Grant No. 1027188) and the Urban Sustainability Research Coordination Network (Grant No. 1140070). The Walton Sustainable Solutions Initiative at ASU funded collaborative travel between Phoenix and Strasbourg, including P. Bois' travel in summer 2015. The Long-Term Ecological Research Network from France and the Strasbourg Long-Term Ecological Research Program (ZAEU) funded P. Bois' travel in summer 2014. We thank Hilairy Hartnett and Joshua Nye at ASU for the use of their fluorometer and lab space, Ben Warner for his contributions early in the project, Nich Weller for leading the macrophyte data collection efforts for the first three years of the project, the City of Phoenix Water Services Department for their support and for providing access to Tres Rios and key datasets, Dakota Tallman for coordinating much of the research

conducted in 2013, and the many student volunteers who helped with the field and laboratory work.

Literature Cited

Bauer, P., G. Thabeng, F. Stauffer, and W. Kinzelbach. 2004. Estimation of the evapotranspiration rate from diurnal groundwater level fluctuations in the Okavango Delta, Botswana. Journal of Hydrology 288:344–355.

Bauer-Gottwein, P., T. Langer, H. Prommer, P. Wolski, and W. Kinzelbach. 2007. Okavango Delta Islands: interaction between density-driven flow and geochemical reactions under evapo-concentration. Journal of Hydrology 335:389–405.

Bazante, J., G. Jacobi, H. Solo-Gabriele, D. Reed, S. Mitchell-Bruker, D. L. Childers, L. Leonard, and M. Ross. 2006. Hydrologic measurements and implications for tree island formation within Everglades National Park. Journal of Hydrology 329: 606–619.

Bodin, H., A. Mietto, P. M. Ehde, J. Persson, and S. E. B. Weisner. 2012. Tracer behaviour and analysis of hydraulics in experimental free water surface wetlands. Ecological Engineering 49:201–211.

Bouma, T. J., L. A. van Duren, S. Temmerman, T. Claverie, A. Blanco-Garcia, T. Ysebaert, and P. M. J. Herman. 2007. Spatial flow and sedimentation patterns within patches of epibenthic structures: combining field, flume and modelling experiments. Continental Shelf Research 27:1020–1045.

Bowmer, K. H. 1987. Nutrient removal from effluents by an artificial wetland: influence of rhizosphere aeration and preferential flow studied using bromide and dye tracers. Water Research 21:591–597.

Chang, N. B., A. J. Crawford, G. Mohiuddin, and J. Kaplan. 2015. Low flow regime measurements with an automatic pulse tracer velocimeter (APTV) in heterogeneous aquatic environments. Flow Measurement and Instrumentation 42:98–112.

Childers, D. L. 1994. Fifteen years of marsh flumes—A review of marsh-water column interactions in Southeastern USA estuaries. Pages 277–296 *in* W. Mitsch, editor. Global wetlands. Elsevier, Amsterdam, The Netherlands.

Childers, D. L., M. L. Cadenasso, J. M. Grove, V. Marshall, B. McGrath, and S. T. A. Pickett. 2015. An ecology *for* cities: a transformational nexus of design and ecology to advance climate change resilience and urban sustainability. Sustainability 7: 3774–3791.

Childers, D. L., and J. W. Day Jr. 1988. A flow-through flume technique for quantifying nutrient and materials fluxes in microtidal estuaries. Estuarine, Coastal and Shelf Science 27:483–494.

Childers, D. L., and J. W. Day Jr. 1990*a*. Marsh-water column interactions in two Louisiana estuaries. I. Sediment dynamics. Estuaries 13:393–403.

Childers, D. L., and J. W. Day Jr. 1990*b*. Marsh-water column interactions in two Louisiana estuaries. II. Nutrient dynamics. Estuaries 13:404–417.

Childers, D. L., D. Iwaniec, D. Rondeau, G. Rubio, E. Verdon, and C. Madden. 2006. Primary productivity in Everglades marshes demonstrates the sensitivity of oligotrophic ecosystems to environmental drivers. Hydrobiologia 569:273–292.

Childers, D. L., S. T. A. Pickett, J. M. Grove, L. Ogden, and A. Whitmer. 2014. Advancing urban sustainability theory and action: challenges and opportunities. Landscape & Urban Planning 125:320–328.

Daoust, R., and D. L. Childers. 1998. Quantifying aboveground biomass and estimating productivity in nine Everglades wetland macrophytes using a non-destructive allometric approach. Aquatic Botany 62:115–133.

Davis III, S. E., D. L. Childers, J. W. Day Jr., D. T. Rudnick, and F. H. Sklar. 2001*a*. Wetland-water column exchanges of carbon, nitrogen, and phosphorus in a Southern Everglades dwarf mangrove. Estuaries 24:610–622.

Davis III, S. E., D. L. Childers, J. W. Day Jr., D. T. Rudnick, and F. H. Sklar. 2001*b*. Nutrient dynamics in vegetated and unvegetated areas of a southern Everglades mangrove creek. Estuarine, Coastal and Shelf Science 52:753–768.

Fonder, N., and T. Headley. 2010. Systematic classification, nomenclature, and reporting for constructed treatment wetlands. Pages 191–219 *in* J. Vymazal, editor. Water and nutrient management in natural and constructed wetlands. Springer Science + Business Media B.V., Dordrecht, The Netherlands.

Fonder, N., and T. Headley. 2013. The taxonomy of treatment wetlands: a proposed classification and nomenclature system. Ecological Engineering 51: 203–211.

Gendron, P. O., F. Avaltroni, and K. J. Wilkinson. 2008. Diffusion coefficients of several rhodamine derivatives as determined by pulsed field gradient-nuclear magnetic resonance and fluorescence correlation spectroscopy. Journal of Fluorescence 18:1093–1101.

Giraldi, D., M. de'Michieli Vitturi, M. Zaramella, A. Marion, andR. Iannelli. 2009. Hydrodynamics of vertical subsurface flow constructed wetlands: tracer tests with rhodamine WT and numerical modeling. Ecological Engineering 35:265–273.

Greenway, M. 2005. The role of constructed wetlands in secondary effluent treatment and water reuse in subtropical and arid Australia. Ecological Engineering 25:501–509.

Grimm, N. B., S. H. Faeth, N. E. Golubiewski, C. L. Redman, J. Wu, X. Bai, and J. M. Briggs. 2008. Global change and the ecology of cities. Science 319:756–760.

Grove, J. M. 2009. Cities: managing densely settled social-ecological systems. Pages 281–294 *in* F. S. Chapin III, G. P. Kofinas, and C. Folke, editors. Principles of ecosystem stewardship: resilience-based natural resource management in a changing world. Springer, New York, New York, USA.

Harvey, J. W., G. B. Noe, L. G. Larsen, D. J. Nowacki, and L. E. McPhillips. 2011. Field flume reveals aquatic vegetation's role in sediment and particulate phosphorus transport in a shallow aquatic ecosystem. Geomorphology 126:297–313.

Kadlec, R. H., and S. D. Wallace. 2009. Treatment wetlands. Second edition. CRC Press, Boca Raton, Florida, USA.

Kaplan, D., M. Bachelin, R. Munoz-Carpena, and W. Rodriguez-Chacon. 2011. Hydrological importance and water quality treatment potential of a small freshwater wetland in the humid tropics of Costa Rica. Wetlands 31:1117–1130.

Kaplan, D., M. Bachelin, C. Yu, R. Munoz-Carpena, T. L. Potter, and W. Rodriguez-Chacon. 2015. A hydrologic tracer study in a small, natural wetland in the humid tropics of Costa Rica. Wetlands Ecology and Management 23:167–182.

Keefe, S. H., L. B. Barber, R. L. Runkel, J. N. Ryan, D. M. McKnight, and R. D. Wass. 2004. Conservative and reactive solute transport in constructed wetlands. Water Resources Research 40:W01201.

Kjellin, J., A. Worman, H. Johansson, and A. Lindahl. 2007. Controlling factors for water residence time and flow patterns in Ekeby treatment wetland, Sweden. Advances in Water Resources 30:838–850.

Laurent, J., P. Bois, M. Nuel, and A. Wanko. 2015. Systemic models of full-scale Surface Flow Treatment Wetlands: determination by application of fluorescent tracers. Chemical Engineering Journal 264:389–398.

Leonard, L. A., and A. L. Croft. 2006. The effect of standing biomass on flow velocity and turbulence in Spartina alterniflora canopies. Estuarine, Coastal and Shelf Science 69:325–336.

Leonard, L. A., and M. E. Luther. 1995. Flow hydrodynamics in tidal marsh canopies. Limnology and Oceanography 40:1474–1484.

Levenspiel, O. 1998. Chemical reaction engineering. Third edition. Wiley, New York, New York, USA.

Lightbody, A. F., and H. M. Nepf. 2006. Prediction of velocity profiles and longitudinal dispersion in emergent salt marsh vegetation. Limnology and Oceanography 51:218–228.

McLaughlin, D. L., and M. J. Cohen. 2014. Ecosystem specific yield for estimating evapotranspiration and groundwater exchange from diel surface water variation. Hydrological Processes 28:1495–1506.

Melosi, M. V. 2000. The sanitary city: environmental services in urban America from colonial times to the present. Johns Hopkins University Press, Baltimore, Maryland, USA.

Meselhe, E., T. Peeva, and M. Muste. 2004. Large scale particle image velocimetry for low velocity and shallow water flows. Journal of Hydraulic Engineering 130:937–940.

Metson, G., R. Hale, D. Iwaniec, E. Cook, J. Corman, C. Galletti, and D. Childers. 2012. Phosphorus in Phoenix: a budget and spatial representation of phosphorus in an urban ecosystem. Ecological Applications 22:705–721.

Nivala, J., T. Headley, S. Wallace, K. Bernhard, H. Brix, M. van Afferden, and R. A. Müller. 2013. Comparative analysis of constructed wetlands: the design and construction of the ecotechnology research facility in Langenreichenbach, Germany. Ecological Engineering 61:527–543.

Pickett, S. T. A., C. G. Boone, B. P. McGrath, M. L. Cadenasso, D. L. Childers, L. A. Ogden, M. McHale, and J. M. Grove. 2013. Ecological science and transformation to the sustainable city. Cities 32: S10–S20.

Ramberg, L., and P. Wolski. 2008. Growing islands and sinking solutes: processes maintaining the endorheic Okavango Delta as a freshwater system. Plant Ecology 196:215–231.

Sanchez, C. A., D. L. Childers, L. Turnbull, R. Upham, and N. A. Weller. 2016. Aridland constructed treatment wetlands II: Plant mediation of surface hydrology enhances nitrogen removal. Ecological Engineering 97:658–665.

Smart, P. L., and I. M. S. Laidlaw. 1977. An evaluation of some fluorescent dyes for water. Water Resources Research 13:15–33.

Sullivan, P., R. M. Price, F. Miralles-Wilhelm, M. S. Ross, L. J. Scinto, T. W. Dreschel, F. H. Sklar, and E. Cline. 2014. The role of recharge and evapotranspiration as hydraulic drivers of ion concentrations in shallow groundwater on Everglades tree islands, Florida (USA). Hydrological Processes 28: 293–304.

Tanner, C. C., J. P. S. Sukias, T. R. Headley, C. R. Yates, and R. Stott. 2012. Constructed wetlands and denitrifying bioreactors on-site and decentralized water treatment: comparison of five alternative configurations. Ecological Engineering 42:112–123.

Troxler-Gann, T., and D. L. Childers. 2006. Relationships between hydrology and soils describe vegetation

patterns in tree seasonally flooded tree islands of the southern Everglades, Florida. Plant and Soil 279:271–286.

Variano, E. A., D. T. Ho, V. C. Engel, P. J. Schmieder, C. Matthew, and M. C. Reid. 2009. Flow and mixing dynamics in a patterned wetland: kilometer-scale tracer releases in the Everglades. Water Resources Research 45:W08422.

Wallace, S. D., and R. L. Knight. 2006. Small-scale constructed wetland treatment systems: feasibility, design criteria, and O&M requirements. Water Environment Research Foundation (WERF), Alexandria, Virginia, USA.

Weller, N. A., D. L. Childers, L. Turnbull, and R. F. Upham. 2016. Aridland constructed treatment wetlands I: macrophyte productivity, community composition, and nitrogen uptake. Ecological Engineering 97:649–657.

White, W. N. 1932. A method of estimating groundwater supplies based on discharge by plants and evaporation from soil: results of investigations in Escalante Valley, Utah. U.S. Geological Survey Water Supply Paper: 659-A. U.S. Department of the Interior, Geological Survey, Washington, USA.

Williams, C. F., and S. D. Nelson. 2011. Comparison of Rhodamine-WT and bromide as a tracer for elucidating internal wetland flow dynamics. Ecological Engineering 37:1492–1498.

Worman, W., and V. Kronnas. 2005. Effect of pond shape and vegetation heterogeneity on flow and treatment performance of constructed wetlands. Journal of Hydrology 301:123–138.

Supporting Information

Additional Supporting Information may be found online at: http://onlinelibrary.wiley.com/doi/10.1002/ecs2.1756/full

Science of the Total Environment 615 (2018) 1099–1109

Contents lists available at ScienceDirect

Science of the Total Environment

journal homepage: www.elsevier.com/locate/scitotenv

Seasonal and ageing effect on the behaviour of 86 drugs in a full-scale surface treatment wetland: Removal efficiencies and distribution in plants and sediments

Maximilien Nuel [a,b], Julien Laurent [a], Paul Bois [a], Dimitri Heintz [b], Adrien Wanko [a,*]

[a] Icube, UMR 7357, ENGEES, CNRS, Université de Strasbourg, 2 rue Boussingault, 67000 Strasbourg, France
[b] Plant Imaging and Mass Spectrometry, Institut de Biologie Moléculaire des Plantes, UPR 2357, CNRS, 12 rue du Général Zimmer, 67084 Strasbourg, France

HIGHLIGHTS

- Data were collected during 2 years of field work on a full-scale SFTW.
- Over two years, the SFTW drug removal ability decreased due to the ageing effect.
- In summer, drugs are accumulated in the mud and released from it in winter.
- Drug compounds were dissimilarly transferred from water to local plants in the SFTW.
- The SFTW drug removal efficiency increases during warm periods.

GRAPHICAL ABSTRACT

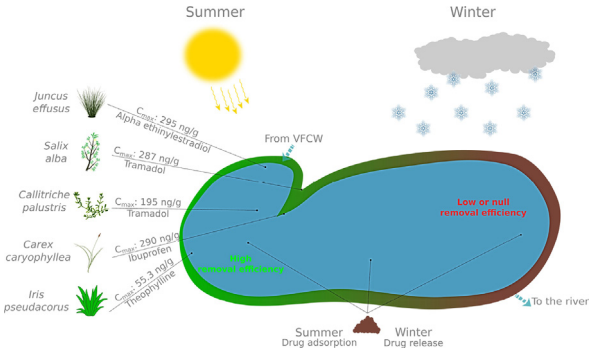

ARTICLE INFO

Article history:
Received 4 August 2017
Received in revised form 7 October 2017
Accepted 7 October 2017
Available online xxxx

Editor: D. Barcelo

Keywords:
Pharmaceutical compounds
Seasonality
Sediment
Plants
Removal efficiency
Ageing

ABSTRACT

The presence of human drugs in the aquatic environment is partly due to an incomplete and insufficient removal process of wastewater treatment plants (WWTPs). Thus, drug traces are observed at different concentrations in water bodies, sediments and aquatic plants all over the world. At the same time, Surface Flow Treatment Wetlands (SFTWs) at the outlet of WWTPs are commonly observed in small municipalities as complementary treatment. However, little is known regarding the role of SFTWs in the complementary mitigation of emerging contaminants, such as drugs, and the interactions between drugs, plants and sediment throughout the seasons. For that reason, we conducted sampling sessions over a period of two years on a full-scale SFTW downstream of a vertical-flow constructed wetland. At each session, the SFTW influent and effluent, as well as five different plant species and one composite sediment sample, were sampled. We detected more than fifty pharmaceutical compounds in the inflow and outflow water. The compounds most frequently detected were bisoprolol and ketoprofen. We emphasized that the SFTW removal ability was better in the summer than in the winter, due to the impact of weather on physicochemical parameters. Large variations of removal efficiencies were also observed when considering all of the detected compounds. Large seasonal variations were also observed for each compound. In addition, the study of the five plants showed their ability to uptake drugs from water and soil to

Abbreviation: Aut, autumn; BOD, biochemical oxygen demand; COD, chemical oxygen demand; CW, constructed wetland; HLB, hydrophilic lipophilic balance; K_d, solid-liquid partition coefficient; K_{ow}, octanol-water partition coefficient; MS/MS, tandem mass spectrometry; NK, Kjeldahl nitrogen; PE, population equivalent; QL, quantification limit; RE, removal efficiencies; SFTW, surface flow treatment wetland; SPE, solid phase extraction; SS, suspended solids; Sum, summer; TP, total phosphorus; TTT, treatment; UPLC, ultra performance liquid chromatography; VFCW, vertical-flow constructed wetland; Win, winter; WWTP, wastewater treatment plant.

* Corresponding author.
E-mail addresses: mnuel@engees.eu (M. Nuel), julien.laurent@engees.unistra.fr (J. Laurent), p.bois@unistra.fr (P. Bois), dimitri.heintz@ibmp-cnrs.unistra.fr (D. Heintz), wanko@unistra.fr (A. Wanko).

https://doi.org/10.1016/j.scitotenv.2017.10.061
0048-9697/

Constructed wetland
Polishing treatment

the leaves in a species-specific manner. The pharmaceutical composition of the sediment was also correlated with the season: the maximum occurrence was reached in summer, and the minimum was reached in winter. Finally, the continuous decrease in removal efficiencies highlights the ageing effect on SFTW removal ability.

1. Introduction

Surface Flow Treatment Wetlands (SFTWs) can be used for wastewater and storm water treatment. SFTWs have water flowing in a horizontal direction above the surface of a permanently saturated soil, flowing through macrophytic vegetation (Fonder and Headley, 2013). SFTWs generally have a shallow sealed basin or sequence of basins and water surface above the substrate (Kadlec and Knight, 1996), acting as a polishing treatment. In France, since 2009, there has been an increase in SFTW between wastewater treatment plants (WWTPs) and the receiving aquatic environment. They are considered as a treatment complementary to the WWTP but no regulations on removal efficiencies apply. Considering international references, this study approaches the case of a pond. Nevertheless, to be consistent with the French context and previous studies (Laurent et al., 2015; Nuel et al., 2015; Nuel et al., 2017a, 2017b, 2017c), the acronym SFTW is used in this study.

The main ecosystem services we are looking at are those related to regulation (Malamaire, 2009): (i) particulate matter retention, (ii) limitation of hydraulic and pollutant loads to surface waters through infiltration, evapotranspiration or evaporation (Boutin et al., 2010), (iii) hydraulic peak attenuation and (iv) additional pollutant mitigation (Verlicchi and Zambello, 2014). The main mechanisms likely to be involved are (Toet et al., 2005): infiltration, evapotranspiration, biological degradation, nutrient uptake by plants, photodegradation or transformation and settling.

Municipal wastewater is the major pathway for pharmaceuticals to reach the aquatic environment (Kolpin et al., 2002; Zorita et al., 2009). Many studies have indicated that the elimination of pharmaceuticals in municipal wastewater treatment plants is often incomplete (Ternes, 1998; Writer et al., 2013). CWs have also been found to remove a variety of pharmaceuticals with promising results (Verlicchi and Zambello, 2014). Several processes are involved in the removal of pharmaceuticals in CWs, including plant uptake, photodegradation, hydrolysis and microbial degradation. Plants seem to contribute to the removal of pharmaceuticals from water (Matamoros et al., 2012a, 2012b), and there is also evidence for a direct uptake of pharmaceuticals by several plant species (Shenker et al., 2011; Carvalho et al., 2014). In addition to direct uptake, plants may facilitate the removal of pharmaceuticals by the release of root exudates into the rhizosphere (Zhang et al., 2011). The root exudates released by plants, such as sugars and organic acids can provide organic carbon and a nutrient source for microorganisms in the rhizosphere (Vanek et al., 2010). Although several studies have documented a significant removal of pharmaceuticals in CWs, data on the direct uptake of pharmaceuticals by wetland plants are sparse and restricted to a few selected compounds and plant species (Dordio et al., 2011; Matamoros et al., 2012a, 2012b; Zhang et al., 2011).

The fate and behaviour of pharmaceuticals and their metabolites in wastewater treatment plants (WWTPs) and surface waters have been the subject of numerous studies (Ellis, 2006; Gros et al., 2006; Vazquez-Roig et al., 2010). The results of these studies indicated that conventional WWTPs are not able to completely remove these micropollutants from wastewaters and they are consequently discharged into the aquatic environment. However, most of the studies on the fate of pharmaceuticals in WWTPs and river water are focused on the aqueous phase, as the determination of compound concentrations in the solid fraction (suspended solids, sediment or sludge) is complex. Nevertheless, Verlicchi and Zambello (2015) reviewed 59 papers published between 2002 and 2015, referring to approximately 152 drug compound concentrations in different kinds of WWTP sludge. They reported that many drug compounds were detected in the sludge, with a high variability of concentrations between 0.1 ng/g and 10 μg/g. The screening of sewage sludge showed that these micropollutants are present in this medium (Petrović et al., 2005; McClellan and Halden, 2010; Verlicchi and Zambello, 2015), and an accumulation in sediments was also reported for several compounds (Nilsen, 2007; Vazquez-Roig et al., 2010; Verlicchi and Zambello, 2015).

The aim of this paper is to highlight the different behaviours and the transfer to plants and sediment of >80 pharmaceutical compounds in a full-scale SFTW. The results are based on sampling sessions carried out during 20 months on inlet water, outlet water, 5 plant species and one composite sediment from a pond as an SFTW.

2. Materials and methods

2.1. Study site

The studied SFTW is located in Lutter (Alsace, France) and was described in Nuel et al. (2017a, 2017b). Briefly, the upstream WWTP is a two-stage Vertical Flow Constructed Wetland (VFCW), designed and operated according to the French guidelines (Molle et al., 2005). Before the first stage, a screening device is used as pretreatment to remove the largest particles. The WWTP receives only municipal wastewater from 970 population equivalent (PE) and was commissioned in 2009. The SFTW receives water from the VFCW second-stage outlet and from WWTP bypasses in the case of extreme rain events. The SFTW characteristics and inlet macropollutant concentrations expected are summarized in Table 1. Currently, natural vegetation is present only near the banks.

2.2. Monitoring of environmental parameters

The physicochemical parameters of the water at the SFTW inlet and outlet were monitored with a multi-parameter probe (YSI Incorporated,

Table 1
SFTW general characteristics.

Characteristics		Lutter
Design		Pond
Bank slope		1/4
Water depth (m)		0.1–0.2
Maximal width (m)		13
Maximal length (m)		40
Surface (m^2)		750
Surface per PE (m^2)		0.77
Volume (m^3)		425
Theoretical hydraulic residence time (h)		84 (±31)
Mean residence time derived from tracer experiments (h)[a]		15 (±7.8)
Mud thickness (m)		0.117 (±0.104)
Inlet concentrations (mg L^{-1})[b]	Biological oxygen demand (BOD)	28.5
	Chemical oxygen demand (COD)	38
	Suspended solids (SS)	46
	Kjeldahl nitrogen (NK)	2.5
	Total phosphorus (TP)	3.9

[a] Data from Nuel et al. (2017a, 2017b, 2017c).
[b] Data from Nuel et al. (2017b).

Yellow Springs OH, USA) to allow for the assessment of the effluent quality and their potential impact on pollutant removal capacities. For each sampling session, pH, conductivity, temperature, dissolved oxygen and redox potential were monitored every 5 min. The SFTW inlet and outlet flow rates were continuously monitored by built-in exponential section venturis (ISMA, Forbach, France) and ultrasonic probes (IJINUS, MELLAC, France). An in situ weather station (ADCON Telemetry, Klosterneuburg, Austria) collected weather data, including rain characteristics, wind speed, air hygrometry, solar radiation and atmospheric pressure. These data were used to estimate the evaporated volumes (due to the free-water surface) by the Rohwer equations (Rohwer, 1931) and the evapotranspired volumes (due to the development of plants) by the Penman-Monteith equation (Monteith and Unsworth, 1990). These losses/gains of water were used to compute the water mass balance for each sampling session.

2.3. Sample collection

The sampling sessions began on July 2015 and occurred on a regular basis during a period of 24 months. Overall, 7 sampling sessions were achieved. The SFTW inlet and outlet water (7 samples of each), plants (20 samples) and sediments (7 samples) were collected as described in Fig. 1.

2.3.1. Water

The SFTW inlet and outlet water samples were collected in glass bottles by automated refrigerated samplers (TELEDYNE ISCO, Lincoln, Nebraska) and kept cold (between 0 and 3 °C). Flow-proportional samples were taken to get representative average samples. The minimum sampling frequency was set at 150 samples (50 mL each) over a period of 24 h. Depending on the weather and flow patterns, between seven and 14 L per sampler were thus collected.

2.3.2. Plants

The SFTW vegetation is characterized by the planted local species (*Juncus effusus* and *Salix alba*) and the natural development of endogenous plants. Vegetation has naturally evolved since 2009. For this study, five target plants were sampled; white willow (*Salix alba*), yellow flag (*Iris pseudacorus*), soft rush (*Juncus effusus*), callitriche (*Callitriche palustris*) and sedge (*Carex caryophyllea*) (Fig. 1); only the leaves were collected to maintain the safety of the plants. The plants were chosen to be located around the SFTW influent pipe and near the preferential flow (as previously determined by dye tracer experiments in Laurent et al., 2015 and Nuel et al., 2017a). Willow, soft rush, callitriche and sedge were located <50 cm from the inlet whereas yellow flag was located 2 m away from the inlet. Approximately 150 g of each species was cut and kept in a cooler (between 0 and 3 °C) during transport. Samples were stored in a freezer (−20 °C) prior to pharmaceutical extractions and analysis.

2.3.3. Sediment

The SFTW presents an important mud thickness due to the ageing effect (Nuel et al., 2017a): between 10 and 50 cm of mud have been deposited at the bottom of the SFTW. Three samples of superficial mud from the SFTW inflow pipe, middle system and outflow pipe provided a composite sample of approximately 100 g (Fig. 1) that was kept in a cooler (between 0 and 3 °C) during transport, until extraction and analysis for pharmaceutical compounds.

2.4. Sample preparation

Sample preparation and drug extraction methodologies are fully described in Nuel et al. (2017c). Nevertheless, a summarized description of these methodologies is proposed below.

2.4.1. Drug extraction from aqueous samples

Water collected (200 mL) from the SFTW inflow and outflow (Fig. 1) was filtered through glass fibre filters at 1.22 μm and 0.45 μm. The resulting sample was then concentrated using a tandem specific-phase extraction (SPE) C18 and 1 g of the Hydrophilic-Lipophilic Balance (HLB) cartridge system (Imchem-Waters, Versailles, France). After concentration, the cartridges were eluted into glass vials with 10 mL of methanol. Next, the samples were dried using a SpeedVac (Savant Thermo Scientific, Villebon sur Yvette, France) and stored at −80 °C until analysis.

2.4.2. Drug extraction from plants

The collected plant tissues (150 g fresh weight) were lyophilized. A total of 20 g dry weight of each sample was ground with a Tissue Lyser I (QIAGEN, Courtaboeuf, France). The resulting powder was solubilized in 1 L acetonitrile with 0.5% formic acid (v:v) under gentle mixing over a period of 24 h at 4 °C. The supernatant was filtered through a 1.22 μm glass fibre filter. Then, the samples were concentrated using an SPE SiO_2 cartridge system (Imchem-Waters, Versailles, France). After concentration, the cartridges were eluted into glass vials with 10 mL of methanol:water (20:80 v:v). Next, the samples were dried using a SpeedVac (Savant Thermo Scientific, Villebon sur Yvette, France) and stored at −80 °C until analysis.

2.4.3. Drug extraction from sediment

One hundred grams of drained sludge was macerated in 1 L of acetonitrile with 0.5% formic acid during a period of 24 h at 4 °C. Next, the solution was filtered through a 1.22 μm glass fibre filter. Pharmaceutical compounds were extracted from the filtered solution as previously described (2.4.2 Plants).

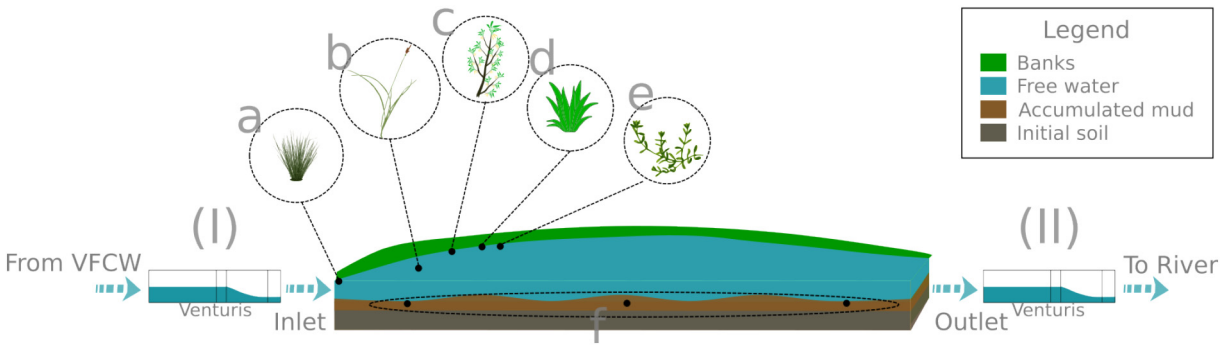

Fig. 1. SFTW operational principles in Lutter with: (I) and (II) respectively inlet and outlet SFTW samples, a: *Juncus effusus*, b: *Carex caryophyllea*,c: *Salix alba*, d: *Iris pseudacorus*, e: *Callitriche palustris* and f: mud, with: green area: SFTW banks, blue area: SFTW free water, light brown area: accumulated SFTW mud and dark brown: initial soil under the SFTW. (For interpretation of the references to colour in this figure legend, the reader is referred to the web version of this article.)

2.5. Sample analysis

Drug detection and quantification methodologies have been fully described in Nuel et al. (2017c). In all, 81 drug compounds and 4 metabolites (clofibric acid, ibuprofen acyl-β-D-glucuronide, *O*-desmethylnaproxen, *O*-desmethyltramadol and Paracetamol β-D-glucuronide) were investigated (Table 1S). A summarized description of these methodologies is given below.

2.5.1. Drug detection

Each plant, sediment and water sample was dried after extraction in a vacuum concentrator without heating and stored at −80 °C. On the day of the analysis, samples were solubilized in 400 μL of ultrapure water/methanol solution (90:10 v:v). After gentle vortexing for 12 h in a cold room, the samples were centrifuged for approximately 45 min at 16000 rpm and 300 μL of the remaining supernatant was used for ultra performance liquid chromatography coupled to mass spectrometry (UPLC-MS/MS) for drug identification and quantification. (Table 1S). For more details about the UPLC-MS/MS analysis and the detection of selected metabolites refer to Nuel et al. (2017c).

2.5.2. Drug quantification

Drugs detected in a sample were quantified using standard curves (from 1 μg L^{-1} to 10 mg L^{-1}). Regression coefficients were obtained by the linear correlation between the peak area and drug concentration, and the R^2 correlation of determination was always >0.96. Furthermore, RO 48–8071 was used as an internal standard and was injected at 10 μg L^{-1}. Drug concentrations were obtained using standard curve coefficients and the drug peak areas were all divided by the RO 48-8071 peak area. Thus, UPLC-MS/MS sensitivity differences between the establishment of standard curves and the samples analyses were considered. Finally, drug quantity injected on the UPLC-MS/MS was determined and extrapolated to the initial sample amount (i.e., volume for liquid samples, mass for solid samples).

2.6. Data processing

2.6.1. Treatment efficiency

SFTW Removal Efficiencies (RE) were calculated as follows:

$$RE(\%) = \frac{C_{Inlet} \cdot V_{Inlet} - C_{Outlet} \cdot V_{Outlet}}{C_{Inlet} \cdot V_{Inlet}} \quad (1)$$

where

- C_{Outlet}: Outlet concentration (μg L^{-1});
- V_{Outlet}: Outlet daily volume (m^3/d);
- C_{Inlet}: Inlet concentration (μg L^{-1});
- V_{Inlet}: Inlet daily volume (m^3/d).

To calculate RE, all concentration data were considered according to their own analytical precisions and quantification limits (QL). Concentrations below the QL were considered equal to the QL. Furthermore, removal efficiencies were calculated only if the inlet and outlet concentrations belonged to strictly different intervals. If not, RE was considered as zero. Moreover, for more convenient interpretation of results, removal efficiencies were ranked into 6 classes, in order of increasing efficiency: <0%, 0%,]0:30],]30:70],]70:90] and]90:100].

The calculation of RE considered only one compound and not the association of the parent drug and its metabolite. In addition, an RE of 100% does not mean that the compound was fully mineralized, but that it was not detected any more at the SFTW outlet. The reason for this disappearance could be volatilization, transfer to groundwater or uptake by plants, crops, animals, grass growing on the land, adsorption on mud (or sludge) (Monteiro and Boxall, 2010). It could also be subject to conjugation processes, which change the compound structure and properties (compounds resulting from conjugation processes were not measured in this study).

2.6.2. Database

Data acquisition and analysis were performed with MassLynx software V4.3 (Waters, Guyancourt, France). Peak integration and validation were done with QuanLynx software V4.1 (Waters, Guyancourt, France). All results were extracted as text files. Custom-programmed automatic programmes in Visual Basic for Applications 7.0 (Microsoft Corporation, Washington, United States) were used to format and integrate text data to Microsoft Access (Microsoft Corporation, Washington, United States). The aim of this database was to collect all area drugs and thanks to the range of the standards, to automatically calculate the concentrations of drugs for each sample. Thus, data-processing mistakes were limited and a high repeatability of results was provided.

2.6.3. Statistical analyses

Statistical analyses, such as Student's or Wilcoxon tests or ANOVA, were performed with R software (R Development Core Team, 2008).

3. Results

During these 2 years of study in a complex environment, physicochemical, meteorological and water quality data were collected. They characterized the different sampling sessions considering abiotic parameters. We will start by characterizing the local weather and physicochemical parameters for the eight sessions. Then, we will comment on the water budget, as removal efficiencies were calculated from the daily pollution load. Thereafter we will analyse drug concentrations in the influent, effluent, plants and sediment. We will eventually propose a qualitative and quantitative analysis of the removal efficiencies.

3.1. SFTW local weather

The weather parameters were significantly different at each sampling session: wind speed (p-value < 2.2E−16), solar radiation(p-value = 5E−11), hygrometry (p-value = 5.7E−08) and barometric pressure (p-value = 4.5E−04). Air temperature was significantly different but to a lower extent (p-value = 1.6E-02).

According to the air temperature (Table 2), experiments are considered as seasonal averages for each season (Lameteo.org, 2017). During 5.Wint16 sampling session, the VFCW second treatment stage was clogged for a few days before the session.

3.2. Water budget

The SFTW influent and effluent flow rates were all compared using the Student test. According to these results, the inlet and outlet flow rates were significantly different.

Table 2
Weather data (±standard deviation) during the sampling sessions. For each session, the table displays average values for air temperature, hygrometry and wind speed while solar radiation values are summed. The following abbreviations are used: Spri: Spring; Sum: Summer, Aut: Autumn and Win: Winter. Each session is identified by its rank, the season and the year. 1. Sum15 means the first during summer 2015.

Season	Month	Temperature (°C)	Solar radiation (W/m^2)	Hygrometry (%)
1. Sum15	July	21.9 (±6)	31,104	64.6 (±21.1)
2. Sum15	September	15 (±3.9)	18,590	79.9 (±16.1)
3. Aut15	November	−2.3 (±3.4)	6919	88.2 (±9.8)
5. Wint16	Marsh	2.9 (±3.8)	11,770	81.9 (±13.6)
7. Sum16	July	15.1 (±3.1)	8229	88.8 (±9.3)
8. Sum16	September	20.8 (±5.6)	16,674	76.5 (±17.8)
9. Aut16	November	−0.5 (±3.2)	6490	91.9 (±8.2)

In most cases, the SFTW peak flow attenuation was about 9% (Fig. 2). Globally, the water budget was influenced by evaporation and tidal range whereas infiltration and evapotranspiration were limited respectively due to clay on the SFTW bottom (to ensure imperviousness) and to the low vegetation density. During 1.sum15 and 9.Aut16 sampling sessions, the SFTW water level decreased (visual observation), which impacted the SFTW water balance. The water level in this system can evolve because of the tidal range.

3.3. Physicochemical parameters affected by SFTW

The inlet and outlet physicochemical parameters (pH, temperature, conductivity, redox potential and dissolved oxygen) were monitored during each sampling session. All these parameters characterize the SFTW influent and effluent and can help in characterizing removal processes. Considering all these physicochemical parameters (Table 2S), their variability and average were different between the inlet and the outlet, as exemplified by the parameter of water temperature: on 1.sum 15 the inlet average was at 9.1 °C (±0.2 °C) whereas the outlet average was at 6 °C (±2 0 °C). The SFTW abiotic and subsequently biotic processes could be strongly influenced by the daily variation in weather. According to the seasons, the SFTW had a strong impact on the inlet dissolved oxygen and redox potential parameters (p-value = 2.2E − 16 for both parameters). Actually, redox potential measurements allow characterizing the water as an oxidizing (high values) or reducing (low value) environment. The value of the redox potential at the inlet is larger than at the outlet whereas its variability is higher at the outlet than at the inlet (the inlet parameters were buffered by the upstream VFCW whereas the outlet parameters were impacted by the SFTW). Actually, there were exceptions on 5.wint16 and 9.aut16 where the inlet and outlet redox potential values were not significantly different (according to their associated standard deviations). At 5.wint16 session, the inlet redox potential was unusually low, certainly due to the clogging of the VFCW second stage (Section 3.1 *SFTW local weather*) during many days. At the 9.Aut16 session, the inlet and outlet flow rates were highest which suggested a short and unusual residence time. Thus, the SFTW buffer effect on this parameter was limited. Overall, redox potential values were highly impacted by the pond. Thus, the SFTW provides a more reducing water environment at the outlet than at the inlet. This change, from an oxidative to a reducing environment, may impact biochemical processes occurring inside this SFTW, especially for the efficiency of drug removal (Tiwari et al., 2017). The redox potential decrease can be explained by the prevalence of reduction reactions occurring in the SFTW over oxygen transfer between the atmosphere and the SFTW water surface.

Comparing all the sampling sessions, we clearly observe that the seasons have a significant impact on the SFTW physicochemical parameters and these variations may play an important role in the drug removal efficiency by the SFTW throughout the seasons. In most cases, flow attenuation occurs in this SFTW. Does this lead to a decrease in drug concentration in the outflow water thanks to plants and/or mud dispersion or on the contrary, to an increase of drug concentration in the SFTW?

3.4. Drug occurrence

Drug concentrations are presented in the Supplementary data (Fig. 1S and Table 3S for water samples, Table 4S for plant samples and Fig. 2S for sediment samples).

3.4.1. Seasonal drug variations in water samples

During all sessions, between 22 and 33 and 19 to 35 compounds were detected, respectively at the inlet and at the outlet of the system (Fig. 3). Furthermore, we observed the highest number of drugs during the winter and the lowest one during the summer. Human drug consumption and upstream WWTP removal ability during the summer could explain this observation but these were not studied here. In addition, during warm periods, the number of drugs along the SFTW was lower than during cold ones.

Throughout the sampling sessions (Fig. 1S and Table 3S), the three most frequent compounds at the SFTW inflow were alpha ethinylestradiol (1140.62 μg L^{-1}; ±1131.54 μg L^{-1}; n = 3), tramadol (222.36 μg L^{-1}; ±161.89 μg L^{-1}; n = 7) and theophylline (31.80 μg L^{-1}; ±38.28 μg L^{-1}; n = 7) whereas at the outflow, they were alpha ethinylestradiol (901.62 μg L^{-1}; ±1328.53 μg L^{-1}; n = 4), tramadol (193.72 μg L^{-1}; ±160.74 μg L^{-1}; n = 5) and losartan (22.87 μg L^{-1}; ±27.12 μg L^{-1}; n = 7). At both sampling points, indomethacin was present the least frequently (inlet: 1.25 10^{-3} μg L^{-1}; n = 1; outlet: 1.87 10^{-3} μg L^{-1}; ±27.12 μg L^{-1}; n = 7). Finally, prednisolone, amoxicillin and topiramate were detected only in the inflow water, which suggests a complete transformation of these molecules. In contrast, sulfadiazine, sertraline, gemfibrozil and haloperidol were only detected in the outflow water. Deconjugation of the drug molecules must have occurred during transport in the SFTW (Verlicchi and Zambello, 2014).

We emphasize that drug analyses on water samples were done for only the dissolved pollutants. Indeed, water samples were filtered to at least 0.22 μm to preserve SPE cartridges. Thus, compounds adsorbed on suspended solids reaching the river were not quantified here but they can play an important role in case of high turbidity or algae development.

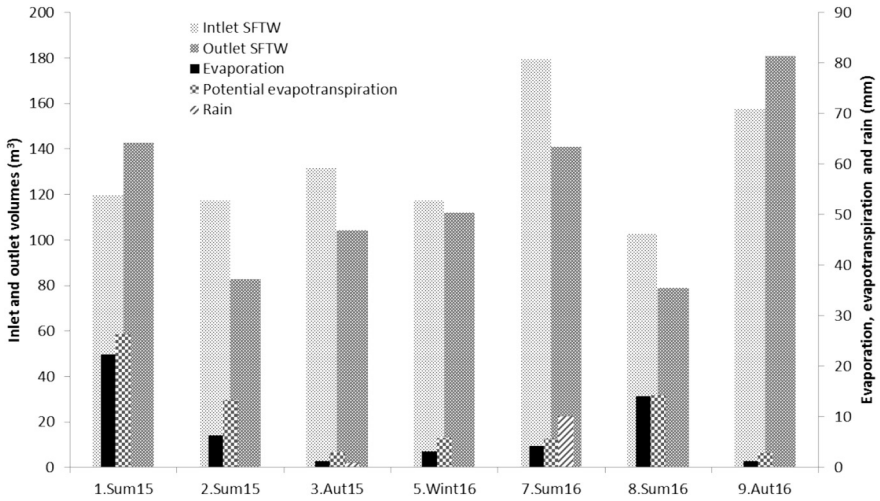

Fig. 2. SFTWs water budget: total inlet and outlet volumes (left axis) and evaporation, potential evapotranspiration and rainfall depth (right axis) during the seasonal sampling sessions.

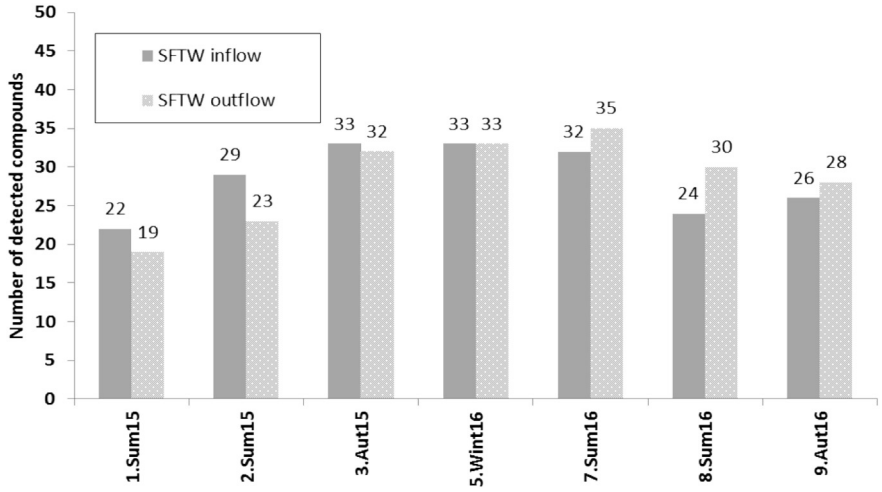

Fig. 3. Number of detected compounds.

3.4.2. Drug distribution in plants and sediment samples

Sediments were sampled for each sampling session whereas plants were sampled when there were enough leaves to compose a complete sample (approximately 150 g; refer to Section 2.3.2 *Plants*) and to ensure the development of the plants until the next sessions. It can be noted that callitriche disappeared after 7.Sum16 session (Fig. 4).

3.4.2.1. Drug and metabolites frequently up taken by plants. Between 5 (sedge on 8.Sum16) and 23 (willow on 2.Sum15) drug compounds were detected in the plant samples (Fig. 4). The three highest average drug concentrations were reported for each plant sample (Table 4S):

- Callitriche: tramadol at 194.66 ng/g, telmisartan at 29.4 ng/g (also detected in rush) and ofloxacin 12.92 ng/g. The pharmaceutical uptake ability of callitriche is poorly studied in the literature. Nevertheless, Wilkinson et al. (2016) detected acetaminophen and diclofenac in callitriche sampling from the Thames River (Great Britain);
- Sedge: ibuprofen at 290.12 ng/g, tramadol at 77.70 ng/g and prednisolone at 60.97 ng/g. There is no published result on pharmaceutical uptake from sedge samples;
- Iris: theophylline at 55.25 ng/g, losartan at 52.85 ng/g (also detected in willow) and tramadol at 31.05 ng/g. Drug transfers from wastewater to the iris plant were already observed by (Mackul'ak et al., 2015a) where they detected cotinine (239 ng/g), methamphetamine (127 ng/g), tramadol (578 ng/g), venlafaxine (112 ng/g) and oxazepam (37 ng/g);
- Rush: alpha ethinylestradiol at 294.75 ng/g (also detected in willow), tramadol at 74 ng/g and ibuprofen acyl-β-D-glucuronide at 29.66 ng/g (also detected in iris and willow). The compound Ibuprofen was also detected at 12.56 ng/g. In addition, it can be nearly completely removed, metabolized and stored equally in the leaves and roots (Y. Zhang et al., 2016; Matamoros et al., 2012a);

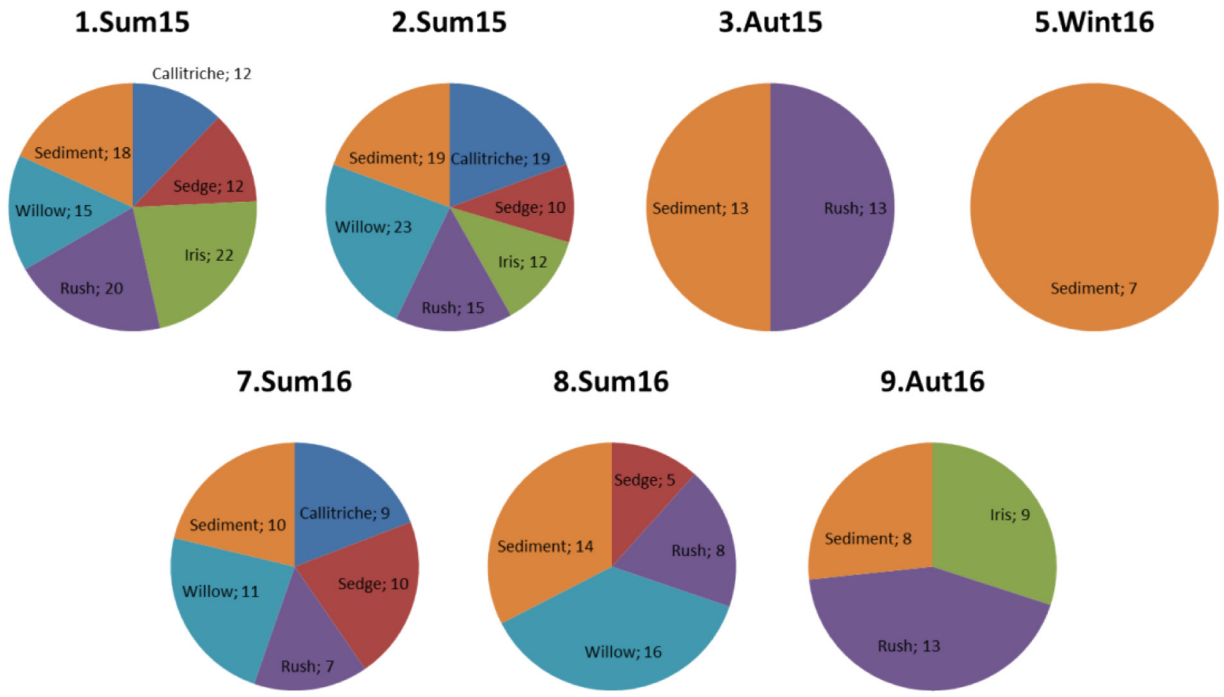

Fig. 4. Drug compound number in plants and sediment throughout the sampling campaign. The following abbreviations were used: Sum: Summer, Aut: Autumn and Win: Winter. Each campaign is identified by its rank, the season and the year. 1.Sum15 means the first campaign during summer 2015.

- Willow: tramadol at 286.51 ng/g, mefenamic acid at 206.36 ng/g and alpha ethinylestradiol at 157.48 ng/g. Specific attention must be paid to the willow sample because it was the only tree sample whereas others were annual plants. Actually, willow appeared to have an annual and continuous increase in the variety of drugs over time (Fig. 4). It may be the consequence of the high water consumption by willow (Persson, 1995; Martin and Stephens, 2006) which is mainly related to plant size, leaf surface area and tends to increase in the late summer (Pellis et al., 2004; Ceulemans et al., 1996).

Tramadol was detected at fairly high concentrations in plants, sediment and in the SFTW influent (an average maximum concentration of 273.74 μg L^{-1}). Regularly detected in relatively high concentration in both the inflow and outflow, tramadol appears to be poorly eliminated (<22%) by WWTPs (Mackuľak et al., 2015b). However, during a mean residence time of 96 h, its uptake capacity by aquatic plants (*C. caroliniana, L. sessiliflora* and *E. najas*) ranged between 29% and 59% (Mackuľak et al., 2015a). In addition, drug distributions in plants were different in each sample analysed even though they were exposed to the same flow. This specific transfer may be due to the plant and properties of the drug molecules. Indeed, it seems that molecules with intermediate polarity could be easily transported to plant shoots (Tanoue et al., 2012).

Furthermore, human organisms generally eliminate active drug compounds by excretion into urine. Thus many metabolites can originate from a single compound. In this study, one of the major metabolites of clofibrate (clofibric acid), ibuprofen (ibuprofen acyl-β-D-glucuronide), naproxen (*O*-desmethylnaproxen), paracetamol (paracetamol acyl-β-D-glucuronide) and tramadol (*O*-desmethyltramadol) were observed:

- Ibuprofen is oxidized into temporary intermediate compounds (carboxyibuprofen and hydroxyibuprofen) that are then conjugated into an acyl glucuronide: ibuprofen acyl-β-D-glucuronide. Ibuprofen was detected in all plant samples whereas ibuprofen acyl-β-D-glucuronide was detected only in iris (3.15 ng/g), rush (29.66 ng/g ± 1.65 ng/g) and willow (0.86 ng/g);
- Naproxen is metabolized to *O*-desmethylnaproxen by organisms. Although naproxen was present in callitriche (4.02 ng/g), iris (4.11 ng/g) and willow (3.28 ng/g), its metabolite was not found in plants. However, it was detected both in the influent (7.44 ng L^{-1}) and the effluent (11.83 ng L^{-1});
- Although up to 55% of paracetamol can be metabolized into its acyl glucuronide metabolite (DrugBank, 2017), this metabolite was not detected in the samples.
- Approximately 30% of a tramadol dose is excreted in the urine unchanged, whereas 60% of the dose is excreted as 11 different metabolites (Pubchem, 2017). *O*-desmethyltramadol is the most common of them and it is still pharmacologically active in animal models. In this study, *O*-desmethyltramadol was detected in the SFTW influent (average of 1,46 μg L^{-1}), effluent (average of 1,8 μg L^{-1}; ±0.4 μg L^{-1}) and sediment (average of 7.57 ng/g). It was not found in any plants (Table 4S).

These results show how crucial it is to search for active drug compounds and their metabolites. Indeed, only a few metabolites were investigated in this study, but their detection in plant and water samples suggests complex conjugation/deconjugation processes, influenced by the season as the exports to plants is higher during the summer. Among the five plant species observed, sedge seems to be less efficient in the uptake of drugs from water than are rush and willow. Considering the annual uptake, willow contains more drugs and at higher concentrations than does rush. This interpretation could be enriched by the knowledge of each biomass species variety in the SFTW to compute the total drug mass uptake.

3.4.2.2. Complex mechanisms involving drugs in sediments. Maximal average concentrations were reached by tramadol (81.73 ng/g; ±46.88 ng/g; n = 5), estriol (22 ng/g; n = 1) and *O*-desmethyltramadol (7.57 ng/g; n = 1); minimal concentrations were reached by lamotrigine (42.49 10^{-3} ng/g; n = 1), clindamycin (10.17 10^{-3} ng/g; ±12.70 10^{-3} ng/g; n = 3) and ketoprofen (6.93 10^{-3} ng/g; n = 1) (Fig. 2S). Paracetamol and propafenone compounds were systematically detected in soil samples at respectively 0.16 ng/g (±0.3) and 3.14 ng/g (+/− 6.19). Finally, atenolol, bisoprolol, paracetamol and propafenone were detected in every sediment sample.

During both years, the maximum number of drugs detected in the sediment was reached at the second summer session whereas the minima were reached during winter (Fig. 4). As a reminder, the highest number of drugs in water samples was during the winter and the lowest was during the summer (Fig. 3). We also emphasize that sediment samples were a mix of material accumulation in large part and fresh mud input from the VFCW and WWTP by-passes to a lesser extent. Thus drug composition reflected degradation processes occurring in mud. We can note that session after session, the sediment drug composition varied strongly (7 compounds on 5.Wint16 to 19 ones on 2.Sum15), which suggests complex and various mechanisms and reactions as biotic (plants, microorganisms, animals, bioturbation as a physical mixing process, etc.) and abiotic (hydrologic effects, flowrate, physicochemistry, weather, different chemical properties among the parent pharmaceuticals, etc.) parameters permanently interact.

Drugs behaviour in sediment depends on many factors, such as the characteristics of the compounds (molecular structure, chemical properties (octanol-water distribution coefficient (Kow) and solid-liquid partition coefficient (Kd)), sludge properties (organic fraction, cation exchange capacity, SS size) and environmental conditions (pH for example) (Verlicchi and Zambello, 2015). In addition, biological degradation is meant to be the key mechanism responsible for the maximum removal of organic micropollutants, as pharmaceutical compounds, in a WWTP (Tiwari et al., 2017). As most of the microbial community can be found in the sediment and rhizosphere of wetlands (Brix, 2003), the variation in drug number throughout the season in sediment samples could be partly explained by the growth cycle of plants.

These concentrations in plants and sediment samples show that (i) the concentration range is fairly large, (ii) drug transfer to plants appears to be specific for each studied plant and (iii) a large part of the detected compounds are present in all plants and soil.

3.5. Drug residue removal efficiencies

3.5.1. Qualitative seasonal variation

As described in Section 2.6.1 *Treatment efficiency*, the drug removal efficiencies were gathered by their efficiency class (Fig. 5). Drug removal efficiencies are detailed in Table 5S.

First, there is a drug variability repartition into efficiency classes, although throughout all the sampling sessions, the null efficiency class was the most populated one. In decreasing order, it is followed by the <0%,]0:30]]30:70],]70:90] and]90:100] classes. As a reminder, the SFTW is located downstream of a two-stage VFCW, thus it must be considered as a tertiary treatment and its influent water quality as treated water.

Second, we observe a correlation between the removal class efficiency and seasons. Indeed, positive removal efficiencies were higher during the summer and their number decreased until the winter period. In contrast, the null efficiency class presence was higher in winter. Throughout the entire campaign, the negative efficiency class continuously increased until 8.Sum16. As previously noted in Section 3.1 *SFTW local weather*, local climate impacted directly and indirectly on the water pollutant degradation process (Hijosa-Valsero et al., 2011a, 2011b;

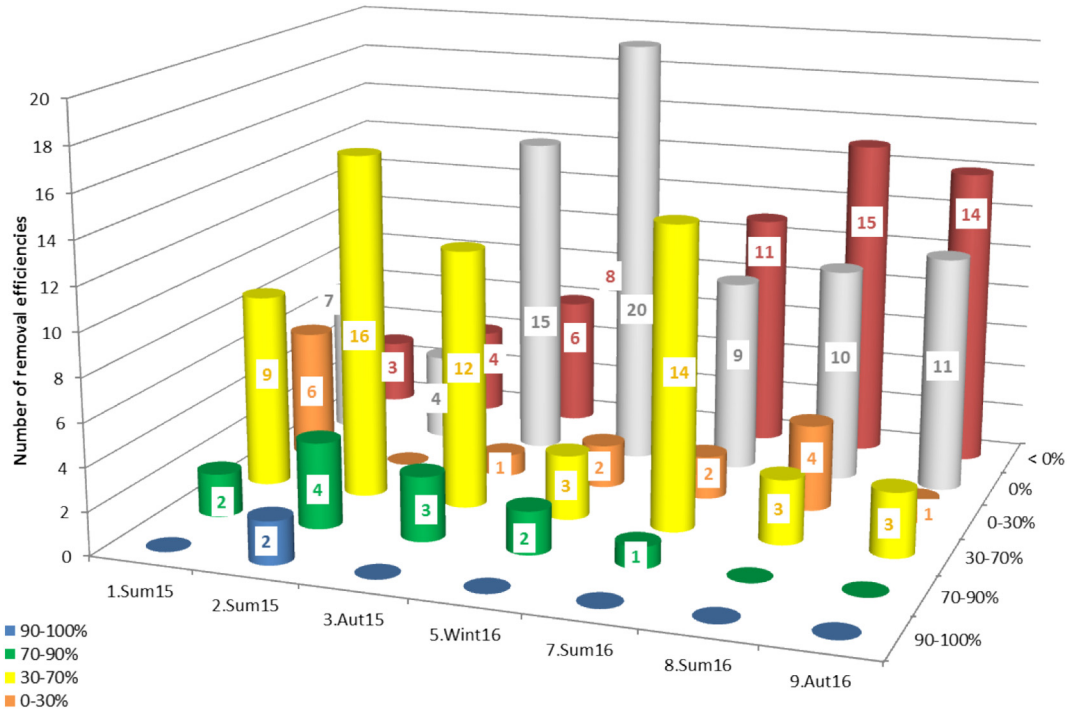

Fig. 5. SFTW drug removal gathered by class efficiency.

Matamoros et al., 2012a; Reyes-Contreras et al., 2011; Nuel et al., 2017b). In fact, we see two major weather parameters that are able to influence removal efficiency:

- Solar radiation penetration into SFTW water, which induces direct and indirect photodegradation, especially in ponds during the summer (Rühmland et al., 2015). Direct photodegradation corresponds to the direct lysis of molecules after UV action. Indirect photodegradation generates strong oxidant molecules as, for example, O_2 (Haag and Hoigne, 1986) or H_2O_2 (Draper and Crosby, 1983) which in turn oxidize other molecules such as pharmaceutical compounds. In part Section 3.1 *SFTW local weather*, we already observed that throughout all the monitoring sessions, solar radiation strongly varied (from 6489.8 W/m^2 (9.Aut16) to 31,103.7 W/m^2 (1.Sum15)) and should impact the drug degradation processes.
- Temperature influences water microorganism communities (slowing activity during cold periods and favouring activity during warm periods) which are the first responsible for organic pollutant degradation (Hijosa-Valsero et al., 2011b). In part Section 3.3 *Physicochemical parameters affected by SFTW* we observed that the SFTW outlet water temperature varied daily during sessions and that it depended on the season under consideration. In addition, in case of a frozen water surface, solar radiation penetrations are strongly limited, and consequently so is photodegradation. High or low seasonal temperatures strongly influence the development of plants and associated mechanisms.

These observations can explain why better removal efficiencies were observed during warm periods. In contrast, low water temperature and low solar radiation during winter periods could explain why a major part of the RE was negative or null in winter.

Furthermore, the presence of many negative removal classes can be explained by the presence of conjugated compounds in the SFTW influents due to VFCW treatment process (not studied here), thus the drug substances themselves were seen at low levels. At the same time, deconjugation processes occurred, due to photodegradation or microorganisms, and the drug substances were quantified at high levels in the effluent (Verlicchi and Zambello, 2014). Another reason for the increase of negative removal efficiencies during autumn and winter can be a release from the soil compartment. The drug number decreases (Fig. 4) from summer to winter (Fig. 4) and the total mud volume in the SFTW can be estimated at >80 m^3 (results not shown); Thus, even if there were drugs at trace concentrations (Fig. 2S), a drug release may have significant impacts on the effluent flow drug concentration. In addition, we previously highlighted that there is a strong ageing effect on this SFTW due to the sedimentation process of suspended solids coming from the VFCW overflows and bypasses (M. Nuel et al., 2017a). The SFTW hydrodynamic behaviour changes over the years and we suppose that it becomes less efficient for drug removal as ageing occurs.

Considering the three highest average concentrations (Fig. 1S), alpha ethinylestradiol, theophylline and tramadol, their removal efficiency varied throughout the sampling sessions (Table 5S). Alpha ethinylestradiol was detected at the 1.Sum15, 7.Sum16 and 9.Aut16 sessions with, respectively, null, −191% and −144% removal efficiencies. Theophylline and tramadol were always detected in the inlet and outlet water. Theophylline removal efficiencies were between 0% and 72% whereas tramadol appeared to be a refractory compound among the SFTW removal processes (between −253% (1.Sum15) and 60% (9.Aut16)).

In seven sessions, bisoprolol, candesartan, carbamazepine, gabapentin, nefopam, paracetamol, sotalol and telmisartan compounds were the most released compounds. Furthermore, a large part of them was present in the 8.Sum16 and 9.Aut16, sessions with the higher negative efficiency class score.

Lastly, two compounds had an elimination efficiency above 90% in the 2.Sum15 session only: estriol (93%) and paracetamol (96%). Estriol was also significantly detected in the inflow and outflow during 3.Aut15 but its RE was null. Paracetamol was detected in every sampling session and was gathered in many efficiency classes: <0 in (5.Wint16, 8.Sum16, 9.Aut16), in]30:70] in (3.Aut15, 7.Sum16), in]70:90] in (1.Sum15) and in 95%]90:100] in (2.Sum15).

3.5.2. Drug RE quantification

Considering the eight sampling sessions, all the efficiency classes on drugs are reported in Fig. 6. They are sorted from the most-frequently to the least-frequently detected compound.

Thirteen compounds were always detected in both the influent and effluent. According to removal class colour codes, their associated RE varied greatly throughout the sampling sessions and may correlate with seasonal weather (Section 3.5.1 *Qualitative seasonal variation*). As can be observed in Fig. 6, all the drug compounds had one negative or/and null RE rates (expected for eprosartan and metoprolol) at least. On the other hand, even drug residues that sometimes were >70% degraded (amitriptyline, atorvastatin, caffeine, estriol, fenoprofen, ketoprofen, paracetamol, phloroglucinol, and ramipril) also had negative or null removal rates. Through many publications, Verlicchi and Zambello (2014) also reported high removal efficiency variations for one compound considered. In the case of estriol, for example, it was detected two times and its associated removal efficiencies were null (3.Aut15, in autumn) and [30–100%] (2.Sum15, in summer). As a reminder, removal efficiencies were calculated from compound concentrations and the daily volumes of inflow and outflow. Thus, removal efficiency value variations need to be correlated with the inflow volume reduction (Fig. 2), especially during summer periods (Table 2). Additionally, physicochemical processes and microbial activity variations were correlated to seasonal weather fluctuations and may affect drug removal efficiencies.

In this part we emphasized that pharmaceutical removal efficiencies were variable according to the drug compound detection frequency, RE rate variations throughout the season observed and a continuous increase of drug release from the SFTW. In addition, the question of the behaviour of pharmaceutical compound in the SFTW as a tertiary treatment is a complex problem with many variables where abiotic parameters, a seasonal effect or physicochemical parameters play an important role in global RE.

4. Conclusions

This study shows that the behaviour of human drug residues in the SFTW is influenced by many factors. First, compounds were not always detected in water in each sample session. Obviously, it depended on their consumption by homes connected to the sewage collection network and on the removal capacity of the upstream WWTP. Second, the properties of the studied drugs rule their behaviour within the SFTW. Biodegradation, molecular photodegradability, sediment adsorption, plant uptake ability, and transformation to many different metabolites by microorganisms have to be considered to interpret the drug RE rates. Additionally, the seasons play an important role in the removal

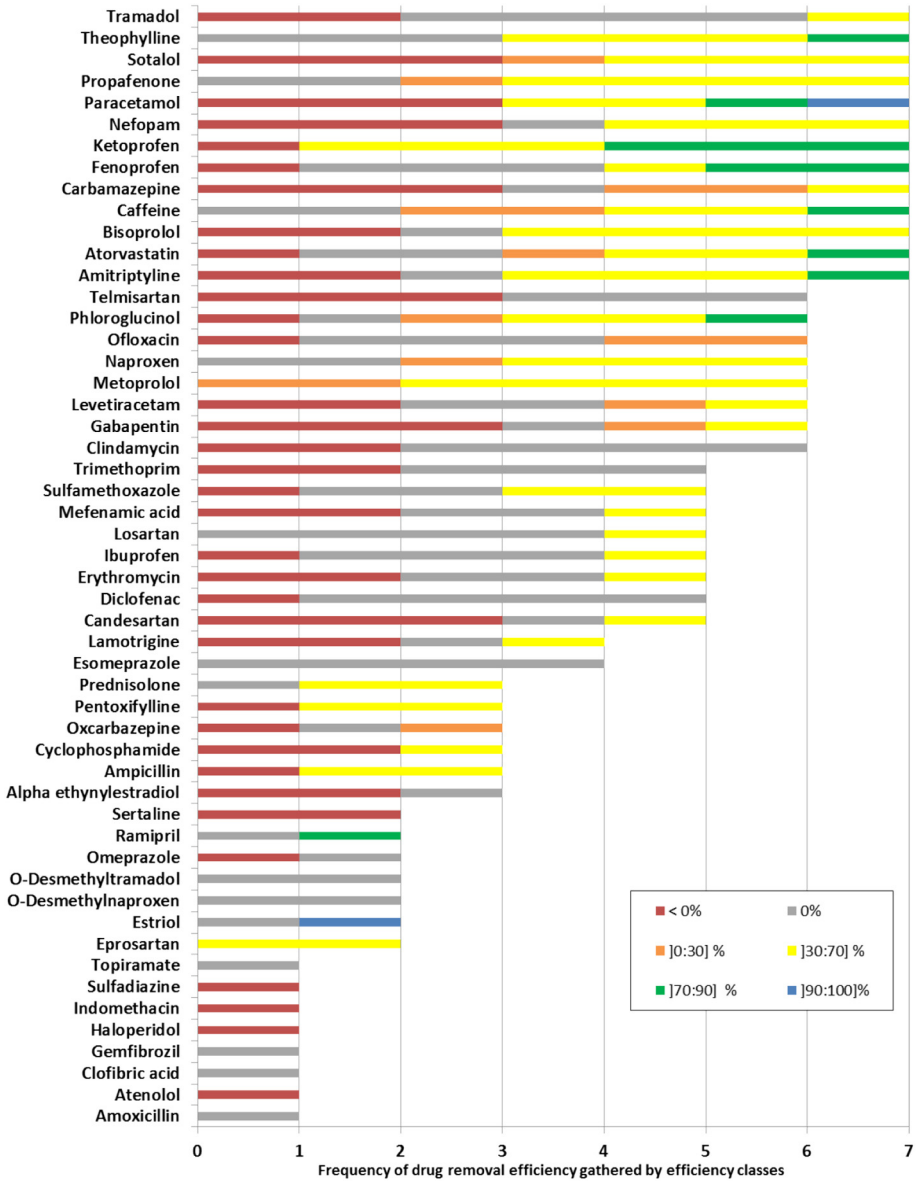

Fig. 6. Removal efficiency classes reported for each drug compound detected during the eight sampling session.

capacity of the wetland, especially solar radiation and air temperature which significantly influence the physicochemical parameters and biological processes. Considering all these parameters, it is difficult to define a typical behaviour for each drug in an SFTW. Overall, the inlet SFTW drug concentrations ranged between 1 ng L^{-1} and 1 mg L^{-1} and one active compound can be metabolized into many others that are usually not monitored.

However, we highlighted that drug removal efficiency within the SFTW followed a seasonal trend, with the best results occurring in the summer. There is also a seasonal effect on sediment uptake ability since a somewhat dynamic transfer was observed with a maximum drug accumulation in summer and a release during the winter period. This seems to be linked to a physicochemical parameter variation due to a seasonal effect. We also observed a specific drug transfer from water and soil to leaves according to plant species, even if plants are only present during a few months of the year around the SFTW. Furthermore, in the SFTW each drug was degraded and global RE values were better in the summer than in the winter. As the SFTW can be considered as a tertiary treatment process, it could be interesting to compare the relative efficiencies of the SFTW vs. the VFCW.

Finally, we observed a continuous degradation of removal efficiency. It may mean that the ageing of the SFTW goes along with a decrease in drug removal ability, in addition to the seasonal effect. It could also be used as an indicator for sludge extraction requirements. This sludge, especially if used agriculturally, should be assessed as potentially containing various drug compounds.

Acknowledgements

This study was funded by the Agence de l'Eau Rhin-Meuse, Région Alsace and Ecole Nationale du Génie de l'Eau et de l'Environnement (ENGEES). The authors wish to thank the Lutter local authorities for allowing us to perform experiments on their WWTP.

Appendix A. Supplementary data

Supplementary data to this article can be found online at https://doi.org/10.1016/j.scitotenv.2017.10.061.

References

Boutin, Catherine, Iwema, Arthur, Lagarrigue, Céline, 2010. Point Sur Les Zones de Dissipation Végétalisées: Vers Une Protection Supplémentaire Du Milieu Récepteur de Surface? http://epnac.irstea.fr/wp-content/uploads/2012/08/Expertise_cemagref_RMC_ZRV_juin_2010.pdf

Brix, Hans, 2003. Plants used in constructed wetlands and their functions. Proceedings of the 1st International Seminar on the Use of Aquatic Macrophytes for Wastewater Treatment in Constructed Wetlands, Lisboa, Portugal. 810, p. 81109 (https://www.researchgate.net/profile/Hans_Brix/publication/230563384_Plants_used_in_constructed_wetlands_and_their_functions/links/00b4952c01bcfede04000000.pdf).

Carvalho, Pedro N., Clara, M., Basto, P., Marisa, C., Almeida, R., Brix, Hans, 2014. A review of plant–pharmaceutical interactions: from uptake and effects in crop plants to phytoremediation in constructed wetlands. Environ. Sci. Pollut. Res. 21 (20), 11729–11763.

Ceulemans, R., McDonald, A.J.S., Pereira, J.S., 1996. A comparison among eucalypt, poplar and willow characteristics with particular reference to a coppice, growth-modelling approach. Biomass Bioenergy, Model. Short Rotation For. Growth 11 (2):215–231. https://doi.org/10.1016/0961-9534(96)00035-9.

Dordio, A.V., Maria, Belo, Martins Teixeira, D., Palace Carvalho, A.J., Dias, C.M.B., Picó, Yolanda, Pinto, Ana Paula, 2011. Evaluation of carbamazepine uptake and metabolization by *Typha* spp., a plant with potential use in phytotreatment. Bioresour. Technol. 102 (17), 7827–7834.

Draper, William M., Crosby, Donald G., 1983. The photochemical generation of hydrogen peroxide in natural waters. Arch. Environ. Contam. Toxicol. 12 (1), 121–126.

Acetaminophen. In: DrugBank (Ed.), DrugBank (https://www.drugbank.ca/drugs/DB00316).

Ellis, John Bryan, 2006. Pharmaceutical and personal care products (PPCPs) in urban receiving waters. Environ. Pollut. 144 (1), 184–189.

Fonder, Nat, Headley, Tom, 2013. The taxonomy of treatment wetlands: a proposed classification and nomenclature system. Ecol. Eng. 51 (February):203–211. https://doi.org/10.1016/j.ecoleng.2012.12.011.

Gros, Meritxell, Petrović, Mira, Barceló, Damiá, 2006. Development of a multi-residue analytical methodology based on liquid chromatography–tandem mass spectrometry (LC–MS/MS) for screening and trace level determination of pharmaceuticals in surface and wastewaters. Talanta 70 (4):678–690. https://doi.org/10.1016/j.talanta.2006.05.024.

Haag, Werner R., Hoigne, Juerg, 1986. Singlet oxygen in surface waters. 3. Photochemical formation and steady-state concentrations in various types of waters. Environ. Sci. Technol. 20 (4), 341–348.

Hijosa-Valsero, Maria, Matamoros, Victor, Pedescoll, Anna, Martin-Villacorta, Javier, Becares, Eloy, Garcia, Joan, Bayona, Josep M., 2011a. Evaluation of primary treatment and loading regimes in the removal of pharmaceuticals and personal care products from urban wastewaters by subsurface-flow constructed wetlands. Int. J. Environ. Anal. Chem. 91 (7–8), 632–653.

Hijosa-Valsero, M., Matamoros, V., Sidrach-Cardona, R., Pedescoll, A., Martín-Villacorta, J., García, J., Bayona, J.M., Bécares, E., 2011b. Influence of design, physico-chemical and environmental parameters on pharmaceuticals and fragrances removal by constructed wetlands. Water Sci. Technol. 63 (11):2527. https://doi.org/10.2166/wst.2011.500.

Kadlec, R.H., Knight, R.L., 1996. Treatment Wetlands. CRC, Baca Raton, FL.

Kolpin, Dana W., Furlong, Edward T., Meyer, Michael T., Michael Thurman, E., Zaugg, Steven D., Barber, Larry B., Buxton, Herbert T., 2002. Pharmaceuticals, hormones, and other organic wastewater contaminants in U.S. streams, 1999 to 2000 a national reconnaissance. Environ. Sci. Technol. 36 (6):1202–1211. https://doi.org/10.1021/es011055j.

Lameteo.org, 2017. Normales Climatiques 1981–2010: Mulhouse' (Accessed June 15. http://www.lameteo.org/index.php/climatologie/1637-normales-climatiques-1981-2010-mulhouse).

Laurent, J., Bois, P., Nuel, M., Wanko, A., 2015. Systemic models of full-scale surface flow treatment wetlands: determination by application of fluorescent tracers. Chem. Eng. J. 264 (March):389–398. https://doi.org/10.1016/j.cej.2014.11.073.

Mackul'ak, Tomáš, Mosný, Michal, Škubák, Jaroslav, Grabic, Roman, Birošová, Lucia, 2015. Fate of psychoactive compounds in wastewater treatment plant and the possibility of their degradation using aquatic plants. Environ. Toxicol. Pharmacol. 39 (2):969–973. https://doi.org/10.1016/j.etap.2015.02.018.

Mackul'ak, T., Grabic, R., Birosova, L., 2015. Aquatic plants as a possible way for physchoactive pharmaceuticals and drugs removal from wastewater. Proceedings of the 14th International Conference on Environmental Science and Technology (September. http://cest2015.gnest.org/papers/cest2015_00385_poster_paper.pdf).

Malamaire, G., 2009. GUIDE: Les Zones de Rejets Intermédiaires – Des Procédés Naturels Pour Réduire L'impact Du Rejet Des Stations D'épuration Sur Les Milieux Aqautiques. http://www.arpe-paca.org/files/20090831_zrimaquetteZRI.pdf.

Martin, Peter J., Stephens, William, 2006. Willow growth in response to nutrients and moisture on a clay landfill cap soil. II: water use. Bioresour. Technol. 97 (3):449–458. https://doi.org/10.1016/j.biortech.2005.03.004.

Matamoros, Víctor, Nguyen, Loc Xuan, Arias, Carlos A., Salvadó, Victòria, Brix, Hans, 2012a. Evaluation of aquatic plants for removing polar microcontaminants: a microcosm experiment. Chemosphere 88 (10):1257–1264. https://doi.org/10.1016/j.chemosphere.2012.04.004.

Matamoros, Víctor, Sala, Lluís, Salvadó, Victòria, 2012b. Evaluation of a biologically-based filtration water reclamation plant for removing emerging contaminants: a pilot plant study. Bioresour. Technol. 104, 243–249.

McClellan, Kristin, Halden, Rolf U., 2010. Pharmaceuticals and personal care products in archived US biosolids from the 2001 EPA National Sewage Sludge Survey. Water Res. 44 (2), 658–668.

Molle, P., Liénard, A., Boutin, C., Merlin, G., Iwema, A., 2005. How to treat raw sewage with constructed wetlands: an overview of the French systems. Water Sci. Technol. 51 (9), 11–21.

Monteiro, Sara C., Boxall, Alistair B.A., 2010. Occurrence and fate of human pharmaceuticals in the environment. Rev. Environ. Contam. Toxicol.:53–154 https://doi.org/10.1007/978-1-4419-1157-5_2.

Monteith, John Lennox, Unsworth, M.H., 1990. Principles of Environmental Physics. Butterworth-Heinemann.

Nilsen, Elena B., 2007. Pharmaceuticals and personal care products detected in sediments of the Lower Columbia River Basin. 6th International Conference on Pharmaceuticals and Enocrine Disrupting Chemicals in Water (https://ngwa.confex.com/ngwa/pharm6/techprogram/P4483.HTM).

Nuel, M., Laurent, J., Bois, P., Mose, R., Heintz, D., Wanko, A., 2015. 'Seasonal and Aging Effects on Hydraulic Behaviour of Two Surface Flow Treatment Wetlands – Fluorescent Tracers Application in Field Conditions'. presented at the WETPOL 2015 - 6th International Symposium on Wetland Pollutant Dynamics and Control, Cransfield, September.

Nuel, M., Laurent, J., Bois, P., Heintz, D., Mose, R., Wanko, A., 2017a. Seasonal and ageing effects on SFTW hydrodynamics study by full-scale tracer experiments and dynamic time warping algorithms. Chem. Eng. J.

Nuel, M., Laurent, J., Bois, P., Heintz, D., Wanko, A., 2017b. Seasonality vs. typology in SFTW: battle of the influences on global performances. J. Environ. Chem. Eng. (Manuscript submitted for publication).

Nuel, M., Laurent, J., Bois, P., Heintz, D., Wanko, A., 2017c. Occurrence and distribution of 83 pharmaceuticals in water, sediments, invertebrate and plants in a constructed Wetland ecosystem. Sci. Total Environ. (Manuscript submitted for publication).

Pellis, A., Laureysens, I., Ceulemans, R., 2004. Growth and production of a short rotation coppice culture of poplar I. Clonal differences in leaf characteristics in relation to biomass production. Biomass Bioenergy 27 (1):9–19. https://doi.org/10.1016/j.biombioe.2003.11.001.

Persson, Gunn, 1995. Willow stand evapotranspiration simulated for Swedish soils. Agric. Water Manag. 28 (4):271–293. https://doi.org/10.1016/0378-3774(95)01182-X.

Petrović, Mira, Hernando, Maria Dolores, Silvia Díaz-Cruz, M., Barceló, Damià, 2005. Liquid chromatography–tandem mass spectrometry for the analysis of pharmaceutical residues in environmental samples: a review. J. Chromatogr. A 1067 (1), 1–14.

Pubchem, 2017. Tramadol|C16H25NO2 - PubChem (Accessed June 6. https://pubchem.ncbi.nlm.nih.gov/compound/Tramadol).

R Development Core Team, 2008. R: a language and environment for statistical computing. Vienna, Austria: R Foundation for Statistical Computing. http://www.R-project.org.

Reyes-Contreras, C., Matamoros, V., Ruiz, I., Soto, M., Bayona, J.M., 2011. Evaluation of PPCPs removal in a combined anaerobic digester-constructed wetland pilot plant treating urban wastewater. Chemosphere 84 (9), 1200–1207.

Rohwer, 1931. Evaporation From Free Water Surfaces. Technical Bulletin. United States Department of Agriculture, Washington, D. C., p. 271 (https://scholar.google.com/scholar_lookup?title=Evaporation%20from%20Free%20Water%20Surface&author=C..%20Rohwer&journal=USDA%20Tech.%20Null.&volume=217&pages=1-96&publication_year=1931).

Rühmland, S., Wick, A., Ternes, T.A., Barjenbruch, M., 2015. Fate of pharmaceuticals in a subsurface flow constructed wetland and two ponds. Ecol. Eng. 80 (July):125–139. https://doi.org/10.1016/j.ecoleng.2015.01.036 (Special Issue: 5th international Symposium on Wetland Pollutant Dynamics and Control),.

Shenker, Moshe, Harush, Daniella, Ben-Ari, Julius, Chefetz, Benny, 2011. Uptake of carbamazepine by cucumber plants–a case study related to irrigation with reclaimed wastewater. Chemosphere 82 (6), 905–910.

Tanoue, Rumi, Sato, Yuri, Motoyama, Miki, Nakagawa, Shuhei, Shinohara, Ryota, Nomiyama, Kei, 2012. Plant uptake of pharmaceutical chemicals detected in recycled organic manure and reclaimed wastewater. J. Agric. Food Chem. 60 (41): 10203–10211. https://doi.org/10.1021/jf303142t.

Ternes, Thomas A., 1998. Occurrence of drugs in German sewage treatment plants and rivers1. Water Res. 32 (11):3245–3260. https://doi.org/10.1016/S0043-1354(98)00099-2.

Tiwari, Bhagyashree, Sellamuthu, Balasubramanian, Ouarda, Yassine, Drogui, Patrick, Tyagi, Rajeshwar D., Buelna, Gerardo, 2017. Review on fate and mechanism of removal of pharmaceutical pollutants from wastewater using biological approach. Bioresour. Technol. 224 (January):1–12. https://doi.org/10.1016/j.biortech.2016.11.042.

Toet, Sylvia, Van Logtestijn, Richard S.P., Kampf, Ruud, Schreijer, Michiel, Verhoeven, Jos T.A., 2005. The effect of hydraulic retention time on the removal of pollutants from sewage treatment plant effluent in a surface-flow wetland system. Wetlands 25 (2):375–391. https://doi.org/10.1672/13.

Vanek, Tomas, Podlipna, Radka, Fialova, Zuzana, Petrova, Sarka, Soudek, Petr, 2010. Uptake of xenobiotics from polluted waters by plants. Xenobiotics in the Urban Water Cycle. Springer, pp. 431–444 (http://link.springer.com/chapter/10.1007/978-90-481-3509-7_23).

Vazquez-Roig, Pablo, Segarra, Ramón, Blasco, Cristina, Andreu, Vicente, Picó, Yolanda, 2010. Determination of pharmaceuticals in soils and sediments by pressurized liquid extraction and liquid chromatography tandem mass spectrometry. J. Chromatogr. A 1217 (16), 2471–2483.

Verlicchi, Paola, Zambello, Elena, 2014. How efficient are constructed wetlands in removing pharmaceuticals from untreated and treated urban wastewaters? A review. Sci. Total Environ. 470–471 (February):1281–1306. https://doi.org/10.1016/j.scitotenv.2013.10.085.

Verlicchi, P., Zambello, E., 2015. Pharmaceuticals and personal care products in untreated and treated sewage sludge: occurrence and environmental risk in the case of application on soil — a critical review. Sci. Total Environ. 538 (December):750–767. https://doi.org/10.1016/j.scitotenv.2015.08.108.

Wilkinson, John L., Swinden, Julia, Hooda, Peter S., Barker, James, Barton, Stephen, 2016. Accumulation of Pharmaceuticals, Perfluorinated Compounds, Plasticisers and Illicit Drug Metabolite in Aquatic Sediment and Plants. Kingston University London.

Writer, Jeffrey H., Antweiler, Ronald C., Ferrer, Imma, Ryan, Joseph N., Michael Thurman, E., 2013. In-stream attenuation of neuro-active pharmaceuticals and their metabolites. Environ. Sci. Technol. 47 (17), 9781–9790.

Zhang, Dong Qing, Tan, Soon Keat, Gersberg, Richard M., Sadreddini, Sara, Zhu, Junfei, Tuan, Nguyen Anh, 2011. Removal of pharmaceutical compounds in tropical constructed wetlands. Ecol. Eng. 37 (3):460–464. https://doi.org/10.1016/j.ecoleng.2010.11.002.

Zhang, Yang, Lv, Tao, Carvalho, Pedro N., Arias, Carlos A., Chen, Zhanghe, Brix, Hans, 2016. Removal of the pharmaceuticals ibuprofen and iohexol by four wetland plant species in hydroponic culture: plant uptake and microbial degradation. Environ. Sci. Pollut. Res. 23 (3):2890–2898. https://doi.org/10.1007/s11356-015-5552-x.

Zorita, Saioa, Martensson, Lennart, Mathiasson, Lennart, 2009. Occurrence and removal of pharmaceuticals in a municipal sewage treatment system in the south of Sweden. Sci. Total Environ. 407 (8), 2760–2770.

Science of the Total Environment 645 (2018) 854–864

Contents lists available at ScienceDirect

Science of the Total Environment

journal homepage: www.elsevier.com/locate/scitotenv

Micropollutants removal and storage efficiencies in urban stormwater constructed wetland

M. Walaszek *, P. Bois, J. Laurent, E. Lenormand, A. Wanko

ICube, UMR 7357, ENGEES/CNRS/Université de Strasbourg, 2 rue Boussingault, 67000 Strasbourg, France

HIGHLIGHTS

- Stormwater from the studied catchment is characterized by a high amount of Zn and a high PAH variety at low concentrations.
- The stormwater constructed wetland removal efficiencies vary from 50% (naphthalene) to 100% (zinc).
- Due to the incoming flow, the accumulated SS decrease the pond removal efficiency for particulate micropollution.
- The vertical subsurface flow sand filter catches the major part of both dissolved and particulate micropollutants.
- Storage study during dry period highlights micropollutants accumulation in soils and water at steady state conditions.

GRAPHICAL ABSTRACT

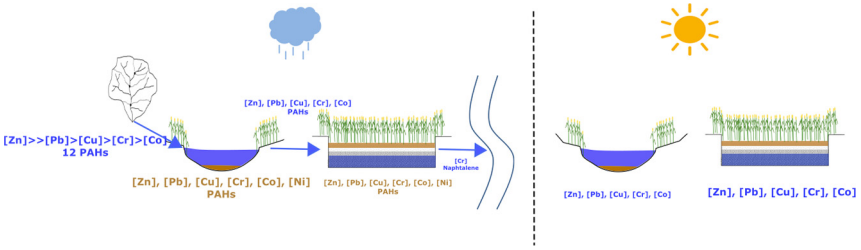

ARTICLE INFO

Article history:
Received 3 November 2017
Received in revised form 23 April 2018
Accepted 11 July 2018
Available online xxxx

Keywords:
Stormwater constructed wetland
Heavy metal
Micropollutant
PAH
Dry period

ABSTRACT

Stormwaters is identified as a major source of pollution in waterbodies. Particularly, heavy metals (HMs) and Polycyclic Aromatic Hydrocarbons (PAHs) in stormwater are highly toxic compounds for living organisms. To limit the impact of these micropollutants on hydrosystems quality, stormwater constructed wetlands (SCWs) have been built worldwide. This study aims to i) assess the efficiency of a SCW that combines a sedimentation pond followed by a vertical flow sand filter in urban area (Strasbourg 67, France) and ii) determine micropollutants storage in water and soils during dry periods. Stormwater quality was analysed during 13 sampling sessions and the SCW storage ability during dry period was highlighted. The rainfall events sampled are characterized by very high variability: dry periods lasted from 5 h to 10 d, rain durations varied from 15 min to 22 h and the return periods were between 2 and 4 wk. and 3–6 mo. The inflow stormwater included a high amount of Zn and a variety of PAHs. Cu, Zn and some PAHs concentrations are impacted by hydrological characteristics. During a rain event, the filter catches the majority of both dissolved and particulate micropollutants and the mobilization of particulate micropollution by incoming flow decreases pond removal efficiency. The treatment removal efficiency varied from 50% (naphthalene) to 100% (particulate Zn). Four HMs (Co, Cu, Pb, Zn) were found in the pond and seven (Cd, Cr, Co, Cu, Ni, Pb, Zn) in the filter during a dry period at high concentrations compared to their occurrence in rainfall. A release of HMs from the filter sand to the interstitial water is highlighted. In water and the soil matrix, PAHs occurrence was consistent with their water solubility, logKow and logKoc.

Abbreviations: HAC, hierarchical ascendant classification; HM, heavy metal; LOQ, limit of quantification; PAH, polycyclic aromatic hydrocarbon; PCA, principal component analysis; RE, removal efficiency; SCW, stormwater constructed wetland; Q, water flow; VFCW, vertical flow constructed wetland.

* Corresponding author.
E-mail address: mwalasze@engees.eu (M. Walaszek).

https://doi.org/10.1016/j.scitotenv.2018.07.156
0048-9697/

1. Introduction

In 2000 the European Water Framework Directive (CE, 2000) gave objectives for improving the quality of water bodies across Europe. By 2027 (with first intermediate deadline in 2015), all European water bodies such as rivers and water surfaces have to display good chemical, physical and biological states. Across Europe, stormwater is identified as a major source of pollution for waterbodies (Göbel et al., 2007; Revitt et al., 2014). In fact, stormwater from urban catchments (with considerable impervious surfaces coverages) contains wastes (e.g., cigarette butts and drink cans), suspended solids, oxidable matter (e.g., dissolved organic carbon and biological oxygen demand for five days), nutrients (e.g., nitrogen and phosphorus), minerals (i.e. heavy metals (HMs)) and organic (hydrocarbons and pesticides) micropollutants and microorganisms such as bacteria. The sources of these pollutants are numerous: initial rain water quality, the atmosphere, runoff from roofs and road catchments and the sewer system (Ahyerre et al., 1998). Among these pollutants, trace HMs and Polycyclic Aromatic Hydrocarbons (PAHs) are the most toxic compounds for living organisms (Guittonny-Philippe et al., 2014). HMs are non-biodegradable and are bioaccumulated in living organisms and/or accumulated in sediments (EPA, 2007) whereas PAHs are bioassimilable and their degradability depends on environmental conditions (EPA, 1984). Major sources of PAHs in the atmosphere include wood and coal combustion for domestic heating and automobile exhaust gases (Bressy et al., 2012). PAHs are also present as dry deposits on urban surfaces. HMs are, in most part, present on urban surfaces: Cu and Zn are used in roofs, gutters, and down pipes, while Pb and other HMs may be present in roofing materials (Göbel et al., 2007). Rain water collects micropollutants from the atmosphere and from runoff on roofs and roads. In most cases, polluted stormwater is directly discharged into waterbodies.

To limit the impact of stormwater on hydrosystems quality, water sensitive urban designs have been constructed worldwide. Stormwater can be managed by either decentralized or centralized strategies. The former captures rainwater where it falls and allows infiltration and evaporation on site: this is known as green stormwater infrastructure (GSI). These systems can be green roofs (Gregoire and Clausen, 2011), wells, or bioswales (Lorant, 1992). The latter catches stormwater after runoff on urban surfaces and in the sewer system. They store, infiltrate in soils, evaporate or release stormwater in waterbodies. They utilize infiltration basins (Birch et al., 2004; Dechesne et al., 2004), detention basins (Nix et al., 1988), or biofilters (Bavor et al., 2001; Carleton et al., 2000; Guardo et al., 1995). Several studies have shown that the most efficient decentralized treatment system is a wet pond followed by a biofilter (Strassler et al., 1999). The pond allows settling of particulate pollution and the biofilter improves the treatment by filtering the remaining particulate pollution and by catching the dissolved pollution.

Numerous studies have been performed on stormwater treatment systems that focus on infiltration basins, storage basins or point-source devices (Bressy et al., 2012; Lamprea and Ruban, 2011; Sébastian et al., 2014; Zgheib et al., 2011). Few have considered pond-filters as a stormwater treatment device in field conditions (Al-Rubaei et al., 2017; Schmitt et al., 2015) and at the laboratory scale (Zhang et al., 2015).These studies highlight stormwater quality and constructed wetland efficiency during rain events, but, to our knowledge, no study has explored the stormwater constructed wetland (SCW) micropollutant dynamic during dry periods. Yet some authors have shown that physico-chemical changes in SCWs can be dramatic and can control the release of stored HMs from sediments to the water column (Bradl, 2004; Flores-Rodrîguez et al., 1994; Kar et al., 2008).

The objectives of this study were to evaluate the efficiency of a constructed wetland to remove micropollutants from urban stormwater and to investigate micropollutant dynamics during both rain events and extended dry periods. We first present a classical approach for the study of a stormwater treatment system. We assessed the quality of stormwaters and the treatment performance of a 6-year-old SCW for micropollutants such as HMs and PAHs. We then present the dynamics of micropollutant storage in the system during dry periods, as it might differ significantly between the wet and dry periods. The HMs and PAHs concentrations in water during dry periods were tracked to develop an understanding of micropollutant distribution between water and solid substrates (i.e., sediment or sand). Micropollutant storage in the accumulated sediments along the treatment system was studied in order to propose best management practices for the system.

2. Material and methods

2.1. Study site description

2.1.1. Catchment area

The experimental site was in Strasbourg (67, France). The urban and residential catchment is 27,100 m^2 (Fig. 1). Its land cover consists of 44% low-traffic roads, 43% green areas (garden, field, and playground) and 13% roof (made up with tiles and Zn gutters). The runoff coefficient is 0.33. Stormwater runoff is drained by a separate sewer network and was previously directly discharged into the adjacent urban stream (Ostwaldergraben).

2.1.2. Treatment facilities

The constructed wetland design is presented in Fig. 2. It was built in 2011 and is made up of a sedimentation pond followed by a vertical subsurface flow constructed wetland (hereafter called "filter").

The pond is fed by runoff from the watershed. During dry periods, 28 m^3 of water in the pond is permanent. The maximum allowable volume during rain periods is 53 m^3. This is supposed to promote sedimentation. A floating weir feeds the filter when the water level in the pond is high enough. The water feeding of the system is episodic, due to the stochastic nature of rain. The pond was not originally planted but has been naturally vegetated by different plant species over the years.

The filter is made of three layers (from top to bottom): 20 cm of fine sand ($d = 0–4$ mm, $d_{10} = 0.16$ mm, $d_{60} = 1.38$ mm, hence a uniformity coefficient (UC) of 8.62), 25 cm of fine gravel ($d = 4–8$ mm) and 20 to 30 cm of drainage layer (coarse gravel, $d = 16–22$ mm). The filter is 90 m^2 in area (1% of the watershed active surface). It is designed to receive a 50 $m.yr^{-1}$ hydraulic load. The sand filter hydraulic conductivity is $2.6.10^{-4}$ $m.s^{-1}$. Aerobic processes are allowed as a result of natural ventilation through vertical aerated pipes. The filter is planted with *Phragmites australis*. A permanent water volume (from 28 cm water level during dry periods to 40 cm during discharge) is kept at the bottom to prevent plant hydric stress during extended dry periods.

2.2. Micropollutants in the water

2.2.1. Sampling campaigns

Sampling campaigns were performed during dry and wet periods.

For campaigns during rainfall, water was sampled at three strategic locations in the system by three automatic refrigerated samplers (Endress & Hauser, Reinach, Switzerland):

- Sampling point #1 in the inlet pipe (untreated stormwater),
- Sampling point #2 in the floating weir between the pond and the filter (settled water), and
- Sampling point #3 at the outlet of the filter (settled and filtered water).

Sampling locations are shown in Fig. 2-a.

Water was regularly sampled during a defined period according to the estimated rainfall duration (point #1), and the hydraulic residence time through the pond (point #2) and the filter (point #3). For sampling points #1 and #2, 200 mL of water was sampled every 3 min over 6 h. For sampling point #3, 200 mL of water was sampled every hour over 5 d. Finally, 24 1-L samples of water were sampled at each point. A composite sample was then created according to water level data and thus

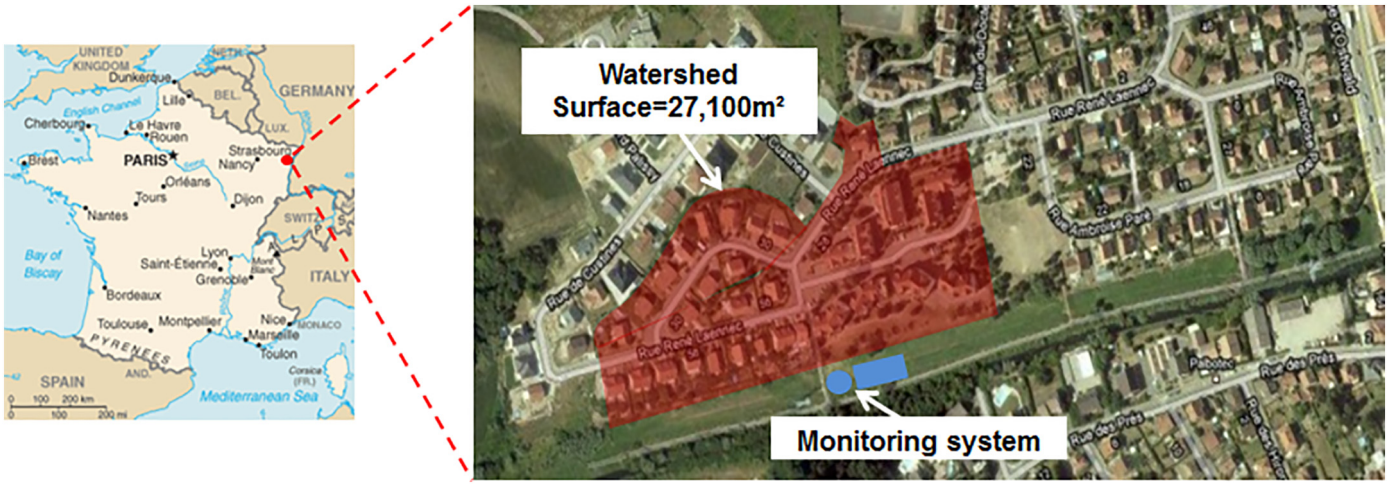

Fig. 1. Study site location in Strasbourg (France).

flow rate during the rain event (Schmitt et al., 2015). Water levels were recorded along the SCW by three sensors (inlet: ultrasonic sensor, Siemens, Munich, Germany; pond and filter: pressure sensor, Endress & Hauser; outlet: radar, Endress & Hauser). More details about the water sampling strategies are given in Schmitt et al. (2015).

Rainfalls characteristics were determined using an on-site weather station (ADCON, Klosterneuburg, Austria).

During dry periods, 2 L of water was also sampled at three points in the system using a sampling pole:

- In the pond (settled water in equilibrium),
- In the filter (water in equilibrium at the bottom through piezometer), and
- At the outlet of the filter.

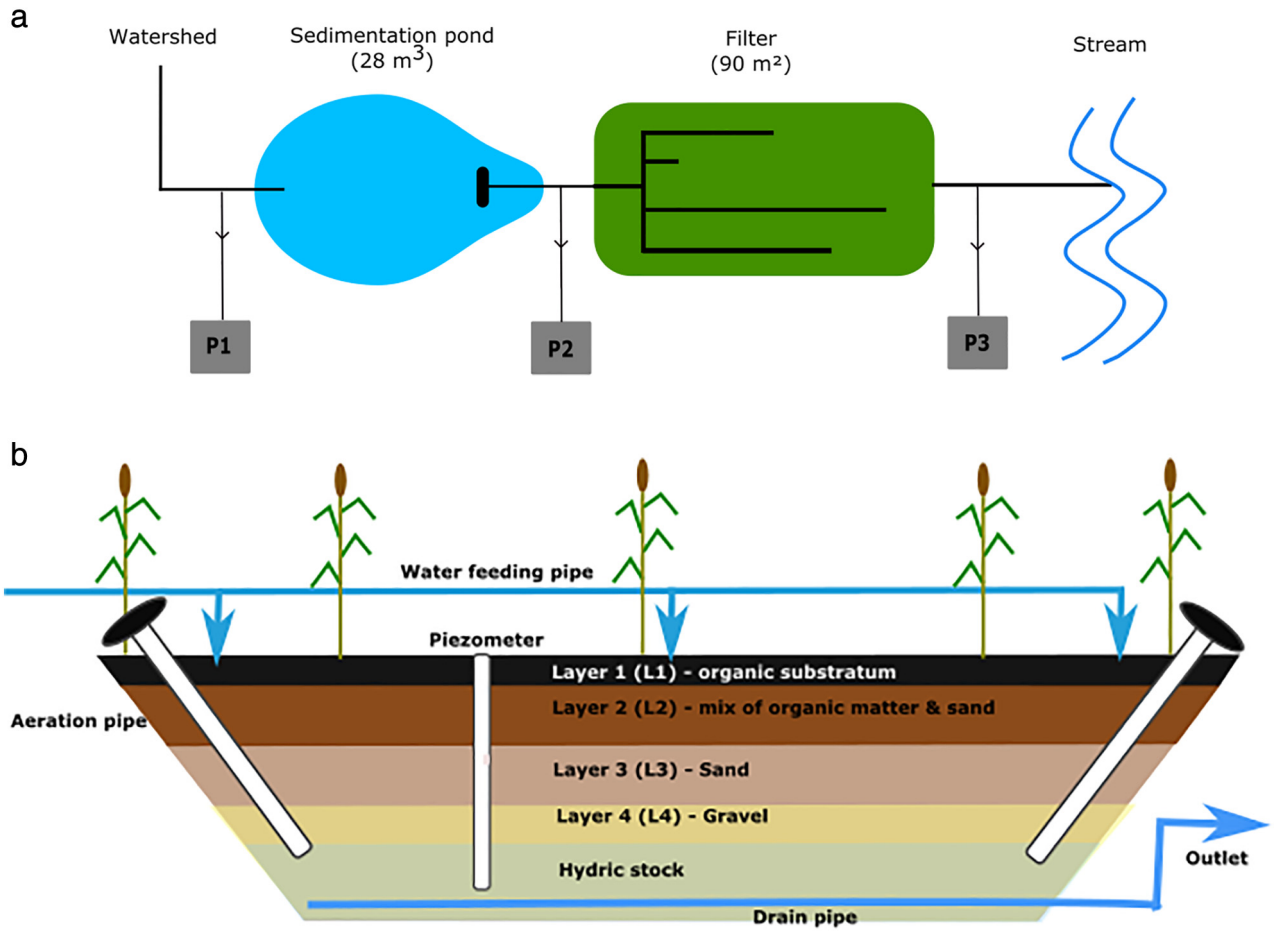

Fig. 2. Stormwater constructed wetland design and sampling points for (a) water sampling campaigns during rainy events (P1, P2, P3), and (b) water and soil sampling campaigns during dry periods (via piezometer, form layers 1 to 3) (a) Design of the constructed wetland and localization of the three water samplers (P1, P2, and P3) (b) Vertical cross-section of the filter with piezometer localizations and substrate layer (L1 to L4) distribution.

2.2.2. Chemical analyses

HMs (Cd, Cr, Co, Cu, Ni, Pb and Zn) concentrations were determined in both raw and filtered samples. Particulate and dissolved fractions were analysed with an ICP/AES (NF EN ISO 11885). Samples for dissolved fraction determination were filtered through a cellulose nitrate membrane (0.45 μm pore size).

PAH (benzo(a)pyrene, fluorine, phenanthrene, anthracene, fluoranthene, pyrene, benzo(a)anthracene, chrysene, benzo(b)fluoranthene, benzo(k)fluoranthene, dibenzo(a,h)anthracene, naphtalene, acenaphthylene, acenaphtene, benzo(ghi)perylene, and indeno(1,2,3-cd) pyrene) concentrations were determined in raw samples with GC/MS after hexane extraction (NF EN ISO 17993).

2.2.3. Removal efficiency

The removal efficiency (RE) of a given compound was evaluated in the pond and in the filter using Eq. (1).

$$\text{Removal efficiency } (\%) = \frac{[X]_{inlet} \times V_{inlet} - [X]_{outlet} \times V_{outlet}}{[X]_{inlet} \times V_{inlet}} \times 100 \quad (1)$$

where $[X]_{inlet}$ and $[X]_{outlet}$ are respectively the concentrations of the micropollutant X at the inlet and the outlet of the pond or the filter, and V_{inlet} and V_{outlet} are respectively the volume runoff at the inlet and the outlet of the pond or the filter. Finally, the REs were calculated in terms of mass to appreciate the real SCW storage capacity and in terms of concentration to assess the environmental impact. Volumes are computed using a hydrologic budget, as shown in Eq. (2):

$$\frac{\Delta V}{\Delta t} = Q_{inlet} - Q_{outlet} - Q_{evaporation} - Q_{infiltration} - Q_{evapotranspiration} \quad (2)$$

where $\Delta V/\Delta t$ is the water storage dynamic, Q_{inlet} is the the inlet flow rate in the pond or the filter, Q_{outlet} the outlet flow rate through the floating weir in the pond or the drainage pipe of the filter. $Q_{evaporation}$, $Q_{inflitration}$ and $Q_{evapotranspiration}$ are respectively the flow rates due to evapotranspiration, evaporation and infiltration through the clay layers at the bottom. They are negligible at the event scale.

REs were calculated according to Choubert et al. (2011a, 2011b), as follows: (i) if both inlet and outlet concentrations are below 10 times the limit of quantification (LOQ), the RE is not calculable (analytical uncertainty above 50%), and, if the inlet or outlet concentration is below the LOQ, half of the LOQ is used for the RE calculation (Fig. 3). An error propagation calculation has been conducted using the measurement errors of volumes and concentrations. RE results are given with an uncertainty of <23%.

2.2.4. Statistical analyses

Statistical analyses were performed using the opensource R (R Core Team, 2016). Concentrations below the LOQ are replaced by half of the LOQ in the dataset. A Shapiro-Wilk test was performed on the dataset, and the data are not normally distributed (p-value < 0.05). Also non-parametric tests were used. Concentrations below the LOQ are replaced by half of the LOQ. A Hierarchical Ascendant Classification (HAC) was performed on the hydrological characteristics of the sampled rainfalls. The number of clusters was determined by calculating the intra-cluster inertia. The partition with the higher relative loss of inertia was used. A Spearman correlation test was run to investigate the link between particulate HMs and suspended solids and a Krustal-Wallis rank sum test to determine any significant difference between stormwater, pond and output micropollutants concentrations or contents. Then, a HAC was performed on the principal components of a Principal Component Analysis (PCA) to determine any link between the hydrological characteristics of the sampled rainfalls and the micropollutants concentrations in stormwater.

2.3. Micropollutants in soils

2.3.1. Soil and sediments sampling campaigns

Two soil analysis sessions were performed along the treatment system to determine the storage dynamics of micropollutants, in May 2016 and April 2017.

Sediments were sampled in the pond and soils in the filter. Previous work (Walaszek et al., 2015) on the influence of the filter feeding device (Fig. 2-a) highlighted a non-uniform water distribution at the top of the filter. Thus, the filter was separated into two areas: the first one regularly fed with water, populated with fully developed reeds and the second one seldom fed with water, populated with only a few reeds. We assumed that the difference in water feeding in the filter leads to a difference in micropollutants contents. The filter soil was sampled at three random points in each area and at three depths for each point to get a representative sample: organic deposit (first layer), sand under the organic deposit (second layer) and so-called deep sand (third layer). A composite sample was made for the two sampling areas by mixing together layers from the same depth (Fig. 2-b).

2.3.2. Chemical analyses

Samples were dried, ground and sieved (2 mm sieve size, NF ISO 11464). Then, HMs (Cr, Co, Cu, Ni, Pb, and Zn) were mineralized with *aqua regia* (NF EN ISO 13346) and analysed using ICP/OES (NF EN ISO 11885).

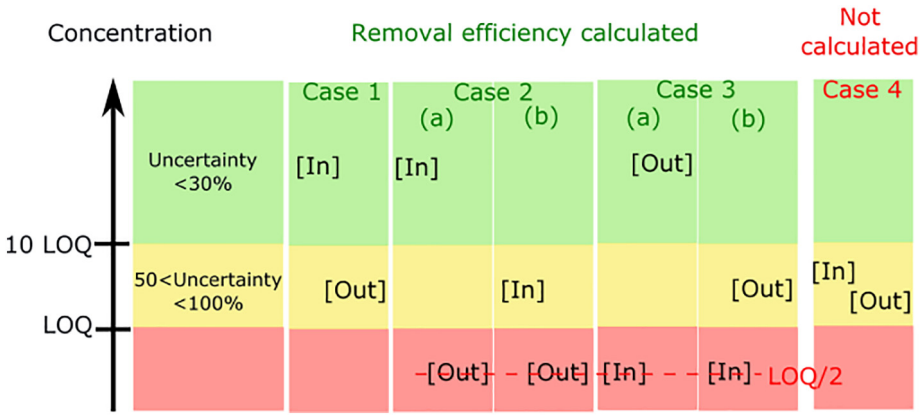

Fig. 3. Calculation rules for micropollutant removal efficiencies according to Choubert et al. (2011a, 2011b) ([in]: inlet concentration; [out]: outlet concentration; LOQ: limit of quantification).

3. Results and discussion

3.1. Micropollutant removal

3.1.1. Rain event descriptions

Thirteen stormwater sampling sessions were performed from October 2015 to June 2017 (Table 1). Hydrological parameters varied strongly across the sampled rainfalls: dry periods lasted from 5 h to 10 d (mean: 4 d) and rain durations varied from 15 min to 22 h (mean: 8 h). Return periods were between 2 and 4 wk. to 3–6 mo. During these two years of monitoring we sampled all types of rainfall.

The sampled rainfalls were ranked in hydrological groups using a HAC. According to antecedent dry period, rain duration and maximum intensity, two groups were characterized.

Hydrological groups were discriminated by antecedent dry periods. The dry periods of group #1 (events 3 through 9 and 11 through 13) were significantly shorter than those of the other group (p-value = 0.0016, group #1 dry period average: 2.2 ± 0.96 d, overall average: 3.6 ± 2.7 d). Group #2 (events 1, 2, and 10) is characterized by long dry periods (group #2 dry period average: 8.06 ± 1.51 d). The types of micropollutants and their concentrations in rain water may be influenced by antecedent dry period, as shown by Li et al. (2017).

Concentrations of HMs and PAHs along the SCW are shown in Table 2.

3.1.1.1. Heavy metals in stormwater

3.1.1.1.1. The Zn predominance. Among the seven monitored HMs, Cr, Co, Cu, Pb and Zn were detected in stormwater. In this study, stormwater was characterized by high Zn concentrations (Table 2): its concentration ranged between 110 and 360 μg/l (mean = 194 ± 69 μg/l). These high Zn amounts can be explained by the presence of numerous gutters made of Zn in the watershed. Göbel et al. (2007) show that runoff from roofs with Zn gutters are five times more concentrated in Zn than runoff from roofs without Zn gutters (mean Zn concentrations for runoff with Zn gutters: 1851 μg/l, for runoff without zn gutters: 370 μg/l). A concentration peak (360 μg/l) was observed on 03/25/2016 (event 4), which corresponds to a high rainfall duration event (10*h*). Cu and Pb were also present in stormwater, to a lesser extent. Their concentrations ranged between 4 and 10 μg/l for Cu (mean = 6 ± 2 μg/l) and 2 and 4 μg/l for Pb (mean = 3 ± 1.2 μg/l). Cr and Co were less present in stormwater. Cr is detected five times at low concentrations, from 0.5 to 5 μg/l (mean = 1.5 ± 1.9 μg/l) and Co once (event 10), at 0.22 μg/l.

All detected HMs were mostly bound to the particulate fraction (Cr: 80%, Co: 100%, Cu: 100%, and Pb: 85%), except Zn which was mainly present in the dissolved fraction. 75% of the Zn total concentration was found in the dissolved phase. These results are in accordance with many studies showing that Cr, Co, Cu and Pb are mainly particle-bound (e.g., Gromaire-Mertz et al., 1999; Zgheib et al., 2011; Schmitt et al., 2015). There is no overall trend for Zn. Gromaire-Mertz et al. (1999) found 48% of dissolved Zn, Lamprea, 2009 97% and Zgheib et al. (2011) only 12%. Lamprea (2009) showed that the partitioning of HMs depends on the type of impervious surface.

These concentrations were compared with the results of two studies in France and Poland. Lamprea (2009) analysed stormwater in a residential watershed in Nantes (area: 310,000 m^2, runoff coefficient: 0.49) and Walęga and Wachulec (2018) studied an urban watershed in Kraków (area: 332,900 m^2, runoff coefficient: 0.74). Lamprea (2009) found 6 HMs in variable concentrations (mean concentrations for Zn: 146 μg/l, Pb: 21 μg/l, Cu: 31 μg/l, Cr: 7.5 μg/l, Ni: 5 μg/l, and Cd: 0.7 μg/l) and Walęga and Wachulec (2018) found 5 HMs with low to high concentrations (mean concentrations for Fe: 0.1 μg/l, Cd and Zn: 10 μg/l, Pb: 100 μg/l, and Cr: 11 mg/l). HMs concentrations from our study were in the same range of Lamprea (2009), but smaller than those of Walęga and Wachulec (2018). This can be explained by the differences of land use and runoff coefficient between our study and Walęga and Wachulec's study (residential/urban; 33%/74%).

3.1.1.1.2. SCW efficiency: the HM release risk. The HM concentrations at the output of the pond are in the same range as in the stormwater. Only dissolved Zn concentrations were less significant. Both dissolved and particulate Zn were almost totally removed by the SCW (RE = 98%). As expected, dissolved Zn is trapped by the filter (RE = 97%). But the particulate Zn is also mainly trapped by the filter (RE = 93%), instead of the pond (RE = −6%). Particulate Zn REs are negative on average in the pond, as well as for suspended solids (RE = −100%, not presented in Table 3). Particulate Zn binds to settled solids in the pond, and particulate Zn and suspended solids concentrations are correlated in the treatment system (Spearman rank test, $r^2 = 0.69$, $p < 0.01$). Incoming flow to the pond during a rain event causes the resuspension of these solids and the associated Zn. But there is no significant correlation between the incoming flow in the pond and the Particulate Zn or the suspended solids resuspension. Zn RE were compared with the results of Al-Rubaei et al. (2017), who studied a pond followed by a wetland (Bäckaslöv wetland) in Sweden (catchment area: 320,000 m^2, pond area: 18,000 m^2, wetland area; 50,000 m^2). Zn RE in that pond were much higher (respectively 84 and 64% for particulate and dissolved Zn) than in our case (respectively 24 and − 22%). Indeed, the maximum specific inflow rate (peak inflow rate divided by pond surface) of our study (1.19e–3 $m^3/s/m^2$) is ten times greater than that of the Bäckaslöv pond ($1.25e^{-4}$ $m^3/s/m^2$). Moreover the shallow pond depth in our study (0.3 m) compared to the Bäckaslöv pond depth (1.6 m) should promote suspended solid resuspension. It is interesting to note, however, that the global RE is similar: 92% for particulate Zn in both cases, 81% (Al-Rubaei et al., 2017) and 100% (our study) for dissolved Zn. Al-Rubaei et al. studied a pond followed by a wetland, while our system is a pond followed by a filter. Despite its small size, the filter is as efficient as the large Bäckaslöv wetland.

Pb and Cu are largely removed by the filter (RE = 90% for Pb and 70% for Cu). The same removal dynamics as Zn were observed for these bound-to-particles HMs: negative REs were observed in the pond and HMs were mostly trapped by the filter. Cr was detected all along the

Table 1
Characteristics of sampled rainfalls from October 2015 to June 2017.

Event	Date	Antecedent dry period (d)	Duration (h)	Maximum intensity for 15 min (mm/h)	Depth (mm)	Return period
1	4/10/2015	10.1	4.5	4	6.2	3 to 6 mo
2	9/12/2015	7.7	3.3	4.8	5	3 to 6 mo
3	23/2/2016	2.9	5.3	2.4	8	3 to 6 mo
4	25/3/2016	1.6	10.3	1.6	2.8	1.5 to 3 mo
5	26/4/2016	1.4	4.8	0.8	2.4	1.5 to 3 mo
6	23/5/2016	3.8	21.8	2.4	11	1.5 to 3 mo
7	21/10/2016	2.5	0.3	0.8	0.2	2 wk. to 1 mo
8	28/2/2017	0.2	0.5	3.2	1	1.5 to 3 mo
9	21/3/2017	3.1	17.0	1.6	11	6 mo to 1.5 y
10	26/4/2017	6.4	10.8	0.8	4.6	1.5 to 3 mo
11	4/5/2017	2.6	6.5	3.2	3.8	1.5 to 3 mo
12	13/5/2017	1.6	4.3	20.8	13.2	1.5 to 2 y
13	3/6/2017	2.6	19	5.6	16.4	3 to 6 mo

Table 2
Concentrations in μg/L of dissolved (D), particulate (P), total (T) heavy metals and PAHs (minimum – maximum [average]) and number of detection (ND) along the SCW.

($n = 13$)	LOQ (μg/L)	Stormwater (μg/L)	ND	Pond output (μg/L)	ND	Filter output (μg/L)	ND
Cr-D	0.5	7	1	7	1	<LOQ	0
Cr-P	0.5	0–5 [1.84]	4	0.7–5 [2.25]	3	5	1
Cr-T	0.5	0–7 [1.07]	5	0.7–7 [3.32]		5	1
Co-D	0.2	<LOQ	0	<LOQ	0	<LOQ	0
Co-P	0.2	0.22	1	0.29–0.39 [0.34]	2	0.22–0.31 [0.27]	2
Co-T	0.2	0.22	1	0.29–0.39 [0.34]		0.22–0.31 [0.27]	2
Cu-D	0.5	<LOQ	0	<LOQ	0	<LOQ	0
Cu-P	0.5	4.11–9.7 [6.44]	4	2.78–11.5 [6.19]	4	1.41–3.03 [2.22]	2
Cu-T	0.5	4.11–9.7 [6.44]	4	2.78–11.5 [5.63]		1.41–3.03 [2.22]	2
Pb-D	0.5	6	1	6	1	<LOQ	0
Pb-P	0.5	1.95–4.15 [3.11]	4	1.75–6.73 [4.40]	4	<LOQ	0
Pb-T	0.5	1.95–6 [1.19]	5	1.75–11.3 [5.63]	5	<LOQ	0
Zn-D	5	70–300 [146.5]	13	40–120 [91.7]	12	<LOQ	0
Zn-P	5	20–281 [90.1]	13	10–197 [69.9]	13	5.9	1
Zn-T	5	110–360 [194]	13	100–197 [145.6]	13	5.9	1
Acenaphtene	0,01	0.01	1	<LOQ	0	<LOQ	0
Benzo(a)pyrene	0,01	0.053	1	<LOQ	0	<LOQ	0
Fluorene	0,01	0.01–0.02 [0.013]	4	0.01–0.02 [0.013]	4	<LOQ	0
Phenanthrene	0,01	0.01–0.06 [0.028]	12	0.01–0.09 [0.036]	9	0.01–0.02 [0.014]	3
Anthracene	0,01	<LOQ	0	0.05	1	<LOQ	0
Fluoranthene	0,01	0.01–0.17 [0.036]	9	0.01–0.04 [0.025]	8	0.02	1
Pyrene	0,01	0.01–0.12 [0.033]	7	0.01–0.03 [0.02]	7	0.01	1
Benzo(a)anthracene	0,01	0.06	1	<LOQ	0	<LOQ	0
Chrysene	0,01	0.05	1	<LOQ	0	<LOQ	0
Benzo(b)fluoranthene	0,01	0.01–0.06 [0.035]	2	0.01	1	<LOQ	0
Benzo(k)fluoranthene	0,01	0.03	1	<LOQ	0	<LOQ	0
Naphtalene	0,01	0.01–0.06 [0.02]	7	0.01–0.02 [0.015]	8	0.01–0.03 [0.016]	7

REs of the SCW and of each compartment (pond and filter) are presented in Table 3 in term of both mass and concentration.

treatment system at low concentrations (≤7 μg/l, Table 2). Dissolved Cr was removed partially by the filter (RE = 64%) while Cr bound to the particulate fraction was neither retained by the pond nor by the filter (RE = 0%). Cr was found in the outlet of the system and subsequently released in the river, at low concentrations (5 μg/l).Co was detected twice and was not trapped by the system. Its output concentration was low (0.22 μg/l.

Li et al. (2017) reported lower REs for a sedimentation pond-horizontal flow CW (pond area: 100 m^2, CW area: 330 m^2) treating stormwater from a residential watershed (1643 m^2) in China (mean RE for total HMs: Pb: 61%, Cu: 46%, Cr: 42%, and Zn: 67%). As well, Birch et al. (2004) studied a sedimentation pond-CW (pond area: 100m^2, CW area: 700 m^2) in a residential watershed (480,000 m^2) in Australia that removed HMs as efficiently as our treatment system (mean RE for total HMs: Pb: 65%, Cu: 65%, Cr: 64%, and Zn: 52%) and which exhibited negative RE for Zn and TSS for some storm event. No correlation between negative suspended solid and Zn concentrations was examined in this study.

3.1.1.2. PAHs in stormwater

3.1.1.2.1. Low PAH occurrence. Seven PAHs (acenaphtene, fluorene, phenanthrene, fluoranthene, pyrene, benzo(b)fluoranthene and

Table 3
Removal efficiency (RE) of the SCW, the pond and the filter to remove dissolved (D), particulate (P) heavy metals and PAHs (minimum – maximum [average]) (—: below limit of detection; ND: number of detection; *: RE not calculable because of a null output volume).

Micropollutants	Pond RE (%)		Filter RE (%)		SCW RE (%)		ND
	Conc.	Mass	Conc.	Mass	Conc.	Mass	
Chromium-D	–	87	96	100	96	100	1
Chromium-P	0–54 [27]	−67-100 [44]	0–76 [38]	97	0–54 [27]	94–100 [97]	3
Cobalt-D	–	100	–	*	–	100	2
Cobalt-P	−77	58–100 [86]	21	93	−41	97–100 [98]	3
Copper-D	–	59	–	99	–	100	1
Copper-P	19–56 [6]	48–100[83]	49–91 [70]	99	47–96 [70]	100	3
Lead-D	0	75–100 [90]	96	94–100 [99]	96	100	11
Lead-P	−74-10 [−38]	63–100 [88]	86–95 [91]	91–100 [98]	87–94 [90]	100	12
Zinc-D	−20-67 [37]	100	94–98 [97]	*	96–99 [98]	100	1
Zinc-P	−200-57 [−6]	100	75–99 [93]	*	88–99 [93]	100	1
Acenaphtene	50	84–100 [97]	–	88–100 [94]	50	98–100 [99]	5
Benzo(a)pyrene	91	59–100 [86]	–	30–100[44]	91	93–100 [99]	11
Fluorene	0–50 [38]	100	50–75 [56]	*	50–75 [56]	100	1
Phenanthrene	−100-75 [2]	38–100 [82]	50–92 [74]	97–100 [98]	50–92 [68]	98–100 [100]	9
Anthracene	–	59–100 [84]	90	94–100 [97]	–	98–100 [99]	6
Fluoranthene	−100-76 [8]	100	50–88 [71]	*	50–88 [71]	100	1
Pyrene	0–75 [11]	100	67–75 [74]	*	75–92 [77]	100	1
Benzo(a)anthracene	92	100	–	*	92	98-100 [100]	2
Chrysene	90	100	–	*	90	100	1
Benzo(b)fluoranthene	0–92 [46]	−25-100 [80]	50	16–100 [76]	50–92 [71]	66–100 [94]	10

* RE not calculable because of a null output volume).

naphthalene) were detected among the 16 tracked. Their concentrations are shown in Table 2. Phenanthrene was detected in most every rain events (frequency of detection = 72%) while benzo(b) fluoranthene was rarely detected in the inlet (frequency of detection = 9%).

Lamprea (2009) found 9 PAHs among the 16 researched in higher concentrations than the present study (total PAHs concentrations for Lamprea (2009): 0.104 μg/l, our study: 0.07 μg/l). This difference can be explained by the larger watershed size of the study (Lamprea (2009): 310,000 m^2, our study: 27,000 m^2).

3.1.1.2.2. SCW removal efficiency. Among the seven PAHs found in stormwater, only acenaphtene was not detected in the pond output. The six other PAHs were present in average concentrations from 0.01 μg/l (Benzo(b)fluoranthene) to 0.03 μg/l (phenanthrene). Due to smaller concentrations, PAH REs were smaller than those for HMs. This might be an effect of the smaller concentration levels rather than a true feature of the system. Among the 7 PAHs found, only 3 had REs >70% (phenanthrene, fluoranthene and pyrene). The others had REs between 45% (naphthalene) and 56% (fluorene). PAHs were mostly removed by the filter, except naphthalene which was removed either by the pond or the filter. Naphalene is highly soluble in water (solubility in water at 25 °C: 32 mg/l) compared to the other PAHs (from 3.42 mg/l for acenaphtene to 0.001 mg/l for benzo(b)fluoranthene) (EPA, 1984). Thus, naphthalene did not seem to settle in the pond, nor was it sorbed in the filter. Fluorene, phenanthrene and fluoranthene had negative REs in the pond. According to the literature, PAHs are mostly bound to the particulate fraction (Bressy, 2010; Zgheib et al., 2011). As for Zn, incoming flow in the pond could cause PAHs resuspension and therefore an increase in PAH concentrations in the water.

3.1.1.3. Rain characteristics effects on micropollutant. We hypothesized that hydrological characteristics have an impact on micropollutants concentrations. Rainfall after a long dry period or rainfall with a long duration or high intensity may cause an important micropollutant load in stormwater. The PCA loading in Fig. 4 provides an overview of the variables that can affect the HMs and PAHs concentrations in stormwater.

Particulate Cu (cu_p), dissolved Zn (zn_d), benzo(a)anthracene (baa), rainfall duration (tp) and depth (h) are grouped together along the second dimension (dim2). This suggests that concentrations of particulate Cu, dissolved Zn, and benzo(a)anthracene are significantly and positively influenced by rainfall duration and depth. On the contrary, particulate Zn (zn_p) is grouped along the first dimension (dim1) and opposite rainfall duration and depth, suggesting that these hydrological parameters influence significantly and negatively particulate Zn concentrations in stormwater. The first dimension indicates that three PAHs (phenanthrene (phen), pyrene (pyr) and fluoranthene (flutn)) are significantly and negatively influenced by dry periods (dts). To conclude, for the 13 sampled rainfall events, long rainfall duration and high depth caused high particulate Cu and benzo(a)anthracene concentrations and low particulate Zn concentrations. Then, long dry periods generated low phenanthrene, pyrene and fluoranthene concentrations in stormwater.

3.2. Heavy metal storage dynamics

3.2.1. Concentrations in water during dry periods

The pond is colonized by a wide variety of plants and provides a habitat for many species (such as green toads). This ecosystem is actually made of the water from the SCW, which operates most of the times during dry weather (in one year, 70% dry weather and 20% wet). As the pond is an artificial water body, its micropollutant concentrations have to be below the limit concentrations in water per the European and French regulations (CE, 2000; RF, 2010).

To verify this, one SCW water sampling campaign was performed in April 2017 during a dry period. We tracked micropollutants in the pond water, in the water at the subsurface of the filter, and at the system outlet. The results for HM and PAH concentrations in water along the SCW are shown in Fig. 5.

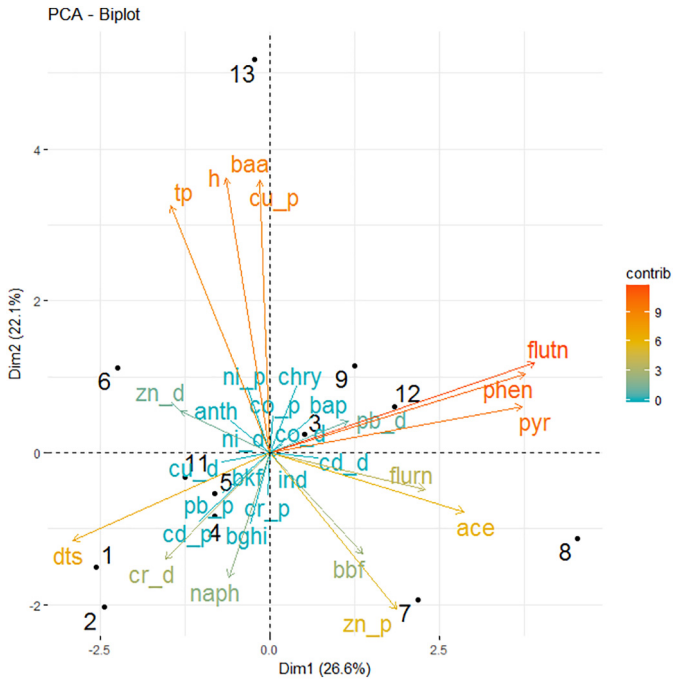

Fig. 4. Principal components 1 and 2 obtained from a PCA of rainfall duration (tp), depth (h), dry period (dts), dissolved and particulate HM and PAH concentrations in stormwater as variables and rainfall events (1 through 13) as individuals. The contribution of variables is from high (in red) to low (in blue). Dim1 explains 26.6% of the variance in the data and Dim 2 21.2%.

3.2.1.1. Heavy metals. Four HMs (Co, Cu, Pb, and Zn) were found in pond water and seven (Cd, Cr, Co, Cu, Ni, Pb, and Zn) in the subsurface filter water during the dry period, while only five were detected in stormwater samples during rainfall events (Cr, Co, Cu, Pb, and Zn). LOQs are provided in Table 2. No other HMs were found at the filter outlet except Cu (0.85 μg/l). In the pond, no Cd and Cr were detected during the dry period but they were found in stormwater. Cu, Pb, and Zn concentrations were lower in the pond water during the dry period than in the stormwater. As for the stormwater, the most present HM in the SCW during the dry period was Zn. Concentrations in the pond were 4.5 times higher than the French legislation concentration limit (7.8 μg/l) (RF, 2010) and 606 times higher in the filter. Other HM concentrations abide by the European (CE, 2000) and French legislations, but not in the filter where they are above limit concentrations (European limit concentrations for Cd: 0.08 μg/l and Pb: 1.2 μg/l, French limit concentrations for Cr: 3.4 μg/l, and Cu: 1 μg/l). Still, the measured Zn concentrations could be harmful for the species living in the SCW, as toxic effects occur at concentrations from 68 μg/l for *Daphnia magna*, a common crustacean in waterbodies (Nys et al., 2017). All HMs concentrations in the filter were higher than in the pond and in the stormwater (Average stormwater concentrations for Cr: 1.5 ± 2 μg/l, Co: 0.22 μg/l, Cu: 6.5 ± 2 μg/l, Pb: 3 ± 1 μg/l, and Zn: 194 ± 69 μg/l; pond concentrations for Co: 0.32 μg/l, Cu: 1.53 μg/l, Pb: 0.87 μg/l, and Zn: 35.6 μg/l; filter concentrations for Co: 2.13 μg/l, Cu: 74.8 μg/l, Pb: 25.8 μg/l, Zn: 4730 μg/l, Cd: 0.37 μg/l, and Cr: 6.29 μg/l). Yet the permanent water level in the filter is not high enough (around 30 cm) to be in contact with the upper sand layer of the filter. This result suggests a release of HMs from filter sand to interstitial water, where they are then leached to the bottom of the filter during discharging rain events.

3.2.1.2. PAHs. Among the seven PAHs detected in stormwater during the rainfall event, only five were found in the pond (acenaphtene, fluorene,

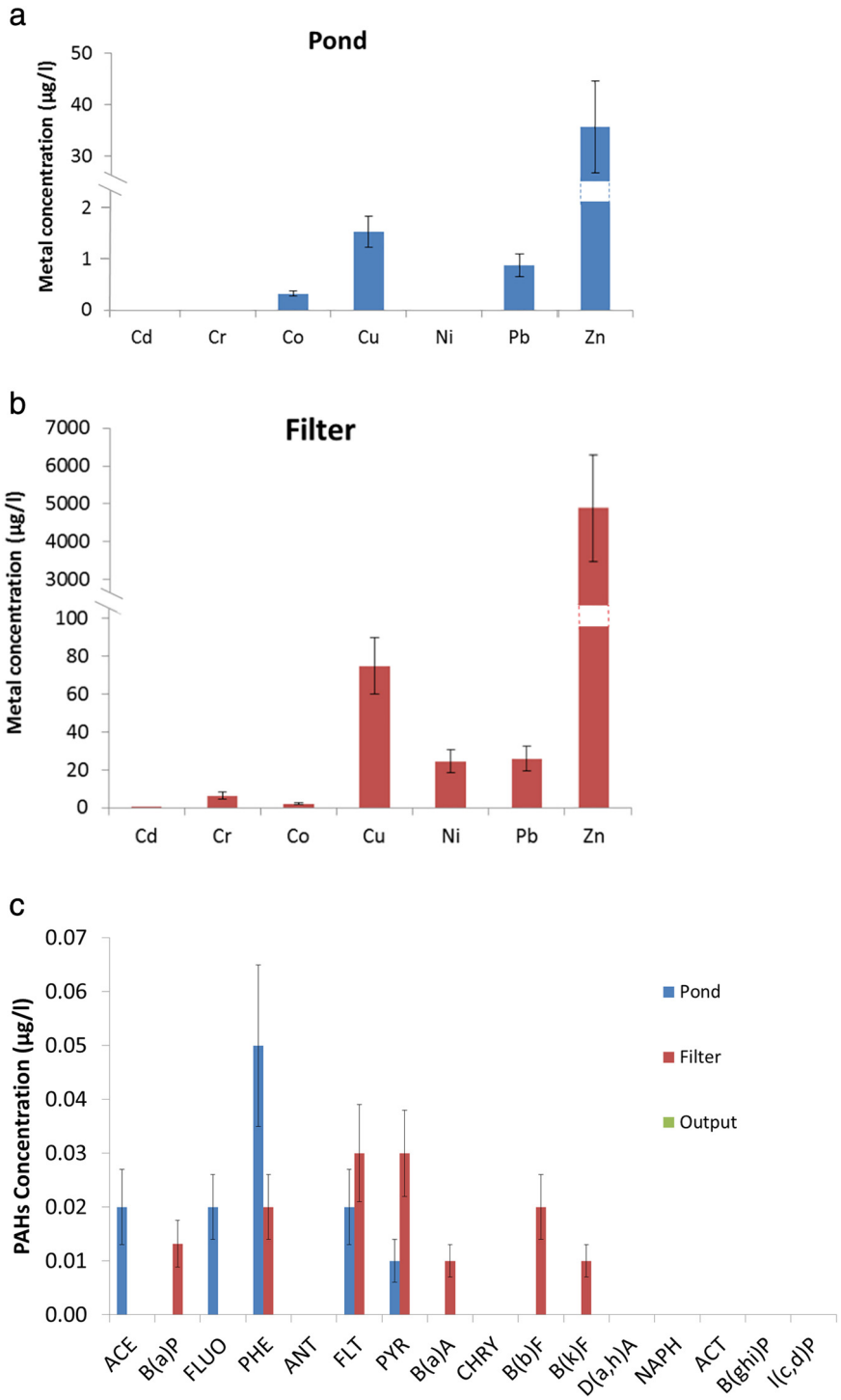

Fig. 5. Concentrations (µg/l) of heavy metal during a dry period in (a) the water pond and (b) the water filter and (c) concentrations (µg/l) of PAHs in water along the SCW at equilibrium (April 2017) (a) HM concentrations during a dry period in the pond water phase (b) HM concentrations during a dry period in the filter water phase (c) PAHs concentrations along the SCW (ACE = acenaphtene, B(a)P = benzo(a)pyrene, FLUO = fluorene, PHE = phenanthrene, ANT = anthracene, FLT = fluoranthene, PYR = pyrene, B(a)A = benzo(a)anthracene, CHRY = chrysene, B(b)F = benzo(b)fluoranthene, B(k)F = benzo(k)fluoranthene, D(a,h)A = dibenzo(a,h)anthracene, NAPH = naphthalene, B(ghi)P = benzo(ghi)perylene, and I(c,d)P = indeno (1,2,3-cd)pyrene).

phenanthrene, fluoranthene, and pyrene) and four in the filter (phenanthrene, fluoranthene, pyrene, and benzo(b)fluoranthene) during the dry period. Naphtalene was not detected in the SCW solid matrix. In fact, naphtalene is characterized by the highest water solubility (32 mg/l) and the highest Henry constant (48.9 $Pa.m^3.mol^{-1}$) at 25 °C, hence it has a great ability for volatilization. Alson note that acenaphtene and naphtalene provide the lowest partition coefficient for octanol/water (log Kow): log Kow = 3.98 and 3.3, respectively. This means that there is a weak potential accumulation of these PAHs in lipids. PAHs concentrations along the SCW were in the same range as in stormwater (pond concentrations for acenaphtene: 0.02 µg/l, fluorene: 0.02 µg/l, phenanthrene: 0.05 µg/l, fluoranthene: 0.02 µg/l, and pyrene: 0.01 µg/l; filter concentrations for phenanthrene: 0.02 µg/l, fluoranthene: 0.03 µg/l, pyrene: 0.03 µg/l, and benzo(b)fluoranthene: 0.02 µg/l). These concentrations are below the limit concentrations of the French legislation (French limit concentrations for acenaphtene:

0.7 μg/l, fluorene: 0.3 μg/l, phenanthrene: 0.11 μg/l, fluoranthene: 0.1 μg/l, pyrene: 24 μg/l, and benzo(b)fluoranthene: 30 μg/l) (RF, 2007).

In summary HM and PAH concentrations in pond water during a dry period were explained by the stormwater input. This was not the case for HM concentrations in the filter which were much higher than in stormwater and pond water. Aside from the pond load, another potential HM source of HMs detected in water during the dry period is the storage of HMs in the sand of the filter.

3.2.2. Heavy metal storage in sediments and soils

Analyses of Pb, Zn, and Cu contents along the SCW were performed twice, in 2016 and 2017. Cr, Ni, Co and PAHs were tracked only in 2017. The results of HM and PAH contents are presented respectively in Fig. 6 and Fig. 7.

3.2.2.1. Heavy metals. In the pond, Pb, Zn and Cu contents in 2017 were much higher than in 2016 (contents in 2016 for Pb: 10.1 mg/kg, Zn: 426 mg/kg, and Cu = 13.71 mg/kg and in 2017 for Pb: 260 mg/kg, Zn: 2270 mg/kg, and Cu = 97.1 mg/kg). In only one year, pond sediments were 5 times richer in Zn, 7 times in Cu, and 26 times in Pb. In the filter, HM contents in 2016 and 2017 werre not significantly different (Mann Whitney-Wilcoxon test, $p > 0.01$). Moreover, there was no significant difference in HM content between the high and the low-supplied filter areas, which shows that our hypothesis (differential water feeding causes a significant differential distribution of HMs) was wrong. Still the HM content differs according to the substrate and the depth in the filter. The first (organic deposit, 0–10 cm) and the second (sand mixed with organic deposit, 10-20 cm) layers of substrates are significantly more concentrated in HMs than the deep sand (20–40 cm). Thus, HMs are more likely stored in the organic deposit and the first few centimetres of sand. Lin and Chen (1998) already showed that an increase in organic matter content in river sediments causes a better sorption potential of heavy HMs.

3.2.2.2. PAHs. In the pond sediments, 12 PAHs were detected at high levels compared to the 5 found in water during the dry period (contents in pond sediments for acenaphthylene: 0.13 mg/kg, phenanthrene: 0.66 mg/kg, anthracene: 0.2 mg/kg, fluoranthene: 1.3 mg/kg, pyrene: 0.79 mg/kg, benzo(a)anthracene: 0.4 mg/kg, chrysene: 0.54 mg/kg, benzo(b)fluoranthene: 0.73 mg/kg, benzo(k)fluoranthene: 0.49 mg/kg, benzo(a)pyrene: 0.41 mg/kg, benzo(ghi)perylene: 0.34 mg/kg, and indeno(1,2,3-cd)pyrene: 0.49 mg/kg). Among the four other PAHs, one was not detected in stormwaters along the SCW (dibenzo(a,h) anthracene) and the three others (naphtalene, acenaphtene, and fluorene) were detected in stormwater (except naphtalene was detected only in stormwater). Bidaud and Tran-Minh (1998) showed that PAHs with a small number of carbons in their structure (2 to 4 carbons) are 90% biodegradable in soils. On the contrary, PAHs with a high number of carbons (5 to 6) are slightly or not biodegradable. In our case, the three PAHs not found in pond sediments contains two carbons (naphtalene) or three (acenaphtene, fluorene). They are volatilized (naphtalene) or biodegraded (acenaphtene, fluorene) in the sediments by microorganisms. Indeed, these molecules provide the lowest partition coefficients for octanol/soil organic carbon (log Koc): log Koc = 3.66 for acenaphtene and log Koc = 3.15 for naphtalene (EPA, 1984). Hence, a weak ability to bind to soil or sediment organics.

As for HMs, there was no significant difference between PAH contents in the input and output of the filter. PAHs were detected only in the organic deposit (first layer) in both the input and output filter. In total, 5 PAHs were detected in lower concentrations than in pond sediments (contents in the organic layer L1 of the input filter for: fluoranthene: 0.091 mg/kg, pyrene: 0.053 mg/kg, benzo(b)fluoranthene: 0.076 mg/kg, and indeno(1,2,3-cd)pyrene: 0.052 mg/kg; of the output filter for: fluoranthene: 0.071 mg/kg, benzo(ghi)perylene: 0.053 mg/kg, and indeno(1,2,3-cd)pyrene: 0.064 mg/kg).

These results show that the pond stores the majority part of the micropolluant loads in the SCW. However, the RE results for HMs (Section 2.1.2) indicate that the filter is responsible for trapping most. This can be explained by the mobility of HMs in the filter. Indeed, we saw that, during a dry period, the HM concentrations in the filter water were much higher than in the pond water and in the stormwater. During dry periods, changes in physico-chemicals properties in the filter could cause a change of speciation and thus a release of HMs in the interstitial water. Yeh et al. (2009) showed in pilot-scale CW that the speciation of HMs determines their fate in the system (i.e. released, stored or uptaken by plants or microorganisms).

Another striking result is that the organic deposit in the filter also stores a large part of the retained micropollutants load. This deposit is made of particulate pollution blocked by the layer of sand and dead plants. The organic deposit in the filter and the sediment layer in the pond is growing every year, thus, the proper functioning of the SCW could be threatened by a filling of the pond with sediments and a clogging of the filter by the deposit layer. So far, during the six years of SCW operation, the pond sediments have never been dredged nor the filter cleaned. There seems to now be a need for SCW maintenance. French regulations allow for the use of sediments and muds as roadway backfill

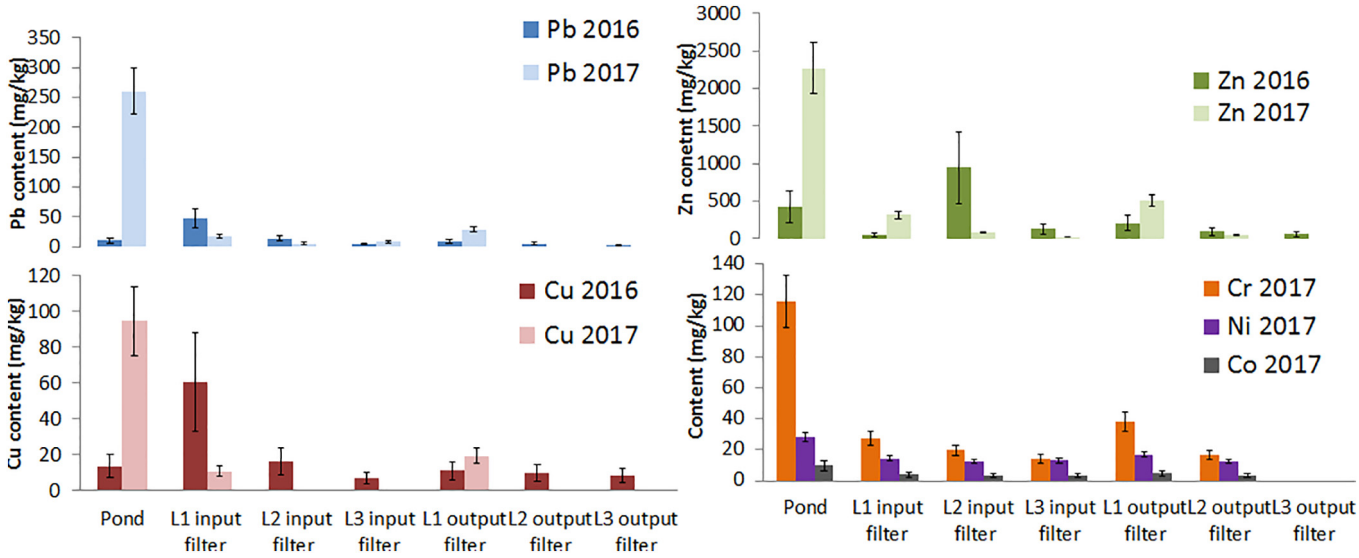

Fig. 6. Heavy metal contents (mg/kg of dry matter) in the sediment of the pond, and in the three layers (L1, L2, L3) of the input and the output filter in 2016 and 2017.

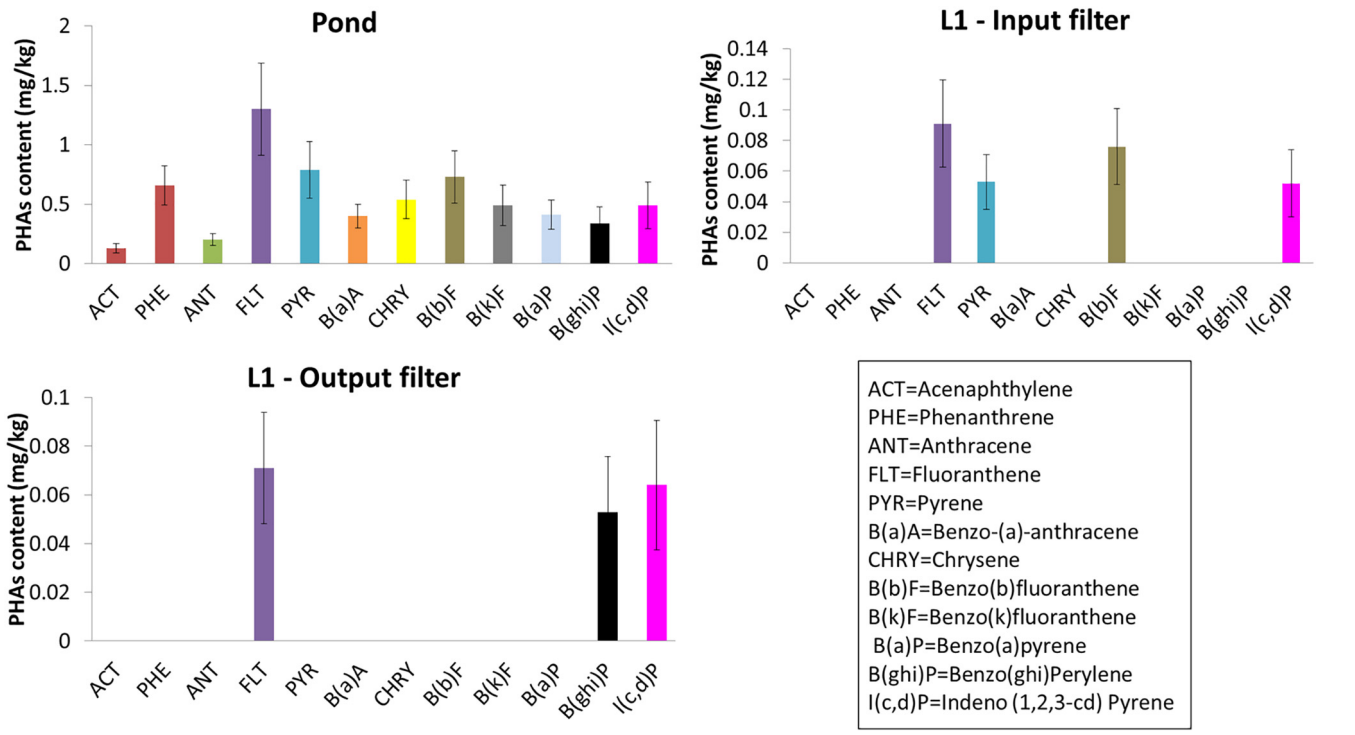

Fig. 7. PAHs contents (mg/kg of dry matter) in the sediment of the pond and in the first layers (L1) of the input filter and the output filter in 2017. No PAHs have been detected in the two other layers (L2 and L3) of the input and the output filter.

as long as the substrate contains HMs and PAHs under the following contents (BRGM, 2002): Cr: 65 mg/kg, Cu: 95 mg/kg, Ni: 70 mg/kg, Zn: 4500 mg/kg, and naphtalene: 23 mg/kg. The current contents in the sediment are above the limit for Cr. In the organic deposit, the contents are below the limits. Reuse of sediments as roadway backfill is a cost-effective alternative to manage SCW waste, especially in contrast to landfill storage, which is very expensive. However, the environmental risk posed by this reuse remains to be assessed. In fact, dredged pond sediments are often dried before disposal at landfill facilities, which could lead to a change of HM mobile fraction distribution (Blecken et al., 2017).

4. Conclusion

In order to determine the stormwater micropollution impacts along the rain characteristics and SCW REs, 13 sampling campaigns were performed during 3 years (2015 through 2017). The incoming stormwater from a small residential watershed was characterized by a high amount of Zn and a variety of PAHs. Additionally Cu, Zn and PAH concentrations in stormwater were impacted by hydrological characteristics. At the scale of a rain event, the filter catches the majority of both dissolved and particulate micropollutants, and the suspension of particulate micropollution by the incoming flow decreases the pond RE. The treatment RE of the SCW system varies from 50% (naphthalene) to 100% (particulate Zn). Because of the suspension of particulate micropollution, REs in the pond can be negative for particulate micropollutants. The study of the SCW during a dry period highlights the release of HMs from filter sand to interstitial water. In fact, HM concentrations during a dry period were much higher than during rain events in the SCW; we even detected more micropollutants in the filter water during the dry period. An assessment of micropollutant storage in the SCW showed that the pond stored the majority of micropollutants, then the organic deposit in the filter, contrary to what the REs indicate. There seems to be no difference in micropollutant load between the largely-fed and the poorly-fed areas of the filter. Finally, current micropollutant contents in the substrate filters could allow for reuse as roadway backfill, an economical alternative to landfill storage.

The release of HMs, especially Zn, is the next operational challenge for SCWs. The physico-chemical variations in the SCW can cause a change in HM speciation and possibly a release into the incoming water. There is a need to investigate the interactions between the filter sand and HMs, and to anticipate HM saturation and subsequent HM release.

Acknowledgements

This study was supported financially and technically by the Strasbourg Eurometropole and the Lumieau-Stra project, laureate of the national call for projects "control strategies for urban water micropollutants" (June 2013) by the French biodiversity agency. The authors thank Martin Fisher for his technical support during the sampling campaigns, Carole Lutz, Marie-Pierre Ottermatte and Eric Pernin of the ENGEES laboratory for their support during the analyses. Finally, the authors would like to acknowledge the Agence de l'Eau Rhin-Meuse and the Zone Atelier Environnementale Urbaine (French LTSER) of Strasbourg for the funding they provided.

References

Ahyerre, M., Chebbo, G., Tassin, B., Gaume, E., 1998. Storm water quality modelling, an ambitious objective? Water Sci. Technol. 37, 205–213.

Al-Rubaei, A.M., Engström, M., Viklander, M., Blecken, G.-T., 2017. Effectiveness of a 19-year old combined pond-wetland system in removing particulate and dissolved pollutants. Wetlands,1–12 https://doi.org/10.1007/s13157-017-0884-6.

Bavor, H.J., Davies, C.M., Sakadevan, K., 2001. Stormwater treatment: do constructed wetlands yield improved pollutant management performance over a detention pond system? Water Sci. Technol. 44, 565–570.

Bidaud, C., Tran-Minh, C., 1998. Polycyclic aromatic hydrocarbons (PAHs) biodegradation in the soil of a former gasworks site: selection and study of PAHs-degrading microorganisms. J. Mol. Catal. B Enzym. 5, 417–421.

Birch, G.F., Matthai, C., Fazeli, M.S., Suh, J.Y., 2004. Efficiency of a constructed wetland in removing contaminants from stormwater. Wetlands 24,459–466. https://doi.org/10.1672/0277-5212(2004)024[0459:EOACWI]2.0.CO;2.

Blecken, G.-T., Hunt III, W.F., Al-Rubaei, A.M., Viklander, M., Lord, W.G., 2017. Stormwater control measure (SCM) maintenance considerations to ensure designed functionality. Urban Water J. 14, 278–290.
Bradl, H.B., 2004. Adsorption of heavy metal ions on soils and soils constituents. J. Colloid Interface Sci. 277, 1–18.
Bressy, A., 2010. Flux de micropolluants dans les eaux de ruissellement urbaines. Effets de différents modes de gestion des eaux pluviales.
Bressy, A., Gromaire, M.-C., Lorgeoux, C., Saad, M., Leroy, F., Chebbo, G., 2012. Towards the determination of an optimal scale for stormwater quality management: micropollutants in a small residential catchment. Water Res. 46,6799–6810 (Special Issue on Stormwater in urban areas). https://doi.org/10.1016/j.watres.2011.12.017.
BRGM, 2002. Gestion des sites (potentiellement) pollués. Annexe 5C révision du 09/12/2002 - Valeurs guides en matière de pollution des eaux et des sols (13 p.).
Carleton, J.N., Grizzard, T.J., Godrej, A.N., Post, H.E., Lampe, L., Kenel, P.P., 2000. Performance of a constructed wetlands in treating urban stormwater runoff. Water Environ. Res. 72, 295–304.
CE, 2000. Directive 2000/60/EC of the European Parliament and the Council of 23 October 2000 Establishing a Framework for Community Action in the Field of Water Policy.
Choubert, J.M., Martin Ruel, S., Budzinski, H., Coquery, M., 2011a. Removal of micropollutants by domestic conventional wastewater treatment plants and advanced tertiary process: Specific method and results of the Amperes project. Tech. Sci. Mét. 106, 44–62.
Choubert, J.M., Martin Ruel, S., Budzinski, H., Miège, C., Esperanza, M., Soulier, C., Lagarrigue, C., Coquery, M., 2011b. Evaluer les rendements des stations d'épuration. Apports Méthodologiques Résultats Pour Micropolluants En Filières Conv. Avancées Extr. Numér. Tech. Sci. Méthodes N. 12.
Dechesne, M., Barraud, S., Bardin, J.-P., 2004. Spatial distribution of pollution in an urban stormwater infiltration basin. J. Contam. Hydrol. 72, 189–205.
EPA, 1984. Health Effects Assessment for Polynuclear Aromatic Hydrocarbons (PAH) (No. U.S. Environmental Protection Agency, Office of Health and Environmental Assessment, Environmental Criteria and Assessment Office). U.S. Environmental Protection Agency, Office of Health and Environmental Assessment, Environmental Criteria and Assessment Office, Cincinnati, OH.
EPA, 2007. Framework for metals risk assessment (No. 120/R-07/001). United States Environmental Protection Agency. Office of the Science Advisor. Risk Assessment Forum, Washington, DC.
Flores-Rodrîguez, J., Bussy, A.-L., Thevenot, D.R., 1994. Toxic metals in urban runoff: physico-chemical mobility assessment using speciation schemes. Water Sci. Technol. 29, 83–93.
Göbel, P., Dierkes, C., Coldewey, W.G., 2007. Storm water runoff concentration matrix for urban areas. J. Contam. Hydrol. 91, 26–42.
Gregoire, B.G., Clausen, J.C., 2011. Effect of a modular extensive green roof on stormwater runoff and water quality. Ecol. Eng. 37, 963–969.
Gromaire-Mertz, M.C., Garnaud, S., Gonzalez, A., Chebbo, G., 1999. Characterisation of urban runoff pollution in Paris. Water Sci. Technol. Innovative Technologies in Urban Storm Drainage 1998 (Novatech '98) Selected Proceedings of the 3rd NOVATECH Conference on Innovative Technologies in Urban Storm Drainage 39, pp. 1–8. https://doi.org/10.1016/S0273-1223(99)00002-5.
Guardo, M., Fink, L., Fontaine, T.D., Newman, S., Chimney, M., Bearzotti, R., Goforth, G., 1995. Large-scale constructed wetlands for nutrient removal from stormwater runoff: an Everglades restoration project. Environ. Manag. 19, 879–889.
Guittonny-Philippe, A., Masotti, V., Höhener, P., Boudenne, J.-L., Viglione, J., Laffont-Schwob, I., 2014. Constructed wetlands to reduce metal pollution from industrial catchments in aquatic Mediterranean ecosystems: a review to overcome obstacles and suggest potential solutions. Environ. Int. 64,1–16. https://doi.org/10.1016/j.envint.2013.11.016.
Kar, D., Sur, P., Mandai, S.K., Saha, T., Kole, R.K., 2008. Assessment of heavy metal pollution in surface water. Int. J. Environ. Sci. Technol. 5, 119–124.
Lamprea, K., 2009. Caractérisation et origine des métaux traces, hydrocarbures aromatiques polycycliques et pesticides transportés par les retombées atmosphériques et les eaux de ruissellement dans les bassins versants séparatifs péri-urbains. (phdthesis). Ecole Centrale de Nantes (ECN).
Lamprea, K., Ruban, V., 2011. Characterization of atmospheric deposition and runoff water in a small suburban catchment. Environ. Technol. 32, 1141–1149.
Li, Y.C., Zhang, D.Q., Wang, M., 2017. Performance evaluation of a full-scale constructed wetland for treating stormwater runoff. CLEAN–Soil Air Water 45.
Lin, J.-G., Chen, S.-Y., 1998. The relationship between adsorption of heavy metal and organic matter in river sediments. Environ. Int. 24, 345–352.
Lorant, F.I., 1992. Effects of piped median vs. open ditch drainage on stormwater quality.
Nix, S.J., Heaney, J.P., Huber, W.C., 1988. Suspended solids removal in detention basins. J. Environ. Eng. 114, 1331–1343.
Nys, C., Janssen, C.R., de Schamphelaere, K.A., 2017. The effect of pH on chronic zinc toxicity differs between daphnid species: development of a preliminary chronic zinc Ceriodaphnia dubia bioavailability model. Environ. Toxicol. Chem. 36, 2750–2755.
R Core Team, 2016. R: a Language and Environment for Statistical Computing. R Foundation for Statistical Computing, Vienna, Austria.
Revitt, D.M., Lundy, L., Coulon, F., Fairley, M., 2014. The sources, impact and management of car park runoff pollution: a review. J. Environ. Manag. 146, 552–567.
RF, 2007. Circulaire du 07/05/07 définissant les “normes de qualité environnementale provisoires (NQEp)” des 41 substances impliquées dans l'évaluation de l'état chimique des masses d'eau ainsi que des substances pertinentes du programme national de réduction des substances dangereuses dans l'eau.
RF, 2010. Arrêté du 25 janvier 2010 relatif aux méthodes et critères d'évaluation de l'état écologique, de l'état chimique et du potentiel écologique des eaux de surface pris en application des articles R. 212-10, R. 212-11 et R. 212-18 du code de l'environnement.
Schmitt, N., Wanko, A., Laurent, J., Bois, P., Molle, P., Mosé, R., 2015. Constructed wetlands treating stormwater from separate sewer networks in a residential Strasbourg urban catchment area: micropollutant removal and fate. J. Environ. Chem. Eng. 3, 2816–2824.
Sébastian, C., Barraud, S., Gonzalez-Merchan, C., Perrodin, Y., Visiedo, R., 2014. Stormwater retention basin efficiency regarding micropollutant loads and ecotoxicity. Water Sci. Technol. 69, 974–981.
Strassler, E., Pritts, J., Strellec, K., 1999. Preliminary Data Summary of Urban Storm Water Best Management Practices. U. S. Environ. Prot. Agency Off. Water (Httpwww Epa Govwaterscienceguidestormwater Nsbd).
Walaszek, M., Bois, P., Laurent, J., Wanko, A., 2015. Ponding water ultrasonic measurements in urban stormwater constructed wetland: clogging monitoring and *Phragmites australis* allometric parameters survey. Presented at the 6th International Symposium on Wetland Pollutant Dynamics and Control, Wetpol, York, United Kingdom, p. 158.
Walega, A., Wachulec, K., 2018. Effect of a Retention Basin on removing pollutants from Stormwater: a case study in Poland. Pol. J. Environ. Stud. 27,1795–1803. https://doi.org/10.15244/pjoes/76797.
Yeh, T.Y., Chou, C.C., Pan, C.T., 2009. Heavy metal removal within pilot-scale constructed wetlands receiving river water contaminated by confined swine operations. Desalination 249, 368–373.
Zgheib, S., Moilleron, R., Saad, M., Chebbo, G., 2011. Partition of pollution between dissolved and particulate phases: what about emerging substances in urban stormwater catchments? Water Res. 45,913–925. https://doi.org/10.1016/j.watres.2010.09.032.
Zhang, K., Deletic, A., Page, D., McCarthy, D.T., 2015. Surrogates for herbicide removal in stormwater biofilters. Water Res. 81, 64–71.

Applied Geochemistry 97 (2018) 167–180

Contents lists available at ScienceDirect

Applied Geochemistry

journal homepage: www.elsevier.com/locate/apgeochem

Sorption behavior of copper, lead and zinc by a constructed wetland treating urban stormwater

M. Walaszek[a,*], M. Del Nero[b], P. Bois[a], L. Ribstein[b], O. Courson[b], A. Wanko[a], J. Laurent[a]

[a] ICube, UMR 7357, ENGEES/CNRS/Université de Strasbourg, 2 rue Boussingault, 67000, Strasbourg, France
[b] Institut Pluridisciplinaire Hubert Curien, UMR 7178 CNRS-UdS, 23, rue du Loess, 67037, Strasbourg Cedex 2, France

ARTICLE INFO

Editorial handling by Michael Kersten

Keywords:
Constructed wetland
Heavy metals
Sorption
Stormwater

ABSTRACT

Sorption behaviors of copper (Cu), lead (Pb) and zinc (Zn) in a stormwater constructed wetland (CW) have been investigated by combining CW sample analysis and batch sorption experiments. The mass balance calculations suggest retention/remobilization along the CW sequence for Zn, unlike Pb and Cu. According to the mixed Tessier-BCR sequential extractions results, Pb and Zn are both mainly associated to residual fractions (incorporated in the lattice or at surfaces of primary clays, or in heavy minerals) and to Fe/Mn oxihydroxyde fractions, whereas Cu is possibly associated to carbonates minerals in the CW. In CW field conditions (metals at trace concentrations and pH lower than 7.5), batch experiment results suggest that the global affinity of the CW substrate for metals attends the following order: Pb = Cu > Zn. Pb and Cu form surface complexes on high and weak affinity sites of the substrate, as hydroxyl groups of iron oxides. Zn is involved in ion exchange and/or compensation of negative charges at the surface of CW substrate (pH < 5). The metals sorption capacities of the substrate reveal that Zn is potentially desorbable from the substrate under the field conditions, on the contrary Cu and Pb removal efficiencies are above 90%.

1. Introduction

Naturally-occurring heavy metals or metalloids (HMs) such as zinc (Zn), copper (Cu), lead (Pb), nickel (Ni), chromium (Cr) and cadmium (Cd) are ubiquitous in all compartments of surface systems, due to their release upon weathering of primary rocks and their subsequent participation to a variety of biogeochemical processes, including secondary processes of retention (sorption) in soils, formation of dissolved or (pseudo)colloidal species transported through soil/surface waters, and uptake by plant roots followed by a delocalization to foliage which may favor further transfers of HMs along the trophic chain. It is well recognized that a multitude of human activities since the past decades, such as those related to ore mining and reprocessing, industrialization and urbanization, have led to a multiplicity of introductory pathways (air, effluents …) of HMs in the environment, contributing thereby to an increase of HMs contents in rain and surface waters (Bressy, 2010; Kar et al., 2008; Sekabira et al., 2010), which can have a negative effect on aquatic ecosystems such as, for example, a health hazard to fishes (Fu et al., 2013). One of the multiple sources of human-derived HMs in surface waters is urban runoff water. Runoff water remobilizes HMs from urban soil (Flores-Rodriguez, 1992) and is a main vector of dissemination/transport of HMs like Zn (130–160 µg/l), Pb (3–29 µg/l), Cu (8–31 µg/l) and to a lesser extent Cr, Ni and Cd (Bressy, 2010; Lamprea, 2009; Schmitt et al., 2015). Stormwater constructed wetlands (CW) can be used to trap HMs transported via runoff waters and to limit the contamination of surface water by HMs. The main process involved in the retention of HMs depends on HMs partitioning between the aqueous and particulate phases: particulate HMs settle in sedimentation pond or are mechanically filtered in filtering basins whereas dissolved HMs are rather sorbed at surfaces of (nano)particles such as clays, metal oxides and hydroxides, metal carbonates, phosphates and organic matter (OM) in suspension, in pond sediments or in basin substrate (Bradl, 2004).

Sorption processes responsible for retention of HMs in soils include a variety of mechanisms (Sposito, 1981) such as ion exchange (McBride, 1994), (co)precipitation (Heike B Bradl, 2004) and surface complexation (Srivastava et al., 2005). Consistently, the main processes of HMs retention reported for CWs are adsorption on surfaces of mineral and organic constituents, diffusion in primary and secondary mineral structures and precipitation as secondary phases (Sipos et al., 2008). The partitioning of HMs between mineral surfaces and solution is actually controlled by their speciation (Lee et al., 1998), which depends on multiple parameters such as the affinity of the metals for dissolved ligands and/or for ligands sorbed at the mineral-solution interfaces (e.g. Land et al., 1999), the structure and the stability of the

* Corresponding author.
E-mail address: mwalasze@engees.eu (M. Walaszek).

https://doi.org/10.1016/j.apgeochem.2018.08.019
Received 15 January 2018; Received in revised form 22 August 2018; Accepted 22 August 2018
Available online 24 August 2018
0883-2927/

metallic species formed (Braun et al., 1993), and the physico-chemical conditions prevailing in the soil (H. W. Nesbitt, 1979). Main parameters affecting the extent of sorption of a HM include the pH and the ionic strength (Harter, 1981), the presence and concentration of competing or complexing species (Benjamin and Leckie, 1981) and humic substances (Davis, 1984) and the nature and concentration of the substrate (Spark et al., 1995).

Many studies have investigated the sorption behavior of Pb, Cu and Zn in natural soils by means of analytical techniques, e.g. electron microscopy, sequential chemical extractions on soil samples and/or batch sorption experiments in competitive metal systems. Several studies of different soils showed general agreement on the following order of sorption of HMs: Pb > Cu > Zn (Covelo et al., 2007a; Echeverria et al., 1998; Hooda and Alloway, 1998; Jiang et al., 2006; Sipos et al., 2008). Elliott et al. (1986) studied the competitive sorption of divalent trace metals and showed that the presence of humic substances (HS) is likely to change the metal affinity order for soil surfaces. The authors found that the affinity order of Cu, Pb, Cd and Zn for acidic soils corresponds to the order of pKs for the first metal hydrolysis products (i.e., Pb > Cu > Zn > Cd) in the absence of HS, whereas the retention of Cd is favored over that of Zn in the presence of HS. This finding was in agreement with experimental studies showing that the stability constants of dissolved metal-HS complexes increase in the order Pb/Cu > Cd > Zn (Kostic et al., 2011; Pandey et al., 2000; Yang and van den Berg, 2009) and supported the existence of specific interactions between metals and HS sorbed at mineral surfaces of soil. Soil components that have been reported in the literature as the main sorbents of HMs depend on the metal and soil considered. Cu was mostly found to be specifically adsorbed in a non-exchangeable form in soils. According to Bradl (2004), Fe and Mn oxides, soil OM and carbonates are the most important sinks for Cu. In a study on 11 Spanish acid soils, Covelo et al. (2007a) reported that Cu is preferentially sorbed by OM and clay as vermiculite. The high charge/radius ratio of Cu enables it to form stable complexes with OM and with high-surface-charge clays as vermiculite (Covelo et al., 2007a). Atanassova and Okazaki (1997) showed that Cu is mainly sorbed at specific high affinity sites which are provided by Fe and Mn oxides present in the soil clay fraction. Carbonate minerals in soils cause alkaline conditions which favor an increased Cu sorption and the precipitation of metals (Sipos et al., 2008). Regarding Pb, Hooda and Alloway (1998) showed that the calcium carbonate and clay mineral contents are positively and significantly correlated with Pb sorption on the acidic subsoils of the eastern USA unlike the OM content. In contrast, Covelo et al. (2007b) and De Matos et al. (2001) indicated that Pb sorption is correlated with the OM and calcium carbonate mineral contents. Bradl (2004) reported that Mn and Fe oxides have a predominant role on Pb sorption: Pb can be strongly and specifically adsorbed due to its high affinity for the oxide surfaces and/or it may participate to the formation of Pb-Mn minerals such as coronadite. Whereas Cu and Pb exhibit specific sorption on soil components such as OM, Fe and Mn oxides, Zn is widely reported to show a non-specific electrostatic adsorption on soil solid particles. For example, Bradl (2004) reports that 2:1 clays (e.g., montmorillonite and illite) have greater Zn fixing capacities than 1:1 clays because Zn is mostly trapped in at frayed edges of clays interlayers wedges. Zn sorption was also found to be highly correlated to Ca soil contents (De Matos et al., 2001) and to be mainly bound to the carbonate and residual fractions of sequential extraction experiments using soil samples (Marković et al., 2016). In summary, OM, clay minerals and Fe and Mn oxides are the most important soil components determining the extent of sorption of HMs in soils. OM can participate to formation of stable metallo-organic complex with Cu and Pb or may bind them by ionic interaction. Clay minerals and metal oxides sorb Cu, Pb and Zn through surface ion exchange and/or metal(organic) surface complex formation (Covelo et al., 2007b; Sipos et al., 2008). Therefore, the ability of a substrate to bind Cu, Pb and Zn strongly depends on its OM and clays contents.

The literature is plenty of studies focus on metal sorption mechanisms in industrial and acidic mining soils (Di Luca et al., 2011; Sheoran and Sheoran, 2006; Uchimiya et al., 2011; Vega et al., 2006) and in natural media as stream sediments and natural soils (Atanassova and Okazaki, 1997; Covelo et al., 2007b, 2007a; De Matos et al., 2001; Echeverria et al., 1998; Hooda and Alloway, 1998; Jiang et al., 2006; Marković et al., 2016; Pan et al., 2016; Sipos et al., 2008; Xian, 1989; Yun et al., 2003; Zhang et al., 2016).

However no study has so far been focusing on the sorption of HMs on CW substrates, especially for urban stormwater treatment. CWs are used for HM retention purposes by specific substrates (sand rich, low OM contents) whose sorption capacity has to remain constant for decades. Moreover, although HM loads in CWs are lower than in the industrial/mining context, they are much higher than in natural systems. All these features make the sorption mechanisms of HMs an important issue of CWs, in particular with regard to the safety assessment of CWs during ageing.

In this work, we aimed at gaining insights into the sorption mechanisms of Cu, Pb and Zn in an urban stormwater CW by combining CW sample analyses and batch sorption experiments of HMs. The mobility/retention behavior of HMs in CW was investigated by performing chemical analyses of substrate/water samples collected along a studied CW profile. Sequential extraction experiments were also made on collected substrate samples to identify main sorbing phases of HMs in CW. Further information on mechanisms involved in the retention of HMs on the CW substrate was acquired by investigating effects of key parameters on the competitive sorption of HMs on sand, e.g., pH, metal concentration, HM-sand-solution contact time and sand composition. .

2. Material and methods

2.1. Constructed wetland studies

The experimental site takes place in Strasbourg (67, France). The treatment system collects runoff water from an urban catchment (27,000 m^2) and is made up by a pond followed by a CW designed to reduce the amount of HMs released in stream. Sizing data are available in (Walaszek et al., 2018). The present study takes place after a 6-years operating of the experimental site and it focuses on the CW substrate, more precisely on the top layer substrate which is expected to be a main trap for dissolved metals. The CW substrate is a filter composed of three layers of 20–30 cm with a variable granulometry (Fig. 1). The top layer studied here is made by sand (with a grain diameter between 0 and 4 mm), the intermediate layer by thin gravel (grain diameter between 4 and 8 mm), and the bottom layer by coarse gravel (grain diameter between 10 and 14 mm). Stormwater infiltrates from the top to the bottom layer and is drained to the stream. In this work, a core sample of the top sand layer was collected up to 25 cm in depth at one sampling point in the CW and was divided into subsamples at three different depths ($CW_{0\text{-}10}$: from 0 to 10 cm, $CW_{10\text{-}20}$: from 10 to 20 cm, and $CW_{20\text{-}25}$: from 20 to 25 cm).

After sieving (< 1 mm) and homogenization, the subsamples were taken for chemical analysis and sequential extraction experiments. A fresh sub-sample of the initial sand (noted sand #1, purchased from Holcim Bischwiller) that was used for constructing the CW top layer, and another sand sample (noted sand #2, also purchased from Holcim Bischwiller but not used in the CW), were also taken after sieving (< 1 mm) for analysis of their particle-size distribution and of their chemical and mineralogical compositions. The particle-size distribution of sand #1 was determined by size fractionation using wet sieving: nested column of sieves (7 mesh sizes: 500- 250–200 -160-100 µm) and is reported in Table 1. The mineralogical compositions of sand #1 and sand #2 were determined by X-ray diffraction analysis. The measurements were performed on both the whole samples and the clay size (< 2 µm) fraction using a Bruker Endeavor D4 diffractometer. Clay size fraction was isolated by settling, and oriented on glass slides. Three XRD analyses were performed for each sample: a) without treatment, b)

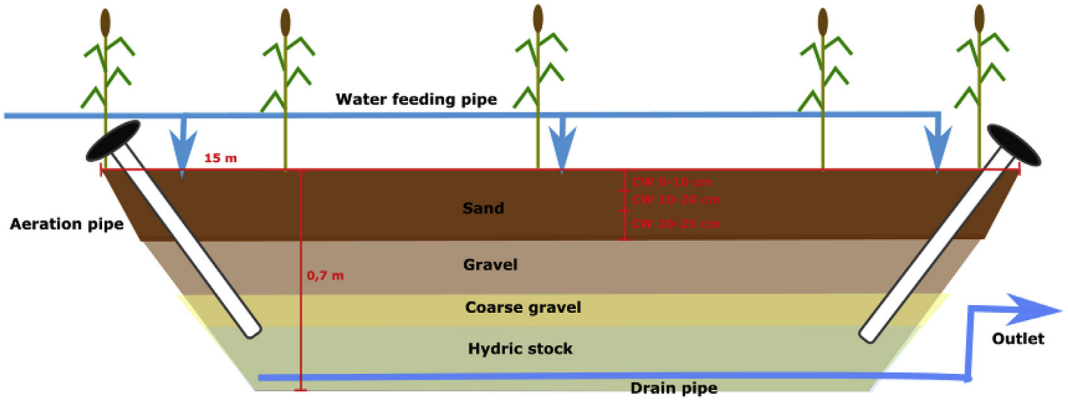

Fig. 1. Design, dimensions and subsamples location in the stormwater constructed wetland.

after saturation for 12 h in ethylene-glycol, c) after heating at 490 °C for 2 h (Bout-Roumazeilles et al., 1999). The clay minerals were identified with their layer and interlayer spacings (Brindley and Brown, 1980). A semi-quantitative estimation of the percentage of each mineral in clay size fraction was performed, with an error in reproducibility of the measurements of less than 5% for each mineral. Quartz and calcite are the major minerals in the sands and plagioclase occur as accessory minerals. The clay fraction is composed by illite (51%) and chlorite (49%).

The chemical analyses of the CW subsamples (CW0-10, CW10-20, and CW20-25) and of the fresh subsample of initial sand (sand#1) were performed to determine the evolution of contents in major and trace elements along the CW top layer of CW and the HM mass balances. Prior to chemical analysis, the subsamples were crushed (< 80 µm), homogenized and dried at 105 °C. They were then digested by alkali fusion with LiBO2 followed by a leaching in a concentrated HNO_3 solution. Major element analysis was made using a Thermo Fisher ICap 6500 inductively coupled plasma optical emission spectrometer (ICP-OES), and trace element analysis was made with a Thermo Elemental ×7 inductively coupled plasma mass spectrometer (ICP-MS). The analytical precision was determined to be < 10% for ICP-OES measurements and < 5% for ICP-MS measurements. The chemical compositions of sand#1 and of the CW subsamples are shown in Table 2 and Table 3 and in Supplementary Information S1, respectively. Contents of Cd, Cu and Zn in sand#1 were under the detection limit. Mass balances of the metals (gain/losses) in the CW subsample at depth from x to y cm were calculated by taking thorium (Th) as invariant element and using the following formula (H. Wayne Nesbitt, 1979):

$$Gain/Loss\ (\%) = \left(\frac{\text{Metal content in } CW_{x-y}/\text{Th content in } CW_{x-y}}{\text{Metal content in sand \#1/Th content in sand \#1}} - 1\right) \times 100$$

Sequential extraction experiments were performed on the CW and on the sand#1 subsamples to help identify main phases of sand that were able to trap HMs in the CW top layer. A procedure combining the Tessier and the BCR methods (Rauret et al., 1999; Tessier et al., 1979) was used. Principle of the sequential extractions is to extract from a same sample the HMs contained in different phases of samples by using extracting reagents of increasing strength. The steps in the procedure were operationally defined in terms of the main targeted forms as follows: exchangeable-weakly sorbed fraction (8 mL, 1 M $MgCL_2$), sorbed and/or carbonate-bound fraction (8 mL, 1M CH_3COONa, pH 5.0), bound to easily reducible manganese oxides and amorphous iron oxides fraction (40 mL, 0.25M $(NH_2OH)2H_2SO_4$, pH = 1.5–2.0), bound to and/or incorporated into organic matter (3 mL, 0.02M HNO_3, 5 mL H_2O_2 30%, pH = 2 then 3 mL H_2O_2 30%, pH = 2 then 5 mL, 3.2M CH_3COONH_4 in HNO_3 20%). The procedure used for 1 g sample is summarized in Table 4. At each step of the procedure, the reagent containing the extracted elements was collected, acidified (except for last reagent) and analyzed for its HM contents by ICP-MS. It should be noted that the fractions extracted by these experiments are actually defined by the operative mode (reagent and extraction conditions) and not from the point of view of the mineralogy/constituent phases of the sample. However, it is common to link these fractions to large classes of soil and sediment constituents. The denomination of the fractions used here corresponds thus to the main phases expected to be targeted by the reagents.

Table 2
Major element composition of sand#1 and sand#2.

	Sand#1	Sand#2
SiO_2 (%)	70.40	83.17
Al_2O_3 (%)	5.70	4.92
Fe_2O_3 (%)	1.26	0.80
MnO (%)	0.036	0.018
MgO (%)	0.89	0.31
CaO (%)	9.68	3.73
Na_2O (%)	1.17	0.93
K_2O (%)	1.70	1.82
TiO_2 (%)	0.17	0.12
P_2O_5 (%)	< L.D.	< L.D.
PF (%)	8.47	3.31
Total (%)	99.48	99.12

2.2. Water analysis

Concentrations of dissolved Cu, Pb and Zn were determined for water samples collected at three strategic points along the treatment system: the pond, the piezometer in the CW and the CW outlet. Samples were filtered at 0.45 µm and analyzed by ICP-MS. Subsamples of the filtered samples were centrifuged for 2 h at 50,000 rpm in order to separate the colloidal and aqueous phases and an aliquot of supernatant was taken for ICP-MS analysis.

Speciation of HMs were calculated using the Cheaqs Pro software

Table 1
Particle size distribution of the CW top layer sand#1.

	> 500 µm	500-315 µm	315-250 µm	250-200 µm	200-160 µm	160-100 µm	< 100 µm
Fraction (%)	11	29	17	18	13	11	2

Table 3
Trace elements composition of sand#1 and sand#2 (L.D: Limit of Detection).

Content (ppm)								
Element	Sand#1	Sand#2	Element	Sand#1	Sand#2	Element	Sand#1	Sand#2
As	5.77	3.96	Ge	1.16	1.28	Sm	2.11	1.55
Ba	265.50	292.40	Hf	1.83	1.67	Sn	6.72	7.37
Be	1.055	0.81	Ho	0.35	0.24	Sr	241.90	126.20
Bi	0.41	< L.D.	In	< L.D.	< L.D.	Ta	0.37	0.37
Cd	< L.D.	< L.D.	La	10.84	8.91	Tb	0.28	0.19
Ce	22.21	17.76	Lu	0.13	0.10	Th	4.056	3.43
Co	3.40	1.89	Mo	< L.D.	< L.D.	Tm	0.13	0.093
Cr	36.81	28,20	Nb	3.60	2.79	U	1.21	0.83
Cs	2.14	2.25	Nd	10.09	7.89	V	17.32	10.37
Cu	< 5	< 5	Ni	17.64	11.25	W	0.73	0.78
Dy	1.69	1.17	Pb	10.32	9.81	Y	10.020	6.77
Er	0.89	0.64	Pr	2.71	2.15	Yb	0.88	0.67
Eu	0.51	0.36	Rb	66.18	67.34	Zn	< 11	< 11
Ga	6.05	4.95	Sc	3.13	< L.D.	Zr	64.20	61.56
Gd	1.77	1.24	Sb	0.53	0.56			

Table 4
Sequential extraction procedure.

Fraction	Reagents	Conditions
Exchangeable	8 mL 1M $MgCL_2$ pH = 7	1 h, Room temperature 50 rpm shaking
Carbonates	8 mL 1M CH_3COONa pH = 5 (acetic acid adjustment)	5 h, Room temperature 50 rpm shaking
Fe and Mn oxides	40 mL 0.25M $(NH_2OH)2H_2SO_4$ pH = 1.5–2 (acetic acid adjustment)	16 h, Room temperature 50 rpm shaking
Organic matter	3 mL 0.02M HNO_3 + 5 mL 30% H_2O_2 (pH = 2) 3 mL 30% H_2O_2 (pH = 2) 5 mL 3.2M CH_3COONH_4 in 20% HNO_3	2 h, 85 ± 3 °C 3 h, 85 ± 3 °C 30 min, Room temperature
Residual	2 mL $HClO_4$ + 10 mL HF 1 mL $HClO_4$ + 10 mL HF 1 mL $HClO_4$ 10 mL HNO_3 10 mL aqua regia 5 mL HNO_3	Total evaporation then repeats in the next acid.

(Verweij, 2014). Equilibrium constants are taken from the NIST database 46 (version 8) (Smith et al., 2004). The speciation calculations were performed considering a partial pressure of CO_2 of $2.14.10^{-4}$ atm (equilibrium with respect at atmospheric CO_2) and a temperature of 25-°C.

2.3. Batch sorption experiments

2.3.1. Procedures

Batch experiments were performed to study the (competitive) sorption of HMs (Cu, Pb, Zn) onto sand #1 and the sand sample noted sand#2. The chemical composition of the latter is given in Tables 2 and 3 Sand#2 displays a lower content of Ca and Fe than Sand#1. The concentration of metal sorbed on sand C_s ($mol.L^{-1}$) was determined by varying in experiments values of pH (pH-edge curves), of HM-sand-solution contact time (kinetic sorption curves) and of initial metal concentration (sorption isotherms). All the solutions were prepared using reagent grade chemicals and ultra-pure water (purity > 18 MΩ cm). Stock metal solutions of 200 µM were prepared by diluting for Cu and Pb 254 µl of 1000 mg/l standard solutions with HNO_3 (0.005%) and for Zn 15 mL of 10 mg/l standard solution with HNO_3 (0.02%). Mono-metal kinetic curves of sorption of Cu, Pb and Zn on sand were obtained from series of mono-metal batch experiments carried out as a function of sand-solution contact (1 h < Tc < 14 days) and pH (2 < pH < 9). Initial suspensions of 1 g.L-1 sand (50.0 ± 0.1 mg of sand in contact with a 49,625 mL of ultrapure water) were prepared in individual 50-ml stoppered High Density Polyethylene (HDPE) tubes. An appropriate volume (375 µl) of a 200 µM Pb, Zn or Cu standard solution was immediately added to the individual tubes to obtain an initial concentration of Pb, Zn or Cu of 1.5 µM. Varied volumes of HNO3 (5%) were also introduced in the tubes to reach a desired value of inital pH (between 2.0 and 4.0). The tubes were then placed in an air-conditioned room (298 K) and shaken at 50 rpm for 1 h to 14 days. The pH-dependent sorption curves were obtained by adding in the initial suspensions appropriate volumes (125 µl) of a solution containing Cu, Zn and Pb at equimolar concentrations (200 µM) or of a solution at a Cu, Pb or Zn concentration of 200 µM (125 µl, 375 µl or 1.25 ml respectively) to reach initial metal concentrations of 0.5 µM, 1.5 µM and 5 µM, respectively. After initial pH adjustment, the tubes were shaken at 298 K and at 50 rpm for 24 h (monometal) or 48 h (multimetal). Monometal sorption isotherms were obtained by adding varied volumes of an appropriate metal solution containing one of the three elements to reach initial concentrations of 5, 10, 20, 30 and 50 µM, varied volumes of distilled-deionized water and HNO3 (5%) to reach pH 2.4 (Zn) or pH 2.6 (Cu, Pb) to 50.0 ± 0.1 mg of sand in 50-ml stoppered HDPE tubes. Suspensions were placed in an air-conditioned room (298 K) and shaken at 50 rpm for 24 h. No attempt was made to adjust ionic strength or pH during the experiments.

After the defined contact time, the final pH values were recorded and suspensions were centrifuged at 9000 rpm for 120 min solution-colloid separation and the supernatants were collected. Supernatants were stored in polyethylene bottle to which a HNO3 (1%) solution containing internal standards was added for sample preservation. Initial metal concentration C_o and final metal concentration C_f in solution were determined by ICP-MS. The percent sorption (%) is calculated as follows:

$$\%\ sorption = \frac{Co - Cf}{Co} \times 100$$

2.3.2. Sand and tube surface effect

Blank experiments were performed to determine the amounts of Cu, Pb and Zn expected to be released in solution from the sands during the batch experiments (contents of Cu and Zn were under the detection limit but Pb content in sand #1 and sand #2 was equal to 10.32 and 9.81 ppm, respectively, cf. Table 3). The blank experiments were carried out for different pH values (2–8) without metal addition. Dissolved metal concentrations of the final solutions in the 2.4–8.2 pH range were below detection limits for Cu, Pb and Zn. Thus no significant amounts of metals were released from the initial sands under the experimental

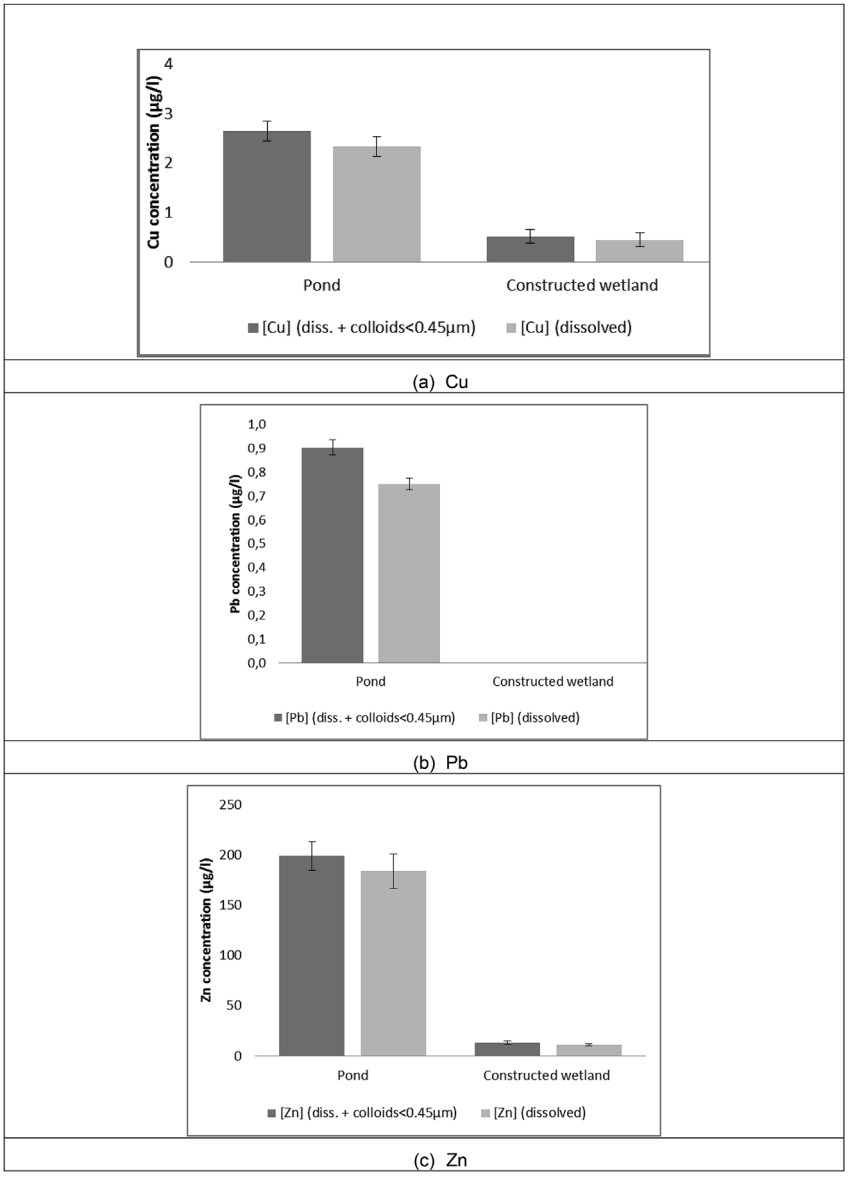

Fig. 2. Concentration of (a) Cu, (b) Pb and (c) Zn in water samples of pond and CW. Fractions "diss. + colloids < 0.45 µm" and "dissolved" refer to analysis of the water samples after filtration at 0.45 µm and after centrifugation of the filtered samples during 2 h, respectively.

conditions used.

Tube surfaces might compete against sand for HM sorption during our batch experiments, particularly at acidic pH and trace metal concentration (< 1 µM). In order to determine the percentage of metal sorbed by the tube walls, the individual tubes used were repeatedly washed (3 times) with distilled water at the end of the sorption experiment, and 10 mL of HNO3 (1%) were added to desorb HMs from tube walls. The tubes were shaken in a cooled room at 298 K. After 24 h, supernatants were collected and stored in polyethylene bottle to which a HNO3 (1%) solution containing internal standards was added for ICP-MS analysis. Fig. 1S (Supplementary Material) reveals that less than 20% of Cu, Pb and Zn is expected to be trapped by tube walls throughout the studied pH range, for the lowest metal concentration used in the sorption experiments (1.5 µM).

3. Results

3.1. Distribution and speciation of metals in CW

3.1.1. Metals in CW water

Fig. 2 presents concentrations of dissolved (and colloidal) Cu, Pb and Zn in the water of the treatment system. A first finding is that sorption/surface complexation of the HMs by colloids is not expected to be a significant mechanism of HM removal in the CW, as there is no significant difference between dissolved metal concentrations and total (dissolved plus colloidal) metal concentrations. Concentrations of dissolved Cu are low along the system, varying from 2.7 µg/l in the pond to 0.45 µg/l in the CW. Dissolved Pb is found to exist at trace level concentration (< 1 µg/L) in the pond and to be below detection limit in the CW. In contrast, dissolved Zn is at a high concentration in the pond (200 µg/l). The metal importance in the system observes the following order: Zn > Cu > Pb.

Solubility and sorption/precipitation behavior of HMs is actually primarily dependent on HM speciation. To know the chemical forms of the metals in entry of the CW, we calculated speciation curves of the

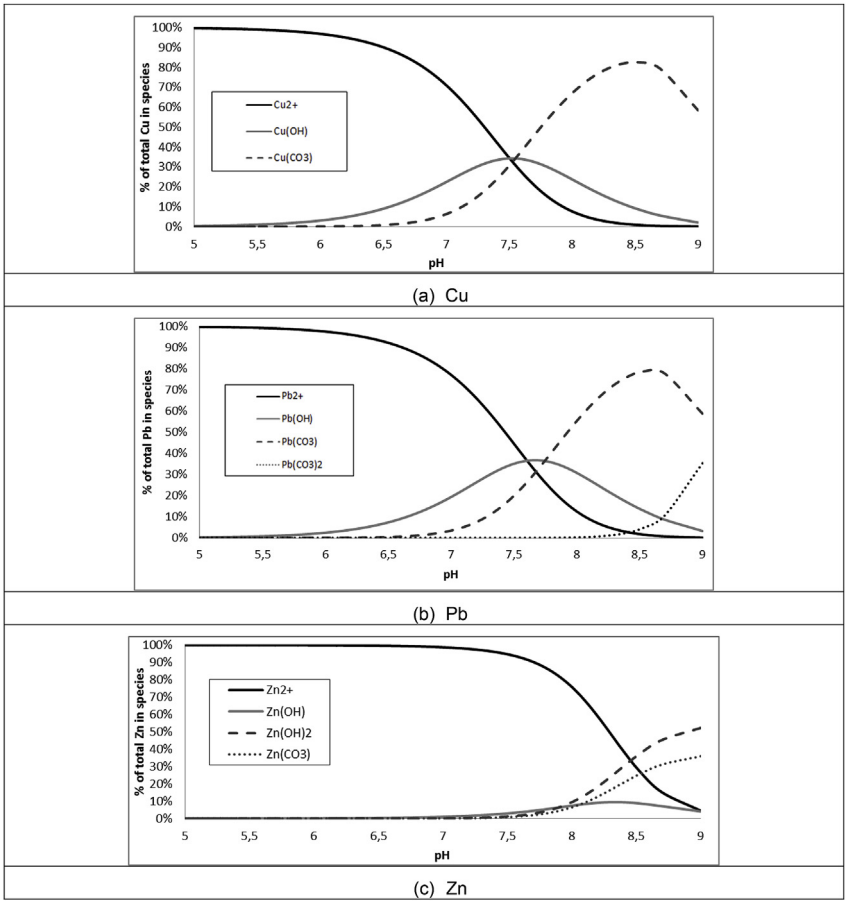

Fig. 3. Calculated speciation of Cu, Pb and Zn using the CHEAQS speciation code. Solutions are considered at equilibrium with atmospheric CO2 and total concentrations of Cu, Pb and Zn equal to 2.5 µg/l, 1 µg/l and 200 µg/l, respectively.

HMs (Fig. 3) at the pond concentrations, for the pH range 5–9. Near-neutral pH values of 7.5 and 7.4 were measured in the pond and in the CW, respectively, during a dry period and cold weather). Cu in the pond outflow is expected to distribute equally in the forms of the metal cation, Cu^{2+}, of its first hydrolysis product, and of 1:1 copper carbonate complexe (calculations were made in the absence of anions others than hydroxide and carbonate anions). Similarly, the principal forms of Pb in the pond are expected to be Pb^{2+}, its first hydrolysis product, and the 1:1 Pb carbonate complex. In contrast, the principal form of Zn is Zn^{2+}. Then at the pond concentrations there is no mineral-carbonates or oxides formation for all HMs at near-neutral pH observed in the pond and the CW. Thus the removal of metals in the system is not caused by the precipitation of HMs.

3.1.2. Distribution profiles of metals along top sequence of CW substrate

First of all, it should be noted that the percentages of major elements for the CW samples do not change significantly with depth and do not show any notable differences with the values obtained for the initial sand, suggesting no significant alteration of sand. Metal contents along the 25 cm of the top layer of CW profile are given in Fig. 4 (a) for Zn and Pb, and in Table 1S (Supplementary Material) for the other metals. Concentrations of Cu remain below detection limit for all the studied samples. Pb concentrations in the CW upper layer are slightly lower than in initial sand (< 10 ppm) and vary slightly with depth. Zn contents vary with depth: they are higher than that of initial sand at depths 0–20 cm and below detection limit (like for sand#1) in sample $CW_{20\text{-}25}$. Gain and losses of metals calculated in the CW profile in the 30 cm of the top layer are given in Fig. 4 (b) for Zn and Pb. Mass balances could not be calculated for Cu as its concentrations are below detection limit along the CW sequence. The mass balance results show that, during 5 years of CW operating, no significant amount of Pb has been stored in the CW profile. Given the analytical uncertainty, this trace metal show moderate (< 20%) or no losses along the CW profile. Similar results were observed for almost all trace metal elements in the CW top layer (Supplementary Information), except for lanthanides and uranium which remained rather immobile. In contrast to Pb, there is a Zn accumulation (+100%) in the first layers. Zn is found to be accumulated and disseminated up to 20 cms in depth, which suggests dynamic retention/remobilization processes of this metal along the CW sequence. Such a difference between Pb and Zn accumulation in the CW can partly reflect the difference between the Pb and Zn inputs in the CW, as shown in §3.1.1. It should indeed be emphasized that these results do not give us information on the relative affinities of the sand with respect to the various metals, since the inputs are different from one metal to another, nor on the sand retention efficiency. They just highlight that the sand shows little or no leaching of metals despite 5 years of flowing of collected runoff waters and that it had also the capacity to trap Zn (whose inputs are important). Whether this storage represents a large or a small part of the inputs is to be determined. Therefore, it is important to carry out sorption experiments under controlled conditions in order to rationalize our knowledge on the sorption efficiency of the sand by estimating the (maximum and relative) sorption capacities of the sand with respect to the various metals and by testing capacity sensitivity to a change of the chemical parameters of the system.

3.1.3. Metals distribution in CW mineral phases

Fig. 5 presents the concentrations of Cu, Pb and Zn extracted (and not extracted) from the five fractions of the mixed Tessier-BCR procedure in the initial sand (sand #1) and along the CW substrates. Results are given with an uncertainty of less than 10%. The data reported

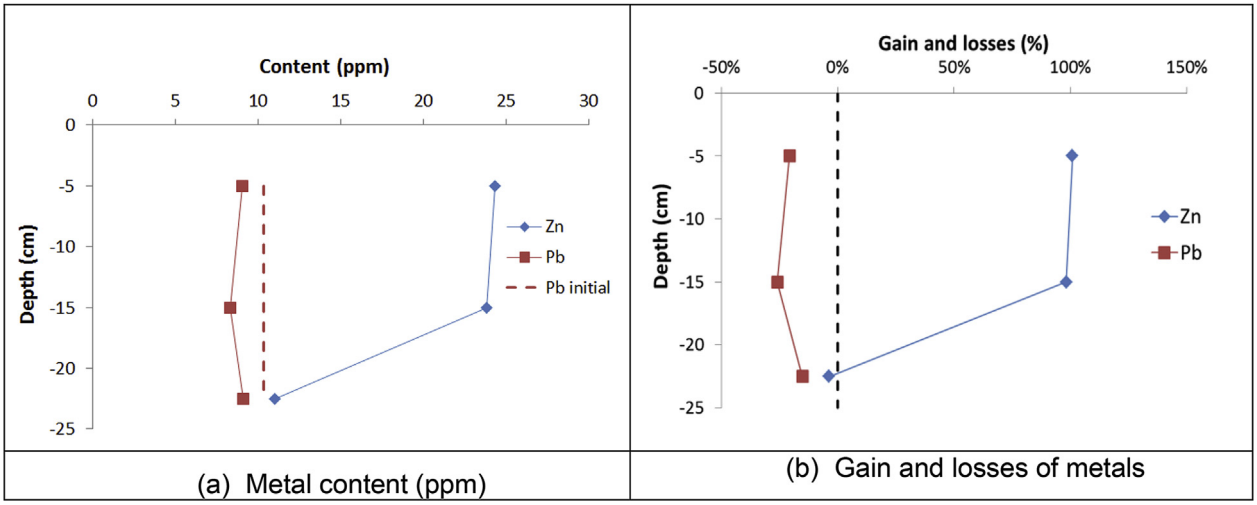

Fig. 4. (a) Metal content (ppm) of initial sand #1 and of sand samples collected at different depths along a vertical sequence in CW and (b) calculated mass balances (gain/losses) of metals (invariant element: Th). Contents of Zn in the initial sand #1 and Cu in all samples are below the detection limit (respectively 11 and 5 ppm).

represent mean values of three replicate experiments, which were found to give self-consistent results except for Cu. It must be kept in mind that a main limit of the method of sequential extractions is its non-selectivity. Indeed, each extractant is capable of acting on several geochemical fractions of the soil (Kheboian and Bauer, 1987). Moreover, when a chemical form of a metal is mobilized, there may be a redistribution of the metal in the different fractions of the soil, which would bias the expected results (Lebourg et al., 1998). Finally,

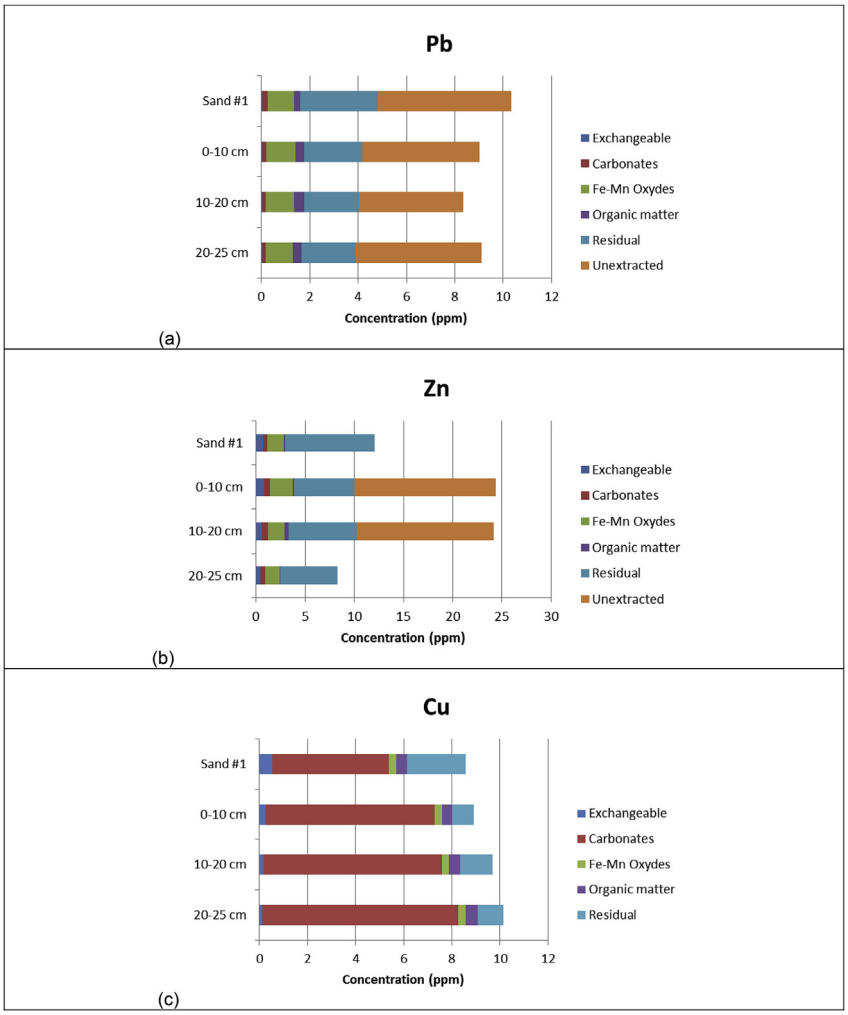

Fig. 5. Results of sequential extraction for (a) Pb, (b) Zn, and (c) Cu performed on sand #1 (initial CW sand) and along the CW substrate depth (up to 25 cm). Mean values of the 3 replicates are presented.

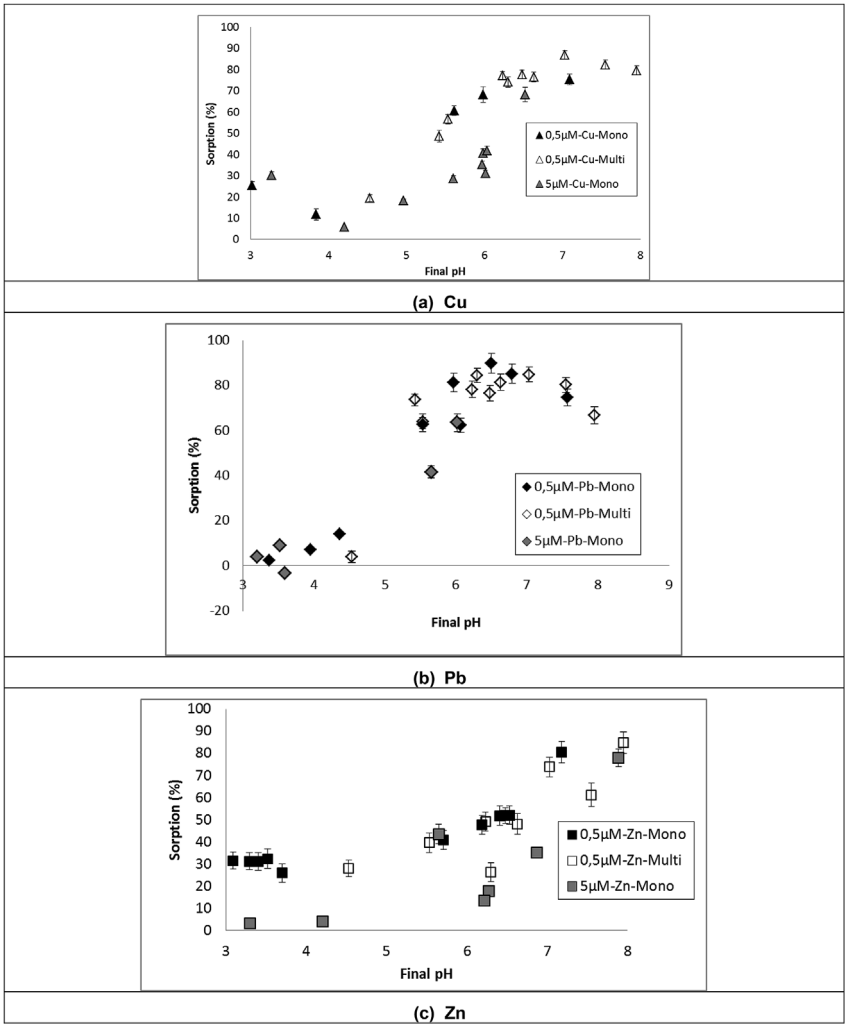

Fig. 6. pH dependence of sorption of (a) Zn, (b) Cu and (c) Pb on sand #2 during experiments at trace metal concentrations ([Cu]tot = [Zn]tot = [Pb]tot = 0.5 and 5 µM). The terms "mono" stands for single-metal experiments (Zn, Cu or Pb in experiment) and "multi" for competitive metal sorption experiments. Sand-solution contact time: 48 h.

efficiency of sequential extractions varies widely depending on a sample, i.e., its mineralogy, its metal composition, etc. The efficiency of the sequential extractions was determined here by calculating the overall extraction yield of a metal as compared to the total metal content of the sample.

A first feature observable in Fig. 5 is that the extraction was not complete in initial sand and CW samples for Pb and in the samples $CW_{0\text{-}10}$ and $CW_{10\text{-}20}$ for Zn: on average, from 52 to 59% of the total metal concentration is extracted and recovered in the five fractions for these samples. Regarding Pb, there was however observed a huge difference in the recovery yield between the replicate experiments: one of them showed a very poor extraction yield whereas the other allowed extracting up to 80–90% of Pb due to a more complete dissolution of the residual fraction (results of the replicates were self-consistent for all other fractions). Differences observed in the recovery yield indicate that a complete dissolution of residual fraction (likely mainly silicates and heavy minerals) is a quite difficult step of the BCR-Tessier procedure used here. The results suggest anyway that most of Pb extracted is found in the residual fraction, i.e., likely in the clay lattices and/or in heavy minerals of initial sand. This is in good accordance with the mass balance results showing no significant accumulation of Pb after a 6-years operating of the CW system. An interesting finding is that a significant part of extracted Pb is likely to be associated with Fe/Mn oxihydroxides, -whereas the contributions to the extracted Pb of the organic matter and the carbonate minerals appear to be quite limited-. Although a redistribution of Pb during extraction experiments can never be ruled out, Fe/Mn oxihydroxides are likely to be main sorbent phases for Pb in the CW top layers as many authors have emphasized its very high affinity for surfaces of Fe-oxihydroxides (Bradl, 2004; Ramos et al., 1994) As for Pb, a predominant influence of residual fraction and Fe/Mn oxihydroxides on metal distribution was also observed for lanthanides and uranium, with the extractions yield varying from moderate to high (Supplementary Information). This is consistent with the widely reported high affinity of these trace metals for Fe-oxihydroxides, too (Dhoum and Evans, 1998; Hu et al., 2006).

The extraction yields for Zn vary from moderate to high depending on the sample and show the lowest values for $CW_{0\text{-}10}$ and $CW_{10\text{-}20}$ in which this metal was found to display absolute accumulations (cf. §3.1.2). The results indicate anyway that residual minerals and Fe/Mn-oxihydroxides are main hosting phases for Zn. Similar results have been reported by other authors (Morera et al., 2001). It is to be noticed that the sequential extractions indicate a contribution (even if small) of exchangeable sites to the Zn distribution, unlike for Pb. Therefore, it is likely that such sites contribute to Zn sorption on the CW substrate, especially considering that this easily extractible fraction of Zn can be largely redistributed on the other sample phases during the subsequent steps of the extraction experiments. Other metals showing a contribution -even if not predominant-of the exchangeable fraction to metal

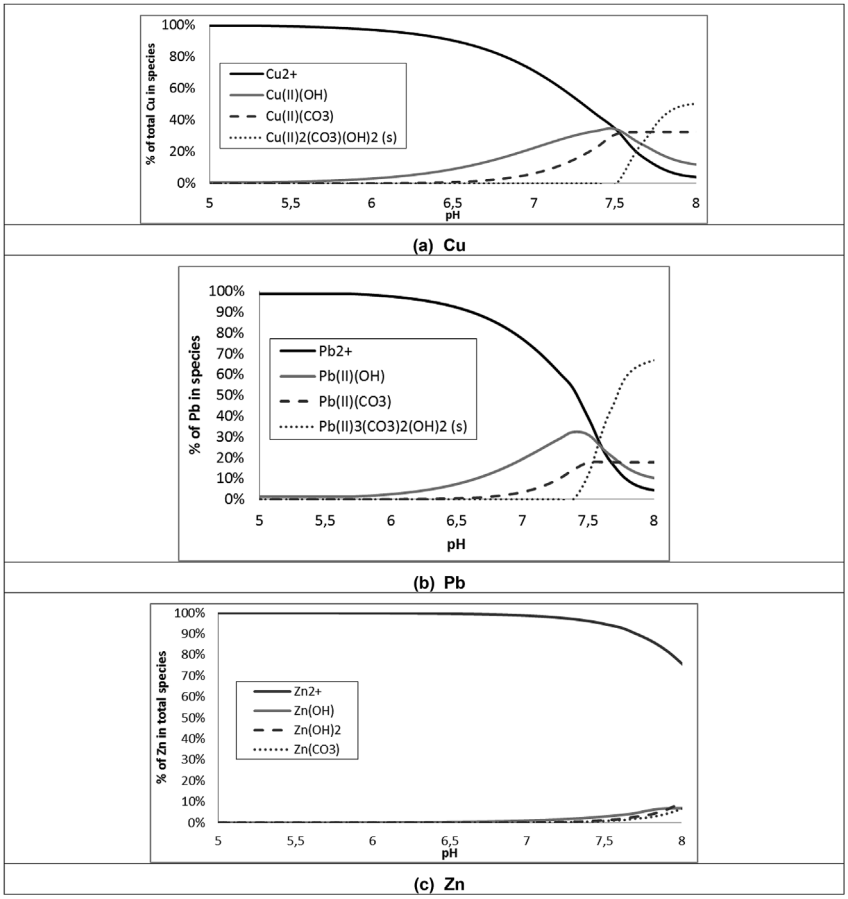

Fig. 7. Calculated speciation of Cu, Pb and Zn using CHEAQS program. Solutions at equilibrium with atmospheric CO2 and total concentrations of Cu, Pb and Zn equal to 0.5 µM.

distribution are Co, Ni (to a lesser extent) and metalloids such as arsenic, chromium and vanadium (cf. supplementary Information).

The results of the sequential extractions in Fig. 5 (mean values) suggest that Cu is mostly bound to carbonate minerals in initial sand and CW substrate. It has been already reported that Cu could be sorbed by carbonate minerals as $CaCO_3$(s) or that it may precipitate with $CoCO\text{-}_3^{2-}$ as $CuCO_3$(s). However, the reproducibility of the Cu results was very low in our experiments regarding the carbonate fraction. Concentrations of Cu extracted in this fraction were found to vary from 0 to 18 µg/g, depending on a replicate. This demonstrates a strong limitation for the application of sequential extraction experiments to low concentrated metals (under detection limit) in a sample, primarily due to a lack of homogeneity of sub-samples with respect to the trace level concentrations.

In summary, our yields evaluation enforces the widely reported observations of sequential extraction limitations including a certain lack of repeatability, which is mainly due here to the difficulty to achieve a complete dissolution of residual factions or to the very low concentration of certain HMs (Chao and Zhou, 1983; Leleyter and Probst, 1999; Mossop and Davidson, 2003; Sahuquillo et al., 1999). However, despite inherent procedure limitations (low yields, non-selectivity, redistribution of extracted trace elements during experiment), the results of the sequential extraction experiments reported here provide some insights into distribution patterns of HMs among the CW constituents. Cu, Pb and Zn distributions are consistent in the initial sand and along the CW depth in accordance with mass balances results. Pb and Zn are both mainly associated/bound to residual fractions (incorporated in the lattice or at surfaces of primary clays or in the heavy minerals). They are also mainly associated to Fe/Mn-oxihydroxide fractions –which are reproducible fractions stable along the CW profile- whereas Cu is possibly associated to carbonate minerals. Zn (and Cu) is also present to a lesser extent in exchangeable sites. Therefore, the results highlight that surfaces of Fe/Mn-oxihydroxides are potentially sorbent surfaces able to trap HMs especially strongly-sorbing metals like Pb in the CW top layer substrate whereas ion exchange may contribute to a certain extent to the sorption of exchangeable metals such as Zn.

3.2. Competitive sorption of metals on sand

3.2.1. Effect of pH and metal concentration on competitive metal sorption at trace levels

Results of the pH-dependency of single or competitive sorption of trace level of Cu, Pb and Zn (0.5 µM for each metal) is given on Fig. 6 for sand#2, which shows lower Ca and Fe contents than sand#1 (cf. Table 3). A sharp increase of percent metal sorption within a narrow pH range is observed for Cu (Fig. 6-a) and Pb (Fig. 6-b). These S-shaped sorption curves for Pb and Cu suggest that surface complex formation governs the sorption behavior at low metal concentration (0.5 µM) below pH7-7.5. For higher pH, secondary precipitation of mixed hydroxide-carbonate minerals of Pb and Cu may contribute to sorption. Calculations of the metal speciation in the absence of sand, actually suggest that precipitation of a mixed hydroxide-carbonate mineral could account for removal from solution of 20%–60% and of 0–40% of Pb and Cu, respectively, when pH is increased from 7.3 to 8 (Fig. 7 –a and –b). The percentage of Pb sorption decreases at pH higher than 7 likely due to a competition between sorption/precipitation processes of Pb and formation of dissolved Pb carbonate complexes (Fig. 7–b). Unlike for Pb and Cu, sorption of Zn is not dependent on pH, for acidic pH lower than 5. Such a feature suggests a process of ion exchange of Zn at

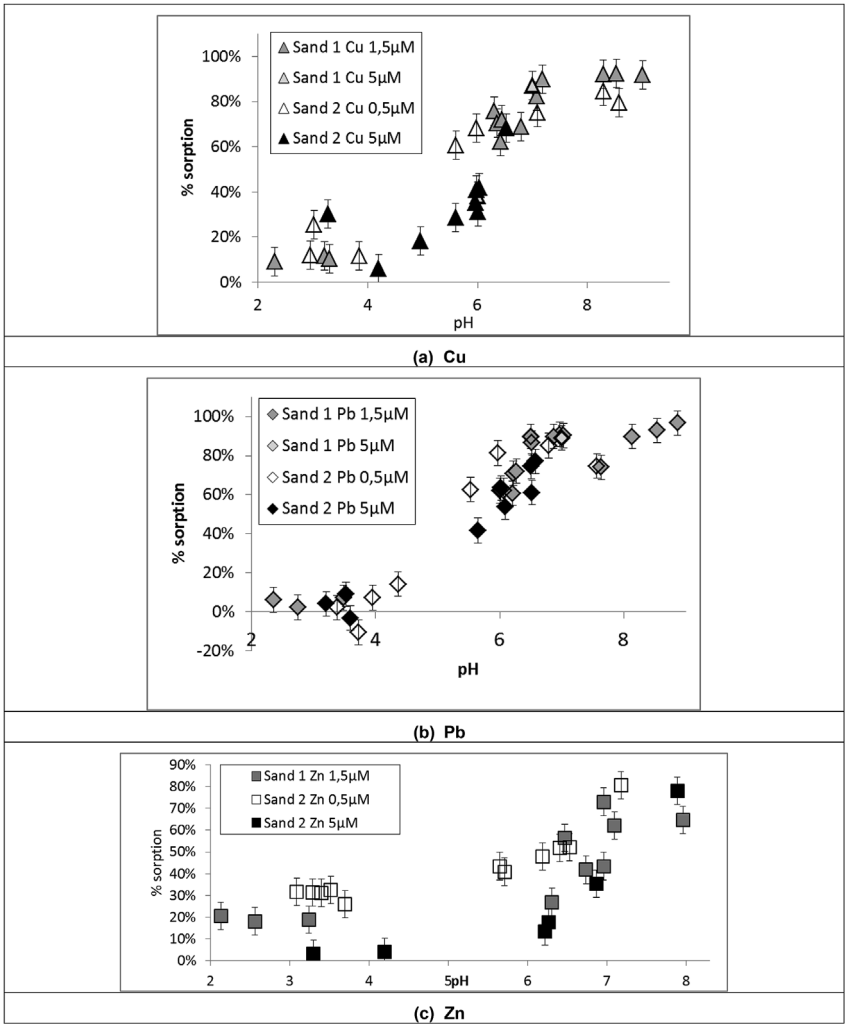

Fig. 8. Influence of sand composition on (a) Cu, (b) Pb and (c) Zn sorption at total metal concentrations equal to 1.5 µM and 5 µM (sand #1), 0.5 µM and 5 µM (sand #2). Experimental conditions: tc = 24 h, sand/solution ratio = 1 g.L-1. Data are not available for Zn at 5 µM using sand #1.

permanently negatively-charged interlayer sites of clays and/or weak sorption of Zn as counter-ions compensating negative charges at deprotonated sites existing at the surface of sand (e.g. onto silica or silicate minerals whose silanol surface sites have a low pKa value (Schindler et al., 1976). From 5 to 7, there was observed only a slight pH dependency of Zn sorption with an increasing of pH, which indicates surface complex formation involving Zn. No secondary mineral precipitation is expected for Zn throughout the pH range investigated (Fig. 7–c) based on speciation calculations. Hence the data suggest that a mechanism of surface complex formation implying the metal and hydroxyl sites at mineral surfaces of sand are responsible for the pH-dependent retention of Pb and Cu in the pH range 4–7.5, with a possible contribution of precipitation of mixed hydroxide-carbonate Pb and Cu minerals being possible at pH higher than 7.3, whereas sorption of Zn is dominated under acidic conditions by a weak sorption process not dependent on pH. The values of PH50 (pH value at which the sorption of half the amount of the initially added metal occurs) is equal to ca. 5.3 for Cu and Pb and to 6.5 for Zn. Therefore the global affinity of the trace metals for sand #2 attends the following order: Pb = Cu > Zn, consistently with previously published studies reporting a positive correlation between the tendency of metals to hydrolyze and their tendency to interact with hydroxylated surfaces (Sigg et al., 2000; Zachara and McKinley, 1993)). No competition between Cu, Pb and Zn was observed for sorption onto sand minerals (Fig. 6–a –b –c, "Multi") as sorption curves recorded for a metal in the monometal and multi-metal systems show no significant differences. This suggests the existence of specific sorption sites for each metal in sand and/or availability of sufficient amounts of sorption sites in the conditions used (low metal concentrations). As regards the effect of a change in metal concentration on sand #2 (0.5–5 µM), there was observed (Fig. 6) a decrease of Cu sorption with an increase of the metal concentration at neutral pH (at pH 6, there is 40% of sorption at 5 µM and 70% at 0.5 µM). Pb sorption data show a lower effect of metal concentration. Finally, at neutral and acidic pH, Zn sorption decreases with an increase of concentration (for pH 3.3, there is 3% of sorption at 5 µM and 20% at 0.5 µM, which corresponds in both cases to an amount of Zn sorbed of ca. 0.1 µmol/g sand). Such a behavior is characteristic of ion exchange (involving Zn, here) at interlayer sites of clays.

3.2.2. *Sand composition effect on metal sorption*

Differences in sand composition -even if small-may modify the metal sorption behaviors especially as regards differences in Fe and Ca contents which indicate different contents in minerals such as Fe-oxi-hydroxides and calcite, respectively. To determine this influence, data of single metal sorption were obtained with the initial CW sand #1, which is richer in Ca and Fe than sand #2 (Table 2). Experiments using sand #1 and sand #2 were performed at a metal concentration of 5 µM. Results are shown in Fig. 8 for Pb and Cu (data are not available for Zn). The composition of sands has no significant influence –or very small effect-on Pb and Cu sorption, within our data dispersion. At pH6, the

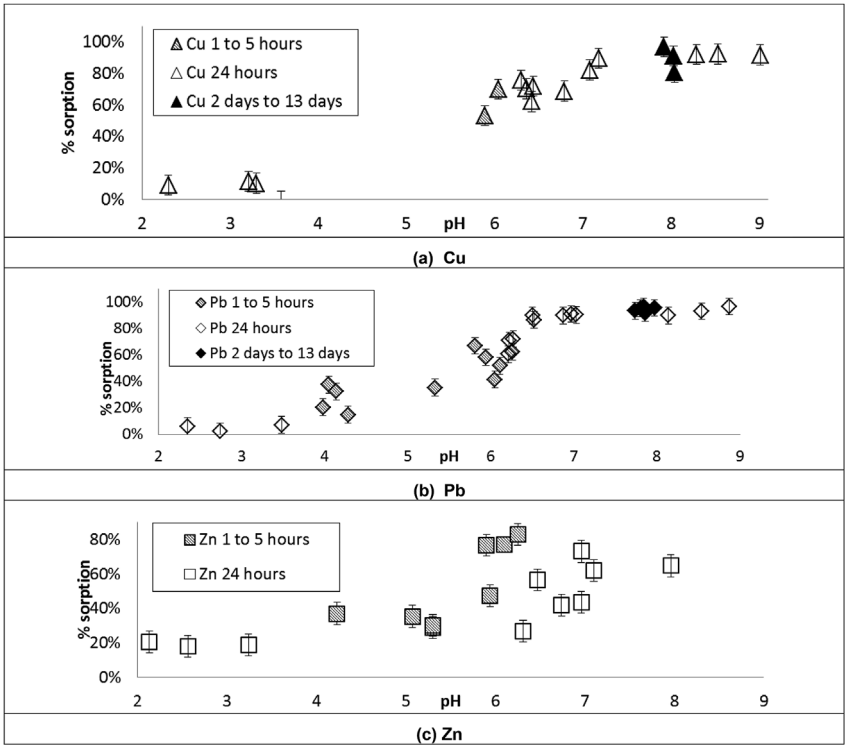

Fig. 9. Influence of sand-solution contact time on the sorption of (a) Cu, (b) Pb and (c) Zn as a function of pH experimental conditions: ([Cu]tot = [Zn]tot = [Pb] tot = 1.5 µM, sand/solution ratio = 1 g.L-1, tc = 1 h to 13 days).

percentages of sorption are, for sand #1 and sand #2, respectively, equal to 38 and 35% for Cu and equal to 62 and 42% for Pb. At pH7, the percentages of sorption are, for sand #1 and sand #2, respectively, equal to 87 and 68% for Cu and equal to 89 and 77% for Pb. Complementary experiments were also performed at Cu, Pb and Zn trace level concentrations (1.5 µM using sand #1and 0.5 µM using sand #2). Cu and Pb sorption curves are S-Shaped for both sands and for all concentrations. At trace level concentrations, the differences in Fe_2O_3 and CaO composition between sands #1 and #2 have no significant influence on sorption of Zn (within our data dispersion), either. Actually, the Zn sorption capacity of sand at interlayer sites poorly depends on the initial Zn concentration: 0.15 ± 0.0090 µmol, 0.3 ± 0.2 µmol and 0.5 ± 0.3 µmol of Zn were found to be sorbed at acidic pH by 1 g of sand for total concentrations of Zn introduced in the system equal to 0.5 µM, 1.5 µM and 5 µM, respectively. This suggests a limited sorption capacity per gram of sand: a tenfold increase of the initial Zn concentration (0.5–5 µM) causes only a slight increase of the quantity of Zn sorbed (+3.4%).

3.2.3. Effect of contact time on metal sorption

Fig. 9 presents the effect of contact time on metal sorption using sand #1. Results are shown for short contact times (1–5 h), intermediate contact time (24 h) and long contact time (2–13 days). Sorption results are highly dispersed for short contact times (1–5 h). The chemical equilibrium is not reached for Cu, Pb and Zn or short contact times don't allowed mixing well the solution with the sand. Sorption pseudo-equilibrium seem to reached at 24 h contact time for Cu, Pb and Zn, as there is no further sorption increase for longer contact times.

3.2.4. Effect of metal concentration on metal sorption

Fig. 10 presents the influence of initial Cu and Pb concentration on the sand #1 sorption for pH6 and pH7. Results are not available for Zn because we didn't succeed to reach the adequate final pH during the experiments. Quantities of Cu sorbed per gram of sand (Fig. 10-b) increase with metal concentration in experiment, until an initial concentration of 30 µM at pH7 and of 10 µM at pH6. For both pH, the sorption percentages decrease for initial Cu concentrations higher than 10 µM (Fig. 10-a). These observations suggest a progressive saturation of hydroxyl functional groups having a strong affinity for Cu and an increasing implication of weak affinity sites with increasing metal concentration (Bradbury and Baeyens, 1999; Strawn et al., 2004) and/or the formation of multiple surface complexes. Sorption calculations show that there is no possible Cu precipitation at pH6. In contrast, at pH7, the increasing Cu sorption can be caused partially by the precipitation of copper carbonates $Cu(II)_2(CO3)(OH)_2(s)$ (from 25% at 10 µM Cu initial concentration to 47% at 50 µM). Pb sorption behavior is similar to that of Cu until an initial concentration of Pb of 20 µM: the sorption percentages decrease (Fig. 10-c) and quantities of Pb sorbed increase (Fig. 10-d) with the initial Pb concentration and are higher at pH7 than at pH6. As for Cu, no mineral formation is possible at pH6 whereas precipitation of $Pb(II)_3(CO_3)_2(OH)_2(_s)$ could participate to Pb removal at pH7 (from 25% at initial Pb concentration of 10 µM–32% at 50 µM according to speciation calculations). Sand affinity for Pb is higher than for Cu: at pH6 and at an initial Pb concentration of 5 µM (no precipitation possible), the sand sorption capacity is equal to 1.9 ± 0.1 µmol per gram of sand for Cu and 3.1 ± 0.2 µmol for Pb.

4. Discussion and conclusion

4.1. Mechanisms of metal sorption

At trace concentration (< 20 µM) and for pH lower than 7.5, Pb and Cu are involved in the formation of surface complexes at high and weak affinity sites of sand mineral surfaces. The surface of the sand consists of several distinct types of sorption sites with varying affinities as reported by Benjamin and Leckie (1981). In our case, sorption sites are probably hydroxyl groups provided by iron oxides. Many authors reported ferrinol −Fe−OH surface sites as strong binding sites for Cu and Pb (Ainsworth et al., 1994; Davies and Bavor, 2000; Strawn et al., 2004). The global affinity for these sorption sites attends the following order:

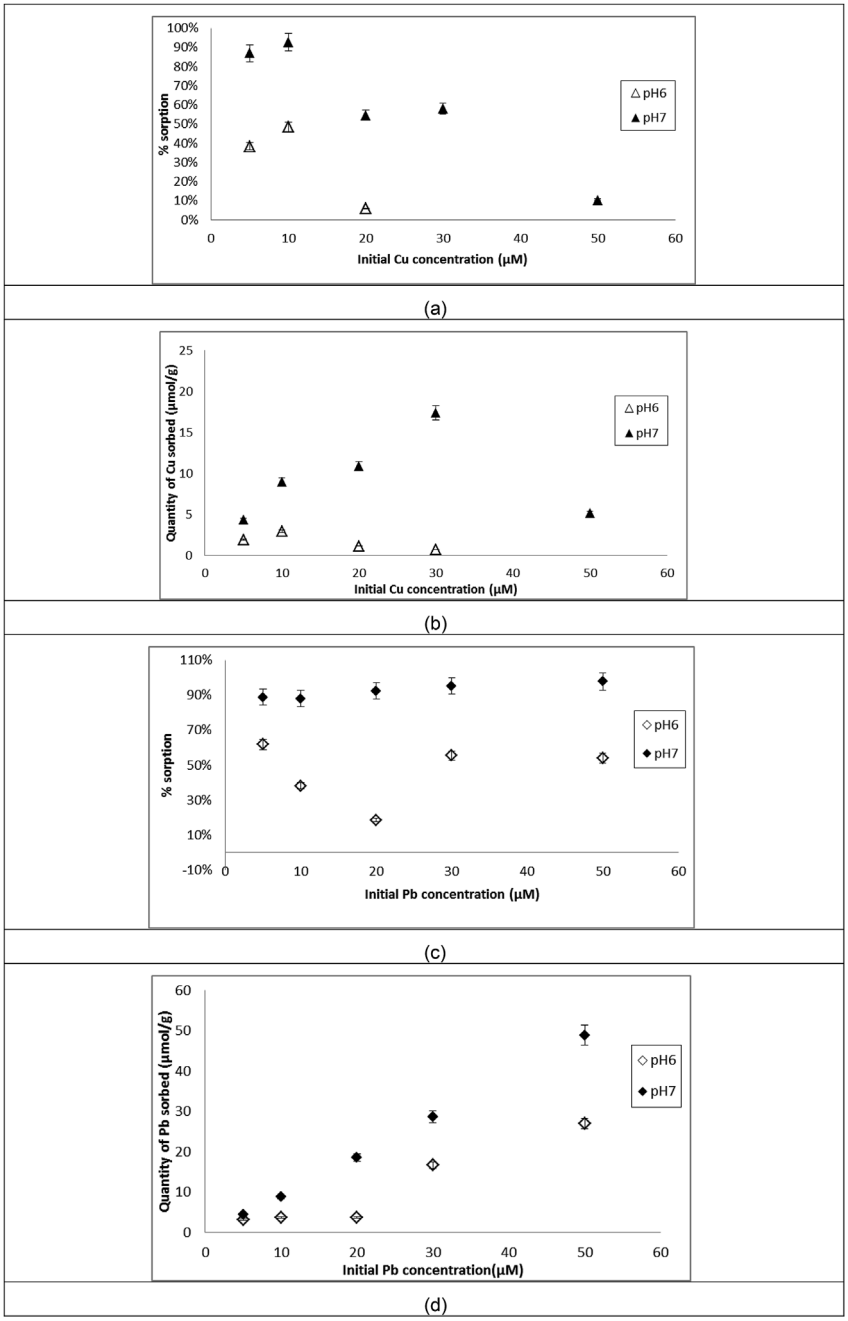

Fig. 10. Influence of initial Cu and Pb concentration on sorption on sand. Results are presented as percent of (a) Cu and (c) Pb sorbed and quantity of (b) Cu and (d) Pb sorbed on sand for two pH values (6 and 7). The ratio soil/solution is 1 g/L.

Pb = Cu > Zn, consistently with the sequential extractions results showing that Pb is mainly trapped by surfaces of Fe/Mn-oxihydroxides (not Cu). Strawn et al. (2004) reported that Cu forms dimers on the surface of smectite with a structural configuration similar to Cu acetate and Morton et al. (2001) showed that Cu precipitate on the surface of montmorillonite with an arrangement similar to the $Cu(OH)_2$ mineral. Roe et al. (1991) demonstrated that at low concentrations (2 mM) Pb forms monomeric and inner-sphere surface complexes whereas it forms surface polymers at higher concentrations (30 mM) on goethite. For higher concentrations (> 20 µM) and neutral pH, Pb sorption is also caused by the precipitation of $Pb(II)_3(CO_3)_2(OH)_{2(s)}$. In contrast, at acidic pH (< 5), Zn is mainly involved in ion exchange and/or in the compensation of negative charges existing at the mineral surfaces of sand (limited to 0.5 µmol/g of sand). This result is consistent with sequential extraction showing that Zn is partially bound to the exchangeable fraction. Then, the sand is made of illite and chlorite, which are built with negatively charged phyllosilicate layers. Scheinost et al. (2002) showed that Zn is a substitute for Al in trioctahedral Al hydroxide layers and fills vacant sites in dioctahedral Al hydroxide layers of a montmorillonite. At higher pH, Zn forms a limited number of surface complexes.

4.2. Implication for metal sorption on CW substrate

Sand sorption by iron and manganese oxides is limited to 3 µmol of Pb and Cu per gram of sand at low metals concentrations. Under the CW conditions (low metals concentrations and neutral pH), Cu and Pb removal efficiencies are above 90%. The ageing of the pond may cause an increase of the metals concentrations in the CW incoming water and so a decrease of the removal efficiency by the sand until 10 µM. The Zn

sorption capacity of sand at interlayer sites is limited to 0.5 μmol of Zn per gram of sand for the concentration observed in input of the CW (ca. 5 μM) and the sorption of Zn on strong sites of the sand is limited compared to Pb and Cu. Thus Zn is potentially desorbable from the sand surface to the infiltrated water in the CW. This partly explains the Zn accumulation up to 20 cms in depth of the CW, in addition to the high Zn inputs. Contrary to previous studies showing Cu and Pb sorption on organic matter (Covelo et al., 2007a; De Matos et al., 2001), the organic fraction of the studied sand doesn't play a significant role in the metals sorption. Finally, HMs concentrations in the treatment system are far below the sand saturation and the pH7 allowed the best sorption capacities for Cu, Pb and Zn by the sand.

Appendix A. Supplementary data

Supplementary data related to this article can be found at https://doi.org/10.1016/j.apgeochem.2018.08.019.

References

Ainsworth, C.C., Gassman, P.L., Pilon, J.L., Van Der Sluys, W.G., 1994. Cobalt, cadmium, and lead sorption to hydrous iron oxide: residence time effect. Soil Sci. Soc. Am. J. 58, 1615–1623.

Atanassova, I., Okazaki, M., 1997. Adsorption-desorption characteristics of high levels of copper in soil clay fractions. Water Air Soil Pollut. 98, 213–228.

Benjamin, M.M., Leckie, J.O., 1981. Multiple-site adsorption of Cd, Cu, Zn, and Pb on amorphous iron oxyhydroxide. J. Colloid Interface Sci. 79, 209–221.

Bout-Roumazeilles, V., Cortijo, E., Labeyrie, L., Debrabant, P., 1999. Clay mineral evidence of nepheloid layer contributions to the Heinrich layers in the northwest Atlantic. Palaeogeogr. Palaeoclimatol. Palaeoecol. 146, 211–228.

Bradbury, M.H., Baeyens, B., 1999. Modelling the sorption of Zn and Ni on Ca-montmorillonite. Geochem. Cosmochim. Acta 63, 325–336.

Bradl, Heike B., 2004. Adsorption of heavy metal ions on soils and soils constituents. J. Colloid Interface Sci. 277, 1–18. https://doi.org/10.1016/j.jcis.2004.04.005.

Braun, J.J., Pagel, M., Herbillon, A., Rosin, C., 1993. Mobilization and redistribution of REEs and thorium in a syenitic lateritic profile: a mass balance study. Geochem. Cosmochim. Acta 57, 4419–4434.

Bressy, A., 2010. Flux de micropolluants dans les eaux de ruissellement urbaines. Effets de différents modes de gestion des eaux pluviales.

Brindley, G.W., Brown, G., 1980. Crystal Structures of Clay Minerals and Their X-ray Identification. Mineralogical Society.

Chao, T.T., Zhou, L., 1983. Extraction techniques for selective dissolution of amorphous iron oxides from soils and sediments. Soil Sci. Soc. Am. J. 47, 225–232.

Covelo, E.F., Vega, F.A., Andrade, M.L., 2007a. Competitive sorption and desorption of heavy metals by individual soil components. J. Hazard Mater. 140, 308–315.

Covelo, E.F., Vega, F.A., Andrade, M.L., 2007b. Simultaneous sorption and desorption of Cd, Cr, Cu, Ni, Pb, and Zn in acid soils: I. Selectivity sequences. J. Hazard Mater. 147, 852–861.

Davies, C.M., Bavor, H.J., 2000. The fate of stormwater-associated bacteria in constructed wetland and water pollution control pond systems. J. Appl. Microbiol. 89, 349–360.

Davis, J.A., 1984. Complexation of trace metals by adsorbed natural organic matter. Geochem. Cosmochim. Acta 48, 679–691.

De Matos, A.T., Fontes, M.P.F., Da Costa, L.M., Martinez, M.A., 2001. Mobility of heavy metals as related to soil chemical and mineralogical characteristics of Brazilian soils. Environ. Pollut. 111, 429–435.

Dhoum, R.T., Evans, G.J., 1998. Evaluation of uranium and arsenic retention by soil from a low level radioactive waste management site using sequential extraction. Appl. Geochem. 13, 415–420.

Di Luca, G.A., Maine, M.A., Mufarrege, M.M., Hadad, H.R., Sánchez, G.C., Bonetto, C.A., 2011. Metal retention and distribution in the sediment of a constructed wetland for industrial wastewater treatment. Ecol. Eng. 37, 1267–1275.

Echeverria, J.C., Morera, M.T., Mazkiaran, C., Garrido, J.J., 1998. Competitive sorption of heavy metal by soils. Isotherms and fractional factorial experiments. Environ. Pollut. 101, 275–284.

Elliott, H.A., Liberati, M.R., Huang, C.P., 1986. Competitive adsorption of heavy metals by soils. J. Environ. Qual. 15, 214–219.

Flores-Rodriguez, J., 1992. Les métaux toxiques dans les eaux pluviales en milieu urbain: caractéristiques physico chimiques (phdthesis). Universite paris XII-Val de Marne.

Fu, J., Hu, X., Tao, X., Yu, H., Zhang, X., 2013. Risk and toxicity assessments of heavy metals in sediments and fishes from the Yangtze River and Taihu Lake, China. Chemosphere 93, 1887–1895.

Harter, R.D., 1981. The relative adsorption selectivities of Pb, Cu, Zn, Cd and Ni by soils developed on shale in New Valley, Egypt. Soil Sci. Soc. Am. J. 47, 47–51.

Hooda, P.S., Alloway, B.J., 1998. Cadmium and lead sorption behaviour of selected English and Indian soils. Geoderma 84, 121–134.

Hu, Z., Haneklaus, S., Sparovek, G., Schnug, E., 2006. Rare earth elements in soils. Commun. Soil Sci. Plant Anal. 37, 1381–1420.

Jiang, K., Sun, T., Sun, L., Li, H., 2006. Adsorption characteristics of copper, lead, zinc and cadmium ions by tourmaline. J. Environ. Sci. 18, 1221–1225.

Kar, D., Sur, P., Mandai, S.K., Saha, T., Kole, R.K., 2008. Assessment of heavy metal pollution in surface water. Int. J. Environ. Sci. Technol. 5, 119–124.

Kheboian, C., Bauer, C.F., 1987. Accuracy of selective extraction procedures for metal speciation in model aquatic sediments. Anal. Chem. 59, 1417–1423.

Kostic, I., Andjelkovic, T., Nikolic, R., Bojic, A., Purenovic, M., Blagojevic, S., Andjelkovic, D., 2011. Copper(II) and lead(II) complexation by humic acid and humic-like ligands. J. Serb. Chem. Soc. 76, 1325–1336.

Lamprea, K., 2009. Caractérisation et origine des métaux traces, hydrocarbures aromatiques polycycliques et pesticides transportés par les retombées atmosphériques et les eaux de ruissellement dans les bassins versants séparatifs péri-urbains (phdthesis). Ecole Centrale de Nantes (ECN).

Land, M., Öhlander, B., Ingri, J., Thunberg, J., 1999. Solid speciation and fractionation of rare earth elements in a spodosol profile from northern Sweden as revealed by sequential extraction. Chem. Geol. 160, 121–138.

Lebourg, A., Sterckeman, T., Ciesielski, H., Proix, N., Gomez, A., 1998. Estimation of soil trace metal bioavailability using unbuffered salt solutions: degree of saturation of polluted soil extracts. Environ. Technol. 19, 243–252.

Lee, S.-Z., Chang, L., Yang, H.-H., Chen, C.-M., Liu, M.-C., 1998. Adsorption characteristics of lead onto soils. J. Hazard Mater. 63, 37–49.

Leleyter, L., Probst, J.-L., 1999. A new sequential extraction procedure for the speciation of particulate trace elements in river sediments. Int. J. Environ. Anal. Chem. 73, 109–128.

Marković, J., Jović, M., Smičiklas, I., Pezo, L., Šljivić-Ivanović, M., Onjia, A., Popović, A., 2016. Chemical speciation of metals in unpolluted soils of different types: correlation with soil characteristics and an ANN modelling approach. J. Geochem. Explor. 165, 71–80. https://doi.org/10.1016/j.gexplo.2016.03.004.

McBride, M.B., 1994. Environmental Chemistry of Soils. Oxford University Press.

Morera, M.T., Echeverria, J.C., Mazkiaran, C., Garrido, J.J., 2001. Isotherms and sequential extraction procedures for evaluating sorption and distribution of heavy metals in soils. Environ. Pollut. 113, 135–144.

Morton, J.D., Semrau, J.D., Hayes, K.F., 2001. An X-ray absorption spectroscopy study of the structure and reversibility of copper adsorbed to montmorillonite clay. Geochem. Cosmochim. Acta 65, 2709–2722.

Mossop, K.F., Davidson, C.M., 2003. Comparison of original and modified BCR sequential extraction procedures for the fractionation of copper, iron, lead, manganese and zinc in soils and sediments. Anal. Chim. Acta 478, 111–118.

Nesbitt, H. Wayne, 1979. Mobility and fractionation of rare earth elements during weathering of a granodiorite. Nature 279, 206–210.

Pan, Y., Bonten, L.T.C., Koopmans, G.F., Song, J., Luo, Y., Temminghoff, E.J.M., Comans, R.N.J., 2016. Solubility of trace metals in two contaminated paddy soils exposed to alternating flooding and drainage. Geoderma 261, 59–69. https://doi.org/10.1016/j.geoderma.2015.07.011.

Pandey, A.K., Pandey, S.D., Misra, V., 2000. Stability constants of metal–humic acid complexes and its role in environmental detoxification. Ecotoxicol. Environ. Saf. 47, 195–200. https://doi.org/10.1006/eesa.2000.1947.

Ramos, L., Hernandez, L.M., Gonzalez, M.J., 1994. Sequential fractionation of copper, lead, cadmium and zinc in soils from or near Donana National Park. J. Environ. Qual. 23, 50–57.

Rauret, G., López-Sánchez, J.F., Sahuquillo, A., Rubio, R., Davidson, C., Ure, A., Quevauviller, P., 1999. Improvement of the BCR three step sequential extraction procedure prior to the certification of new sediment and soil reference materials. J. Environ. Monit. 1, 57–61.

Roe, A.L., Hayes, K.F., Chisholm-Brause, C., Brown Jr., G.E., Parks, G.A., Hodgson, K.O., Leckie, J.O., 1991. In situ X-ray absorption study of lead ion surface complexes at the goethite-water interface. Langmuir 7, 367–373.

Sahuquillo, A., Lopez-Sanchez, J.F., Rubio, R., Rauret, G., Thomas, R.P., Davidson, C.M., Ure, A.M., 1999. Use of a certified reference material for extractable trace metals to assess sources of uncertainty in the BCR three-stage sequential extraction procedure. Anal. Chim. Acta 382, 317–327.

Scheinost, A.C., Kretzschmar, R., Pfister, S., Roberts, D.R., 2002. Combining selective sequential extractions, X-ray absorption spectroscopy, and principal component analysis for quantitative zinc speciation in soil. Environ. Sci. Technol. 36, 5021–5028.

Schindler, P.W., Fürst, B., Dick, R., Wolf, P.U., 1976. Ligand properties of surface silanol groups. I. Surface complex formation with Fe3+, Cu2+, Cd2+, and Pb2+. J. Colloid Interface Sci. 55, 469–475.

Schmitt, N., Wanko, A., Laurent, J., Bois, P., Molle, P., Mosé, R., 2015. Constructed wetlands treating stormwater from separate sewer networks in a residential Strasbourg urban catchment area: micropollutant removal and fate. J. Environ. Chem. Eng. 3, 4. https://doi.org/10.1016/j.jece.2015.10.008 pp. 2816–2824.

Sekabira, K., Origa, H.O., Basamba, T.A., Mutumba, G., Kakudidi, E., 2010. Heavy metal assessment and water quality values in urban stream and rain water. Int. J. Environ. Sci. Technol. 7, 759–770.

Sheoran, A.S., Sheoran, V., 2006. Heavy metal removal mechanism of acid mine drainage in wetlands: a critical review. Miner. Eng. 19, 105–116.

Sigg, L., Behra, Ph., Stumm, W., 2000. Chimie des Milieux Aquatiques, 3rd ed. Dunod, Paris.

Sipos, P., Németh, T., Kis, V.K., Mohai, I., 2008. Sorption of copper, zinc and lead on soil mineral phases. Chemosphere 73, 461–469.

Smith, R.M., Martell, A.E., Motekaitis, R.J., 2004. NIST standard Reference Database 46. NIST Crit. Sel. Stab. Constants Met. Complexes Database Ver 2. .

Spark, K.M., Wells, J.D., Johnson, B.B., 1995. Characterizing trace metal adsorption on kaolinite. Eur. J. Soil Sci. 46, 633–640.

Sposito, G., 1981. The Thermodynamics of Soil Solutions. Clarendon Press, Oxford.

Srivastava, P., Singh, B., Angove, M., 2005. Competitive adsorption behavior of heavy metals on kaolinite. J. Colloid Interface Sci. 290, 28–38. https://doi.org/10.1016/j.jcis.2005.04.036.

Strawn, D.G., Palmer, N.E., Furnare, L.J., Goodell, C., Amonette, J.E., Kukkadapu, R.K.,

2004. Copper sorption mechanisms on smectites. Clay Clay Miner. 52, 321–333.
Tessier, A., Campbell, P.G.C., Bisson, M., 1979. Sequential extraction procedure for the speciation of particulate trace metals. Anal. Chem. 51, 844–851. https://doi.org/10.1021/ac50043a017.
Uchimiya, M., Klasson, K.T., Wartelle, L.H., Lima, I.M., 2011. Influence of soil properties on heavy metal sequestration by biochar amendment: 1. Copper sorption isotherms and the release of cations. Chemosphere 82, 1431–1437.
Vega, F.A., Covelo, E.F., Andrade, M.L., 2006. Competitive sorption and desorption of heavy metals in mine soils: influence of mine soil characteristics. J. Colloid Interface Sci. 298, 582–592.
Verweij, W., 2014. CHEAQS (a Program for Calculating CHemical Equilibria in AQuatic Systems).
Walaszek, M., Bois, P., Laurent, J., Lenormand, E., Wanko, A., 2018. Urban stormwater treatment by a constructed wetland: seasonality impacts on hydraulic efficiency, physico-chemical behavior and heavy metal occurrence. Sci. Total Environ. 637, 443–454.
Xian, X., 1989. Effect of chemical forms of cadmium, zinc, and lead in polluted soils on their uptake by cabbage plants. Plant Soil 113, 257–264.
Yang, R., van den Berg, C.M.G., 2009. Metal complexation by humic substances in seawater. Environ. Sci. Technol. 43, 7192–7197. https://doi.org/10.1021/es900173w.
Yun, S.-I., Choi, W.-J., Choi, Y.-D., Lee, S.-H., Yoo, S.-H., Lee, E.-J., Ro, H.-M., 2003. Distribution of heavy metals in soils of Shihwa tidal freshwater marshes. Korean J. Ecol. 26, 65–70.
Zachara, J.M., McKinley, J.P., 1993. Influence of hydrolysis on the sorption of metal cations by smectites: importance of edge coordination reactions. Aquat. Sci.-Res. Boundaries 55, 250–261.
Zhang, J., Yang, B., Chen, T., Sun, X., Chen, C., 2016. Metal speciation and pollution assessment of Cd and Pb in intertidal sediments of Donghai Island, China. Reg. Stud. Mar. Sci. 6, 37–48. https://doi.org/10.1016/j.rsma.2016.03.006.

Integrated Blue and Green Corridor Restoration in Strasbourg: Green Toads, Citizens, and Long-Term Issues

Paul Bois, Jean-Nicolas Beisel, Carine Heitz, Léa Katinka, Julien Laurent, Marjorie Pierrette, Milena Walaszek and Adrien Wanko

Abstract The Ostwaldergraben is an urban stream located in Strasbourg (northeast of France). Mostly fed by groundwater, it was enlarged some forty years ago, which led to a radical alteration of the flow dynamics and a strong siltation. According to the European Water Framework, the stream displayed a bad status with sediments polluted by discharges of former tanneries. Hence, a project of restoration—both of the stream and the adjacent wasteland—was launched by the City of Strasbourg in 2010 to solve these issues of environmental degradation in accordance with the European regulation. The stream bed was redesigned to energize the flows and to create meanders and vegetated benches. To improve the connectivity between two adjacent wetlands, new habitats and a network of ponds have been created. A hybrid type of stormwater treatment system—a pond followed by a constructed wetland—was implemented to complete the restoration project. In this chapter, we propose to study this project from its construction to its current development, through the lens of ecological engineering and a perspective on long-term issues. We aim at illustrating the facts that nature-based solution management can differ from technological management and that the ecosystem services provided by a nature-based solution result from trade-offs, which requires a global analysis of such restoration project. To reach this goal, the project will be studied from ecological, engineering, and sociological perspectives. Our study shows that the restored socio-ecosystem works on a rustic basis and provides several ecosystem services: supporting services (habitat for

P. Bois (✉) · J.-N. Beisel · J. Laurent · M. Walaszek · A. Wanko
ICube, UMR 7357 ENGEES/CNRS/Unistra, 2 Rue Boussingault,
67000 Strasbourg, France
e-mail: p.bois@unistra.fr

P. Bois · J. Laurent · M. Walaszek · A. Wanko
LTSER France, Zone Atelier Environnementale Urbaine, 3 Rue de L'Argonne,
67000 Strasbourg, France

C. Heitz · M. Pierrette
Irstea, UMR GESTE, ENGEES, 1 Quai Koch, BP61039, 67070 Strasbourg, France

L. Katinka
ENGEES, UMR GESTE, 1 Quai Koch, BP61039, 67070 Strasbourg, France

V. Achal and A. Mukherjee (eds.), *Ecological Wisdom Inspired Restoration Engineering*, EcoWISE, https://doi.org/10.1007/978-981-13-0149-0_9

amphibians), regulating services (water quality enhancement), and cultural services (urban landscape greening).

Keywords Stormwater treatment · Ecosystem services · Green toads
Urban landscape · Restoration

1 Introduction

The main target of the Ostwaldergraben restoration's project (2010–2015) was to create an ecological corridor in an urban area by restoring a length of about 600 m of the Ostwaldergraben stream and its floodplain. The main ambition was then to rebuild the stream's function as a blue and green corridor for a target species (*Bufotes viridis*, commonly referred to as the green toad) between two upstream and downstream sites that were previously restored. In 2008, the upstream zone originally composed of an agricultural area was turned into three ponds located in a compensatory afforestation north of a large one called 'Etang du Bohrie' (Fig. 1). This area is surrounded by a mosaic of different habitats. In 2009, on the downstream area, a wetland was restored around the Ill River at the confluence with the Ostwaldergraben. At this location, the restoration consisted in the creation of various environments (wet meadows, woodlands, reed beds) and a flooded island enclosed by arms with various depths. In less than one year, the site was colonized by at least 12 regionally declining species, of which 7 are listed as endangered (birds, reptiles, and insects such as *Odonata* and *Lepidoptera*). But the stream stretch that connects these two wetlands was preventing these species from spreading or freely moving, especially the green toad. The green toad is a patrimonial species, an important and emblematic element of the regional fauna. The species easily colonizes early successional habitats within its area of occurrence as long as the vegetation is not too developed. This species depends on two major types of habitat: ponds as suitable habitats for breeding and larval development and terrestrial pioneer habitats for juveniles and adults (foraging, hibernating, and/or traveling). Several indications of the presence of *B. viridis* were observed upstream (recurrent use of breeding sites) and seldom downstream the restored area along the Ostwaldergraben in a large pond called 'Etang Gerig.'

In that context, the main aims were (i) to provide *B. viridis* with a corridor to reach and leave reproduction sites, allowing exchanges between two close subpopulations; (ii) to reinforce habitats available to complete its life cycle. Organisms that require two different habitat types to fulfill their life cycles, such as pond-breeding amphibians, are especially vulnerable to habitat loss and degradation (Becker et al. 2007). For them, landscape complementation can be defined as the process by which the proximity of two critical habitat patches of different types essential for a major ontogenetic niche shift complements occupancy, abundance, or persistence in each patch (Dunning et al. 1992). The project was designed to both allow displacement of individuals along the river and increase the landscape complementation in an urban context for the green toad.

Fig. 1 Location of the restored section (white double arrow) between two adjacent sites previously restored for environmental purposes (view extracted from Google earth). The flow direction is from west to east

2 Issues and Potential of the Socio-Ecosystem at Stake

2.1 What Alterations Have Motivated the Restoration Program?

The Ostwaldergraben is an urban stream mostly fed by groundwater. Forty years ago, it was enlarged which led to a radical alteration of the flow dynamics and a strong siltation. The environmental characteristics change along the course of the stream from the upstream part ('Etang du Bohrie') to the downstream one. Before the confluence with the Ill, the stream flows under a bridge dedicated to the trams' and cars' traffic. The wet bed occupied the entire width of the bridge deck, meaning

there were no banks at this point. The passage of terrestrial fauna was impossible there, while the bank vegetation continuity was interrupted and fish passage restricted because of a very low water depth (Fig. 2a). An earthen bund contained the river on the left bank; it abruptly severed the aquatic compartment from the terrestrial one.

In terms of nuisances, pylons of power lines are placed overhang from the stream on the left bank. A regulation obliges the landowners to manage the vegetation that develops under and around the pylon within a radius of 5 m. Since these lines cannot be moved, regular vegetation management operations (cutting of trees and shrubs, mowing) are scheduled.

Before the restoration program, a monitoring highlighted that the stream displayed a bad status, notably because of polluted sediments due to the former tanneries. The district's stormwater was directly discharged into the watercourse without any prior treatment, and the ducts were overhanging the natural environment.

In this context, the challenge was (i) to revitalize the stream in an environment with fine sediments of very poor quality, (ii) to allow the creation of a mosaic of environments favorable to the movements and reproduction of the green toad, (iii) to decrease the negative effects of the passage under the bridge in terms of longitudinal continuity.

2.2 First Project, Public Inquiry, and Social Adjustments

From the aforementioned alterations, the Ostwaldergraben project was first imagined as a three-pronged approach:

1. Stream restoration and creation of an ecological continuum allowing animal species to come back, among them the green toad (*B. viridis*);
2. Stormwater depollution performed by treatment systems (we will explain in the next part why this was included);
3. Creation of a bike lane along the restored stream.

Closing the whole area to the public was also an option considered in the project. A public inquiry was carried out in 2011 as a prior step to the whole project. A public inquiry is a regulatory and mandatory step (French regulation) that takes place prior to any land use planning project. It is meant as a democratic consultation tool, where any citizen or environmental/local associations can freely express their view on a given land use project. Three environmental associations answered the inquiry and insisted mainly on the creation of the bike lane, perceived as in total contradiction with the species comeback. Public meetings were held in 2012 in Strasbourg and Ostwald (the two municipalities at the border of the Ostwaldergraben). The organization of public meetings is the second mandatory requirement in the process of public consultation in a land use planning project. Following the public inquiry and the public meetings, the local authorities gave up

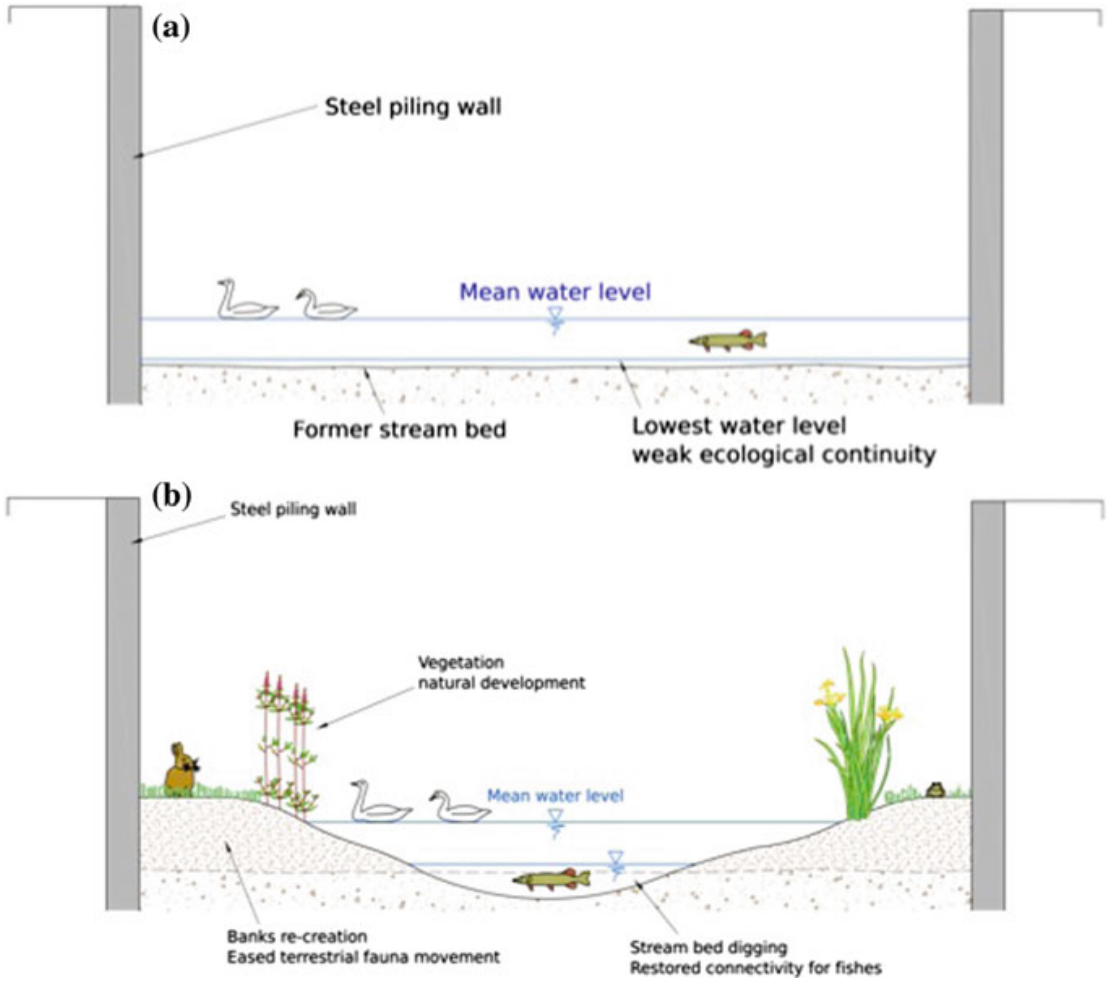

Fig. 2 **a** Former situation. The space under the bridge breaks the terrestrial continuity (banks severed) and the aquatic continuity (low water depth). (Modified from a document produced by the engineering consultant SINBIO), **b** Restored situation. The space under the bridge was modified to tighten the width of the streambed, revitalize the flows, and avoid siltation. The tightening of the minor bed and digging of the middle part of the channel make it possible to obtain water height and flow velocities compatible with fish continuity. The naturally vegetated side banks allow the passage of the terrestrial fauna. (Modified from a document produced by the engineering consultant SINBIO)

on the bike lane project and concluded also that the comeback of given species (e.g., mosquitoes, amphibians, etc.) subsequent to the stream restoration was an issue for some citizens. The stream flow was very low at that time, so mosquitoes were largely able to nest in even before restoration. The report also highlighted that the residents preferred closing the site to avoid burglary or potential nuisances.

The project was eventually carried out in two phases to restore the site (stream and flood channel) over more than 600 m (2015) and setup stormwater treatment systems (2012).

2.3 *The 'Dirty' Stormwater Problem and the Way It Was Solved*

The restoration of a stream relies on its morphologic features, but also on the various water inputs, mainly stormwater in this case. Two main effects are at stake: (i) banks physical alteration due to water discharge and (ii) water pollution through contaminant transports by stormwater.

The first effect is caused by stormwater collection in separate networks and direct discharge into streams; the resulting peak flows during storm events create a physical effect of digging on the riverbanks. This at least disturbs the morphology of the stream, if not reshaping it and may generate suspended solids resuspension in the stream; the consequences unveil very quickly. Additionally, in the case of the Ostwaldergraben stream, the outlet pipes of the separate network were positioned overhang and discharged directly into the water bodies, which increases the physical impact of runoff.

The second effect results from a quite complex chain of processes. When it rains, rainwater loads with airborne pollutants, such as heavy metals, hydrocarbons, pesticides, and gaseous species (Azimi et al. 2005; Scheyer et al. 2007; Fenger 1999). As it reaches the roofs, roads, gardens and if there is enough rain to start runoff, it will collect other compounds either by transport or dissolution. In the case of urban systems, these main compounds are (Barbosa et al. 2012): solid particles from dust, traffic, and animal feces (becoming suspended solids when carried in the water), heavy metals coming mainly from gutter, road and car material, PAHs from traffic, pesticides from gardening activities, bacteria from animal feces and miscellaneous compounds from light-headed point discharges. In the case of the Ostwaldergraben stream, the typical pollutant concentrations for eight runoff events analyzed in 2013 are listed in Table 1. As can be seen from the table, these are low but significant levels, and of course highly variable values. Urban streams are thus directly contaminated by polluted stormwater in case of untreated discharge. Eventually, even at these low levels of contamination, stormwater was shown to display ecotoxicological effects on aquatic ecosystems (Gosset et al. 2017; Chong et al. 2013); stormwater treatment is mandatory to keep the stream in a good state once restored.

To alleviate this environmental degradation and help maintaining the stream at a good status, many options can be chosen, from the most classically engineered ones to ecologically engineered ones, sometimes called nature-based solutions (NBS) (Erickson et al. 2013). Classically, engineered systems are generally characterized by a large environmental footprint due to the use of exogenous material and of their complex structures arranged with the intensive use of machines powered with fossil fuels. Eventually, the recycling of the materials at the end of their lifecycle is not neutral. Although the environmental footprint of NBS exists as well, it is greatly reduced compared with classically engineered systems (O'Sullivan et al. 2015). In the case of constructed treatment wetlands (CTWs), a large part of the ecological footprint is due to the fact that the basin

Table 1 Contamination levels in the Ostwaldergraben stormwater for eight runoff events in 2013 (adapted from Schmitt et al. 2015). COD = Chemical Oxygen Demand, TSS = Total Suspended Solids, TN = Total Nitrogen, TP = Total Phosphorus

	COD (mg_{O2}/L)	TSS (mg/L)	TN (mg_N/L)	TP (mg_P/L)	Cu (µg/L)	Cr (µg/L)	Pb (µg/L)	Zn (µg/L)
Minimum concentration	25	5	0.8	0	9.6	1.1	1.7	176
Maximum concentration	400	110	11	1.2	42.4	10.6	94.4	640
Number of detections	5	7	8	6	7	5	7	3

must be filled with sand of a given particle size, that is sometimes sampled and transported from afar.

Apart from their ability to clean stormwater and to protect the stream (feature of any stormwater treatment system), the reduced ecological footprint of NBS and the will to create green/blue connections with the to-be-restored stream were the main reasons these systems were set up along the urban stream. More specifically, constructed wetlands were set up. Among the ecosystem services provided by this type of system (Moore and Hunt 2012), regulating services were guiding the construction of a hybrid system composed of a pond and a constructed treatment wetland (CTW). The potential peak flows are buffered by the succession of a pond and a CTW, while the pollutant load is reduced by the combination of settling, photodegradation, physical filtration, biodegradation, and sorption phenomena happening in the pond-CTW system. This system is typical of an ecological engineering approach, as defined by Mitsch (2012): 'the design of sustainable ecosystems that integrate human society with its natural environment for the benefit of both.' It is (among others) characterized by reduced engineering during the construction phase, reduced compulsory maintenance and energy costs and use of natural properties from a complex ecosystem to provide ecosystem services—in this case, regulating services.

3 Tackling the Issues: The Restoration of the Ostwaldergraben Socio-Ecosystem

The implementation of this restoration program, the technical choices, and the construction resulted from the work of a consortium with an owner (City of Strasbourg), a contractor (the engineering consultant SINBIO), an engineering school (Ecole Nationale du Génie de l'Eau et de l'Environnement de Strasbourg), a research laboratory (ICUBE lab.), a water agency (AERM—public establishment of the Ministry for Sustainable Development), a NGO (BUFO—study of Amphibians and Reptiles of Alsace), and citizens. This co-construction exercise

involved a participatory approach that marked the different stages and accomplishments that we describe here.

3.1 Technical Itinerary to Achieve the Restoration Objectives

In order to stimulate the flow and limit the siltation, the bed width was reduced to 2 m. Gently sloping banks likely to be naturally vegetated by helophytes were created as well as windings and meanderings (Fig. 3). Shrub willow cuttings were planted.

The first operations to improve the diversity of the habitats were devoted to the creation of a pond network in the upstream sector where the sediments were not polluted. These ponds have three main functions: They serve as potential breeding habitat for amphibians, they contribute to the habitat diversity available to wildlife, and they collect the water discharging from the stormwater treatment system (see next part). The excavation/embankment operations were conducted to erase the bund; this reconnected the river and its major bed, while removing an awkward feature in this landscape context.

Management operations (mowing) of the vegetation under and around electric pylons must be conducted regularly. These interventions allowed artificially rejuvenating the environment on the left bank where breeding ponds were created, the right bank being left in natural evolution. The fauna and flora thus have a mosaic of aquatic/terrestrial habitats at different stages of plant succession. Mowed habitats are banks of alluvium and sand adequate to the displacements of many species.

Fig. 3 Restored stream. A dead arm can be seen on the left side of the picture, and a meander on the right (*Source* ICube Laboratory)

The biological quality of the Ostwaldergraben was evaluated with biological indicators based on aquatic macroinvertebrates. The biotic index applied highlighted the bad status of the stream stretch. Deposits made during the period of the tanneries' activity resulted in sediment contamination with highly toxic metal trace elements, such as chromium (Table 2). These observations led to remove the bund and dispose of this part of the polluted materials in a nearby dump (the one from the old tanneries). The remaining contaminated sediments corresponded to finer fractions, with sludge dredged from the stream bed. They were confined on created mudflats in a part of the old bed (three sections short-circuited by the re-meandering). The objective was to confine all the polluted muds extracted from the reduced minor bed and the ponds created on the right bank. The mudflats were covered with a geomembrane and a geotextile to avoid contact with the air in case of a drop in the water table. The containment of polluted sediments enabled the project to stay economically realistic compared with an export-and-treatment option. Additionally, it avoids for humans as for animals any possibility of contact or ingestion of the pollutants when visiting the area.

Vegetated embankments were created under the bridge to ease the passage of wildlife under the structure and restore the ecological corridor function for terrestrial species (Fig. 2b). The flow was tightened in a dug channel to promote aquatic continuity, in particular for fish. This panel of technical options was chosen thanks to the property right of the site by the owner builder, the City of Strasbourg.

Table 2 Sediment quality of the stream observed at two locations in 2006. All measured organic compounds are polycyclic aromatic hydrocarbon (PAH). The limit values provided correspond to French guideline values for soil and water pollution

	Units	Location 1	Location 2	Limit value
Dry matter	%	23.5	41.0	/
Cd	mg/kg DM	5	5	<10
Cr	mg/kg DM	**1,600**	**5,700**	<65
Cu	mg/kg DM	**150**	53	<95
Hg	mg/kg DM	1	0.23	<3.5
Ni	mg/kg DM	34	15	<70
Pb	mg/kg DM	190	70	<200
Zn	mg/kg DM	1,100	190	<4,500
Benzo(b)fluoranthene(3,4)	µg/kg DM	1,200	400	/
Benzo(k)fluoranthene(11,12)	µg/kg DM	550	190	/
Benzo(g,h,i)perylene(1,12)	µg/kg DM	700	280	/
Indéno (1,2,3-c,d) pyrène	µg/kg DM	1,300	390	/
Fluoranthene	µg/kg DM	2,200	640	/
Benzo(a)pyrene(3,4)	µg/kg DM	1,100	410	/
Sum of the six PAH	µg/kg DM	7,050	2,310	/

3.2 Setting up the Nature-Based Solutions to Treat Stormwater

Three urban watersheds are discharging runoff water into the stream on the study site, so three nature-based systems were set up; each one collecting and treating the water from one watershed. The sizes of the watersheds are pretty alike (ca. 2 ha) but in order to test the effect of different configurations on treatment efficiency, the constructed wetland varied in size. The choice of the CTW being the variable was somewhat arbitrary, as the pond might have been another variable of choice for different setups. Thus on the location of the initial wasteland were eventually built these treatment systems (Fig. 4), made of (from upstream to downstream):

- An artificial pond followed by a vertical subsurface flow wetland (#1 and #3, with differences in the size of the porous media that were used) followed by a discharge pond;
- An artificial pond followed by a horizontal subsurface flow wetland (#2) followed by a discharge pond.

Of the three systems, only two (#1 and #3) have been studied so far, so we will not develop further on #2. The main geometric, hydraulic, and upstream watershed characteristics of the systems are summarized in Table 3. For each watershed, the {pond + CTW} combination area is around 1–2% of the watershed active area.

As the groundwater table is close to the surface on the premises, the whole system was conceived to be impervious, in order to prevent infiltration of untreated water. As the available soil was not watertight, the main question that arose was how to ensure such imperviousness? The choice was finally made to coat the bottom of the pond and the wetland with 30 cm clay to achieve this at a reasonable cost; luckily this was the most environmental-friendly solution (other solutions were geomembrane or concrete).

The pond is fed through a concrete duct that is the outlet of the separate network collecting runoff water from the urban watershed (Fig. 5). The water flows from the pond to the CTW through a floating weir, whose triggering depends on the initial pond water level and rain events characteristics (intensity, duration, dry period, water level, and return period) and that works only for large enough rain events. The constructed treatment wetland is fed through several PVC pipes reaching different parts of the system to try and feed the system homogeneously. After vertical flow in the CTW, the stormwater is discharged into the last artificial ponds that are hydraulically connected to the stream. Moreover, the first pond is equipped with overflows—made of concrete pipes, which increases the ecological footprint of the system—that discharge directly into the final pond in case of extreme events. This overflow system caused a temporary failure in the system. It is indeed sealed with clay on the edge of the pipe to remain watertight, but a too low water level in the pond at first caused the clay to dry and subsequently retract. When water filled the pond back at a higher level, it started leaking at the joint and the pond drained. More clay was added to solve the problem.

Fig. 4 Hybrid treatment system just after construction. The settling pond is on the lower side of the picture; the constructed treatment wetland is on the upper left side of the picture. A bit further behind, a discharge pond can be seen (*Source* ICube Laboratory)

Table 3 Stormwater treatment system characteristics and hydraulic features (adapted from Schmitt 2014)

		#1	#3
Watershed	Surface (ha)	2.7	1.8
	Active surface (ha)	0.9	0.52
Pond	Size (m × m)	11 × 9	5 × 4.5
	Maximum hydraulic load ($m^3/m^2/day$)	10	10
	Permanent water volume (m^3)	28	2
	Maximum temporary water volume (m^3)	56	10
CTW	Area (m^2)	90	100
	Surface/watershed active surface (%)	1	2
	Maximum hydraulic load ($m^3/m^2/day$)	60	30

From the surface to the bottom of the CTWs, the porous medium is distributed as follows: The top layer is made of 20 cm (CTW #1), respectively, 30 cm (CTW #3) of sand (particle size from 0 to 4 mm); for both CTWs, the intermediate layer is made of 25 cm of fine gravel (particle size from 4 to 8 mm), and the drainage layer is made of 25 cm of gravel (particle size from 16 to 22 mm). The choice and the arrangement of these layers are a crucial and delicate point for CTWs, as it controls the infiltration rate and subsequently the hydraulic residence time, determining the absence or prominence of clogging in the system.

Finally, as the system feeding is by essence stochastic, a minimal water level is maintained at the bottom of the CTWs to reduce the water stress that vegetation, especially wetland plants, could endure during long dry periods. The ponds were

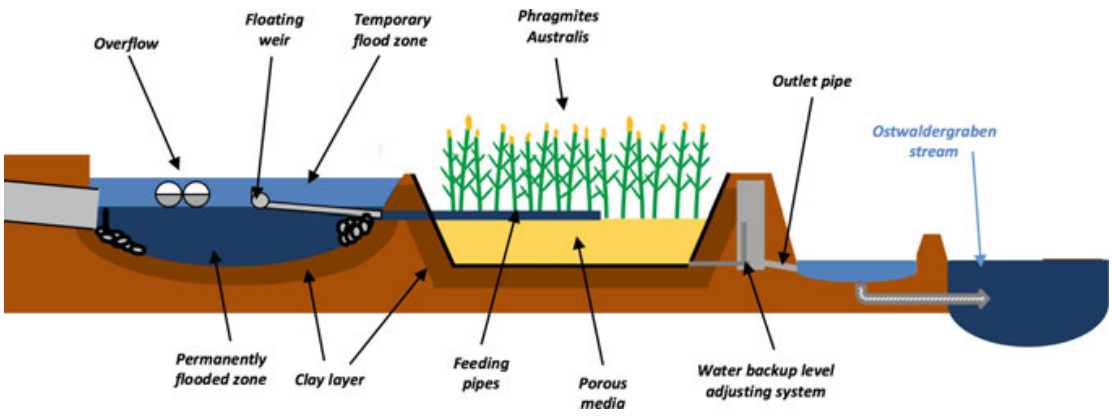

Fig. 5 Side view of the treatment system. From left to right (corresponding also to the water flux), pond, constructed wetland, discharge pond, stream (adapted from Schmitt 2014)

built free of vegetation, while the constructed wetlands were planted with *Phragmites australis* (9 plants/m^2).

4 The Ostwaldergraben's Response: Aftermath of the Restoration Project

4.1 The Creation of a Haven for the Green Toad? A New Face for the Corridor

The operations on the natural environment showed positive changes in a very short time after achievement. For example, the first ponds were created between March and August 2012, and as early as in September immature individuals of green toads were observed in these newly created habitats. In April of the following year (2013), egg clutches of several green toads were observed. The creation of a network of ponds at the upstream site (Bohrie Pond—2008) produced the same trends (Michel and Zrak 2015): a very fast colonization and a rise in the number of use of these environments, at least before the vegetation development (2011). These few results given as examples show the rapidity of spread in new environments by organisms whenever source populations are around.

The notion of a mosaic of habitats has also a central place in this type of project. The amphibian species *Bufotes viridis* acts here as an umbrella species that needs fallow and even cultivated soil to find suitable habitat during its terrestrial phase. This pioneer environmental species needs a constantly rejuvenated environment. Working gravel pits on both sides of the restored site allow the maintenance of pioneer habitats, while the restored site can be considered as a secondary habitat favoring connectivity between subpopulations. To keep this passage interesting and functional for the green toad, vegetation must be managed to avoid too great development and keep this system at a pioneer stage. The maintenance needed to

manage the vegetation under and around the power lines pylons also helps rejuvenating the vegetation along the dispersal corridor, in particular on the bare soil surrounding the artificial breeding ponds. The obligatory status of this management compensates the absence of self-sustaining natural processes to maintain each adequate habitat available in the mid- and long-terms.

4.2 Sustainability of the stormwater treatment: evolution of the hybrid system over 5 years

The responses of the treatment system were observed from the beginning of operation (back in 2012). The hybrid system was meant to provide regulating services on peak flows and water quality. First, less than 20% of the runoff events discharging into the pond actually discharge from the pond to the CTW. Thus, the sizing of the pond provides a strong buffering effect on runoff water discharge into the stream. Second, the pollution of the stormwater is clearly mitigated for both watersheds: major pollution (COD, TSS, TN, TP) (Schmitt et al. 2015) and micropollution (heavy metals and polycyclic aromatic hydrocarbons—PAHs) drops from the inlet to the outlet of the systems. These performances are sustained in time, as sampling sessions from 2013 to 2017 gave similar results.

The ecosystem services expected for the hybrid systems are well provided. The way the system works is also interesting: For instance, in case of runoff a strong shortcut is created by the floating weir because of its arm's length, which largely reduces the hydraulic residence time in the pond—and thus the efficiency of the settling phase (Laurent et al. 2013). This could be easily enhanced by installing a static weir leaving the whole pond surface available. In the CTW, the flow distribution is heterogeneous unlike what was expected: very little water reaches the end of the longest feeding pipes, which creates a feeding gradient.

The accumulation of sediments progressively fills the pond; the organic layer depositing at the surface of the CTW is around 4 cm after 6 years for the most covered CTW and 0 for the less covered. Ponds are colonized (2 out of 3) by macrophytes or algae and transform slowly into wetlands. In the CTWs, a gradient of organic deposit according to the feeding gradient is observed. In both constructed wetlands, trees and grass are appearing and sometimes taking over on macrophytes.

After 6 years of operation, the pollution mitigation is still working. As the pollution that is treated is mainly due to heavy metals and PAH, that are either non-degradable or highly stable compounds, their removal from stormwater means they migrated from the liquid phase to another phase. These pollutants are then logically found in the solid phase (sediments from the pond and organic matter and sand from the constructed wetland)—in the pond sediments, heavy metals were detected at a few mg/kg_{DM} to more than 2,000 mg/kg_{DM} for zinc, and around 1 mg/kg_{DM} of PAHs—and in the vegetation of the constructed wetland—from 1 to 22 mg/kg_{plant_DM} of heavy metals were measured in the reeds growing in the CTW

—(Schmitt et al. 2015). The contamination level in the sediments will rise steadily with time, which makes it first a sink for pollutants, but could also create a source of pollution under changing physicochemical conditions (Semadeni-Davies 2006).

When we look further ahead, the hydraulic functionality is likely to remain as long as sediments' accumulation is not too important. Yet, as the system keeps on retaining suspended solids from stormwater, accumulation will go on and call for sediment dredging, at least in the pond. With a minimal maintenance, this ecosystem service can be easily sustained over time. It is less crucial in the CTW, as the accumulation of mainly organic matter on its surface is much lower than in the pond, as the latter is the first in the system to retain such pollutants. If we look now from an ecotoxicological perspective on this system, the handling and disposal of these sediments appear to be of utmost importance: The toxicity of stormwater sediments was shown for much lower metal concentrations (Hatch and Allen 1999; Snodgrass et al. 2008). And as the treatment system is bound to stay and continue working, this long-term question is critical for the sustainability of the system. Eventually, the issue of the sediment behavior and fate should be carefully thought after.

4.3 Nature-Based Solutions and Citizen Representations: Sociological Aspects of the Project

To study the way this freshly built socio-ecosystem is perceived by the local residents and surveys were carried out during spring 2017. As a first step, seven people living in close proximity to the site were interviewed about their perception of their neighborhood. These semi-structured interviews were focused on the representation of their living environment and the potential nuisances, the representation of the Ostwaldergraben and its utility and on their own practices in terms of water pollution. This step was meant to define precise questions before individual questionnaires would be created. The individual questionnaires summarized the main issues of the interviews and were addressed to all the inhabitants living in the street right next to the site and to the inhabitants living in the street right behind (147 households). The questionnaire contained 23 questions (including 7 questions on the social characteristics of the respondents). It was self-administrated, and the principle of answering to the questions was built on the Likert scale: Respondents had to choose between five modalities (from 1 = 'not at all' to 5 = 'absolutely'). Of the 147 questionnaires mailed, 66 answers were received (45%—without any reminder). The sample was quite similar to the population living in this area: In our sample, we had 53% men and 47% female, the average age was 52 years (σ = 15.1) and there was a strong percentage of retired people (30%). Fifty-eight percent of the respondents had a direct look upon the zone. The questionnaire allowed us to test three main hypotheses: (i) The distance to the Ostwaldergraben site influences the residents' representation of the Ostwaldergraben; (ii) the knowledge of the functionality of the site (depollution) modifies the inhabitants'

behaviors linked to their own pollution in the rainwater network collection; and (iii) there is a typical profile of inhabitants who show a stronger awareness of the link between pollution in the stormwater network collection and the pollution of the Ostwaldergraben stream.

The results showed that distance to the site influenced the representation of pollution of the Ostwaldergraben: The respondents with a direct look on the site preferentially think that the stream is polluted [F (1.61) = 4.0334, $p = 0\ .05$]. Likewise, the respondents with direct look on the site wish that the site remains closed to the public [F (1.60) = 7.1361; $p = 0.01$].

To check the link between the respondents' understanding of the site and their own behaviors (hypothesis #2), further questions were asked (Figs. 6 and 7). The answers to the question on the system's functioning (Fig. 6) showed that the reintroduction function is the most understood, followed by the aesthetics enhancement. On the contrary, the regulating service—pollution mitigation—is poorly understood and the gutter products do not seem to be associated with pollution. To precise things a bit more, the question of the origin of the water entering the pond-CTW system was asked (Fig. 7). These answers showed that people think of the system as only designed to treat 'rainfall,' which means actually direct rainfall, as shows the answers to the last question '[…] gutter-discharged products.' People are aware that this system is not meant to treat wastewater as shows the answer to the second question (…domestic wastewater). Eventually, the understanding of the stream restoration conforms to reality but there is a gap between the {pond-CTW} function and its perception from the respondents. Additionally, an analysis of the variance (ANOVA) of the results shows that reading the information panel does not make a significant difference in the understanding of neither the treatment function of the hybrid system nor the origin of the water discharging in the system. We can conclude that the panels failed to explain the function of the treatment system, and that if deeper understanding of the people is wished by the city of Strasbourg, additional measures should be taken.

To understand the weight of the communication and information in the respondents' understanding of the site functionality, we tested the part of the communication implemented by the city of Strasbourg (public meetings, visits of the site once restored and information panels). Ninety-one percent of the respondents did not attend the public meetings, and 82% did not visit the restored site. Apart from these formal information sequences, 55% of the respondents read the information panels that are displayed on the access doors to the site, but the impact of the panels on the level of understanding is clearly questionable. It also seems that the respondents did not feel informed enough on the site and its functionality (52% of the respondents). Only 31% think that they are informed on that point.

Concerning a typical profile of inhabitants that were more aware on the link between the stormwater pollution and the pollution of the Ostwaldergraben site (hypothesis #3), it seems that the representation of a level of pollution was not linked with social characteristics.

We also tested the future of the site, trying to answer the question of the Ostwaldergraben sustainability and a kind of 'appropriation' of the site by the

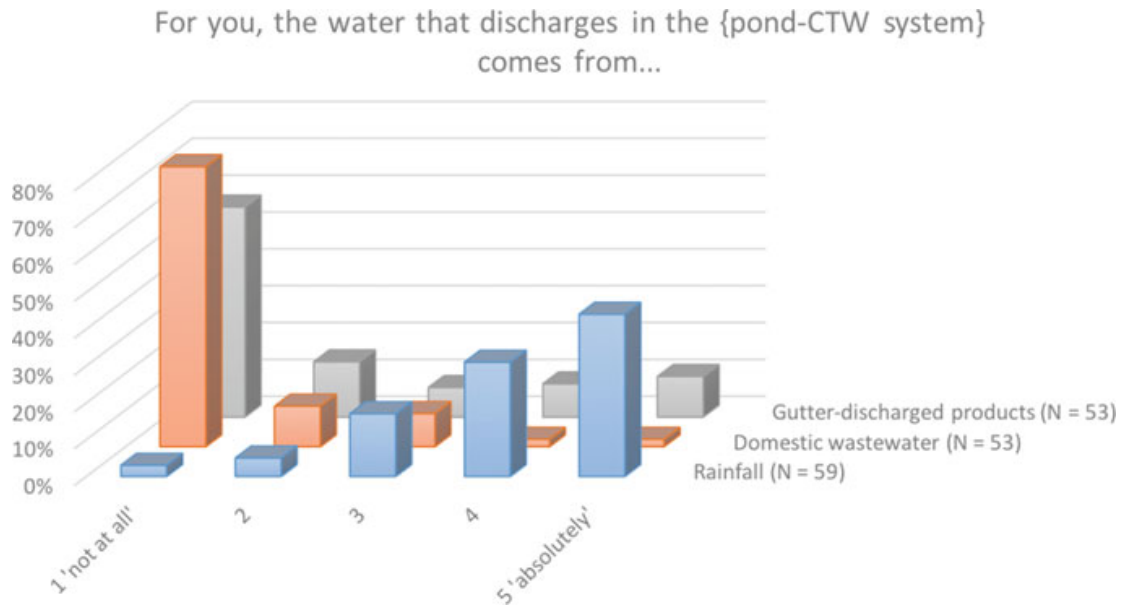

Fig. 6 Results from the questionnaire sent to local communities. The questions were related to the pond and constructed treatment wetland (CTW) in operation phase. Here the origin of the water that flows into the {pond-CTW} system

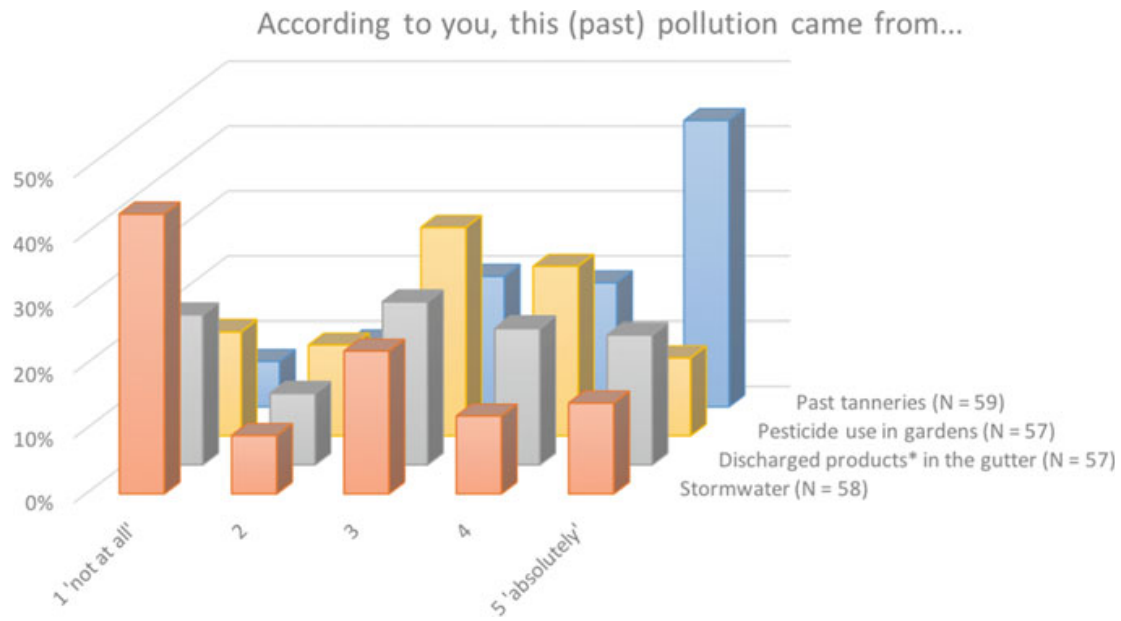

Fig. 7 Results from the questionnaire sent to local communities. The questions were related to the pond and constructed treatment wetland (CTW) in operation phase. Here the origin of the water that flows into the {pond-CTW} system. * paint, oil, water from carwash

inhabitants. A majority of the respondents (56%) wanted it to remain closed, while 30% wanted the opening to be restricted and 14% wanted it to be open. Eventually, we tested the interest of the local community about getting more active in the life of the site and the future vision of the site they had (Table 4). In accordance with the will of having it closed to the public, 46% of the answers about tours open for the

Table 4 Results of the questionnaire sent to residents on the social aspects of the project. The question was: « About the future use of the site, you would like to… » (response expressed in %). 1 = 'not at all,' 5 ='absolutely'

	1	2	3	4	5
Use it for educational purpose (N = 66)	23	3	12	14	48
Get involved in the stewardship of the site (N = 62)	58	10	13	8	11
Have it more used for tours open to the public (N = 65)	46	6	20	8	20
Make it an example for other sites in Strasbourg (N = 65)	20	2	14	11	53

public are 'not at all.' A clear tendency also showed that the inhabitants did not want to get involved in the stewardship of the site (68% of the answers between 1 and 2). They did believe, however, that this system is valuable, in terms of use for educational purpose or as an example to be replicated across Strasbourg.

To summarize, the Ostwaldergraben site seemed mostly 'accepted' and well perceived by the inhabitants. Indeed, the first source of perceived nuisance in the neighborhood was actually youngsters hanging out (20 occurrences at the open question '*In your neighborhood, what kind of nuisances do you perceive (noise pollution, olfactory pollution, visual pollution)*' N = 53). The second nuisance is linked to the amphibians (18 occurrences). Let us remember that the respondents who perceived the most negatively the amphibians are located in one spot, just across the natural pond. Yet, the results showed that the respondents who perceived the amphibians as a nuisance were significantly not favorable to wetland habitats [$F(1.49) = 10.576$; $p = 0.002$].

5 Conclusion: The Trade-Offs of This Project

The target species of this program was *B. viridis*, an endangered amphibian. Many amphibian species have populations structured as patchy networks or metapopulations. Urbanization reduces the ability of these networks of populations to function due to the construction of roads and urban infrastructure that inhibit or discourage amphibian dispersal (Hamer and McDonnell 2008). Stormwater wetlands and their neighboring terrestrial habitats may play an under-appreciated role in the conservation of urban amphibians (Scheffers and Paszkowski 2013). The construction of stormwater ponds is recognized as a useful tool both to mitigate the loss of wetlands, to retain water runoff from impermeable urban surfaces and to treat them, but their ecological value, in particular as breeding habitat for amphibians, remains poorly known (Chester and Robson 2013; Scheffers and Paszkowski 2013). Habitat surrounding stormwater sites also merits attention and preservation considering the importance of small-scale connections between the habitat of immatures and that of adults (Scheffers and Paszkowski 2013).

Controversial views of urban small water bodies are related to their water quality, even if in recent decades the quality of many urban aquatic habitats has

been significantly improved. In green toad, heavy metals like copper and lead have been shown to increase the frequency of morphological malformations (Dorchin and Shanas 2010) but *B. viridis* was already found in heavily contaminated water bodies (Adlassnig et al. 2013). Further, analyses are required to investigate the potential cost for the species of a putative lack of water quality.

The great removal efficiency of the treatment system provides benefits, but the cost of the sediments pollution and long-term solution to this is not to be underestimated. Additionally, taking into account local communities advices could help replicating this type of project and improve its acceptability among the population.

Acknowledgements The research on the Ostwaldergraben system is mainly supported by the Rhin-Meuse Water Agency and the French Biodiversity Agency through the LumiEau-Stra project. Additional research support is provided by the ZAEU (French LTSER network). Ideas for this chapter came through collaborations supported by the Urban Sustainability Research Coordination Network, support by the U.S. National Science Foundation (Grant No. 1140070).

References

Adlassnig W, Sassmann S, Grawunder A, Puschenreiter M, Horvath A, Koller-Peroutka M (2013) Amphibians in metal-contaminated habitats. Salamandra 49(3):149–158

Azimi S, Rocher V, Muller M, Moilleron R, Thevenot DR (2005) Sources, distribution and variability of hydrocarbons and metals in atmospheric deposition in an urban area (Paris, France). Sci Total Environ 337:223–239

Barbosa AE, Fernandes JN, David LM (2012) Key issues for sustainable urban stormwater management. Water Res 46:6787–6798

Becker CG, Fonseca CR, Haddad CFB, Batista RF, Prado PI (2007) Habitat split and the global decline of amphibians. Science 318(5857):1775–1777

Chester ET, Robson BJ (2013) Anthropogenic refuges for freshwater biodiversity: their ecological characteristics and management. Biol Cons 166:64–75

Chong MN, Sidhu J, Aryal R, Tang J, Gernjak W, Escher B, Toze S (2013) Urban stormwater harvesting and reuse: a probe into the chemical, toxicology and microbiological contaminants in water quality. Environ Monit Assess 185:6645–6652

Dorchin A, Shanas U (2010) Assessment of pollution in road runoff using a *Bufo viridis* biological assay. Environ Pollut 158(12):3626–3633

Dunning JB, Danielson BJ, Pulliam HR (1992) Ecological processes that affect populations in complex landscapes. Oikos 65(1):169

Erickson AJ, Weiss PT, Gulliver JS (2013) Stormwater treatment processes. Optimizing stormwater treatment practices. Springer, New York, NY, pp 22–34

Fenger J (1999) Urban air quality. Atmos Environ 33:4877–4900

Gosset A, Durrieu C, Orias F, Bayard R, Perrodin Y (2017) Identification and assessment of ecotoxicological hazards attributable to pollutants in 2 urban wet weather discharges. Environ Sci Process Impacts 19:1150–1168

Hamer AJ, McDonnell MJ (2008) Amphibian ecology and conservation in the urbanising world: a review. Biol Cons 141(10):2432–2449

Hatch AC, Allen G Jr (1999) Sediment toxicity and stormwater runoff in a contaminated receiving system: consideration of different bioassays in the laboratory and field. Chemosphere 39 (6):1001–1017

Laurent J, Finaud-Guyot P, Wanko A, Bois P, Mosé R (2013) Hydrodynamic of artificial wetlands at the outlet of urban catchment: complementarity of the systemic approach and computational fluid dynamics tools. Récents Progrès en Génie des Procédés, 104, Ed. SFGP, Paris, France

Michel V, Zrak E (2015) Bilan de dix années de suivi des indicateurs de la biodiversité en Alsace. Les effectifs de crapauds verts, Bufotes viridis. CICONIA, 39 (2–3):144–151

Mitsch WJ (2012) What is ecological engineering? Ecol Eng 45:5–12

Moore TLC, Hunt WF (2012) Ecosystem service provision by stormwater wetlands and ponds: a means for evaluation? Water Res 46:6811–6823

O'Sullivan AD, Wicke D, Hengen TJ, Sieverding HL, Stone JJ (2015) Life cycle assessment modelling of stormwater treatment systems. J Environ Manage 149:236–244

Scheffers BR, Paszkowski CA (2013) Amphibian use of urban stormwater wetlands: the role of natural habitat features. Landsc Urban Plann 113:139–149

Scheyer A, Morville S, Mirabel P, Millet M (2007) Pesticides analyzed in rainwater in Alsace region (Eastern France): comparison between urban and rural sites. Atmos Environ 41:7241–7252

Schmitt N (2014) Characterization of hybrid systems for the treatment of urban stormwater: fate of emerging pollutants. PhD Thesis. University of Strasbourg. HAL-ID: tel-01214516

Schmitt N, Wanko A, Laurent J, Bois P, Molle P, Mosé R (2015) Constructed wetlands treating stormwater from separate sewer networks in a residential Strasbourg urban catchment area: Micropollutant removal and fate. J Environ Chem Eng 3:2816–2824

Semadeni-Davies A (2006) Winter performance of an urban stormwater pond in southern Sweden. Hydrol Process 20:165–182

Snodgrass JW, Casey RE, Joseph D, Simon JA (2008) Microcosm investigations of stormwater pond sediment toxicity to embryonic and larval amphibians: Variation in sensitivity among species. Environ Pollut 154:291–297

ELEMENTA
Science of the Anthropocene

Childers, DL, et al. 2019. Urban Ecological Infrastructure: An inclusive concept for the non-built urban environment. *Elem Sci Anth,* 7: 46. DOI: https://doi.org/10.1525/elementa.385

REVIEW

Urban Ecological Infrastructure: An inclusive concept for the non-built urban environment

Daniel L. Childers[*], Paul Bois[†], Hilairy E. Hartnett[‡], Timon McPhearson[§,‖,¶], Geneviève S. Metson[**] and Christopher A. Sanchez[††]

It is likely that half of the urban areas that will exist in 2050 have not yet been designed and built. This provides tremendous opportunities for enhancing urban sustainability, and using "nature in cities" is critical to more resilient solutions to urban challenges. Terms for "urban nature" include Green Infrastructure (GI), Green-Blue Infrastructure (GBI), Urban Green Space (UGS), and Nature-Based Solutions (NBS). These terms, and the concepts they represent, are incomplete because they tend to reduce the importance of non-terrestrial ecological features in cities. We argue that the concept of Urban Ecological Infrastructure (UEI), which came from a 2013 forum held in Beijing and from several subsequent 2017 publications, is a more inclusive alternative. In this paper we refine the 2013 definition of UEI and link the concept more directly to urban ecosystem services.

In our refined definition, UEI comprises all parts of a city that support ecological structures and functions, as well as the ecosystem services provided by UEI that directly affect human outcomes and wellbeing. UEI often includes aspects of the built environment, and we discuss examples of this "hybrid infrastructure". We distinguish terrestrial, aquatic, and wetland UEI because each type provides different ecosystem services. We present several examples of both "accidental" UEI and UEI that was explicitly designed and managed, with an emphasis on wetland UEI because these ecotonal ecosystems are uniquely both terrestrial and aquatic. We show how both accidental and planned UEI produces unexpected ecosystem services, which justifies recognizing and maintaining both purposeful and serendipitous types of UEI in cities. Finally, we posit that by incorporating both "ecological" and "infrastructure", UEI also helps to bridge urban scientists and urban practitioners in a more transdisciplinary partnership to build more resilient and sustainable cities.

Keywords: Urban Ecological Infrastructure; Ecosystem services; Hybrid infrastructure; Urban sustainability; Urban resilience

Infrastructure and nature in cities

Homo sapiens is becoming an increasingly urban species (Wigginton et al. 2016; Elmqvist et al. 2018; NSF AC-ERE 2018), a global shift that underscores the profound importance of understanding urban ecosystems. Cities, as concentrated consumers of energy and resources, are producers of various wastes, but they are also centers of innovation, efficiency, social networks, and solutions (David 1995; Grimm et al. 2008; Bettencourt et al. 2009; Pickett et al. 2013; Grimm and Schindler 2018). Cities are designed and built to be human habitats, and the result is urban infrastructure. Infrastructure is typically defined as the physical components of interrelated systems that provide commodities and services essential to enable, sustain, or enhance societal living conditions (*sensu* Neuman and Smith 2010). In its classical definition, infrastructure is generally restricted to the built [and otherwise human-constructed] environment; this is the way architects, engineers, and city planners and managers often think of it. In contrast, our focus here is on non-built "nature in cities" infrastructure and the broader adoption of a more inclusive term and concept for it: Urban Ecological Infrastructure (UEI).

The traditional concept of infrastructure likely began to expand to include nature in cities with the designs

* School of Sustainability, Arizona State University, Tempe, Arizona, US
† ICube (UMR 7357 ENGEES/CNRS/Unistra), Strasbourg, FR
‡ School of Earth and Space Exploration and School of Molecular Sciences, Arizona State University, Tempe, Arizona, US
§ Urban Systems Lab, The New School, New York, New York, US
‖ Cary Institute of Ecosystem Studies, Millbrook, New York, US
¶ Stockholm Resilience Centre, Stockholm, SE
** Theoretical Biology, Department of Physics, Chemistry and Biology (IFM), and Center for Climate Science and Policy Research (CSPR) Linköping University, Linköping, SE
†† Global Institute of Sustainability, Arizona State University, Tempe, Arizona, US
Corresponding author: Daniel L. Childers (dan.childers@asu.edu)

of Frederick Olmstead, then later with the work of Ian McHarg (1969) and, more recently, Frederick Steiner (2006). Awareness of nature in cities began to mature and become more widespread during the environmental movement of the 1960s and 70s. Since then, the importance and value of nature in cities has strengthened with the growth of urban ecology as both a discipline and an approach to understanding urban systems dynamics. With this strengthening has come the prevalence of several terms by European and U.S. urban scientists and practitioners to refer to nature in cities. Green Infrastructure (GI) is one (Tzoulas et al. 2006; Keeley 2011; Andersson et al. 2014; Larsen 2015; Koc et al. 2017); it is typically defined as the interconnected network of natural and semi-natural elements capable of providing multiple functions and ecosystem services encompassing positive ecological, economic, and social benefits for humans and other species (Benedict and McMahon, 2006; Koc et al. 2017). The GI concept has recently been expanded to Green-Blue Infrastructure (GBI), in order to include urban aquatic features (*sensu* Barbosa et al. 2019). Another more recently used term is Urban Green Space (UGS), defined as the natural, semi-natural, and artificial ecological systems within and around a city that comprise a range of habitats (Niemela et al. 2010; Cilliers et al. 2013; Aronson et al. 2017). Additionally, the term Nature-Based Solutions (NBS) has gained considerable traction, particularly in Europe (Eggermont et al. 2015; Cohen-Shacham et al. 2016; Maes and Jacob 2017; Kabisch et al. 2017; Frantzeskaki et al. 2019; Keeler et al. 2019), although this concept seems to be more focused on goal-oriented engineering rather than on the natural infrastructure itself (Nesshover et al. 2017, WWAP/UN-Water 2018). The definitions of GI, GBI, UGS, and NBS overlap considerably, and all are routinely coupled with the ecosystem services concept (e.g., Gomez-Baggethun et al. 2013; Andersson et al. 2015; Locke and McPhearson 2018; Keeler et al. 2019). GI and UGS are more strongly focused on terrestrial ecological features in cities; notably, a recent review and typology of GI by Koc et al. (2017) included no aquatic features, while a review of the GI literature by Haase et al. (2014), that was focused on ecosystem services, did not include urban wetlands. Similarly, applications of the GBI and NBS terms and concepts rarely discuss or include urban wetlands.

The concept of Ecological Infrastructure first appeared in a 1984 report by the United Nations Educational, Scientific, and Cultural Organization's (UNESCO) Man and Biosphere Program. It was several decades before the concept of UEI emerged in the literature, as a product of the 2013 International Ecopolis Forum on "Urban Ecological Infrastructure for New Urbanization" that was held in Beijing, China (Li et al. 2017a). This forum defined UEI as the organic integration of blue, green, and gray landscapes, combined with "exits" (outflows and recycling) and "arteries" (corridors; Li et al. 2017b). This definition included the built urban environment, and thus seems to include all urban infrastructure. The Li et al. (2017b) definition was also complicated by the inclusion of processes both within and between patches of UEI in the urban matrix. Perhaps because this definition was so expansive, the UEI concept has not become known by, let alone resonated with, the larger communities of urban systems scientists or practitioners in Europe, the U.S., or elsewhere beyond China.

Our objectives for this paper include:

1. The presentation of a simplified and more concise definition of UEI that directly connects UEI to the ecosystem services it provides, eliminating the need to include the ecological processes that produce those services explicitly in the definition.
2. A desire to make urban researchers and practitioners from Europe, the U.S., and elsewhere more broadly aware of the UEI concept, in hopes that it will be adopted as a more inclusive concept for nature in cities.
3. Justification for the idea that use of both "ecological" and "infrastructure" in the UEI concept forms a key bridge between urban ecologists and urban practitioners–UEI elevates urban ecological features to the same consideration by the latter as urban built features.
4. Demonstration that terrestrial, aquatic, and wetland types of UEI provide unique ecosystem services, and that a more refined focus on these ecosystem-specific processes may produce "surprise" ecosystem services.

A simplified definition of UEI

Our simplified and more concise definition of UEI encompasses all parts of a city that include ecological structures and functions. Ecological structure is the physical components that make up ecosystems (e.g. species, soils, waterways) while ecological function is the processes that result from interactions among the structural components (e.g. primary production, nutrient cycling, decomposition). UEI forms a critical bridge between nature in cities and the people that live in cities via its purveyance of urban ecosystem services (**Figure 1**). These ecosystem services are, by definition, the benefits that people gain from UEI and the resulting effects on human outcomes. Many of these ecosystem services result from the ecological function of UEI (the arrows in **Figure 1** that connect function to ecosystem services to outcomes), but some are purely structural (the arrow in **Figure 1** that connects UEI with outcomes). For example, urban trees are known for providing a number of function-derived ecosystem services, such as transpirational cooling and soil retention and development. But urban trees also provide services that are strictly tied to their ecological structure, including shade and habitat for wildlife.

Notably, infrastructure must possess ecological structure and function to be considered UEI. For example, swimming pools provide key services such as exercise, recreation, and cooling, but [by design] pools do not have ecological structure or function so they are not UEI. In our broadest of definitions, UEI is effectively all of the physical components of a city *except* the built environment. A building roof that is painted white (or even green) and called a "green roof" because of energy savings is not

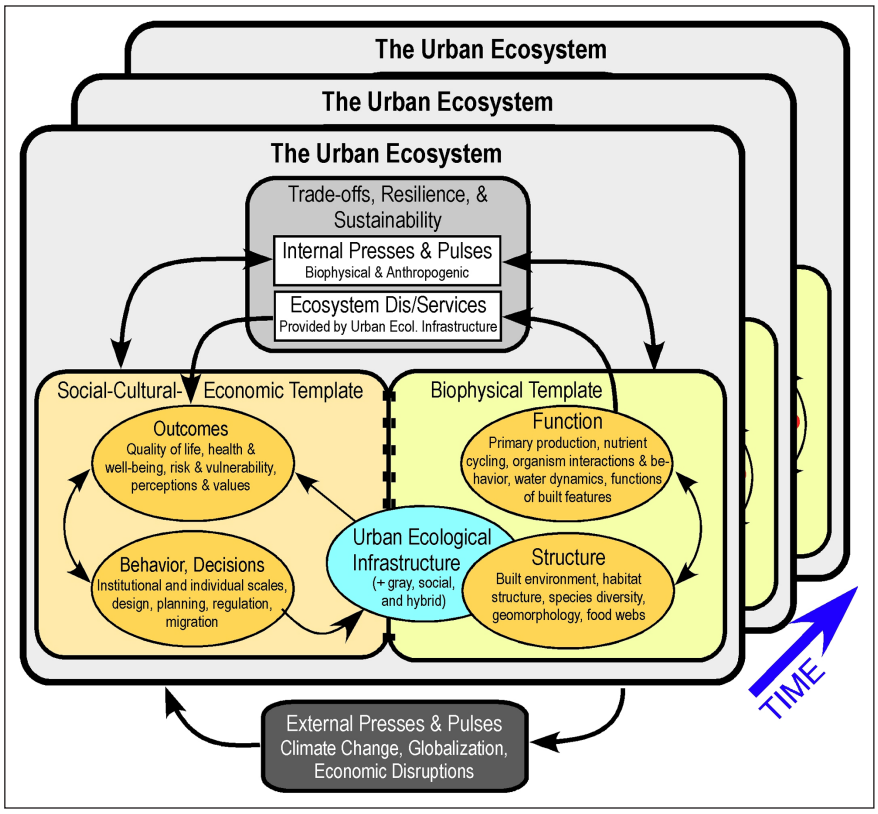

Figure 1: Conceptual framework of the CAP LTER Program. The conceptual framework being used by the Central Arizona-Phoenix Long-Term Ecological Research Program (CAP LTER) to structure and guide its urban ecological research. Note the blue oval in the center that demonstrates how UEI bridges the biophysical and human realms of the urban ecosystem. DOI: https://doi.org/10.1525/elementa.385.f1

UEI, but a green roof that includes soil and plants and is designed and managed for stormwater and heat abatement has ecological structure and function, and thus is UEI. Other examples of UEI include parks, streams, street trees, residential yards, riparian areas, lakes, urban agriculture, vacant lots, and constructed treatment wetlands. To the extent that a planted front porch flowerpot provides aesthetic benefits and food for pollinators, it is also UEI. Thus, UEI occurs at all scales. Finally, UEI is typically designed and managed to varying degrees, but not always. Examples of unplanned and/or unmanaged UEI include "accidental wetlands" (*sensu* Suchy 2016; Palta et al. 2016, 2017), vacant lots (McPhearson et al. 2013), and [seemingly] neglected areas.

Our ecologically inclusive UEI concept [of course] includes all terrestrial ecological features in cities, which we refer to as Green UEI. Bare soil is a particular terrestrial ecological feature that is present in all cities and is often a separate land cover class. Bare soils are sites of important ecological functions, including a host of biogeochemical processes and water infiltration (Herrmann et al. 2016). Thus, we distinguish bare soil from green UEI because it is not vegetated and is generally overlooked in research on GI/UGS and ecosystem services. For example, many vacant lots in Phoenix—a hot, dry desert city—are bare soil because without irrigation few if any plants can survive. Interestingly, vacant lots make up a large fraction of total urban land area, averaging 15% or more (Kremer et al. 2013). For these reasons, we include this unvegetated Brown UEI in our terrestrial ecological categorization.

All cities also have various types of aquatic ecological features, including lakes, streams, rivers, canals, and coastal oceans. We refer to this as Blue UEI. Notably, in their analysis of cultural ecosystem services in cities, Andersson et al. (2014) explicitly discussed both green and blue infrastructure, as do other recent publications (Ioja et al. 2018). In addition, because of the ways that water moves across landscapes, aquatic and wetland UEI features are often highly connected in urban ecosystems, even when those connections are not readily visible (e.g. buried urban streams). Yet urban wetlands are the ecological components that are either left out of discussions, studies, and reviews of nature in cities or are designated as either terrestrial or aquatic. All cities have wetlands of some form—undisturbed or degraded, constructed or restored, or simply accidental (*sensu* Palta et al. 2017). But wetlands have structural and functional characteristics that are both terrestrial and aquatic—they are effectively ecotone systems (Mitsch and Gosselink 2015). This means that wetlands combine the ecological characteristics of both Green and Blue UEI, yet wetlands are uniquely neither terrestrial or aquatic. For this reason we categorize urban wetlands separately, as Turquoise UEI (as first defined in Childers et al. 2015), because when one combines the colors green and blue the result is the color turquoise.

Our four-color approach to defining the UEI concept distinguishes Green, Brown, Blue, and Turquoise UEI because

each type provides a unique set of ecosystem services, and each type has its own management trade-offs because of potential disservices (in **Table 1** we present examples of Blue, Turquoise, and Brown UEI; the literature is rich with examples of Green UEI). Still, having these four categories reunited under the common banner of UEI allows for the connectivity among them (e.g., the same water may flow through Brown, Green, and/or Turquoise UEI before it reaches Blue UEI) to be more readily highlighted and to be managed in more integrated ways.

Why UEI is more inclusive than currently used terms for nature in cities

We argue that UEI as both a term and a concept, is necessary because of the terrestrial-centric nature of GI and UGS. Both GI and UGS seem to downplay or even ignore the importance of aquatic and wetland ecosystems in cities, yet all cities have streams, rivers, canals, lakes, shorelines or coastlines, and various types of wetlands. This emphasis on the terrestrial makes some sense, given that *Homo sapiens* is a land-bound species. Regardless, a focus on only terrestrial ecological features is an incomplete representation of nature in cities. The recent expansion of GI to GBI, so as to include aquatic features, still fails to acknowledge the ecological uniqueness of wetlands and their important contributions to UEI-based urban ecosystem services. While NBS does include aquatic features and wetlands (WWAP/UN-Water 2018), it is a goal-oriented and engineering-based concept that tends to focus on single-service delivery. We know this is insufficient because nature in cities provides multiple, and sometimes conflicting, benefits and these vary because of the social, technological, and ecological context of individual cities (Keeler et al. 2019). Our definition of UEI, detailed above, is considerably less abridged in its inclusion of urban ecological systems.

Another complication with GI is that this same term has a number of enviro-political connotations. Green infrastructure is routinely used to describe environmentally friendly, or "green" policies (e.g., recycling) or technologies (e.g., solar panels). This confusion over what GI actually means may lead to miscommunication or misunderstanding when urban ecologists are working with decision makers or with the public. One person's conception of nature in cities may be another person's idea of environmentally-supportive policies. As urban ecologists are striving to work more with urban designers, engineers, planners, other practitioners, and urban residents, it is important to ensure that we are all talking about the same things.

UEI as a bridge between urban scientists and practitioners

We posit that UEI, as both a term and a concept, will resonate with designers, planners, and managers, strengthening this ecologist-practitioner bridge and thus advancing our ability to move knowledge to action in support of more sustainable urban futures (per Childers et al. 2015; Pickett et al. 2016). An example of this comes from recent work by two authors of this paper (DLC and CAS) on a UEI stormwater management project on the campus of Arizona State University, Tempe AZ USA. A newly-constructed LEED Platinum Student Pavilion building included bioswales and other UEI features in the surrounding landscape to manage stormwater. The university administration also wanted to apply for SITES certification for the site (SITES

Table 1: Select examples of Blue, Brown, and Turquoise UEI, including associated ecosystem services and potential or perceived disservices. Ecosystem service abbreviations: P = provisioning services; R/S = regulating or supporting services; A/C = aesthetic or cultural services. DOI: https://doi.org/10.1525/elementa.385.t1

UEI Type	UEI Color	Ecosystem Services	Potential Ecosystem Disservices
Residential and park lakes	Blue	Enhanced property values (R/S), recreation (A/C), local cooling (R/S), fishing (P)	Disease vectors (e.g. mosquitoes), undesirable algal blooms
Urban streams and rivers	Blue	Flood control (R/S), recreation (A/C), local cooling (R/S), fishing (P), transportation (R/S)	Flooding, disease vectors, undesirable water quality
Riparian areas	Turquoise	Flood control (R/S), water quality enhancement (R/S), local cooling (R/S), wildlife habitat (A/C), recreation (A/C)	Flooding, disease vectors, undesirable wildlife
Water delivery canals	Blue	Water supply (P), local cooling (R/S), recreation (A/C), fishing (P)	Disease vectors, undesirable wildlife
Constructed treatment wetlands	Turquoise	Water quality enhancement (R/S), local cooling (R/S), wildlife habitat (A/C)	Disease vectors, undesirable wildlife
Accidental wetlands	Turquoise	Water quality enhancement (R/S), local cooling (R/S), wildlife habitat (A/C), human habitat (P)	Disease vectors, undesirable wildlife, undesirable people
Vacant lots	Brown	Stormwater regulation (R/S), groundwater recharge (R/S), soil development (R/S), wildlife habitat (A/C)	Sources of blowing dust, aesthetically undesirable
Construction sites	Brown	Stormwater regulation (R/S), groundwater recharge (R/S)	Sources of blowing dust
Fallow urban agricultural plots	Brown	Stormwater regulation (R/S), groundwater recharge (R/S), soil development (R/S), wildlife habitat (A/C)	Sources of blowing dust, aesthetically undesirable

is a certification program similar to LEED that focuses on the ecological efficacy of a building's surrounding landscape). The SITES certification process requires that the applicant empirically demonstrate effective outcomes of UEI solutions, which thus requires monitoring of UEI processes. These practitioners had little to no experience with environmental monitoring, but they did know about our long-term research on stormwater management using UEI through the Central Arizona-Phoenix Long-Term Ecological Research Program (CAP LTER; Hale et al. 2014, 2015).

The subsequent practitioner-researcher collaboration on the Student Pavilion's UEI involved several meetings, workshops, and field trips and resulted in a fully co-produced monitoring design for the site. Our research on this stormwater management UEI not only produced ecohydrological and biogeochemical data, but also included survey data derived from interviews of all practitioners and scientists involved in the monitoring design process (Sanchez 2019).

The architects and engineers involved in the project came into the co-production design process referring to their stormwater management features as GI. When asked to define GI, practitioner definitions of GI were remarkably similar to UEI. Further, it was clear they were aware of the many different perceptions of what GI means, including its enviro-political connotations, and they readily acknowledged the confusion this may produce. When introduced to the UEI concept, it was clear they had never heard of it before but they were quickly receptive to it as a better, more inclusive, and less confusing alternative. We posit that as the UEI concept becomes more prevalent in these design co-production activities, its value as a bridge between urban research and practice will become clearer.

Ecosystem services, and "surprise" services, provided by UEI

The UEI concept, and UEI itself, also forms a critical bridge between nature in cities and the people that live in cities (**Figure 1**). The most important link between these two realms is the ecosystem services provided by UEI. Most of these services derive from the ecological functions of UEI, as shown in **Figure 1**, but some of the benefits people derive from UEI are structural and more direct. For example, trees in a city park provide a number of functionally-based ecosystem services, including cooling via evapotranspiration, soil development, carbon and nutrient sequestration, and stormwater management. But the same trees also provide shade for people and habitat for birds, insects, and other wildlife—these are purely structural ecosystem services. UEI is also an important component of hybrid urban infrastructure, which Grimm et al. (2016) define as components of the urban fabric that are a mix of built and environmental structures in cities. As such, hybrid infrastructures provide benefits via both ecological structure and function (e.g., ecosystem services) and built structures (e.g., services; Depietri and McPhearson 2017).

In this section we present case study examples of ecosystem services provided by UEI. The literature is rich with examples of terrestrial UEI—also known as GI, UGS, or NBS—and the ecosystem services it provides (e.g., **Figure 4** in Haase et al. 2014). For this reason, there is no need to expand on these here. Rather, we focus our UEI case studies on Blue and Turquoise UEI because: 1) these systems have been neglected in GI, UGS, and NBS research and in the urban ecosystem services literature; 2) it is important to demonstrate that urban wetlands provide services that are unique from those of terrestrial or aquatic UEI and; 3) Blue and Turquoise UEI often provides unexpected, or "surprise", ecosystem services. Our point here is that by focusing on the terrestrially-based UEI in our cities, we are often surprised by the additional benefits that people derive from other "wetter" forms of UEI. The following examples document the value of Blue and Turquoise UEI to urban residents, via both the ecosystem services these systems were designed and managed to produce as well as via serendipitous ecosystem services.

1. Blue UEI in Phoenix AZ USA

Tempe Town Lake is a man-made lake that was built in the heart of downtown Tempe AZ in 1999 (**Figure 2A, B**). It was built by constructing dams across the bed of the Salt River, which has been effectively a dry river since the late 1930s. Tempe Town Lake was built to promote economic development, to provide recreational opportunities, and to manage stormwater and flooding. The lake provides effective flood control because the dams can be lowered, allowing the lake to accommodate significant flows during storm events or upstream dam releases. High flow events (>1000 cubic feet per second over a period of days to weeks) have necessitated opening the dams on five occasions since 2005. According to the City of Tempe, the economic impacts of the lake have exceeded $1.5 Billion. More than 2.4 million people spend time at the lake and the associated Tempe Beach Park every year, making it Arizona's second most popular public attraction—after the Grand Canyon (https://www.tempe.gov/city-hall/community-development/tempe-town-lake). Clearly, Tempe Town Lake has provided the three main ecosystem services of design.

In 2012, 68 users of Tempe Town Lake and park were surveyed about their perceptions and attitudes towards six ecosystem services: habitat provisioning, aesthetics, microclimate and stormwater regulation, and recreational and educational opportunities (Wilson 2012). Attitudes towards all of these ecosystem services were positive, and not surprisingly water was the central interest for most park users. Microclimate regulation, aesthetics, and recreational opportunities ranked highest in user preferences, and user attitudes and perceptions aligned reasonably well with the City's design and management goals for the lake and park.

We have monitored water quality in Tempe Town Lake since 2005 as part of the CAP LTER Program. One outcome of this long-term monitoring effort is our discovery of an unexpected ecosystem service: Because the lake is highly productive, it takes up significant amounts of atmospheric CO_2 over most of the year. The primary evidence for high primary production is the consistently alkaline pH (>8.5; **Figure 3A**) due to the uptake of CO_2—which is an acid when dissolved in water—by phytoplankton. Corroborating evidence is found in the consistently high

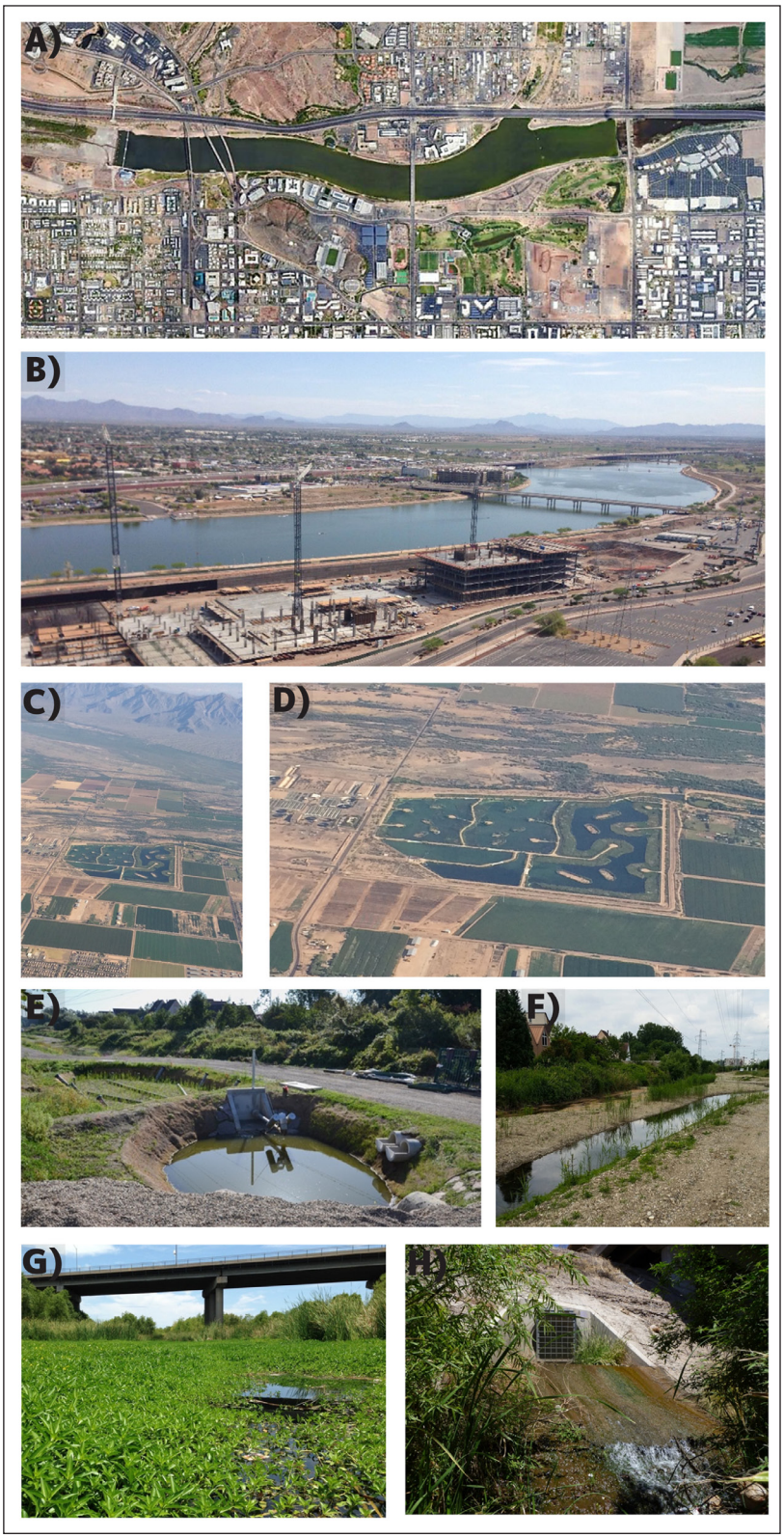

Figure 2: Photographs of the UEI systems described in the case studies. (A) Tempe Town Lake, Tempe AZ. The lake is directly north of downtown Tempe and the ASU campus; **(B)** There has been substantial economic development along the south shore of the lake (Photos A and B: Google Earth images); **(C)** The Tres Rios CTW (center). **(D)** Long-term monitoring and research have been carried out in the L-shaped 42 ha wetland cell on the right, which includes 21 ha of vegetated marsh. The wastewater treatment plant is on the far left of both photos, and the Salt River is immediately above the CTW (Photos by D. Childers); **(E)** The stormwater management UEI at the Ostwaldergraben system in Strasbourg, France shortly after installation. **(F)** The nearby stream shortly after restoration (Photos by P. Bois); **(G)** Accidental wetlands in the Salt River bed, downtown Phoenix AZ USA; **(H)** A stormwater outfall into the river bed with a large enough stormwatershed, or pipeshed, that it produces perennial flow (Photos by A. Suchy). DOI: https://doi.org/10.1525/elementa.385.f2

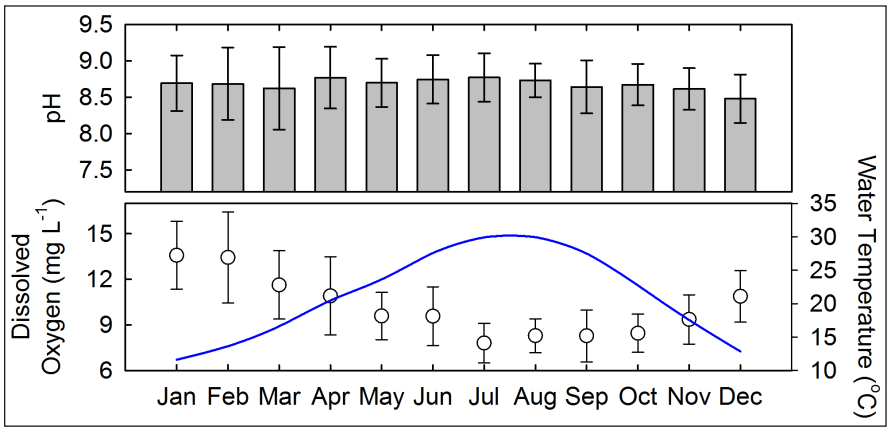

Figure 3: Tempe Town Lake water quality data. Tempe Town Lake monthly average data for pH (top), dissolved oxygen (bottom, open symbols), and water temperature (bottom, blue line). Data are taken from the City of Tempe water quality database; weekly data are grouped by month and monthly averages are calculated for the period 2005 to 2017 (n = ~50 for each month). Error bars are ±1 S.D. of the monthly mean (CAP LTER dataset DOI:10.6073/pasta/59d2e20260ad78d887e9bf3dd8987db4). DOI: https://doi.org/10.1525/elementa.385.f3

dissolved O_2 concentrations (7.8 to 13 mg L^{-1}; **Figure 3B**); on average, the lake is ~12% supersaturated with respect to O_2 throughout the year. The lake has very low nitrogen concentrations (<2 mg NO_3^- L^{-1}; <0.2 mg NH_4^+ L^{-1}) because of high algal productivity. While this carbon sink cannot come close to offsetting the atmospheric carbon sources of Tempe, most of which are associated with transportation, this is a valuable and little-known service of this Blue UEI.

2. Deliberate Turquoise UEI in Phoenix AZ USA

In 2010, the City of Phoenix began using a large constructed treatment wetland (CTW) to provide final tertiary treatment to effluent from its 91st Avenue wastewater treatment plant—the largest in the Phoenix Metro Area (**Figure 2C**). This CTW, known locally as Tres Rios, includes three wetland treatment cells that total roughly 100 ha and the system is capable of treating up to 400,000 m^3 day^{-1} of wastewater effluent. Since 2011, the CAP LTER Program has been quantifying wetland ecosystem processes in the largest of the three wetland cells (**Figure 2D**; Weller et al. 2016). Tres Rios was designed to provide the ecosystem service of surface water treatment in the form of nutrient reduction, and our data confirm that it is meeting this goal quite well (Sanchez et al. 2016). In fact, we have found that if nitrogen makes its way into the vegetated wetland component of this system, it is nearly completely expunged from the water (**Figure 4**).

As part of our long-term research in the Tres Rios CTW, we have also been quantifying and estimating the whole-system water budget. This includes water loss via plant transpiration, which is remarkably high during the hot, dry Sonoran Desert summers (Sanchez et al. 2016). As we analyzed these data, we realized the large volumes of water being lost to the atmosphere from the vegetated marsh must be replaced, and the only possibility for this was via a gradual but persistent flow of surface water into the marsh from the adjacent open water areas. We call this phenomenon the "Biological Tide". It has been verified in the field and represents the first time that anyone has ever documented plant-mediated control of surface hydrology in a wetland (Bois et al. 2017). In addition, the biological tide brings additional nitrogen and pollutants into the vegetated marsh for treatment, enhancing the ecosystem service for which it was designed. This enhanced efficacy of the CTW was an unexpected ecosystem service of this Turquoise UEI. Another surprising ecosystem service is that Tres Rios quickly became a significant habitat for wetland and aquatic wildlife, including being a mecca for birds. This CTW is a seasonal or permanent home to dozens of species of wetland and aquatic birds, including protected species.

3. Deliberate Blue-Turquoise UEI in Strasbourg France

Strasbourg, in NE France, is characterized by a dense network of waterways within the city boundaries. One of them, the Ostwaldergraben, is a small stream fed mostly by groundwater. As the city grew it was strongly channelized and enlarged. It also once received wastewater discharge from former tanneries. The City of Strasbourg launched a program in 2010 to restore the stream and recover it from its "mediocre" ecological state, as assessed by the European Water Framework Directive (EC 2000). The restoration process highlighted that the stream could be morphologically and chemically degraded by stormwater being discharged from the nearby urban residential watershed. Given this information, stormwater inflows were equipped with ponds (Blue UEI) and constructed wetlands (Turquoise UEI; Bois et al. 2019). This UEI was designed to improve water quality and mitigate stormwater flows (**Figure 2E, F**). After six years of operation, we have confirmed that the system is providing the ecosystem services that it was designed to provide: Fewer than 20% of storm events discharge into the stream and the UEI effectively removed suspended sediment, organic matter, nitrogen, phosphorus from the water (**Figure 5**; Schmitt et al. 2015, Walaszek et al. 2018).

A key goal of the stream and associated riparian zone restoration was to help bring back a pioneer and endangered species: The green toad (*Bufotes viridis*). Surprisingly, the artificial ponds, which were initially only designed for stormwater management, have been colonized by this

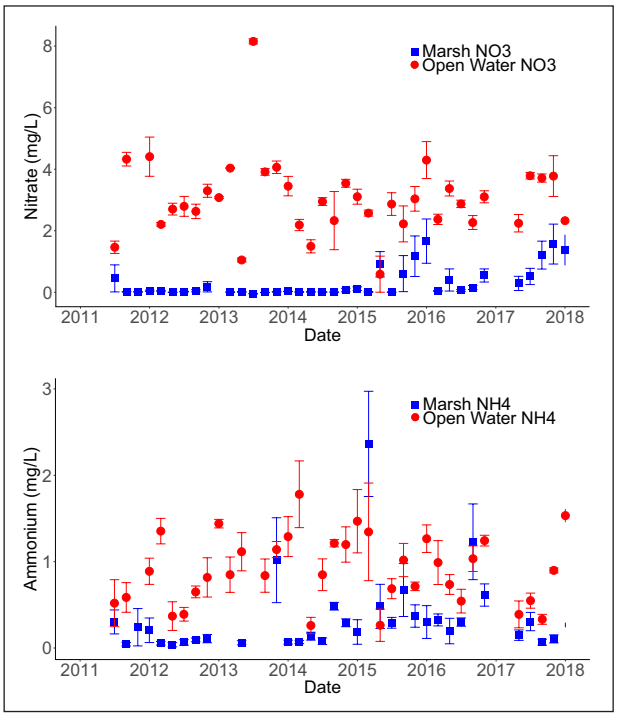

Figure 4: Tres Rios constructed treatment wetland water quality data. Nitrate (top) and ammonium (bottom) concentration data from the Tres Rios CTW. Data are collected bimonthly along three transects within the vegetated marsh; the red circles represent triplicate samples collected at the marsh-water interface and the blue squares are samples collected near the shore. Not that in nearly all samples, nitrate is in very low concentrations near the shore, relative to near the open water. The pattern for ammonium is similar, but not as dramatic. See Sanchez et al. (2016) for methodological details (CAP LTER dataset DOI:10.6073/pasta/3eb1f02c8db033f63a144a6f9d778fa7). DOI: https://doi.org/10.1525/elementa.385.f4

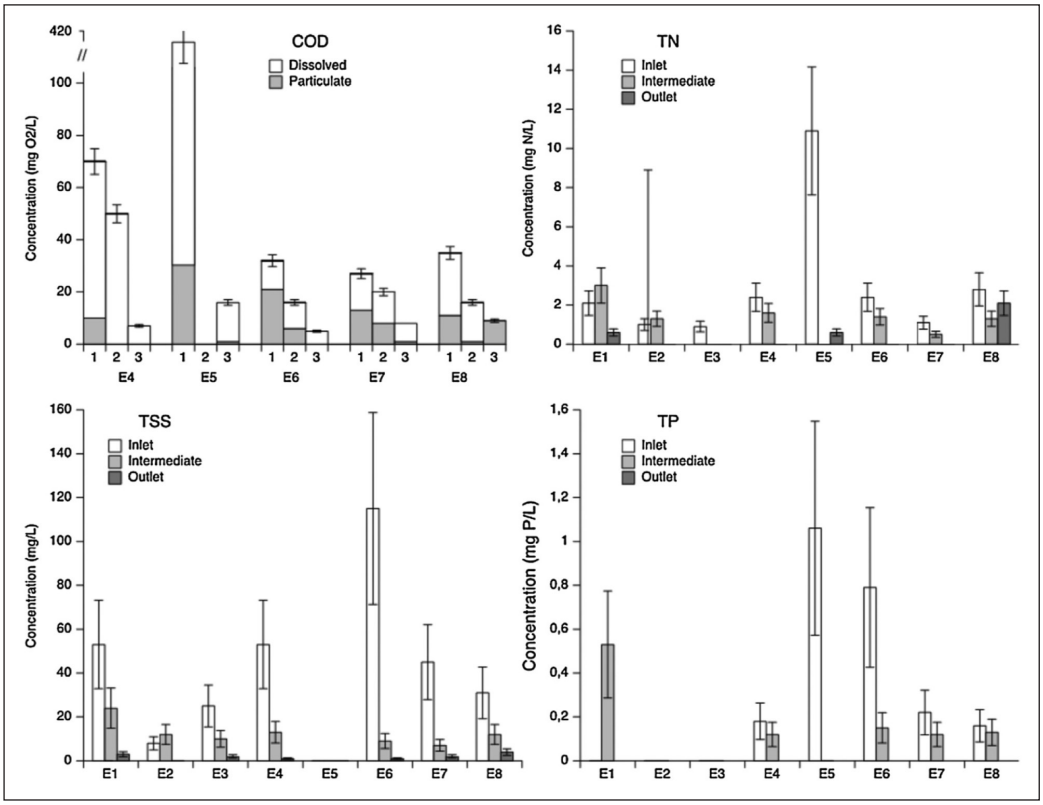

Figure 5: Ostwaldergraben stormwater treatment wetland water quality data. Change in pollutant concentration from the inlet to between the pond and the constructed treatment wetland (intermediate) to the outflow in the Ostwaldergraben system shown in Figure 2E, F (from Schmitt et al. 2015). COD = chemical oxygen demand; TN = total nitrogen; TSS = total suspended solids; TP = total phosphorus. DOI: https://doi.org/10.1525/elementa.385.f5

endangered toad as well as by other amphibians, thus providing an unexpected ecosystem service. The results of questionnaires from our semi-structured interviews of nearby residents have shown that they recognize and value this new habitat for amphibians (Bois et al. 2019) as well as the aesthetic enhancements provided by the restored stream and associated stormwater management UEI. Interestingly, the water quality and quantity regulating services provided by this UEI are still poorly perceived by local communities. This suggests an opportunity for scientists working in the system to expand their education and outreach activities in these neighboring communities.

4. Accidental Turquoise UEI in Phoenix AZ USA

The Salt River that runs through central Phoenix was once a perennial river. In prehistoric times its flow supported the agricultural and cultural productivity of the Hohokam people for nearly 1000 years (Murphy 2012). With the arrival of European settlers about 150 years ago, though, a lack of resilience to, and tolerance for, flooding became a major issue. By the late 1930s, the last of seven dams and reservoirs had been built upstream of Phoenix, on the Salt and Verde Rivers, sequestering 100% of the flow of both rivers for urban and agricultural use in the Phoenix metropolitan area. The Salt River has effectively not been a river since that time, except in extreme but rare events.

A lack of water in an urban riverbed does not necessarily preclude the possibility of wetlands, even in the arid southwestern U.S. As it turns out, Phoenix is a rather "leaky" city; storm drains that empty into the Salt River flow frequently, predictably, and even continuously, depending on the size of their urban pipe-sheds (Palta et al. 2017). The result is an array of "accidental" wetlands in the riverbed itself that provide unmanaged and unexpected ecosystem services, including nitrogen processing and removal and wildlife habitat (**Figure 2G, H**; Suchy 2016; Palta et al. 2017; Suchy et al. in press.). But an even more surprising collection of ecosystem services provided by these accidental wetlands was discovered when we began conducting field research in these systems. These perennial stormwater outflows and their associated Turquoise UEI are regularly used by homeless or indigent people throughout the Phoenix Metro area and provide many benefits, including cooling, bathing, and even food. These transient populations often prefer the wetlands to local shelters or cooling centers and have developed local knowledge of which outfalls have "good" (i.e., high quality) water and which do not (Palta et al. 2016). These accidental wetlands in the Salt River, that are not designed or managed, thus provide an array of unexpected ecosystem services to a diversity of city residents.

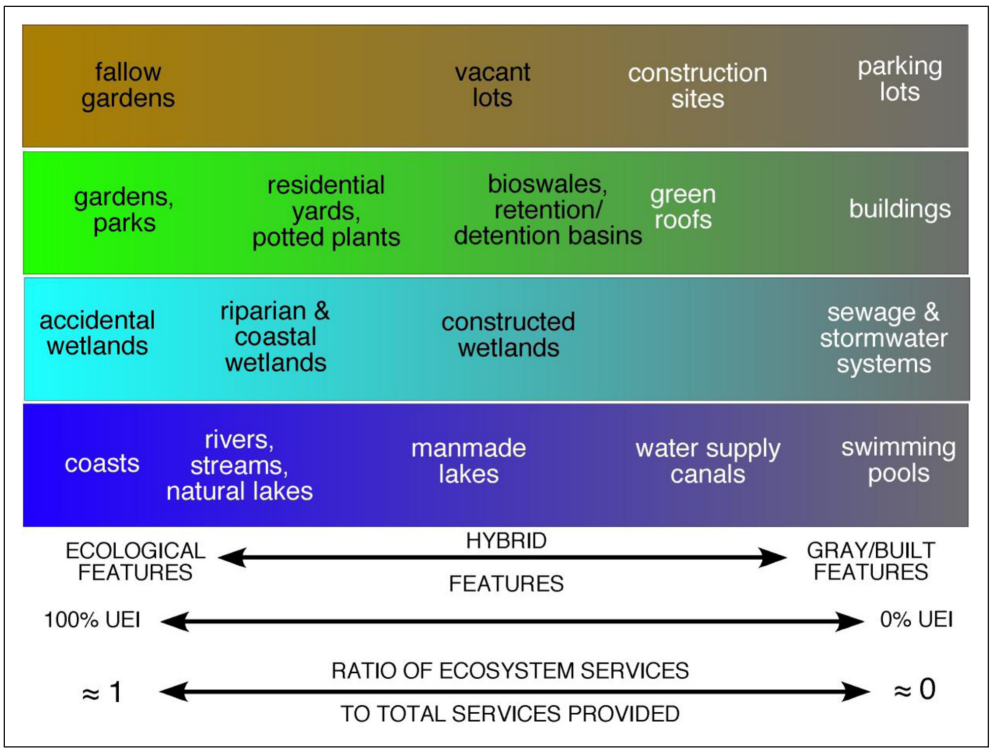

Figure 6: Schematic of the infrastructure hybridity gradient from 100% UEI to 100% built. Conceptual depiction of a gradient from ecological to hybrid to built features for the four colors of UEI. Note that while cities contain a great deal of purely gray/built infrastructure which does not include UEI (far right), they often contain few examples of pure UEI (far left); most UEI is actually hybrid infrastructure. For each UEI color, several examples and their approximate location on the ecological ←→ built gradient are shown. The gradient in the ratio of total services provided to those that result from ecological structure and function is also shown; ≈1 is where virtually all are ecosystem services from UEI, ≈0 is virtually none of the services are ecosystem services. The infrastructure types from the four case studies are also shown (stormwater retention/detention basins, accidental wetlands, constructed wetlands, and manmade lakes). DOI: https://doi.org/10.1525/elementa.385.f6

Synthesis and Conclusions

In this paper we present a more inclusive and simpler definition of Urban Ecological Infrastructure, refined from the earlier use of the concept by Li et al. (2017), that explicitly addresses all urban ecological components, including aquatic and wetland systems. We argue that UEI, as both a term and a concept, is preferable because the many existing terms for this idea are focused on goals and outcomes rather than on the ecological components themselves. For example, concepts such as ES and NBS merge functions and benefits and have required myriad papers to disentangle them. Additionally, existing related concepts (e.g., GI and UGS) are terrestrial-centric and thus downplay the importance of aquatic and wetland ecosystems in cities. In fact, all cities have aquatic components, including streams, rivers, canals, lakes, shorelines or coastlines, and all cities have various types of wetlands. A focus on mainly terrestrial ecological features is therefore an incomplete representation of nature in cities. Our refined definition of UEI is unabridged and includes all types of urban ecological systems. We use metaphorical colors to distinguish the different characteristics of, and services that come from, terrestrial, aquatic, and wetland ecosystems: Green, Blue, and Turquoise UEI, respectively. We include Brown UEI as a fourth type because non-vegetated terrestrial features are also common in all cities and urban soils as UEI provide important ecosystem functions and services.

But cities also contain a wide array of hybrid infrastructure types that span a full gradient from completely UEI to completely human-made (**Figure 6**; Grimm et al. 2016; Depietri and McPhearson 2017). As hybrid infrastructure incorporates more ecological characteristics and fewer built characteristics, a larger fraction of total benefits derived from it will be ecosystem services (**Figure 6**). Additionally, focusing on one single targeted service, as is often the case with NBS approaches, might prevent managers and stakeholders from recognizing, managing for, and benefitting from other ecosystem services that may be provided by UEI. It is this concept of hybridity in urban infrastructure, from mostly UEI to all built, that makes the UEI concept both fully inclusive and powerful. None of the other terms for nature in cities captures this fusion of the built and ecological features that we find throughout all cities.

An important advantage of the UEI concept is that the term itself includes both "ecological" and "infrastructure". Thus, the concept forms a key bridge between urban researchers and urban practitioners, and we anticipate that it will elevate urban ecological features to the same consideration by those practitioners as urban built features. This is key as cities expand their use of UEI in diverse biophysical and social contexts. At present, even without considering unintended benefits or consequences, UEI can deliver mixed outcomes. For example, although the use of bioretention swales is supposed to mitigate stormwater runoff and aid in pollutant removal, storm size and frequency alter the effectiveness of the swales (Norton et al. 2017). It is thus imperative that we continue to incorporate scientific knowledge into designs and management practices.

UEI may also allow practitioners from different sectors to account for synergies and tradeoffs among the services for which each sector is responsible. For example, vacant land may be managed as wildlife habitat, as a productive food landscape, or for storm water management (Kremer et al. 2013; McPhearson et al. 2013), depending on who takes leadership in management. But not all transformations from Brown to Green UEI result in the same ecosystem services. For example, although urban agriculture may provide food and pollinator habitat (Clinton et al. 2018), the over-application of fertilizers and other soil amendments by hobby gardeners (Metson et al. 2015; Lewis et al. 2018) may result in downstream water degradation rather than increasing water quality through stormwater retention. The UEI concept should allow diverse stakeholders (e.g., food policy councils, local water quality authorities, and zoning authorities in the example above) to talk to one another about how a parcel might be used to maximize benefits while avoiding damaging trade-offs. This is an advantage of the fact that UEI, as both a term and a concept, should resonate with designers, planners, and managers, strengthening the ecologist-practitioner bridge while advancing our ability to move knowledge to action in support of more sustainable and resilient urban futures. Our experience with co-producing a stormwater UEI monitoring design demonstrated this bridging effect. And this is already happening in our Strasbourg case study: The city's Urban Ecology and Water Department worked with both scientists and local communities to define, design, and implement the restoration of the Ostwaldergraben (Bois et al. 2019).

The UEI concept has important implications for the future of cities. For example, there are projections that by 2050 four in five people will live in cities. This means that as much as half of the areas that will be urban in the future have yet to be built—a huge opportunity for not just "thinking out of the box", but for "thinking of a whole new box" in terms of what urban development looks like and how it behaves (McPhearson et al. 2016; Alberti et al. 2018). With multiple social and environmental pressures, operating at myriad scales (e.g., climate change as an existential threat through extreme events, especially in coastal cities), the UEI concept provides a critical entry point for rethinking urban development so that it meets both sustainability and resilience goals. We argue that a key to this new vision of urban development is the transdisciplinary fusion of ecology and design, *sensu* Childers et al. (2015). Urban planners and designers, including architects, engineers, and landscape architects, need to be coaxed into thinking beyond a single project and urban scientists need to be coaxed into using their knowledge about urban ecosystems to make cities better places to live. The UEI concept inherently includes ecological connectivity, via a variety of hybrid UEI-built infrastructure types, as well as the spatial heterogeneity that characterizes all cities.

The literature is replete with analyses that demonstrate how UEI-based solutions are more adaptive and flexible than hard-engineered solutions, such that "safe to fail" infrastructure can impart resilience to urban systems

while "fail-safe" infrastructure often does not (Chester and Allenby 2018). There is also copious evidence that the co-production of knowledge, designs, and solutions by urban practitioners and researchers is a key to more sustainable future pathways for cities—those that exist today and those yet to be built (Elmqvist et al. 2018). We argue that UEI is the best term and concept for nature in cities because it conceptually, and perhaps literally, bridges the worlds of knowledge generation and action. It should thus be a critical conduit for enhancing the co-production of urban sustainability solutions that will lead to more resilience cities.

Acknowledgements

Thanks to S.T.A. Pickett for helpful comments on a late draft, and to two anonymous reviewers for their input.

Funding information

The U.S. National Science Foundation supported this work through the Central Arizona-Phoenix Long-Term Ecological Research Program (Grant Nos. DEB-1026865, DEB-1637590, and DEB-1832016). G.S.M was supported by FORMAS, the Swedish research council for sustainable development (Grant #942-2016-69 992023). The Rhin-Meuse Water Agency and the French Biodiversity Agency supported the Ostwaldergraben work through the LumiEau-Stra Research Project. Additional research support was provided to P.B. by the ZAEU (French LTSER network). TM was supported by the Urban Resilience to Extreme Weather-Related Events Sustainability Research Network (UREx SRN; NSF Grant No. SES-1444755), SETS Resilience project (NSF Grant No. GCR-1934933) and NATURA network (NSF Grant No. Accel-Net 1927167).

Competing interests

The authors have no competing interests to declare.

Author contributions

The authors of this paper contributed equally to the conception and refining of the ideas, to the case study examples and related data, and to the writing of the manuscript. All authors approved the final version for publication.

References

Alberti, M, McPhearson, T and **Gonzalez, A.** 2018. Embracing urban complexity. In: *The Urban Planet: Knowledge towards sustainable cities.* Cambridge, UK: Cambridge University Press.

Andersson, E, Barthel, S, Borgstrom, S, Colding, J, Elmqvist, T, Folke, C and **Gren, A.** 2014. Reconnecting cities to the biosphere: Stewardship of green infrastructure and urban ecosystem services. *Ambio* **43**: 445–453. DOI: https://doi.org/10.1007/s13280-014-0506-y

Andersson, E, Tengo, M, McPhearson, T and **Kremer, P.** 2015. Cultural ecosystem services as a gateway for improving urban sustainability. *Ecosystem Services* **12**: 165–168. DOI: https://doi.org/10.1016/j.ecoser.2014.08.002

Aronson, MFJ, Lepczyk, CA, Evans, KL, Goddard, MA, Lerman, SB, MacIvor, JS, Nilon, CH and **Vargo, T.** 2017. Biodiversity in the city: Key challenges for urban green space management. *Frontiers in Ecology & the Environ* **15**(4): 189–196. DOI: https://doi.org/10.1002/fee.1480

Barbosa, A, Martin, B, Hermoso, V, Arévalo-Torres, J, Barbiére, J, Martínez-López, J, Domisch, S, Langhans, SD, Balbi, S, Villa, F, Delacámara, G, Teixeira, H, Nogueira, AJA, Lillebø, AI, Gil-Jiménez, Y, McDonald, H and **Iglesias-Campos, A.** 2019. Cost-effective restoration and conservation planning in green and blue infrastructure designs. A case study on the Intercontinental Biosphere Reserve of the Mediterranean: Andalusia (Spain) – Morocco. *Science of the Total Environment* **652**:1463–1473. DOI: https://doi.org/10.1016/j.scitotenv.2018.10.416

Benedict, MA and **McMahon, ET.** 2006. *Green infrastructure: Linking landscapes and communities*. Island Press.

Bettencourt, L, Lobo, J and **West, G.** 2009. The self-similarity of human social organization and dynamics in cities. In: *Complexity Perspectives in Innovation and Social Change*. Volume 7, Methods Series. Rotterdam, Netherlands; Springer. DOI: https://doi.org/10.1007/978-1-4020-9663-1_8

Bois, P, Beisel, JN, Heitz, C, Katinka, L, Laurent, J, Pierrette, M, Walaszek, M and **Wanko, A.** 2019. Integrated Blue and Green Corridor Restoration in Strasbourg: Green Toads, Citizens, and Long-Term Issues. In: *Ecological Wisdom Inspired Restoration Engineering*. Singapore: Springer. DOI: https://doi.org/10.1007/978-981-13-0149-0_9

Bois, P, Childers, DL, Corlouer, T, Laurent, J, Massicot, A, Sanchez, CA and **Wanko, A.** 2017. Confirming a plant-mediated "Biological Tide" in an aridland constructed treatment wetland. *Ecosphere* **8**(3): 1–16. DOI: https://doi.org/10.1002/ecs2.1756

CAP LTER Tempe Town Lake water quality data. DOI: https://doi.org/10.6073/pasta/59d2e20260ad78d887e9bf3dd8987db4

CAP LTER Tres Rios water quality data. DOI: https://doi.org/10.6073/pasta/3eb1f02c8db033f63a144a6f9d778fa7

Chester, M and **Allenby, BR.** 2018. Toward Adaptive Infrastructure: Flexibility and Agility in a Non-stationarity Age. *Sustainable and Resilient Infrastructure* **3**(1): 1–19.

Childers, DL, Cadenasso, ML, Grove, JM, Marshall, V, McGrath, B and **Pickett, STA.** 2015. An ecology *for* cities: A transformational nexus of design and ecology to advance climate change resilience and urban sustainability. *Sustainability* **7**(4): 3774–3791. DOI: https://doi.org/10.3390/su7043774

Cilliers, S, Cilliers, J, Lubbe, R and **Siebert, S.** 2013. Ecosystem services of urban green spaces in African countries—perspectives and challenges. *Urban Ecosystems* **16**: 681–702. DOI: https://doi.org/10.1007/s11252-012-0254-3

Clinton, N, Stuhlmacher, M, Miles, A, Uludere Aragon, N, Wagner, M, Georgescu, M, Herwig, C and **Gon, P.** 2018. A global geospatial ecosystem services estimate

of urban agriculture. *Earth's Future* **6**: 40–60. DOI: https://doi.org/10.1002/2017EF000536

Cohen-Shacham, E, Walters, G and **Janzen, C.** 2016. Nature-based Solutions to address global societal challenges. Gland, Switzerland: IUCN. DOI: https://doi.org/10.2305/IUCN.CH.2016.13.en

David, F. 1995. Network cities: Creative urban agglomerations for the 21st century. *Urban Studies* **32**(2): 313–327. DOI: https://doi.org/10.1080/00420989550013103

Depietri, Y and **McPhearson, T.** 2017. Integrating the grey, green, and blue in cities: Nature-based solutions for climate change adaptation and risk reduction. In: *Nature-based Solutions to Climate Change in Urban Areas: Linkages Between Science, Policy, and Practice.* New York, NY: Springer. DOI: https://doi.org/10.1007/978-3-319-56091-5_6

EC. 2000. Directive 2000/60/EC of The European Parliament and of the Council of 23 October 2000 Establishing a Framework for Community Action in the Field of Water Policy. *Official Journal of the European Communities* L327.

Eggermont, H, Balian, E, Azevedo, J, Manuel, J, Beumer, N, Brodin, V, Claudet, J, Fady, B, Grube, M, Keune, H, Lamarque, P, Reuter, K, Smith, M, van Ham, C, Weisser, W and **Le Roux, X.** 2015. Nature-based Solutions: New Influence for Environmental Management and Research in Europe. *GAIA – Ecological Perspectives for Science and Society* **24**(4): 243–248. DOI: https://doi.org/10.14512/gaia.24.4.9

Elmqvist, T, Bai, X, Frantzeskaki, N, Griffith, C, Maddox, D and **McPhearson, T.** 2018. *Urban Planet: Knowledge towards Sustainable Cities*. Cambridge, UK: Cambridge University Press. DOI: https://doi.org/10.1017/9781316647554

Frantzeskaki, N, McPhearson, T, Collier, MJ, Kendal, D, Bulkeley, H, Dumitru, A, Walsh, C, Noble, K, van Wyk, E, Ordóñez, C, Oke, C and **Pinter, L.** 2019. Nature-based solutions for urban climate change adaptation: linking the science, policy, and practice community for evidence-based decision-making. *BioScience*. DOI: https://doi.org/10.1093/biosci/biz042

Gómez-Baggethun, E, Gren, Å, Barton, DN, Langemeyer, J, McPhearson, T, O'Farrell, P, Andersson, E, Hamstead, Z and **Kremer, P.** 2013. Urban Ecosystem Services. In: *Cities and Biodiversity Outlook: Urbanization, Biodiversity and Ecosystem Services: Challenges and Opportunities*. Rotterdam, Netherlands: Springer. DOI: https://doi.org/10.1007/978-94-007-7088-1_11

Grimm, NB, Cook, EM, Hale, RL and **Iwaniec, DM.** 2016. A broader framing of ecosystem services in cities: benefits and challenges of built, natural, or hybrid system function. In: *Handbook on urbanization and global environmental change*. New York, NY: Routledge.

Grimm, NB, Faeth, SH, Golubiewski, NE, Redman, CL, Wu, J, Bai, X and **Briggs, JM.** 2008. Global change and the ecology of cities. *Science* **319**(5864): 756–760. DOI: https://doi.org/10.1126/science.1150195

Grimm, NB and **Schindler, S.** 2018. Nature of cities and nature in cities: prospects for conservation and design of urban nature in human habitat. In: *Rethinking Environmentalism: Linking Justice, Sustainability, and Diversity* **23**. Strüngmann Forum Reports. Cambridge, MA: MIT Press.

Haase, D, Larondelle, N, Andersson, E, Artmann, M, Borgström, S, Breuste, J, Gomez-Baggethun, E, Gren, Å, Hamstead, Z, Hansen, R, Kabisch, N, Kremer, P, Langemeyer, J, Rall, EL, McPhearson, T, Pauleit, S, Qureshi, S, Schwarz, N, Voigt, A, Wurster, D and **Elmqvist, T.** 2014. A quantitative review of urban ecosystem service assessments: concepts, models, and implementation. *Ambio* **43**: 413–33. DOI: https://doi.org/10.1007/s13280-014-0504-0

Hale, RL, Turnbull, L, Earl, S, Childers, DL and **Grimm, NB.** 2015. Stormwater infrastructure controls runoff and dissolved material export from arid urban watersheds. *Ecosystems* **18**(1): 62–75. DOI: https://doi.org/10.1007/s10021-014-9812-2

Hale, RL, Turnbull, L, Earl, S, Grimm, NB, Riha, K, Michaelski, G, Lohse, K and **Childers, DL.** 2014. Sources and transport of nitrogen in arid urban watersheds. *Environ. Sci. Technol.* **48**(11): 6211–6219. DOI: https://doi.org/10.1021/es501039t

Herrmann, DL, Shuster, WD and **Garmestani, AS.** 2016. Vacant urban lot soils and their potential to support ecosystem services. *Plant Soil* **413**: 45–57. DOI: https://doi.org/10.1007/s11104-016-2874-5

Ioja, I, Oscaci-Costache, G, Breuste, J, Hossu, CA, Gradinaru, SR, Onose, DA, Nita, MR and **Skokanova, H.** 2018. Integrating urban blue and green areas based on historical evidence. *Urban Forestry & Greening* **34**: 217–225. DOI: https://doi.org/10.1016/j.ufug.2018.07.001

Kabisch, N, Korn, H, Stadler, J and **Bonn, A.** 2017. *Nature-based Solutions to Climate Change in Urban Areas: Linkages Between Science, Policy, and Practice*. Springer. DOI: https://doi.org/10.1007/978-3-319-56091-5_1

Keeler, BL, Hamel, P, McPhearson, T, Hamann, Donahue, MM, Meza Prado, K, Arkema, K, Bratman G, Brauman, K, Finlay, J, Guerry, A, Hobbie, S, Johnson, J, MacDonald, G, McDonald, R, Neverisky, N and **Wood, S.** 2019. Social-ecological and technological factors moderate the value of urban nature. *Nature Sustainability* **2**: 29–38. DOI: https://doi.org/10.1038/s41893-018-0202-1

Keeley, M. 2011. The green area ratio: An urban site sustainability metric. *Jour. Environ. Planning and Manage* **54**(7): 937–958. DOI: https://doi.org/10.1080/09640568.2010.547681

Koc, CB, Osmond, P and **Peters, A.** 2017. Towards a comprehensive green infrastructure topology: A systematic review of approaches, methods, and typologies. *Urban Ecosystems* **20**: 15–35. DOI: https://doi.org/10.1007/s11252-016-0578-5

Kremer, P, Hamstead, Z and **McPhearson, T.** 2013. A Social-Ecological Assessment of Vacant Lots

in New York City. *Landscape and Urban Planning*, 218–233. DOI: https://doi.org/10.1016/j.landurbplan.2013.05.003

Larsen, L. 2015. Urban climate and adaptation strategies. *Frontiers in Ecology and the Environment* **9**(13): 486–492. DOI: https://doi.org/10.1890/150103

Lewis, O, Home, R and **Kizos, T.** 2018. Digging for the roots of urban gardening behaviours. *Urban Forestry & Urban Greening* **34**: 105–113. DOI: https://doi.org/10.1016/j.ufug.2018.06.012

Li, F, Liu, H, Huisingh, D, Wang, Y and **Wang, R.** 2017a. Shifting to healthier cities with improved urban ecological infrastructure: From the perspectives of planning, implementation, governance, and engineering. *Jour. Cleaner Prod.* **163**: S12–S18. DOI: https://doi.org/10.1016/j.jclepro.2016.11.151

Li, F, Liu, X, Zhang, X, Zhao, D, Liu, H, Zhou, C and **Wang, R.** 2017b. Urban ecological infrastructure: An integrated network for ecosystem services and sustainable urban systems. *Jour. Cleaner Prod.* **163**: S1–S11. DOI: https://doi.org/10.1016/j.jclepro.2016.02.079

Locke, DH and **McPhearson, T.** 2018. Urban areas do provide ecosystem services. *Frontiers in Ecology & the Environment* **16**(4): 203–205. DOI: https://doi.org/10.1002/fee.1796

Maes, J and **Jacobs, S.** 2017. Nature-Based Solutions for Europe's Sustainable Development. *Conservation Letters* **1**: 121–124. DOI: https://doi.org/10.1111/conl.12216

McHarg, IL. 1969. *Design with Nature*. New York, NY: Natural History Press.

McPhearson, T, Kremer, P and **Hamstead, Z.** 2013. Mapping Ecosystem Services in New York City: Applying a Social-Ecological Approach in Urban Vacant Land. *Ecosystem Services*, 11–26. DOI: https://doi.org/10.1016/j.ecoser.2013.06.005

McPhearson, T, Parnell, S, Simon, D, Gaffney, O, Elmqvist, T, Bai, X, Roberts, D and **Revi, A.** 2016. Scientists must have a say in the future of cities. *Nature* **538**: 165–166. DOI: https://doi.org/10.1038/538165a

Metson, GS and **Bennett, EM.** 2015. Phosphorus cycling in Montreal's food and urban agriculture systems. *PLoS ONE* **10**(3): e0120726. DOI: https://doi.org/10.1371/journal.pone.0120726

Mitsch, WJ and **Gosselink, JG.** 2015. *Wetlands*. New York, NY: John Wiley & Sons.

Murphy, JT. 2012. Exploring complexity with the Hohokam water management simulation: A middle way for archeological modeling. *Ecological Modelling* **241**: 15–29. DOI: https://doi.org/10.1016/j.ecolmodel.2011.12.026

Nesshover, C, Assmuth, T, Irvine, KN, Rusch, GM, Waylen, KA, Delbaere, B, Haase, D, Jones-Walters, L, Keune, H, Kovacs, E, Krauze, K, Kulvik, M, Rey, F, van Dijk, J, Vistad, OE, Wilkinson, ME and **Wittmer, H.** 2017. The science, policy, and practice of nature-based solutions: An interdisciplinary perspective. *Science of the Total Environment* **579**: 1215–1227. DOI: https://doi.org/10.1016/j.scitotenv.2016.11.106

Neuman, M and **Smith, S.** 2010. City planning and infrastructure: Once and future partners. *Journal of Planning History* **9**: 21–42. DOI: https://doi.org/10.1177/1538513209355373

Niemelä, J, Saarela, S, Soderman T, Kopperoinen, L, Yli-Pelkonen, V, Vare, S and **Kotze, DJ.** 2010. Using the ecosystem services approach for better planning and conservation of urban green spaces: A Finland case study. *Biodiversity Conservation* **19**: 3225–3243. DOI: https://doi.org/10.1007/s10531-010-9888-8

Norton, RA, Harrison, JA, Kent Keller, C and **Moffett, KB.** 2017. Effects of storm size and frequency on nitrogen retention, denitrification, and N_2O production in bioretention swale mesocosms. *Biogeochemistry* **134**: 353–370. DOI: https://doi.org/10.1007/s10533-017-0365-2

NSF Advisory Committee for Environmental Research and Education. 2018. *Sustainable Urban Systems: Articulating a Long-Term Convergence Research Agenda*. Alexandria, VA: National Science Foundation.

Palta, MM, du Bray, M, Stotts, R and **Wutich, AY.** 2016. Ecosystem services and disservices for a vulnerable human population: Findings from urban waterways and wetlands in an American desert city. *Human Ecology* **44**(4): 463–478. DOI: https://doi.org/10.1007/s10745-016-9843-8

Palta, MM, Grimm, NB and **Groffman, PM.** 2017. "Accidential" urban wetlands: Ecosystem functions in unexpected places. *Frontiers in Ecology and the Environment* **15**(5): 248–256. DOI: https://doi.org/10.1002/fee.1494

Pickett, STA, Boone, CG, McGrath, BP, Cadenasso, ML, Childers, DL, Ogden, LA, McHale, M and **Grove, JM.** 2013. Ecological science and transformation to the sustainable city. *Cities* **32**: S10–S20. DOI: https://doi.org/10.1016/j.cities.2013.02.008

Pickett, STA, Cadenasso, ML, Childers, DL, McDonnell, MJ and **Zhou, W.** 2016. Evolution and future of urban ecological science: Ecology in, of, and for the city. *Ecosystem Health & Sustainability* **2**(7): e01229. DOI: https://doi.org/10.1002/ehs2.1229

Sanchez, CA. 2019. *Designing and implementing ecological monitoring urban ecological infrastructure: A case study*. MS Thesis. Tempe, AZ, USA: Arizona State University.

Sanchez, CA, Childers, DL, Turnbull, L, Upham, R and **Weller, NA.** 2016. Aridland constructed treatment wetlands II: Macrophyte-driven control of the wetland water budget makes the system more efficient than expected. *Ecological Engineering* **97**: 658–665. DOI: https://doi.org/10.1016/j.ecoleng.2016.01.002

Steiner, FR. 2006. *The Essential Ian McHarg: Writings on Design and Nature*. West Palm Beach, FL: Island Press.

Suchy, AK. 2016. *Denitrification in accidental urban wetlands: Exploring the roles of water flows and plant patches*. Ph.D. Dissertation. Tempe, AZ: Arizona State University.

Suchy, AK, Palta, MM, Stromberg, JC and **Childers, DL.** In press. Spatial and temporal patterns of potential denitrification in accidental urban wetlands in Phoenix AZ. *Ecosystems*.

Tzoulas, K, Korpela, K, Venn, S, Yli-Pelkonen, V, Kazmierczak, A, Neimelä, J and **James, P.** 2006. Promoting ecosystem and human health in urban areas using green infrastructure: A literature review. *Landscape & Urban Planning* **81**: 167–178. DOI: https://doi.org/10.1016/j.landurbplan.2007.02.001

Walaszek, M, Bois, P, Laurent, J, Lenormand, E and **Wanko, A.** 2018. Urban stormwater treatment by a constructed wetland: Seasonality impacts on hydraulic efficiency, physico-chemical behavior and heavy metal occurrence. *Science of the Total Environment* **637–638**: 443–454. DOI: https://doi.org/10.1016/j.scitotenv.2018.04.325

Weller, NA, Childers, DL, Turnbull, L and **Upham, R.** 2016. Aridland constructed treatment wetlands I: Macrophyte productivity, community composition, and nitrogen uptake. *Ecological Engineering* **97**: 649–657. DOI: https://doi.org/10.1016/j.ecoleng.2015.05.044

Wigginton, NS, Fahrenkamp-Uppenbrink, J, Wible, B and **Malakoff, D.** 2016. Cities are the future. *Science* **352**(6288): 904–905. DOI: https://doi.org/10.1126/science.352.6288.904

World Water Assessment Programme. 2018. The United Nations World Water Development Report 2018: Nature-Based Solutions for Water. Paris: UNESCO.

How to cite this article: Childers, DL, Bois, P, Hartnett, HE, McPhearson, T, Metson, GS and Sanchez, CA. 2019. Urban Ecological Infrastructure: An inclusive concept for the non-built urban environment. *Elem Sci Anth,* 7: 46. DOI: https://doi.org/10.1525/elementa.385

Domain Editor-in-Chief: Donald R. Zak, School of Natural Resources & Environment, University of Michigan, US

Associate Editor: Jessica J. Hellmann, Institute on the Environment, University of Minnesota, US

Knowledge Domain: Ecology

Submitted: 17 July 2019 **Accepted:** 23 October 2019 **Published:** 18 November 2019

ELEMENTA Science of the Anthropocene

Elem Sci Anth is a peer-reviewed open access journal published by University of California Press.

OPEN ACCESS